1992

The SYNOP Experiment: Bottom Pressure Maps for the Central Array May 1988 to August 1990

Xiaoshu Qian

D. Randolph Watts
University of Rhode Island, randywatts@uri.edu

GRADUATE SCHOOL OF OCEANOGRAPHY
UNIVERSITY OF RHODE ISLAND
NARRAGANSETT, RHODE ISLAND

THE SYNOP EXPERIMENT:
Bottom Pressure Maps for the Central Array
May 1988 to August 1990

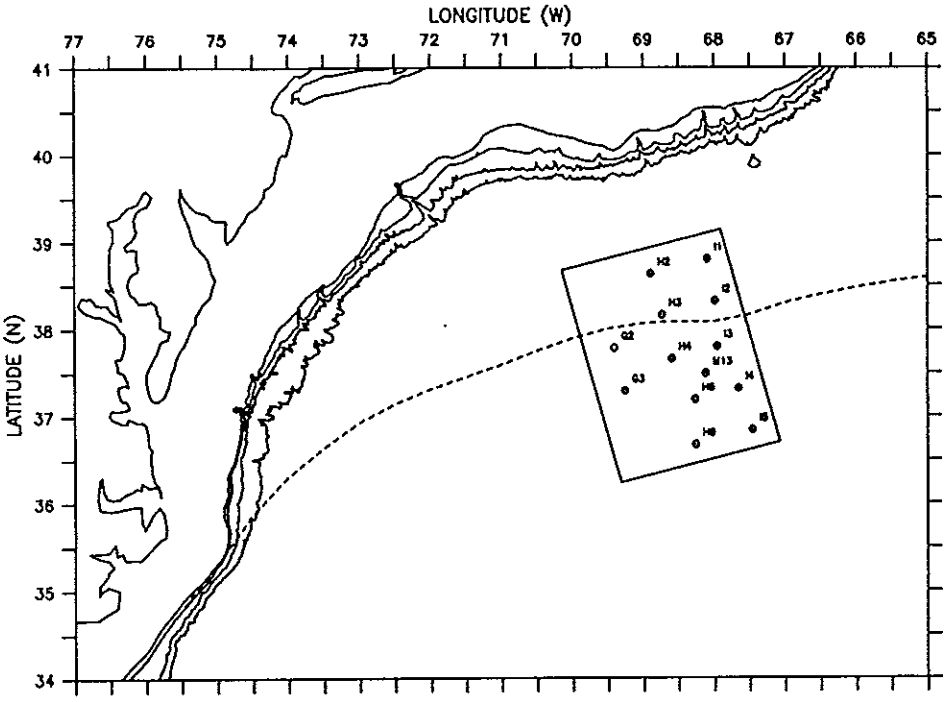

by

Xiaoshu Qian and D. Randolph Watts

GSO Technical Report No. 92-3
July 1992

This research program has been sponsored by the National Science Foundation under grant number OCE87-17144 and by the Office of Naval Research under contract number N00014-90-J-1568.

Abstract

This report documents our procedures and the accuracy of objective maps of bottom pressure in the Synop Central Array region between June 1988 and August 1990. The pressure maps are made by using multivariate objective analysis procedures to combine data from bottom pressure measurements by Inverted Echo Sounders (PIES) and bottom current meter measurements in the Central Array between June 1988 and August 1990.

A key new feature is that all daily maps can be adjusted to a fixed reference level by combining measurements of bottom pressure and near-bottom currents, (P_b, u,v). While objective stream functions mapped from (u,v) alone are spatially consistent, the reference levels vary temporally from map to map. On the other hand, each bottom pressure record P_b has a temporally consistent reference but the reference can vary from site to site. The combination allows us to adjust all to a common, consistent reference level in multivariate objective maps.

The pressure maps and error maps are displayed daily for 26 months with overlaid measured current vectors. Mapping procedures are documented along with error analyses and comparisons with measured fields. The results produce bottom pressure and current fields with typical error of only 2 mbar and 2 cm/sec, compared to typical signal standard deviation of 6 mbar and 9 cm/s.

The report is one of a series of data reports that document aspects of our participation in the SYNoptic Ocean Prediction (SYNOP) experiment.

Contents

List of Tables

List of Figures

1 Introduction

This report documents the procedures and the accuracy of the objective bottom pressure maps in the Synop Central Array region between June 1988 and August 1990. It is one of a series of data reports that document aspects of our participation in the SYNoptic Ocean Prediction (SYNOP) experiment [7, 2, 3, 8, 9, 6]. The study region consists of a sub-region of the Synop Central Array and is shown in Figure 1 and Table 1.

The bottom pressure maps are made by combining data from bottom pressure measurements [2, 3] by Inverted Echo Sounders (PIES) and bottom current meter measurements. The instrument positions are indicated in Figure 1 and detailed in Table 2 and Table 3. For each instrument site, the period when PIES and Current Meter measurements were taken is shown by the time lines in Figure 2 and by the start and end dates in Table 2 and Table 3.

The rest of the report is organized as follows. Section 2 reviews the aspects of multivariate Objective Analysis procedures necessary for mapping the pressure fields from the pressure and current measurements. Section 3 describes the data processing steps. Section 4 evaluates the precision of the resulting pressure maps. The pressure maps are then displayed in section 5 along with the corresponding error maps.

Table 1: Corner positions of the rectangular mapping region

Corner	x (km)	y (km)	Latitude (N)	Longitude (W)
Upper Left	−160	120	38° 40.27	70° 09.10
Lower Left	−160	−160	36° 14.08	69° 18.69
Upper Right	40	120	39° 08.25	67° 54.73
Lower Right	40	−160	36° 42.06	67° 04.32

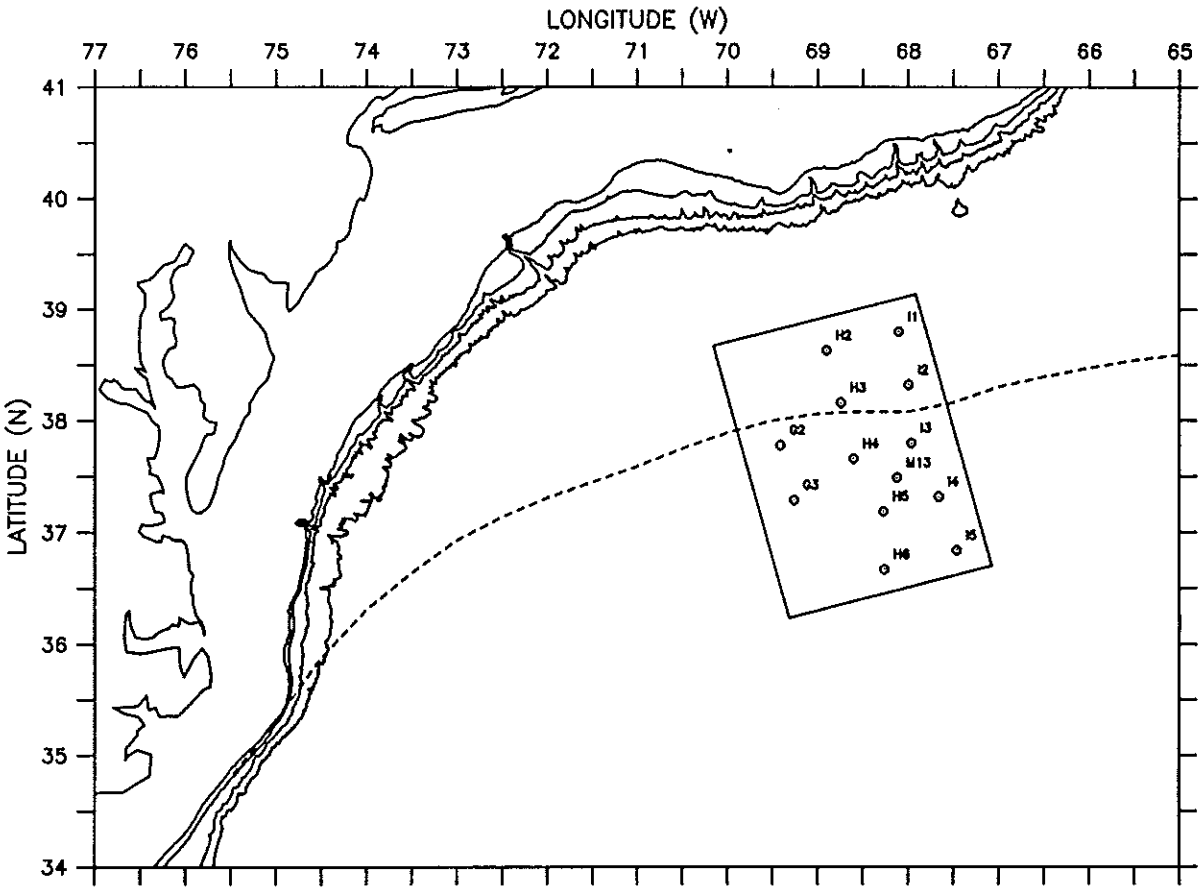

Figure 1: Current meter mooring and PIES sites. The dashed curve indicates the mean path of the Gulf Stream (1975 to 1986) from Gilman and Cornillon [1990].

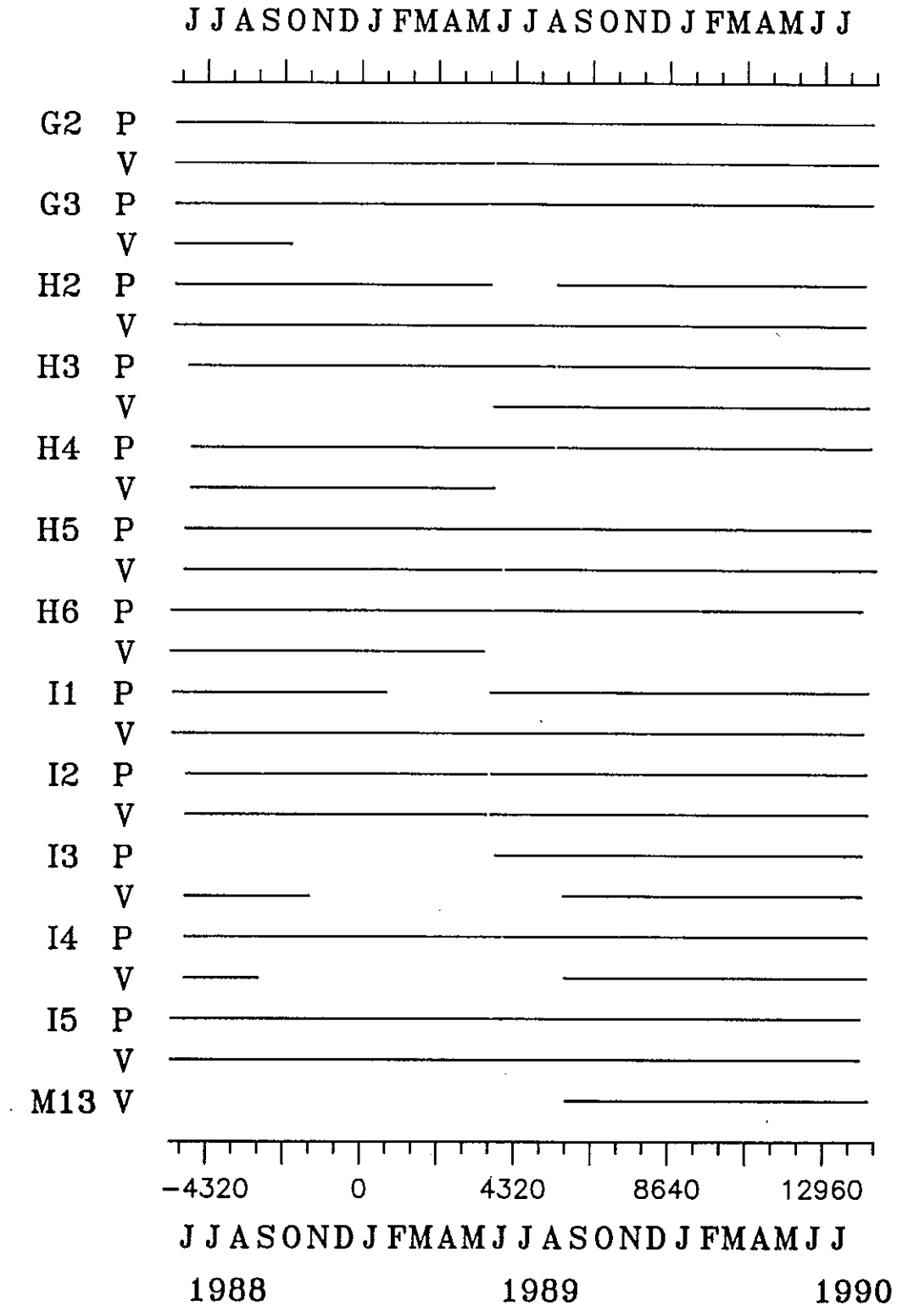

Figure 2: Time lines of the data coverage for current meters and PIES's on all sites

Table 2: Duration and location of the PIES records used in mapping

Site	Start date	End date	Latitude (N)	Longitude (W)	Depth (m)
G2	28-MAY-1988	12-SEP-1989	37° 47.52	69° 24.33	4060
	07-JUN-1989	19-AUG-1990	37° 47.84	69° 24.31	4088
G3	28-MAY-1988	28-MAY-1989	37° 17.40	69° 14.53	4358
	30-MAY-1989	18-AUG-1990	37° 16.99	69° 14.71	4358
H2	28-MAY-1988	01-JUN-1989	38° 37.88	68° 54.20	3458
	17-AUG-1989	10-AUG-1990	38° 37.78	68° 54.90	3458
H3	13-JUN-1988	14-AUG-1989	38° 10.10	68° 43.30	4030
	17-AUG-1989	14-AUG-1990	38° 10.09	68° 43.65	4025
H4	16-JUN-1988	14-AUG-1989	37° 39.80	68° 35.40	4445
	17-AUG-1989	17-AUG-1990	37° 39.57	68° 35.35	4445
H5	09-JUN-1988	13-AUG-1989	37° 10.60	68° 17.00	4790
	16-AUG-1989	17-AUG-1990	37° 10.23	68° 17.83	4800
H6	24-MAY-1988	03-JUN-1989	36° 40.45	68° 15.64	4883
	05-JUN-1989	08-AUG-1990	36° 39.35	68° 15.70	4840
I1	26-MAY-1988	01-FEB-1989	38° 47.54	68° 06.38	3828
	01-JUN-1989	16-AUG-1990	38° 47.58	68° 06.25	3828
I2	11-JUN-1988	29-MAY-1989	38° 20.90	67° 59.60	4720
	02-JUN-1989	15-AUG-1990	38° 19.68	67° 58.71	4270
I3	07-JUN-1989	10-AUG-1990	37° 47.61	67° 58.85	4610
I4	10-JUN-1988	15-JUN-1989	37° 18.50	67° 39.30	4775
	18-JUN-1989	16-AUG-1990	37° 18.88	67° 39.58	4765
I5	25-MAY-1988	02-JUN-1989	36° 49.73	67° 27.57	4975
	05-JUN-1989	07-AUG-1990	36° 50.19	67° 27.36	4975

Table 3: Duration and location of the current meter records used in mapping

Site	Start date	End date	Latitude (N)	Longitude (W)	Depth (m)
G2	28-MAY-1988	03-JUN-1989	37° 47.30	69° 24.50	3500
	06-JUN-1989	24-AUG-1990	37° 47.03	69° 24.66	3500
G3	27-MAY-1988	11-OCT-1988	37° 17.70	69° 14.50	3500
H2	26-MAY-1988	10-AUG-1990	38° 38.02	68° 54.00	3355
H3	03-JUN-1989	14-AUG-1990	38° 09.31	68° 44.28	3500
H4	15-JUN-1988	05-JUN-1989	37° 40.10	68° 35.20	3500
H5	09-JUN-1988	14-JUN-1989	37° 11.05	68° 17.60	3500
	17-JUN-1989	23-AUG-1990	37° 11.50	68° 15.96	3500
H6	23-MAY-1988	25-MAY-1989	36° 40.40	68° 15.85	3500
I1	26-MAY-1988	10-AUG-1990	38° 47.83	68° 06.25	3500
I2	10-JUN-1988	29-MAY-1989	38° 19.40	67° 59.20	3500
	02-JUN-1989	16-AUG-1990	38° 19.18	67° 59.37	3500
I3	10-JUN-1988	03-NOV-1988	37° 47.35	67° 56.20	3500
	26-AUG-1989	09-AUG-1990	37° 47.81	67° 57.82	3500
I4	09-JUN-1988	04-SEP-1988	37° 18.50	67° 38.30	3500
	27-AUG-1989	15-AUG-1990	37° 19.07	67° 39.58	3500
I5	24-MAY-1988	07-AUG-1990	36° 50.10	67° 27.40	3500
M13	28-AUG-1989	17-AUG-1990	37° 29.12	68° 07.18	3500

2 Review of Objective Analysis Procedures

This section reviews Objective Analysis (OA) procedures. We first review the Gauss-Markov problem of estimating a random variable from some other random variables that are correlated to it [5]. The solution to this problem is then applied to mapping the pressure field from pressure and current measurements [1]. Various computational aspects of the procedures are discussed next. Section 2.3 examines the error model underlying the OA procedure we used, followed by a discussion of normalization of the covariance functions in Section 2.4. Programs are discussed in Section 2.5 and listed in Appendix A. For use in later sections, some theoretical relationships between spatial cross covariance functions between pressure and currents are tabulated in section 2.6, and their derivation is provided in Appendix B.

2.1 OA basics

Given N random variables

$$\phi = (\phi_1, \phi_2, ..., \phi_N)^T, \tag{1}$$

where the superscript T denotes the matrix transpose, we want to estimate another random variable θ by a linear relation between θ and ϕ

$$\hat{\theta} = \sum_{s=1}^{N} b_s \phi_s = b^T \phi, \tag{2}$$

where $b = (b_1, b_2, ..., b_N)^T$ is selected in such a way that the resulting mean square error

$$P = E\{(\hat{\theta} - \theta)^2\} \tag{3}$$

is minimum. Note we implicitly assume that $E\{\theta\} = E\{\phi_s\} = 0$, because otherwise the estimator in (2) can be readily improved by adding a constant term to it.

We now show that the optimal estimator and the minimal mean square error in the above problem are given by

$$\hat{\theta} = CA^{-1}\phi \tag{4}$$

$$P = E\{\theta^2\} - CA^{-1}C^T. \tag{5}$$

where A and C are respectively the covariance matrix between the $\phi's$ and the cross-covariance matrix between θ and $\phi's$. Specifically, A is an N by N symmetric matrix

$$A = E\{\phi\phi^T\} \quad or \quad A_{sr} = E\{\phi_s\phi_r\} \tag{6}$$

and C is a *row* vector of length N

$$C = E\{\theta\phi^T\} \quad or \quad C_r = E\{\theta\phi_r\}. \tag{7}$$

To prove the above result, we note that the mean square error P in (3) is a function of b_s and is minimum if all its partial derivatives with respect to b_s are zero. That is, $2E\{(\hat{\theta} - \theta)\frac{\partial\hat{\theta}}{\partial b_r}\} = 2E\{(\hat{\theta} - \theta)\phi_r\} = 0$, $r = 1, 2, ..., N$. To write in matrix form, we have

$$E\{(\hat{\theta} - \theta)\phi^T\} = 0 \tag{8}$$

Inserting (2) into (8), we obtain $b^T E\{\phi\phi^T\} = E\{\theta\phi^T\}$, or

$$b^T A = C \tag{9}$$

By inserting the solution of (9) for b^T into (2) we get the optimal estimator in (4). Next, to obtain the least mean square error in (5), we use (3), (2) and (8) to obtain

$$P = E\{(\theta - \hat{\theta})\theta^T\} - E\{(\theta - \hat{\theta})\phi^T b\} = E\{(\theta - \hat{\theta})\theta\} = E\{\theta^2\} - E\{\hat{\theta}\theta\}$$

Now using right hand side of (4) to replace $\hat{\theta}$ yields

$$P = E\{\theta^2\} - CA^{-1}E\{\phi\theta\},$$

which is the same as (5) by the definition of C in (7).

2.2 Extending basic formulas

We now generalize (4) and (5) for computational convenience. Our main interest is to use the result to estimate a physical parameter θ at some locations, where possibly no direct measurement is available, from measurements ϕ of possibly different parameters at instrument sites.

First we note that $\phi's$ can be measurements of different kinds. For example, we can have N measurement sites measuring M different parameters with N_m sites measuring m^{th} parameter (thus $N = \sum_{m=1}^{M} N_m$). In this report we are interested in estimating pressure, θ, at an arbitrary point from measurement of pressures and currents at instrument sites ($M = 3$). Thus an example with $M = 3$ and $N = 7$ can be

$$\phi = (p_1, p_2, p_3, u_1, u_2, v_1, v_2)^T.$$

Secondly, when we need estimates of θ on several, say G, locations, we can apply (4) and (5) to all G interpolation points one by one

$$\hat{\theta}_g = C_g A^{-1}\phi$$

$$P_g = E\{\theta_g^2\} - C_g A^{-1} C_g^T$$

where subscripts of θ denote interpolation points, C_g denotes row vector C corresponding to g^{th} interpolation point. Stacking those equations together, we can put them in matrix form

$$\hat{\theta} = CA^{-1}\phi \tag{10}$$

$$P = \text{diagonal}[E\{\theta\theta^T\} - CA^{-1}C^T], \tag{11}$$

with θ and P now being column vectors of length G, and C being a G by N matrix. For example, for $G = 4$ we have

$$\hat{\theta} = \begin{pmatrix} \hat{\theta}_1 \\ \hat{\theta}_2 \\ \hat{\theta}_3 \\ \hat{\theta}_4 \end{pmatrix} \quad \text{and} \quad C = \begin{pmatrix} E\{\theta_1\phi_1\} & \dots & E\{\theta_1\phi_N\} \\ E\{\theta_2\phi_1\} & \dots & E\{\theta_2\phi_N\} \\ E\{\theta_3\phi_1\} & \dots & E\{\theta_3\phi_N\} \\ E\{\theta_4\phi_1\} & \dots & E\{\theta_4\phi_N\} \end{pmatrix}. \tag{12}$$

Finally, if we want to estimate a time series (say, of length T) of θ from a corresponding series of ϕ, then under stationarity assumption about both θ and ϕ fields, covariance matrices A and C do not change with time and we can apply (10) at each time point. The result can again be expressed in compact form as (10) with matrix sizes of θ and ϕ now being G by T and N by T respectively. Equation (11) holds without any change in this case because error estimate does not change with time due to stationarity, as can also be seen directly from the right hand side of (11). For an example with $T = 3$, we have

$$(\hat{\theta}(1), \hat{\theta}(2), \hat{\theta}(3)) = CA^{-1}(\phi(1), \phi(2), \phi(3)) \tag{13}$$

where C and each $\hat{\theta}(t)$ can be of the forms in (12) and each $\phi(t)$ can be a column vector of measurements at all instrument sites.

To summarize the above extensions[1] we repeat here the main formulas after the extensions

$$\hat{\theta} = CA^{-1}\phi \quad or \quad \hat{\theta}_{gt} = \sum_{r=1}^{N} C_{gr} \left(\sum_{s=1}^{N} A_{rs}^{-1} \phi_{st} \right); \tag{14}$$

$$P = \text{diagonal}[E\{\theta(t)\theta(t)^T\} - CA^{-1}C^T] \quad or \quad P_g = E\{\theta_g^2(t)\} - \sum_{r,s=1}^{N} C_{gr} A_{rs}^{-1} C_{gs}; \tag{15}$$

$$A = E\{\phi(t)\phi(t)^T\} \quad or \quad A_{sr} = E\{\phi_s(t)\phi_r(t)\}; \tag{16}$$

$$C = E\{\theta(t)\phi(t)^T\} \quad or \quad C_{gr} = E\{\theta_g(t)\phi_r(t)\}; \tag{17}$$

where the dimensions of all matrices are as follows

$\hat{\theta}$: G by T;
P : G by 1 (It would be G by T if either θ or ϕ were non-stationary);
A : N by N;
C : G by N;
ϕ : N by T, (notation: $\phi_{st} \equiv \phi_s(t)$ and $\phi(t)$ is the t^{th} column in ϕ);
θ : G by T (notation: $\theta_{st} \equiv \theta_s(t)$ and $\theta(t)$ is the t^{th} column in θ).

Here is an example of (14) where $N = 7$, $M = 3$, $G = 4$, $T = 3$:

$$\begin{pmatrix} \hat{\theta}_1(1) & \hat{\theta}_1(2) & \hat{\theta}_1(3) \\ \hat{\theta}_2(1) & \hat{\theta}_2(2) & \hat{\theta}_2(3) \\ \hat{\theta}_3(1) & \hat{\theta}_3(2) & \hat{\theta}_3(3) \\ \hat{\theta}_4(1) & \hat{\theta}_4(2) & \hat{\theta}_4(3) \end{pmatrix} = \begin{pmatrix} E[\theta_1 p_1] & E[\theta_1 p_2] & E[\theta_1 p_3] & E[\theta_1 u_1] & E[\theta_1 u_2] & E[\theta_1 v_1] & E[\theta_1 v_2] \\ E[\theta_2 p_1] & E[\theta_2 p_2] & E[\theta_2 p_3] & E[\theta_2 u_1] & E[\theta_2 u_2] & E[\theta_2 v_1] & E[\theta_1 v_2] \\ E[\theta_3 p_1] & E[\theta_3 p_2] & E[\theta_3 p_3] & E[\theta_3 u_1] & E[\theta_3 u_2] & E[\theta_3 v_1] & E[\theta_1 v_2] \\ E[\theta_4 p_1] & E[\theta_4 p_2] & E[\theta_4 p_3] & E[\theta_4 u_1] & E[\theta_4 u_2] & E[\theta_4 v_1] & E[\theta_1 v_2] \end{pmatrix}$$

[1]The extension can also include the case where some $\phi(t \pm n)$, for $n \geq 1$, are also used in estimating $\theta(t)$.

$$\begin{pmatrix} E[p_1p_1] & E[p_1p_2] & E[p_1p_3] & E[p_1u_1] & E[p_1u_2] & E[p_1v_1] & E[p_1v_2] \\ E[p_2p_1] & E[p_2p_2] & E[p_2p_3] & E[p_2u_1] & E[p_2u_2] & E[p_2v_1] & E[p_2v_2] \\ E[p_3p_1] & E[p_3p_2] & E[p_3p_3] & E[p_3u_1] & E[p_3u_2] & E[p_3v_1] & E[p_3v_2] \\ E[u_1p_1] & E[u_1p_2] & E[u_1p_3] & E[u_1u_1] & E[u_1u_2] & E[u_1v_1] & E[u_1v_2] \\ E[u_2p_1] & E[u_2p_2] & E[u_2p_3] & E[u_2u_1] & E[u_2u_2] & E[u_2v_1] & E[u_2v_2] \\ E[v_1p_1] & E[v_1p_2] & E[v_1p_3] & E[v_1u_1] & E[v_1u_2] & E[v_1v_1] & E[v_1v_2] \\ E[v_2p_1] & E[v_2p_2] & E[v_2p_3] & E[v_2u_1] & E[v_2u_2] & E[v_2v_1] & E[v_2v_2] \end{pmatrix}^{-1} \begin{pmatrix} p_1(1) & p_1(2) & p_1(3) \\ p_2(1) & p_2(2) & p_2(3) \\ p_3(1) & p_3(2) & p_3(3) \\ u_1(1) & u_1(2) & u_1(3) \\ u_2(1) & u_2(2) & u_2(3) \\ v_1(1) & v_1(2) & v_1(3) \\ v_2(1) & v_2(2) & v_2(3) \end{pmatrix}.$$

2.3 Modeling measurement errors

The measurement error is assumed to be additive. Thus a measurement ϕ_s is the sum of true signal ϕ_{0s} and a noise term ϵ_s, assumed to be uncorrelated to all the signals in ϕ_0,

$$\phi_s = \phi_{0s} + \epsilon_s.$$

Also by assumption, ϵ_s from different measurement sites are *not* correlated; they all have zero mean but may have different variances.

From those assumptions about measurement error, the covariance matrices A and C can be written as

$$A = A_0 + E \tag{18}$$

$$C = C_0, \tag{19}$$

where A_0 and C_0 are corresponding covariance matrices in the absence of noise and E is a diagonal matrix whose s^{th} diagonal element is the variance of ϵ_s.

In contrast to the measurement error, we will call the least mean square error in (5) *mapping error*. It is sometimes useful to check the mapping error at a measurement site. To this end, we suppose that one of the measurement, say ϕ_k, happens to be the sum of θ and a noise term ϵ

$$\phi_k = \theta + \epsilon,$$

where ϵ has zero mean and variance σ^2 and is independent of θ and all other ϕ_s, then equation (5) reduces to

$$P = \sigma^2(1 - \sigma^2 A^{-1}_{kk}),$$

where A^{-1}_{kk} is the kth diagonal element of A^{-1}. Thus the mapping error is smaller than the measurement error at a measurement site due to the contribution of measurements from other sites.

2.4 Normalization of covariance matrices

Computationally, it is convenient to normalize the covariance matrices A and C. We will denote normalization by a tilde. Let

$$\tilde{\phi} = N_\phi^{-1}\phi, \qquad \tilde{\theta} = N_\theta^{-1}\theta \tag{20}$$

$$\tilde{A} = N_\phi^{-1} A N_\phi^{-1} \tag{21}$$

$$\tilde{C} = N_\theta^{-1} C N_\phi^{-1} \tag{22}$$

$$\tilde{P} = N_\theta^{-2} P \tag{23}$$

where N_ϕ is a diagonal matrix whose s^{th} diagonal element, $(N_\phi)_{ss}$, is the normalization factor for $\phi_s(t)$ and N_θ is a diagonal matrix whose g^{th} diagonal element, $(N_\theta)_{gg}$, is the normalization factor for $\theta_g(t)$. Specifically, we have

$$\tilde{\phi}_s(t) = \phi_s(t)/(N_\phi)_{ss}, \qquad \tilde{\theta}_g(t) = \theta_g(t)/(N_\theta)_{gg}$$

$$\tilde{A}_{rs} = E\{\tilde{\phi}_r(t)\tilde{\phi}_s(t)\} = \frac{A_{rs}}{(N_\phi)_{rr}(N_\phi)_{ss}},$$

$$\tilde{C}_r = E\{\tilde{\theta}_g(t)\tilde{\phi}_r(t)\} = \frac{C_r}{(N_\theta)_{gg}(N_\phi)_{rr}}.$$

Solving (21) and (22) for A and C and then putting them into (14) and (15), we get

$$\hat{\theta} = N_\theta \tilde{C} \tilde{A}^{-1} N_\phi^{-1} \phi \tag{24}$$

$$P = \text{diagonal}[E\{\theta(t)\theta(t)^T\} - N_\theta \tilde{C} \tilde{A}^{-1} \tilde{C}^T N_\theta]. \tag{25}$$

Those two equations are often written in more symmetrical form as

$$\hat{\tilde{\theta}} = \tilde{C} \tilde{A}^{-1} \tilde{\phi} \tag{26}$$

$$\tilde{P} = \text{diagonal}[E\{\tilde{\theta}(t)\tilde{\theta}(t)^T\} - \tilde{C} \tilde{A}^{-1} \tilde{C}^T] \tag{27}$$

where (20) and (23) have been used. In particular, if we choose $(N_\theta)_{gg} = \sqrt{E[\theta_g^2(t)]}$, then (27) becomes

$$\tilde{P} = \text{diagonal}[I_{G\times G} - \tilde{C} \tilde{A}^{-1} \tilde{C}^T] \tag{28}$$

Moreover, if all $E[\theta_g(t)^2]$ have same value σ^2 and we choose

$$N_\phi = \sigma I_{N\times N} \quad \textit{and} \quad N_\theta = \sigma I_{G\times G}. \tag{29}$$

with I being the identity matrix, then (24) can be written as

$$\hat{\theta} = \tilde{C}\tilde{A}^{-1}\phi \tag{30}$$

Note in (30) neither $\hat{\theta}$ nor ϕ is normalized and in (28) $\tilde{P}$ is the mapping error as a fraction of the signal variance $E\{\theta_g(t)^2\}$.

In practice, the normalization factor $(N_\phi)_{ss}$ is often chosen to be proportional to either the total variance $E\{\phi_s^2\}$ or the signal variance $E\{\phi_{0s}^2\}$. The first choice appears to be more natural at first since the total variance is often more readily available than the signal variance. However, we have adopted the second choice because it facilitates handling the case where measurement errors differ at different instrument sites. Under this choice, the measurement errors remain to be constrained in the diagonal elements of matrix $\tilde{A}$ (refer equations (18) and (19)). Thus if different error estimates are used for different measurement sites, the second approach requires only the diagonal elements of matrix $\tilde{A}$ to be changed while the first approach necessitates changes of whole matrix $\tilde{C}$ and all off-diagonal elements of matrix $\tilde{A}$.

In addition to the computational convenience, the normalization also simplifies handling the case of non-uniform variance in the measured fields. In this case, one normalizes ϕ and θ such that $\tilde{\phi}$ and $\tilde{\theta}$ fields in (20) have uniform variance, thus permitting use of homogeneous covariance functions in $\tilde{A}$ and $\tilde{C}$ in (26). This is equivalent to using (14) with A and C calculated from some covariance functions whose values at zero lag (variances) are location dependent.

2.5 Program prototypes

Five programs are listed in Appendix A. Three of them are for mapping pressure fields respectively from pressure measurements, current measurements and the combination of pressure and current measurements. The other two are for mapping current fields respectively from current measurements and the combination of pressure and current measurements. The programs closely follow the formulation in section 2.2. The output error fields are expressed in terms of variance percentage of signal fields and are calculated using (27) (after factoring out the first term). The relationship between input and output fields can be interpretated according to either (14), (26) or (30) depending on the normalization factors used.

A close match between the statements in the programs and the formulas in section 2.2 makes the programs more readable, thus reduces the chance of coding error, and facilitates their adaptation for new situations. We used these programs as the basis for more 'user-friendly' programs and to test different correlation functions. However, little emphasis has been given in these programs to the convenience of input format, input validation and CPU/storage efficiency. Also 'bogus data' is not allowed in the input matrices to these programs.

2.6 Assumed cross-covariance functions between pressure and current

In order to use the OA formulas (14)–(17), we need to supply the covariance matrices A and C. In our application, the elements of these matrices are calculated from the spatial cross covariance functions between current and pressure. This subsection examines some theoretical relationships between these cross-covariance functions for use in section 3.1 to obtain matrices A and C.

We assume that the current is geostrophic and has little vertical shear between the current measurement level at 3500 m depth and the pressure measurement level at the sea floor. Also we assume that pressure field statistics are stationary in time, and homogeneous and isotropic in space, and its spatial covariance function is a Gaussian function. Based on these, we examine here the required forms of the cross-covariance functions between current components (u, v) and pressure p. Further discussions on the above assumptions can be found in Section 3.1.

Specifically, assuming geostrophy, the current and pressure fields are related by

$$u = -\frac{1}{f_0 \rho}\frac{\partial p}{\partial y}, \qquad v = \frac{1}{f_0 \rho}\frac{\partial p}{\partial x}. \tag{31}$$

where $f_0 (= 2\Omega \cdot \sin\alpha)$ is the Coriolis parameter and ρ is the density of the sea water. The values of f_0 and ρ we used correspond to the values for the Central Array around 3500 m depth:

$$\begin{aligned} f_0 &= 2\Omega \cdot \sin\alpha = 2 \times 7.292 \times 10^{-5} \times \sin 38^\circ = 8.9788 \times 10^{-5}\ (s^{-1}); \\ \rho &= 1050\ (\mathrm{kg}/m^3). \end{aligned}$$

The current and pressure were measured, respectively, at 3500 m depth (above the bottom frictional layer) and near ocean bottom. Thus with (31), we have implicitly used the assumption that the current has little vertical shear in the region outside the bottom frictional

layer and between the two measurement levels. With this assumption, the bottom pressure field will be the same as the pressure field at the 3500 m horizon within an overall constant independent of location and time (see also section 3.3.2), because a frictional boundary layer is not expected to alter the pressure from its geostrophic value outside the layer.

From geostrophic relation (31), we see that the velocity field is horizontally non-divergent. Thus a stream function $\psi(x, y, t)$ exists such that

$$u = -\frac{\partial \psi}{\partial y}, \qquad v = \frac{\partial \psi}{\partial x} \tag{32}$$

From this, we can derive all the cross-covariance functions between stream function and current from the covariance function of the stream function. The derivation is given in the Appendix B and the results are listed in Table 4.

Table 4: Cross-covariance functions of stream function and current. γ, α_x and α_y are defined respectively by $\gamma = \{(x_1 - x_2)^2 + (y_1 - y_2)^2\}^{\frac{1}{2}}$, $x_2 - x_1 = \gamma \cos\alpha_x$ and $y_2 - y_1 = \gamma \cos\alpha_y$.

	$\psi(x_2, y_2)$	$u(x_2, y_2)$	$v(x_2, y_2)$
$\psi(x_1, y_1)$	$F(\gamma)$	$-\cos\alpha_y \frac{dF}{d\gamma}$	$\cos\alpha_x \frac{dF}{d\gamma}$
$u(x_1, y_1)$	$\cos\alpha_y \frac{dF}{d\gamma}$	$-\cos^2\alpha_y \frac{d^2F}{d\gamma^2} - (1 - \cos^2\alpha_y)\frac{1}{\gamma}\frac{dF}{d\gamma}$	$\cos\alpha_x \cos\alpha_y \left(\frac{d^2F}{d\gamma^2} - \frac{1}{\gamma}\frac{dF}{d\gamma}\right)$
$v(x_1, y_1)$	$-\cos\alpha_x \frac{dF}{d\gamma}$	$\cos\alpha_x \cos\alpha_y \left(\frac{d^2F}{d\gamma^2} - \frac{1}{\gamma}\frac{dF}{d\gamma}\right)$	$-\cos^2\alpha_x \frac{d^2F}{d\gamma^2} - (1 - \cos^2\alpha_x)\frac{1}{\gamma}\frac{dF}{d\gamma}$

Table 5: Same as the last table except that F is assumed to be a Gaussian function here.

	$\psi(x_2, y_2)$	$u(x_2, y_2)$	$v(x_2, y_2)$
$\psi(x_1, y_1)$	$F(\gamma) = V_\psi \exp(-\lambda\gamma^2)$	$\gamma \cos\alpha_y \cdot 2\lambda F(\gamma)$	$-\gamma \cos\alpha_x \cdot 2\lambda F(\gamma)$
$u(x_1, y_1)$	$-\gamma \cos\alpha_y \cdot 2\lambda F(\gamma)$	$(1 - 2\lambda\gamma^2 \cos^2\alpha_y) \cdot 2\lambda F(\gamma)$	$2\lambda\gamma^2 \cos\alpha_x \cos\alpha_y \cdot 2\lambda F(\gamma)$
$v(x_1, y_1)$	$\gamma \cos\alpha_x \cdot 2\lambda F(\gamma)$	$2\lambda\gamma^2 \cos\alpha_x \cos\alpha_y \cdot 2\lambda F(\gamma)$	$(1 - 2\lambda\gamma^2 \cos^2\alpha_x) \cdot 2\lambda F(\gamma)$

From (31) and (32), we see that the stream function ψ can be chosen in such a way that pressure p is proportional to ψ, namely,

$$p = f_0 \rho \psi. \tag{33}$$

Therefore, all the cross-covariance functions between pressure and current are the same as those between stream function and current except for a constant factor and thus can be readily obtained from Table 4.

In particular, we will assume that the pressure covariance function is a Gaussian function

$$F(\gamma) = E\{[p_i - E(p_i)][p_j - E(p_j)]\} = V_p \exp(-\lambda\gamma^2) \tag{34}$$

where $\gamma = \sqrt{(x_i - x_j)^2 + (y_i - y_j)^2}$ is the distance between site i and site j, and $\lambda = \frac{1}{(\text{Correlation Length})^2}$ is a constant to be fitted by the data, and V_p is the *signal* variance. By Equation (33), the covariance function of the stream function ψ is also a Gaussian function. As shown in Appendix B, the resulting cross covariance functions between current and stream function will be of the forms listed in Table 5.

3 Mapping the pressure fields

This section describes the data processing procedures involved in mapping pressure fields. The major work of objective mapping consists in estimating the noise variance in measurements, modeling the covariance functions and estimating the mean fields based on measured fields. We discuss these problems in the following two subsections. Then the final subsection describes the processing procedures that were applied to the measured pressures and currents and eventually led to a time series of pressure maps.

3.1 Estimating covariance functions

The noise variance in both pressure and current measurements is chosen to be ten percent of the *signal* variance (Table 6) by the following considerations. The typical standard deviation of all the pressure records is about 0.06 decibar. The error in residual pressure is negligible compared to the error in the reference pressure (see section 3.3.2). The error standard deviation of the reference pressure is estimated to be 0.02 decibar. Thus for pressure, $V_n \approx \left(\frac{0.02}{0.06}\right)^2 \approx 0.10$. The typical standard deviation of the deep current records is about 0.1 meter per second while the error standard deviation is estimated to be 0.03 meter per second. Thus for current record, $V_n \approx \left(\frac{0.03}{0.1}\right)^2 \approx 0.10$.

Table 6: Noise variance and correlation length used

Fields	Noise Variance/Signal Variance	Correlation length
Pressure or current	0.10	90 km
Mean pressure or current	0.05	150 km

The cross-covariance functions between pressures (or stream functions) and currents are assumed to be of the forms listed in Table 5. In doing so, we have made following assumptions as discussed in section 2.6. These assumptions are only approximations to reality and they are made to facilitate the data processing and/or make full use of existing measurements in improving the mapped pressure fields.

- geostrophy. The current measurements are typically on the order of 0.2 m/sec with a length scale of about 100 km. Combining these values with the value of Coriolis parameter given below Equation (31) gives a Rossby number of about 0.02. Thus, we expect that geostrophy is a good approximation.

- no vertical shear in currents between 3500m depth where currents were measured and

top of the bottom friction layer; no change in geostrophic pressure through the bottom friction layer to the ocean bottom. Hence the PIES measurement of pressure at the bottom is the same as at the 3500 m horizon except for a dynamically unimportant constant hydrostatic reference offset.

- homogeneity. From our measurements, the fields on the northern part of the array typically have less variance but more high frequency components than their southern counterparts. Although nonhomogeneity of other spectral characteristics often has no simple solution, variation in variance in the measured fields can usually be remedied by normalizing the measurement fields by their standard deviations, then mapping the normalized fields using a homogeneous covariance functions and finally scaling the estimated fields back to the real fields. Nevertheless, we did not scale measured pressure and currents for two reasons. Firstly, non-uniformly scaled pressure and current data will no longer be in geostrophic balance, resulting in much more complex cross-covariance functions between pressure and current. Secondly, in contrast to the near-surface Gulf Stream data, the deep pressures and currents have only small spatial changes in eddy variance; thus scaling by the variance should not be necessary.

- isotropy. Anisotropy of the correlation functions in this region is not justified from our previous experience with mapping the thermocline depth fields [8].

- stationarity. From the time series plots of measured pressures and currents (see Figure 9, 10 and 11 in Appendix C), we see that overall the time series are approximately stationary.

The assumptions above have reduced the problem of estimating covariance functions to one of estimating the correlation length of the pressure field. Fitting a Gaussian function to data covariance estimates in Figure 3 results in a correlation length of about 90 kilometers. In doing the least square fitting, the contribution of each pair of measurement sites is weighted by the length of the concomitant pressure records on both sites; the noise variance in the data cross-covariance is assumed to be 10 percent. Also shown in Figure 3 is the bin averages of the estimated data cross-covariance. Only data cross-covariance estimated by two pressure records longer than 30 days are used in bin averages. The length of each error bar is twice as big as the standard deviation of the bin average.

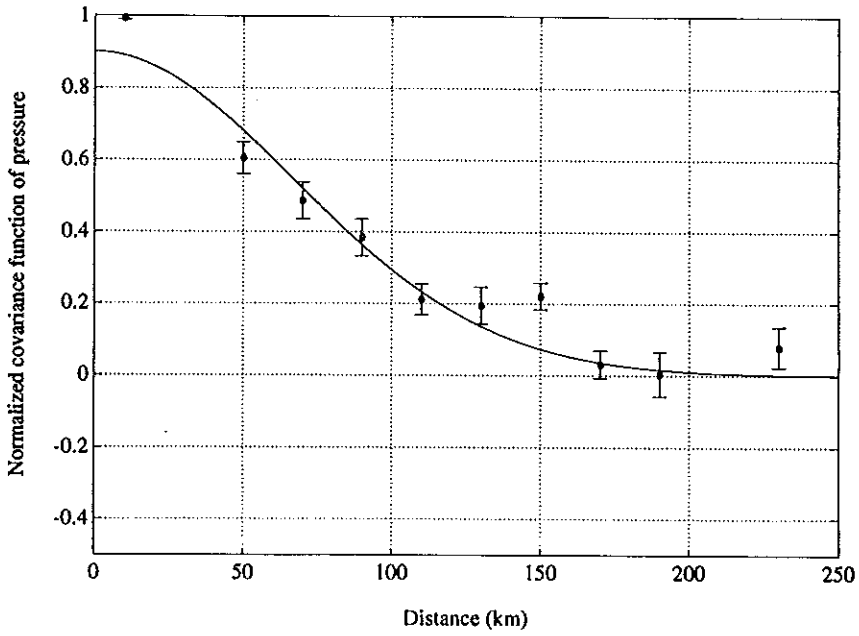

Figure 3: Spatial correlation function of the pressure fields.

In addition, the choice for the values of the noise variance and correlation length in Table 6 were also based on the following experiment. We objectively estimated the currents on each site, first using all available current measurements and then using only measurements other than the site chosen. In both cases, all combinations of noise variance (0.05, 0.10) and correlation lengths from 50 km through 130 km (at 10 km interval) were tried in the OA procedure. The estimated currents were compared with the measured ones and the resulting root mean square errors were compared with OA predicted errors. The parameter values listed in Table 6 produced best overall performance.

The covariance matrices A and C in (14) and (15) are calculated from (18) and (19). In the last two equations, the estimated signal covariance functions are used to calculate the elements of matrices A_0 and C_0; the noise variance estimates are used for the diagonal elements of E.

3.2 Estimating the mean fields

Both measured and estimated fields in OA formulae (14) — (17) are assumed to have zero mean. Accordingly, the measured field should be demeaned before applying the OA procedure, and the estimated perturbation field should have mean fields restored afterwards. This subsection describes how we determine those mean fields.

In essence, we estimate the mean pressure fields from temporally averaged *current* measurements by objectively mapping the stream function. Thus we need to know the noise variance in the averaged measurements and the covariance functions of the average fields. In this case, our best choice is that the noise variance is five percent of the signal variance for both averaged pressure and averaged currents and the correlation length of the averaged pressure fields is 150 kilometers (Table 6). The choice was guided by the experiment that we mentioned near the end of section 3.1, in which we found that our choice is 'best' in the sense that it minimizes the difference between the *mean* estimated currents and the *mean* measured ones.

3.3 Data flow diagrams

The following subsections describe the processing procedures that were applied to the measured pressures and currents to obtain a time series of pressure maps. Figure 4 summarizes the processing steps.

3.3.1 Dedrifting

Several bottom residual pressure records, H3 in year 1, and G2, H2, H3, I1 in year 2, appeared to have trends of about 0.1–0.2 decibar in one year. These records were dedrifted by fitting an exponential-plus-constant curves or straight lines to the residual pressure records by least squares method and subtracting these curves from the records. In addition, there was a slight offset between the two G2 records during the overlapping period of the two deployment years. This offset was removed, at least partly, by adding half the average difference (about 0.01 dbar) to the record for year 2 and subtracting the same amount from the record for year 1. Plots in Figure 5 and 6 show all the relevant PIES records before and after dedrifting.

3.3.2 Reference pressure levels

In order to use *residual* pressure records from PIES pressure measurements in making the *absolute* pressure maps (relative to an overall constant independent of time and space), we need to determine the reference levels for the residual pressure records. Although the residual pressure records themselves are resolved to 0.001 decibars, the directly measured reference levels for these records are only accurate to 1.5 decibar (page 11 in [3]) due to the

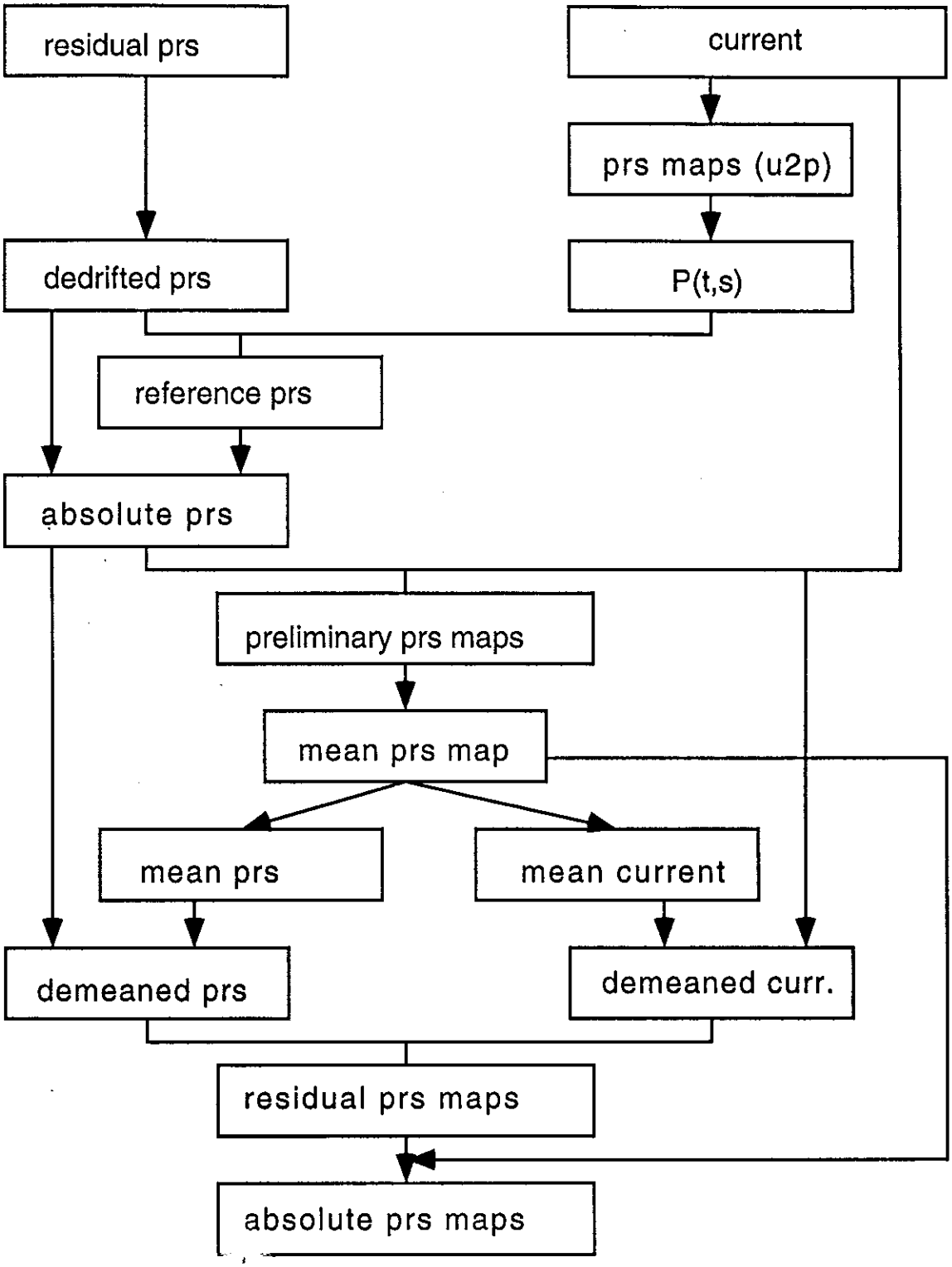

Figure 4: Data processing flowchart

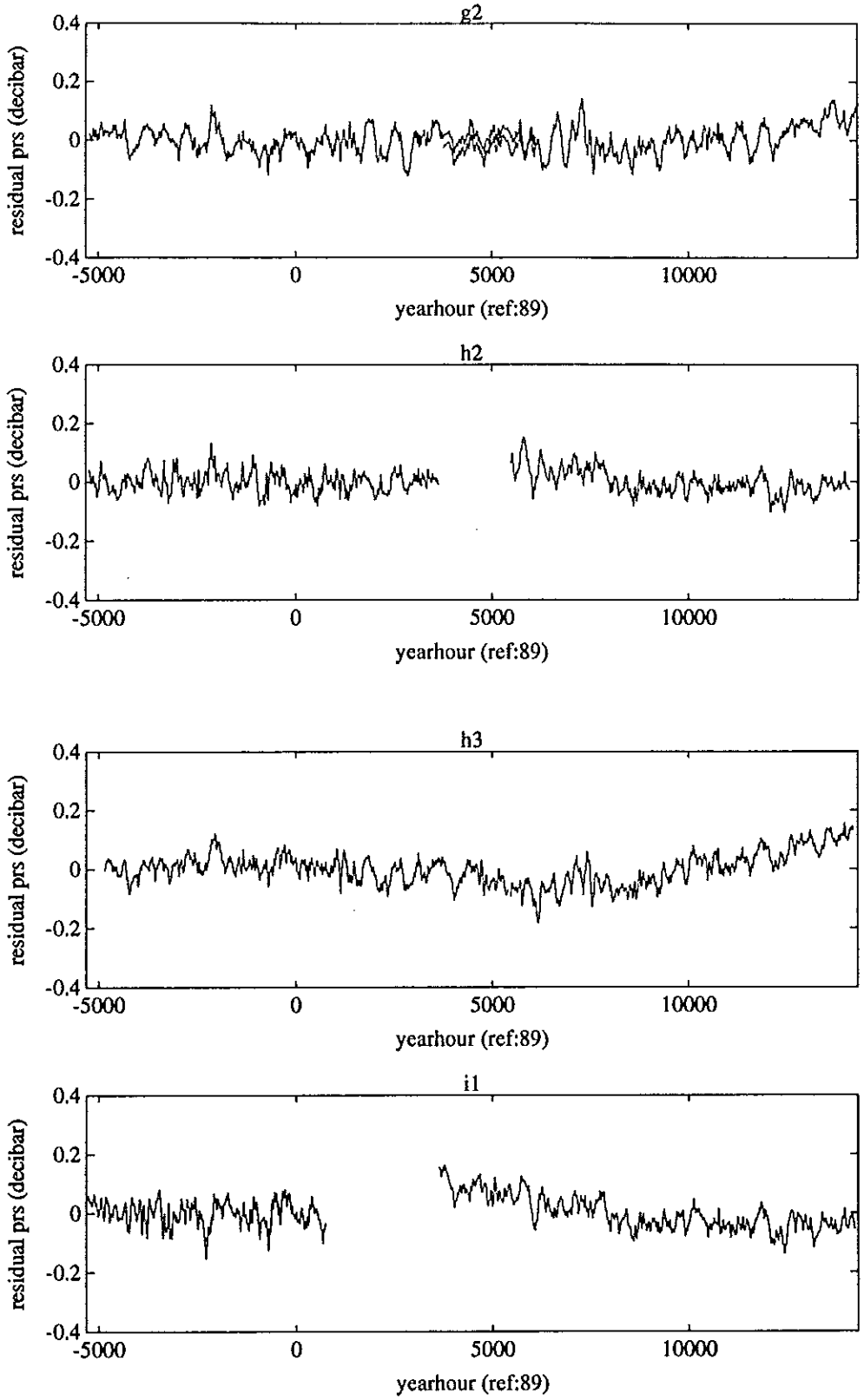

Figure 5: Some PIES records to be dedrifted.

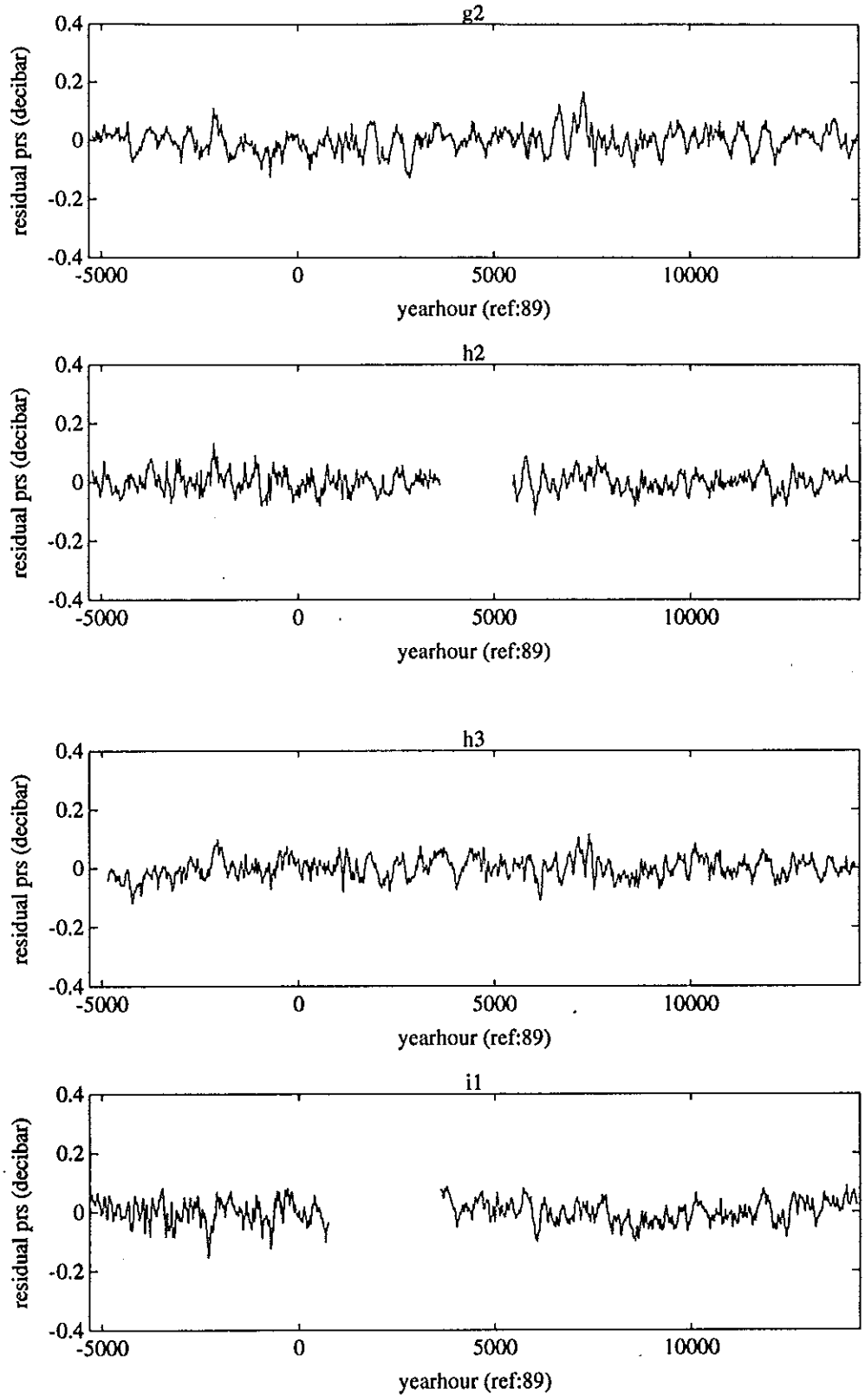

Figure 6: Dedrifted PIES records.

absolute calibration accuracy. This uncertainty is much larger than the standard deviations of these pressure records, which are less than 0.1 decibars. Therefore, we develop in this section a better way of determining these reference levels.

In essence, the mean pressure field mapped from current records was used as reference level for the PIES measured pressure records. The following scheme was used to ensure that the *mean* reference level calculated for a site has the correct average period consistent with measurement period of that site. In the first step, diagrammed at the top of Figure 4, objective analysis was used on the current measurements alone to map pressure fields ("u2p"). In particular, they were interpolated to the PIES instrument sites. Note, however, that while the pressure fields objectively mapped from (u,v) alone are spatially consistent, the reference pressures vary temporally from map to map. On the other hand, the bottom pressure record each has a temporally consistent reference but the reference can vary from site to site. Let $P(t,s)$ and $P_0(t)$ denote the interpolated pressure time series at site s from current meters and its unknown offset from the absolute pressure. Let $p(t,s)$ and $p_0(s)$ represent the measured residual pressure from PIES at site s and its unknown reference level. Since the absolute pressure at a given time and site is unique, we have

$$p(t,s) + p_0(s) = P(t,s) + P_0(t).$$

The unknown $P_0(t)$ may be eliminated by subtracting the above equation for any one site (we used G2) from the equations for all other sites, giving

$$\Delta_s p_0(s) = \Delta_s P(t,s) - \Delta_s p(t,s),$$

where Δ_s is the spatial difference operator with respect to G2; for example, $\Delta_s p(t,s) = p(t,s) - p(t,\mathrm{G2})$.

The left hand term, $\Delta_s p_0(s)$, of the above equation should *not* be a function of time. However, the right hand side, estimated from real data, varies with time due to errors (principally those in mapping $P(t,s)$ each day and from vertical shear changes in $p(t,s)$ above each PIES). In the light of this, the reference level for each site s on the left hand side of the above equation was calculated by the time average of the right hand side.

3.3.3 Multivariate mapping

The next step, midway down Figure 4, is to combine the absolute pressure records (Pb) and current measurement records (u,v) in mutivariate objective analysis, to obtain pres-

sure maps. With (Pb, u,v) inputs, mapping errors are reduced because pressure and its gradient are both specified. We designate these maps "preliminary" because of an iterative refinement that we describe next.

The objective analysis procedure requires that the input data have the mean removed first. Accordingly, we calculated the 26 month temporal mean pressure field and the corresponding geostrophic mean current field. The bottom of Figure 4 shows (a) we subtracted these mean fields from the absolute pressure records and the current records to get "demeaned" records, (b) re-ran the multivariate OA program on the demeaned records, and (c) restored the mean pressure field to obtain final absolute pressure maps.

4 Evaluation of the maps

This section assesses the precision of the objective pressure maps obtained in section 3 by comparing the time series derived from the maps and their statistics with those from the measurements.

4.1 Comparison of mapped fields with measured fields

In this section, the objectively estimated pressure time series at the PIES sites are compared with the "measured" absolute pressures as determined in section 3.3.2. Likewise, the objectively estimated current time series at the current meter sites are compared with the current measurements. The comparison plots are shown in Appendix C and the comparison statistics are tabulated in Tables 7, 8 and 9.

The comparison plots in Appendix C show good agreement between measured and mapped pressure and currents.

In Tables 7, p, p_{meas} and p_{oa} denote respectively the *true* (that is, error free) pressure, the PIES measured pressure and objectively mapped pressure. On most sites, the correlation coefficients ρ_p between p_{meas} and p_{oa} are above 90 percent. In carrying out the OA procedure, we assumed that the std(p) is a constant independent of sites. If we choose std(p) to be a typical value of 0.7 decibar, the OA estimated std($p_{oa} - p$) agree well with "measured" rms($p_{oa} - p_{meas}$). The magnitude of the difference $\bar{p}_{oa} - \bar{p}_{meas}$ is in most cases less than 10 percent of std(p_{meas}) as shown in the bias column in Tables 7. Note the bias is defined here as $\frac{\bar{p}_{oa}-\bar{p}_{meas}}{\text{std}(p_{meas})}$ instead of the more widely used $\frac{\bar{p}_{oa}-\bar{p}_{meas}}{\bar{p}_{meas}}$ because some $\bar{p}_{meas}$'s are effectively zero for the given averaging periods.

In Table 8 and 9, (u, v), (u_{meas}, v_{meas}) and (u_{oa}, v_{oa}) denote respectively the *true* (that is, error free) current, the measured current and objectively mapped current. the correlation coefficients between measured and mapped currents are all 90 percent or over. It appears, however, that the OA procedure 'smoothed' out some variance in small scale motion such that when std(u_{meas}) is large std(u_{oa}) tends to underestimate it and $\frac{\text{std}(u_{oa}-u)}{\text{std}(u)}$ tends to underestimate $\frac{\text{rms}(u_{oa}-u_{meas})}{\text{std}(u_{meas})}$.

4.2 Comparison of predicted fields with measured fields

In this section, we examine how well the percentage error predicted by OA procedure reflects the real one. To do this, we pick one pressure measurement site at a time and remove the

Table 7: Comparison between measured pressure and mapped pressure. (The pressure is in decibar unit and Len denotes record length in days)

Site	Len	$\bar{p}_{meas}$	$\bar{p}_{oa}$	std(p_{meas})	std(p_{oa})	bias	ρ_p	$\frac{\text{rms}(p_{oa}-p_{meas})}{\text{std}(p_{meas})}$	$\frac{\text{std}(p_{oa}-p)}{\text{std}(p)}$
y1g2	472	-0.01	-0.01	0.04	0.04	0.08	0.93	0.37	0.23
y1g3	365	-0.02	-0.02	0.04	0.04	-0.08	0.95	0.30	0.23
y1h2	369	0.01	0.01	0.03	0.03	-0.01	0.93	0.37	0.24
y1h3	427	-0.02	-0.02	0.04	0.03	-0.06	0.92	0.40	0.18
y1h4	424	-0.04	-0.04	0.04	0.04	-0.13	0.91	0.41	0.19
y1h5	430	-0.08	-0.08	0.08	0.06	-0.04	0.92	0.41	0.19
y1h6	374	-0.08	-0.07	0.06	0.05	-0.05	0.91	0.42	0.22
y1i1	250	0.00	0.00	0.04	0.03	0.05	0.73	0.69	0.21
y1i2	352	-0.03	-0.03	0.04	0.03	-0.02	0.84	0.54	0.22
y1i4	370	-0.08	-0.08	0.10	0.08	-0.04	0.95	0.35	0.20
y1i5	373	-0.06	-0.07	0.09	0.08	0.02	0.98	0.24	0.24
y2g2	438	0.01	0.01	0.04	0.04	-0.05	0.92	0.38	0.23
y2g3	445	0.02	0.02	0.05	0.05	0.03	0.98	0.23	0.24
y2h2	358	0.04	0.04	0.03	0.03	0.02	0.90	0.46	0.21
y2h3	362	0.01	0.01	0.03	0.03	0.03	0.87	0.49	0.18
y2h4	365	0.00	0.00	0.06	0.05	0.04	0.95	0.30	0.15
y2h5	366	-0.01	-0.02	0.09	0.09	0.08	0.99	0.16	0.18
y2h6	429	-0.03	-0.03	0.08	0.08	0.01	0.99	0.17	0.25
y2i1	441	0.03	0.03	0.04	0.03	0.05	0.90	0.43	0.21
y2i2	438	0.00	0.00	0.04	0.03	0.05	0.87	0.49	0.18
y2i3	428	-0.02	-0.02	0.08	0.07	0.00	0.97	0.26	0.17
y2i4	424	-0.04	-0.04	0.11	0.10	0.01	0.99	0.11	0.17
y2i5	429	-0.05	-0.05	0.10	0.09	0.00	0.99	0.17	0.23

Table 8: Comparison between measured currents and mapped currents (u component). (The current is in meter/sec. Len denotes record length in days, bias is defined as $\frac{\bar{u}_{oa}-\bar{u}_{meas}}{\mathrm{std}(u_{meas})}$ and ρ_u denotes correlation coefficient between u_{meas} and u_{oa}.)

Site	Len	$\bar{u}_{meas}$	$\bar{u}_{oa}$	std(u_{meas})	std(u_{oa})	bias	ρ_u	$\frac{\mathrm{rms}(u_{oa}-u_{meas})}{\mathrm{std}(u_{meas})}$	$\frac{\mathrm{std}(u_{oa}-u)}{\mathrm{std}(u)}$
y1g2	371	0.01	0.00	0.06	0.05	0.10	0.97	0.26	0.27
y1g3	137	-0.01	-0.02	0.05	0.05	0.14	0.96	0.28	0.26
y1h4	354	-0.06	-0.05	0.10	0.08	-0.04	0.96	0.32	0.23
y1h5	370	-0.03	-0.04	0.08	0.06	0.07	0.90	0.44	0.23
y1i2	352	-0.06	-0.06	0.09	0.08	0.01	0.96	0.30	0.26
y1i3	146	0.00	-0.01	0.09	0.07	0.09	0.92	0.40	0.22
y1i4	87	0.04	0.05	0.04	0.04	-0.36	0.93	0.38	0.23
y2g2	438	0.02	0.02	0.09	0.08	0.01	0.98	0.23	0.27
y2h2	805	-0.07	-0.07	0.08	0.06	-0.01	0.98	0.24	0.27
y2h3	437	-0.03	-0.03	0.10	0.08	0.05	0.94	0.37	0.23
y2h5	427	-0.03	-0.03	0.11	0.10	-0.02	0.97	0.26	0.22
y2h6	365	0.01	0.01	0.06	0.06	0.00	0.97	0.23	0.28
y2i1	806	-0.06	-0.06	0.08	0.07	0.00	0.97	0.26	0.28
y2i2	440	-0.05	-0.05	0.11	0.09	-0.01	0.95	0.33	0.23
y2i3	348	-0.04	-0.03	0.13	0.14	-0.05	0.97	0.24	0.21
y2i4	353	0.00	0.00	0.10	0.09	0.00	0.94	0.33	0.22
y2i5	805	0.04	0.04	0.10	0.10	0.01	0.99	0.16	0.28
y2m13	354	-0.01	-0.01	0.13	0.11	0.02	0.97	0.26	0.20

Table 9: Comparison between measured currents and mapped currents (v component). (See caption of Table 8 for notational convention)

Site	Len	$\bar{v}_{meas}$	$\bar{v}_{oa}$	std(v_{meas})	std(v_{oa})	bias	ρ_v	$\frac{\mathrm{rms}(v_{oa}-v_{meas})}{\mathrm{std}(v_{meas})}$	$\frac{\mathrm{std}(v_{oa}-v)}{\mathrm{std}(v)}$
y1g2	371	0.00	0.00	0.06	0.05	-0.01	0.97	0.25	0.27
y1g3	137	-0.04	-0.06	0.08	0.07	0.15	0.97	0.24	0.26
y1h4	354	-0.05	-0.05	0.08	0.07	-0.01	0.96	0.30	0.23
y1h5	370	-0.05	-0.05	0.10	0.10	0.05	0.97	0.26	0.23
y1i2	352	-0.01	-0.01	0.05	0.04	-0.02	0.95	0.40	0.26
y1i3	146	0.03	0.04	0.08	0.08	-0.12	0.97	0.25	0.25
y1i4	87	0.11	0.12	0.09	0.09	-0.09	0.98	0.19	0.25
y2g2	438	0.01	0.01	0.08	0.07	-0.01	0.98	0.25	0.28
y2h2	805	-0.01	-0.01	0.05	0.04	-0.06	0.93	0.39	0.26
y2h3	437	-0.01	-0.01	0.07	0.05	-0.03	0.91	0.45	0.21
y2h5	427	-0.05	-0.05	0.11	0.11	0.00	0.98	0.20	0.24
y2h6	365	-0.06	-0.05	0.09	0.09	-0.04	0.98	0.18	0.27
y2i1	806	-0.01	-0.01	0.05	0.04	-0.02	0.91	0.43	0.27
y2i2	440	-0.02	-0.02	0.06	0.04	0.00	0.91	0.42	0.25
y2i3	348	-0.05	-0.04	0.09	0.08	-0.06	0.94	0.33	0.22
y2i4	353	-0.03	-0.03	0.10	0.09	0.04	0.99	0.18	0.26
y2i5	805	0.04	0.04	0.12	0.12	0.00	0.99	0.13	0.28
y2m13	354	-0.04	-0.05	0.10	0.10	0.08	0.98	0.22	0.21

pressure measurement record on the site and run the OA procedure as if that pressure record did not exist. As a result, we obtain an interpolated pressure record and a predicted percentage error on the measurement site. Then we compare the observed pressure record with the interpolated one and calculate an observed percentage error. The results, along with other comparison statistics, are displayed in Table 10. Similar results for currents are shown in Table 11 and Table 12.

It may be worth pointing out that this is an extreme test since it leaves such a big hole in the array. Most places were surrounded by closer measurements than in such a case. The predicted errors (last column) in Tables 10, 11 and Table 12 tend to be smaller than the measured errors (second to the last column). Specifically, the discrepancy seems worst on array edges, less in the interior and least at site M13. So the fewer nearby measurements the worse discrepancy. This may be due to the approximate nature of the assumptions in section 3.1. There may be, however, another cause for the discrepancy. In the case of pressure estimate, this can be seen as follows. In estimating p_{oa} on a site, p_{meas} on the site was taken out. Thus the measurement error in p_{meas} should be uncorrelated to the mapping error in p_{oa}. Accordingly, we have

$$\frac{\mathrm{rms}(p_{oa}-p_{meas})}{\mathrm{std}(p_{meas})} = \frac{\mathrm{rms}(p_{oa}-p+p-p_{meas})}{\mathrm{std}(p_{meas})} \approx \frac{\mathrm{rms}(p_{oa}-p)}{\mathrm{std}(p_{meas})} + \frac{\mathrm{rms}(p-p_{meas})}{\mathrm{std}(p_{meas})}.$$

The first and second terms on the right can measure respectively the mapping and measurement errors. Therefore, $\frac{\mathrm{rms}(p_{oa}-p_{meas})}{\mathrm{std}(p_{meas})}$ may overestimate the mapping error in p_{oa} given by $\frac{\mathrm{std}(p_{oa}-p)}{\mathrm{std}(p)}$.

4.3 Checking pressure maps against measured currents

The geostrophic currents from pressure maps are compared with current measurements in section 5.2 by overlaying the observed current vectors on the daily pressure maps. Likewise, the *mean* geostrophic currents from pressure maps are compared with *mean* current measurements in section 5.1 by overlaying the *mean* observed current vectors on the *mean* pressure maps. From visiual inspection, the current vectors in these plots almost always run parallel with the pressure contour lines.

Table 10: Comparison between measured pressure and predicted pressure. (See caption of Table 7 for notational convention)

Site	Len	$\bar{p}_{meas}$	$\bar{p}_{oa}$	std(p_{meas})	std(p_{oa})	bias	ρ_p	$\frac{\text{rms}(p_{oa}-p_{meas})}{\text{std}(p_{meas})}$	$\frac{\text{std}(p_{oa}-p)}{\text{std}(p)}$
y1g2	472	-0.01	-0.01	0.04	0.04	-0.13	0.71	0.78	0.34
y1g3	365	-0.02	-0.01	0.04	0.04	0.15	0.78	0.64	0.34
y1h2	369	0.01	0.01	0.03	0.03	0.04	0.59	0.92	0.38
y1h3	427	-0.02	-0.02	0.04	0.03	0.08	0.81	0.59	0.22
y1h4	424	-0.04	-0.03	0.04	0.04	0.20	0.79	0.63	0.24
y1h5	430	-0.08	-0.08	0.08	0.06	0.06	0.78	0.63	0.26
y1h6	374	-0.08	-0.07	0.06	0.06	0.09	0.58	0.87	0.31
y1i1	250	0.00	0.00	0.04	0.04	-0.11	0.17	1.24	0.30
y1i2	352	-0.03	-0.03	0.04	0.04	0.08	0.47	0.96	0.31
y1i4	370	-0.08	-0.08	0.10	0.07	0.08	0.84	0.55	0.27
y1i5	373	-0.06	-0.06	0.09	0.06	0.01	0.86	0.54	0.36
y2g2	438	0.01	0.01	0.04	0.04	0.13	0.64	0.89	0.35
y2g3	445	0.02	0.01	0.05	0.05	-0.09	0.83	0.56	0.39
y2h2	358	0.04	0.04	0.03	0.04	-0.04	0.74	0.82	0.28
y2h3	362	0.01	0.01	0.03	0.03	-0.05	0.71	0.75	0.23
y2h4	365	0.00	0.00	0.06	0.05	-0.05	0.92	0.40	0.18
y2h5	366	-0.01	-0.02	0.09	0.09	-0.11	0.96	0.27	0.23
y2h6	429	-0.03	-0.04	0.08	0.07	-0.04	0.88	0.47	0.42
y2i1	441	0.03	0.03	0.04	0.04	-0.10	0.67	0.80	0.28
y2i2	438	0.00	0.00	0.04	0.04	-0.07	0.72	0.73	0.23
y2i3	428	-0.02	-0.02	0.08	0.07	-0.02	0.93	0.38	0.20
y2i4	424	-0.04	-0.04	0.11	0.10	-0.02	0.99	0.17	0.21
y2i5	429	-0.05	-0.05	0.10	0.09	-0.01	0.94	0.35	0.34

Table 11: Comparison between measured currents and predicted currents (u component). (See caption of Table 8 for notational convention)

Site	Len	$\bar{u}_{meas}$	$\bar{u}_{oa}$	std(u_{meas})	std(u_{oa})	bias	ρ_u	$\frac{\text{rms}(u_{oa}-u_{meas})}{\text{std}(u_{meas})}$	$\frac{\text{std}(u_{oa}-u)}{\text{std}(u)}$
y1g2	371	0.01	-0.01	0.06	0.05	-0.35	0.52	0.90	0.51
y1g3	137	-0.01	-0.03	0.05	0.05	-0.31	0.58	0.87	0.49
y1h4	354	-0.06	-0.05	0.10	0.07	0.10	0.76	0.65	0.32
y1h5	370	-0.03	-0.04	0.08	0.07	-0.09	0.46	0.98	0.34
y1i2	352	-0.06	-0.06	0.09	0.07	0.02	0.60	0.81	0.48
y1i3	146	0.00	-0.01	0.09	0.07	-0.13	0.63	0.80	0.31
y1i4	87	0.04	0.07	0.04	0.04	0.76	0.63	0.84	0.35
y2g2	438	0.02	0.01	0.09	0.07	-0.04	0.66	0.76	0.52
y2h2	805	-0.07	-0.06	0.08	0.05	0.09	0.48	0.91	0.56
y2h3	437	-0.03	-0.04	0.10	0.08	-0.13	0.63	0.78	0.34
y2h5	427	-0.03	-0.03	0.11	0.09	0.07	0.85	0.53	0.33
y2h6	365	0.01	0.00	0.06	0.08	-0.08	0.68	0.98	0.58
y2i1	806	-0.06	-0.07	0.08	0.06	-0.04	0.28	1.08	0.59
y2i2	440	-0.05	-0.05	0.11	0.09	0.04	0.72	0.71	0.34
y2i3	348	-0.04	-0.03	0.13	0.15	0.08	0.92	0.44	0.28
y2i4	353	0.00	0.00	0.10	0.09	0.00	0.77	0.66	0.32
y2i5	805	0.04	0.03	0.10	0.10	-0.04	0.76	0.68	0.59
y2m13	354	-0.01	-0.01	0.13	0.11	-0.03	0.90	0.43	0.26

Table 12: Comparison between measured currents and predicted currents (v component). (See caption of Table 8 for notational convention)

Site	Len	$\bar{v}_{meas}$	$\bar{v}_{oa}$	std(v_{meas})	std(v_{oa})	bias	ρ_v	$\frac{\text{rms}(v_{oa}-v_{meas})}{\text{std}(v_{meas})}$	$\frac{\text{std}(v_{oa}-v)}{\text{std}(v)}$
y1g2	371	0.00	0.00	0.06	0.06	-0.01	0.47	1.02	0.56
y1g3	137	-0.04	-0.08	0.08	0.07	-0.46	0.65	0.80	0.51
y1h4	354	-0.05	-0.05	0.08	0.06	0.04	0.78	0.63	0.34
y1h5	370	-0.05	-0.06	0.10	0.12	-0.15	0.87	0.58	0.34
y1i2	352	-0.01	-0.01	0.05	0.04	0.07	0.12	1.13	0.47
y1i3	146	0.03	0.06	0.08	0.09	0.33	0.86	0.61	0.40
y1i4	87	0.11	0.13	0.09	0.09	0.23	0.87	0.50	0.41
y2g2	438	0.01	0.01	0.08	0.07	0.04	0.29	1.10	0.60
y2h2	805	-0.01	0.00	0.05	0.05	0.22	0.17	1.24	0.50
y2h3	437	-0.01	-0.01	0.07	0.05	0.04	0.55	0.85	0.29
y2h5	427	-0.05	-0.05	0.11	0.10	0.03	0.87	0.49	0.38
y2h6	365	-0.06	-0.04	0.09	0.11	0.16	0.84	0.67	0.54
y2i1	806	-0.01	0.00	0.05	0.06	0.10	0.02	1.56	0.52
y2i2	440	-0.02	-0.01	0.06	0.05	0.03	0.31	1.11	0.42
y2i3	348	-0.05	-0.04	0.09	0.08	0.12	0.76	0.66	0.31
y2i4	353	-0.03	-0.04	0.10	0.08	-0.12	0.86	0.52	0.43
y2i5	805	0.04	0.04	0.12	0.11	0.01	0.80	0.60	0.58
y2m13	354	-0.04	-0.05	0.10	0.10	-0.14	0.93	0.39	0.27

5 Bottom Pressure Maps

This section displays the mean and daily pressure maps.

5.1 Mean pressure maps

Figure 7 shows mean bottom pressure maps with measured (solid line vectors) and mapped (dash line vectors) mean currents. Contour levels are in decibars. The scale of the currents is 3 kilometer in the maps corresponding to 1 centimeter per second. The mean is taken over the period from June 16, 1988 through May 24, 1989 for year 1, and from August 29, 1989 through August 7, 1990 for year 2. Both pressure and current are averaged over same period. Sites with measured pressure and current records contributing to the maps are respectively indicated by o's and x's. However, mean current vectors are not shown on three current measurement sites in year 1 because the measurements spanned only part of the averaging period shown. A description of the coordinate system is contained in section 5.2.

Figure 7: Mean bottom pressure maps with measured (solid line vectors) and mapped (dash line vectors) mean currents.

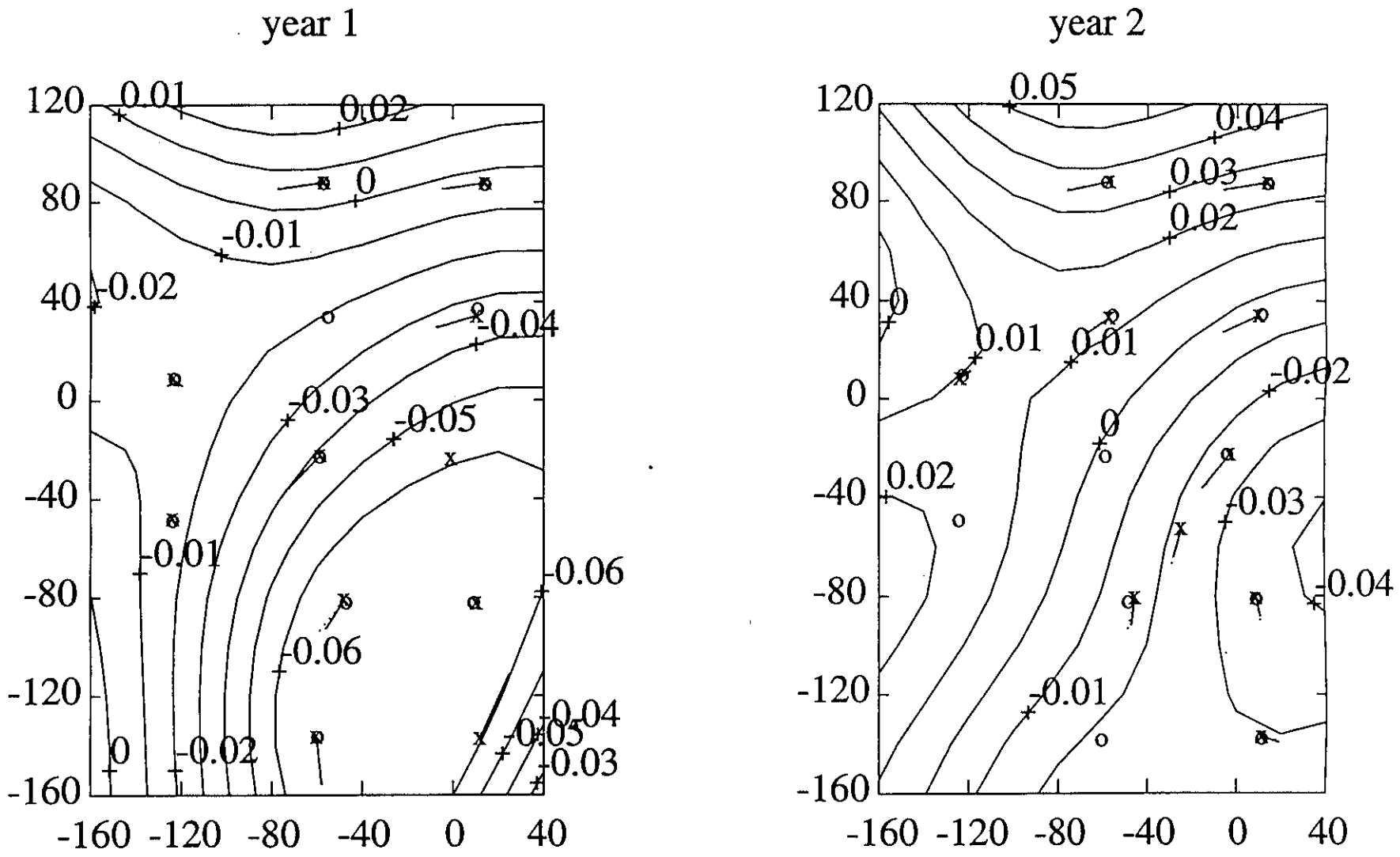

5.2 Daily pressure maps overlaid with current measurements

Bottom pressure maps from June 13, 1988 through August 7, 1990 are shown at daily interval in this section. The original maps were produced at six hour interval but only the ones at 1200 UT are displayed.

The overall format of the pressure maps is designed to facilitate comparison with the thermocline depth maps in the Central Array for the same time period [8]. To this end, the border of the thermocline depth maps in [8] is shown here with each pressure map. The region of the pressure maps corresponds to the boxed area in Figure 1. The latitude and longitude of the four corners of the box are listed in Table 1. The coordinate system used here is the same as that used for the thermocline depth maps in [8]. The origin is located at 38°N, 68°W. The scaling factors converting latitude and longitude to kilometers are 111 km per degree latitude and 82.263 km per degree longitude. The grid is then rotated 15° so that the horizontal axis is directed 075°T and vertical axis 345°T.

Shown in each map are the bottom pressure contours, percentage error contours, observed current vectors, current meter mooring positions and PIES sites. The pressure field is contoured at 0.015 decibar intervals. The negative and positive contour lines are denoted respectively by dashed and solid lines to tell troughs from crests. The estimated errors are represented as percentage of the standard deviation of the pressure field, which is 0.6 decibar on average. Errors are contoured at 3% interval with those over 48% shown by solid contours and those between 30% and 48% by dashed contours. Errors lower than 30% are not contoured. The current vectors are shown by solid lines with 3 kilometer in the maps corresponding to 1 centimeter per second. Small squares and '+' marks denote respectively current meter positions and PIES sites.

Figure 8: Daily pressure maps overlaid with current measurements (pages 33 — 163). See paragraphs above for description.

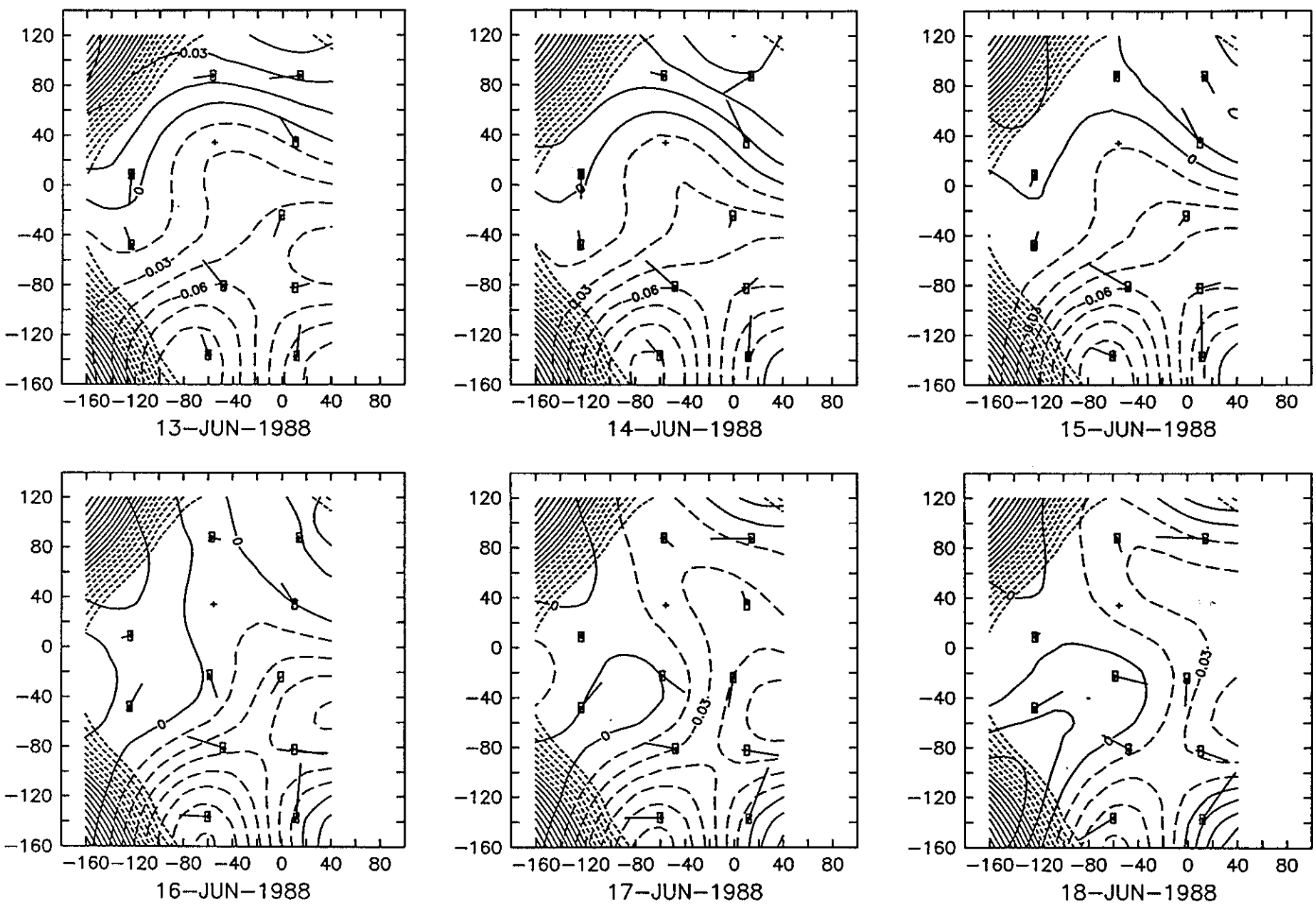
13–JUN–1988
14–JUN–1988
15–JUN–1988
16–JUN–1988
17–JUN–1988
18–JUN–1988
120
80
40
0
−40
−80
−120
−160
−160 −120 −80 −40 0 40 80
0.03
0.06
0

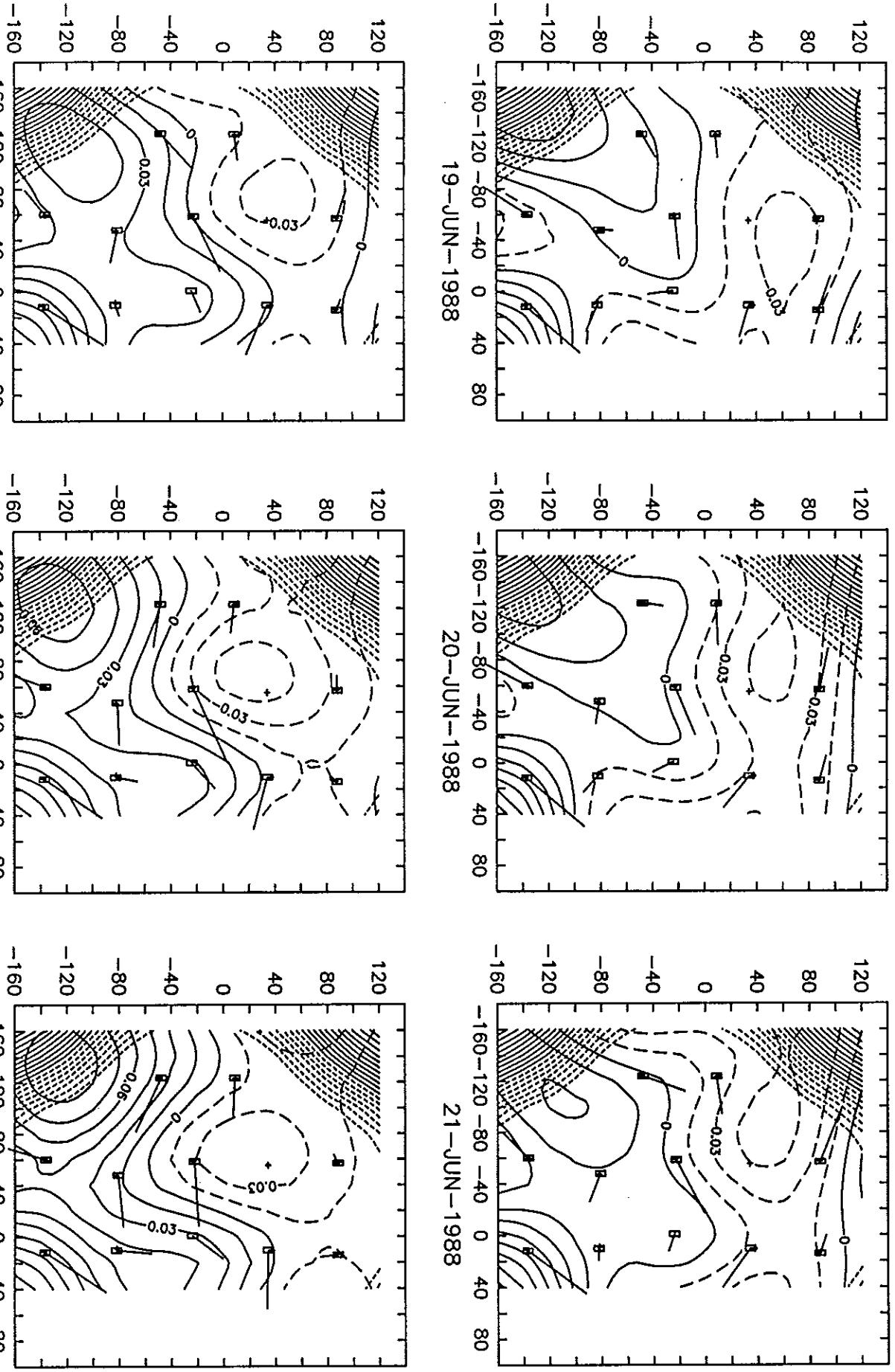
19-JUN-1988
20-JUN-1988
21-JUN-1988
22-JUN-1988
23-JUN-1988
24-JUN-1988

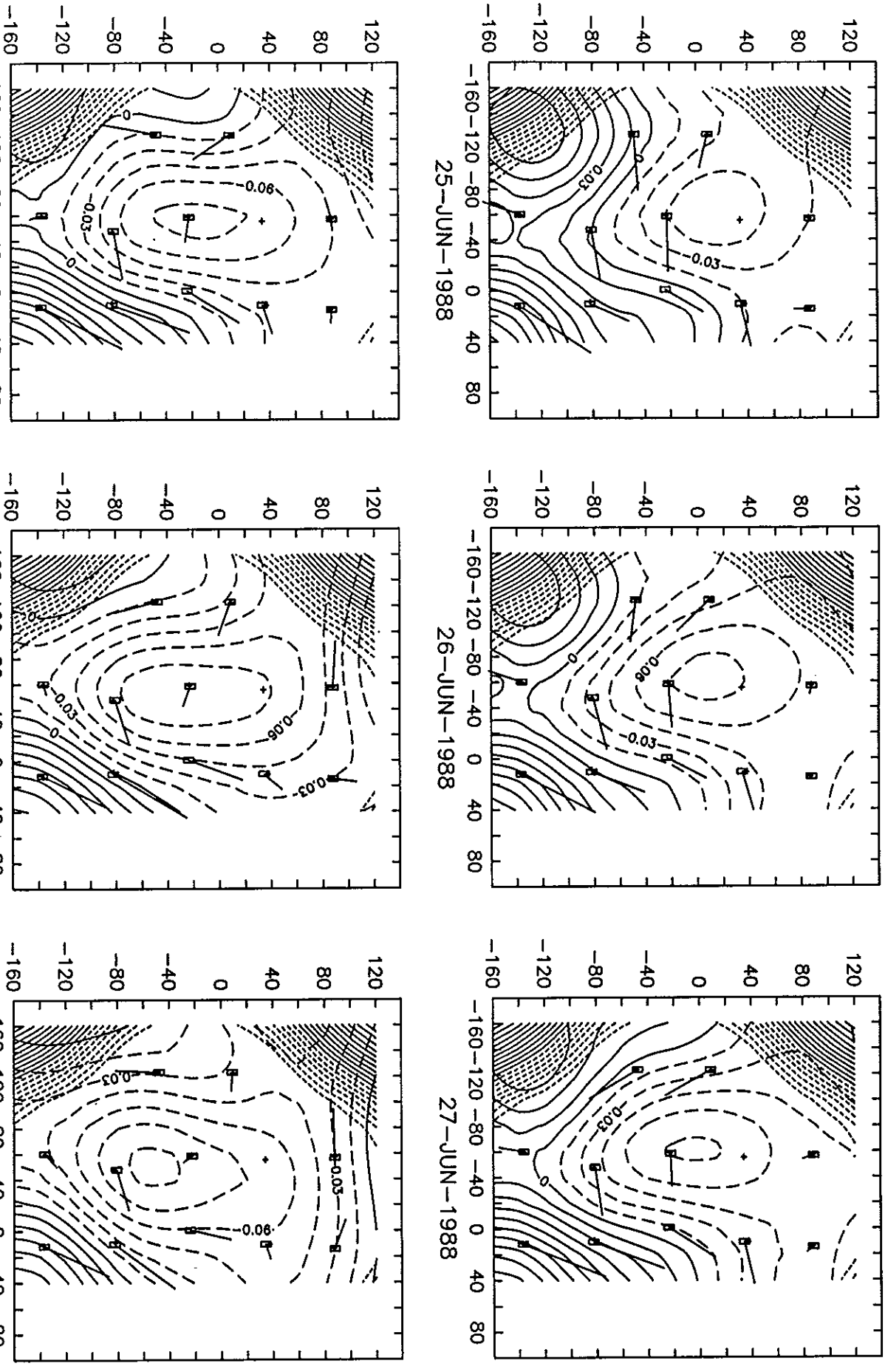
25-JUN-1988
26-JUN-1988
27-JUN-1988
28-JUN-1988
29-JUN-1988
30-JUN-1988

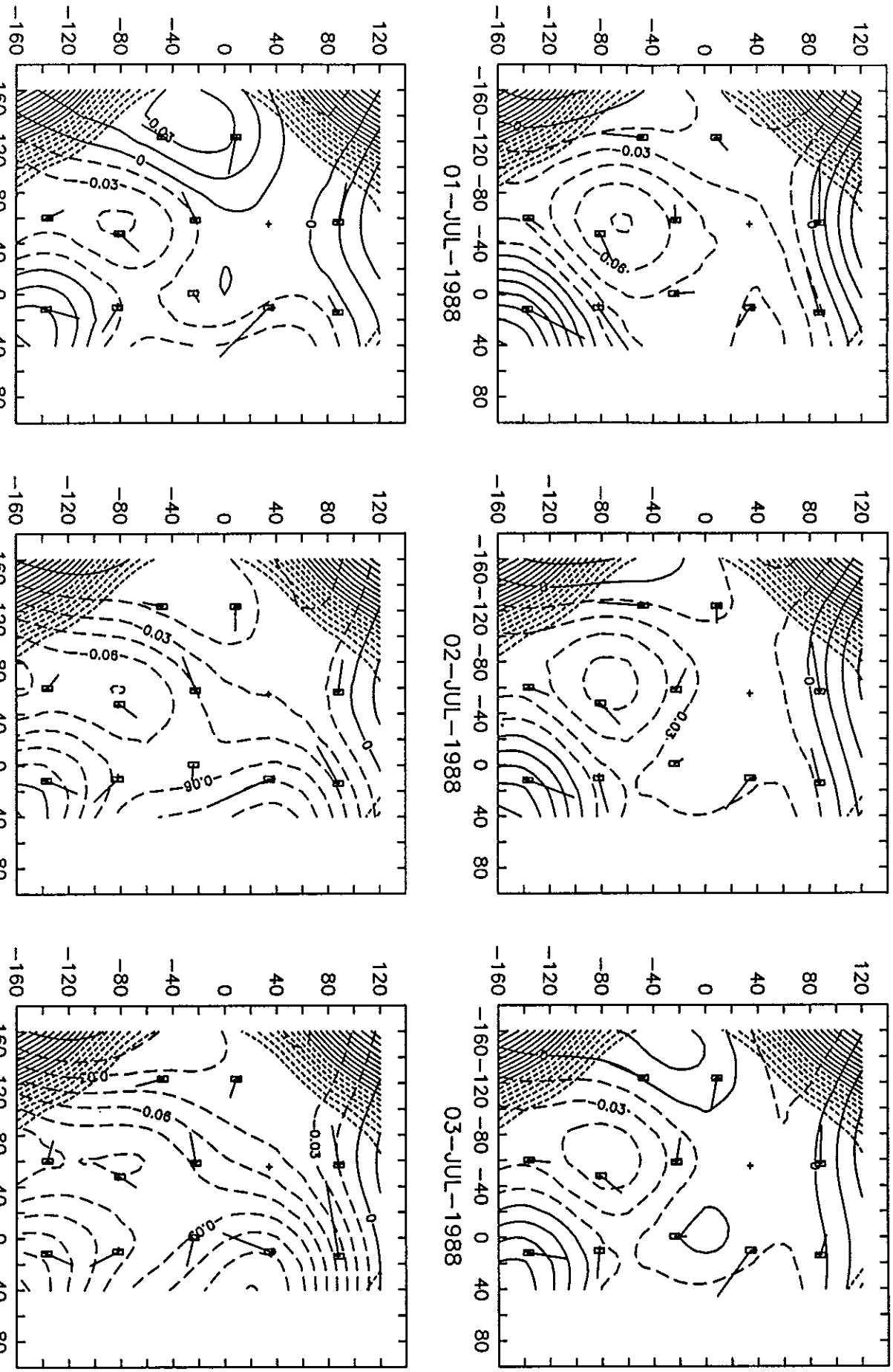
01-JUL-1988
02-JUL-1988
03-JUL-1988
04-JUL-1988
05-JUL-1988
06-JUL-1988

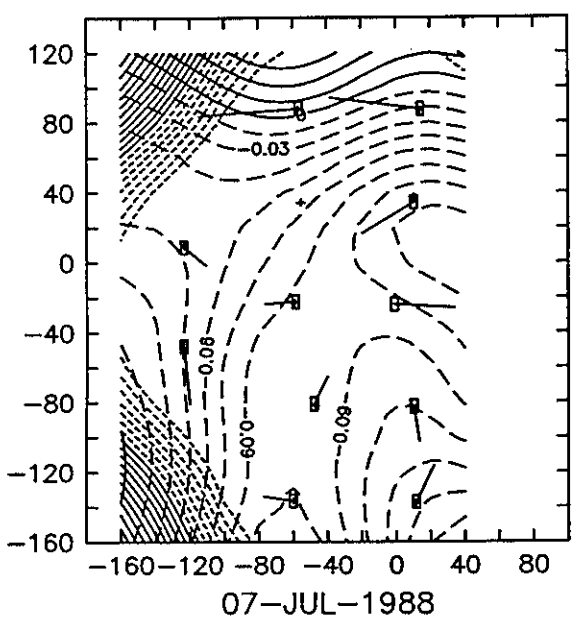
120
80
40
0
−40
−80
−120
−160
−160 −120 −80 −40 0 40 80
07−JUL−1988

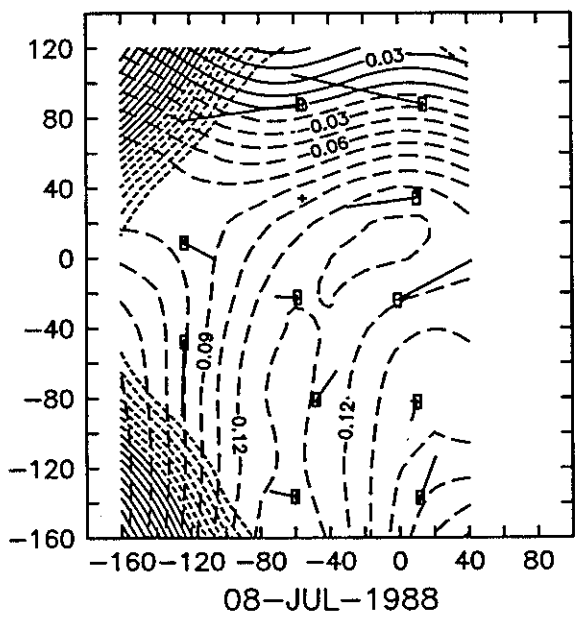
120
80
40
0
−40
−80
−120
−160
−160 −120 −80 −40 0 40 80
08−JUL−1988

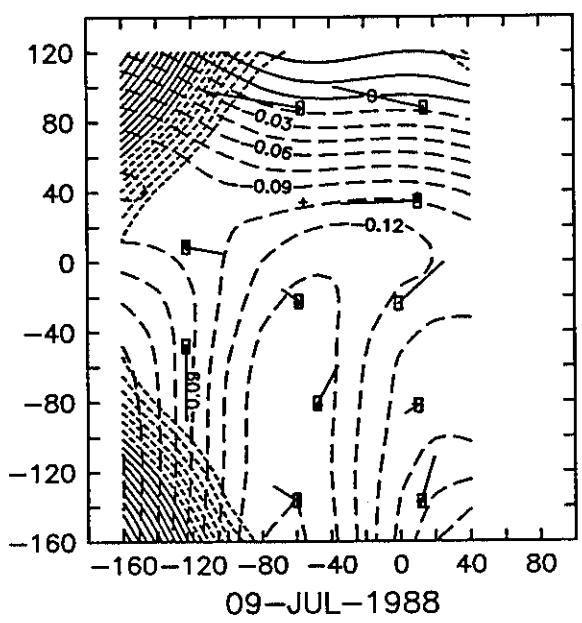
120
80
40
0
−40
−80
−120
−160
−160 −120 −80 −40 0 40 80
09−JUL−1988

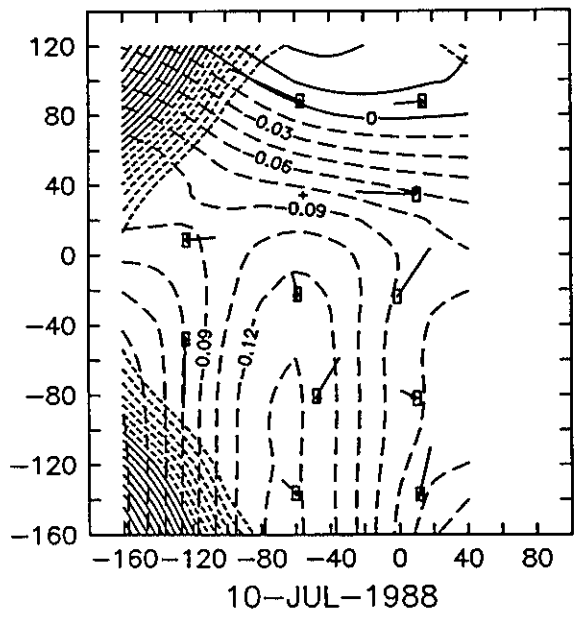
120
80
40
0
−40
−80
−120
−160
−160 −120 −80 −40 0 40 80
10−JUL−1988

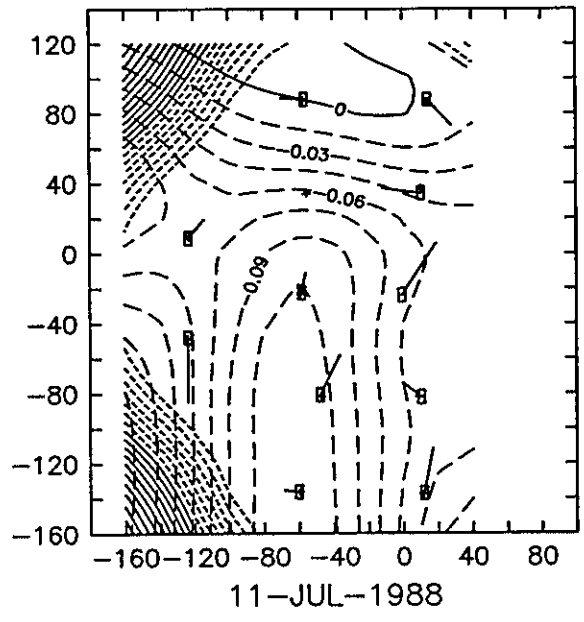
120
80
40
0
−40
−80
−120
−160
−160 −120 −80 −40 0 40 80
11−JUL−1988

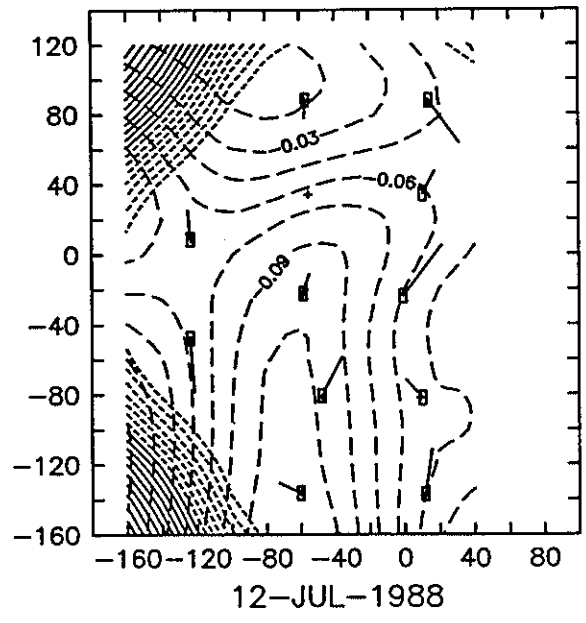
120
80
40
0
−40
−80
−120
−160
−160 −120 −80 −40 0 40 80
12−JUL−1988

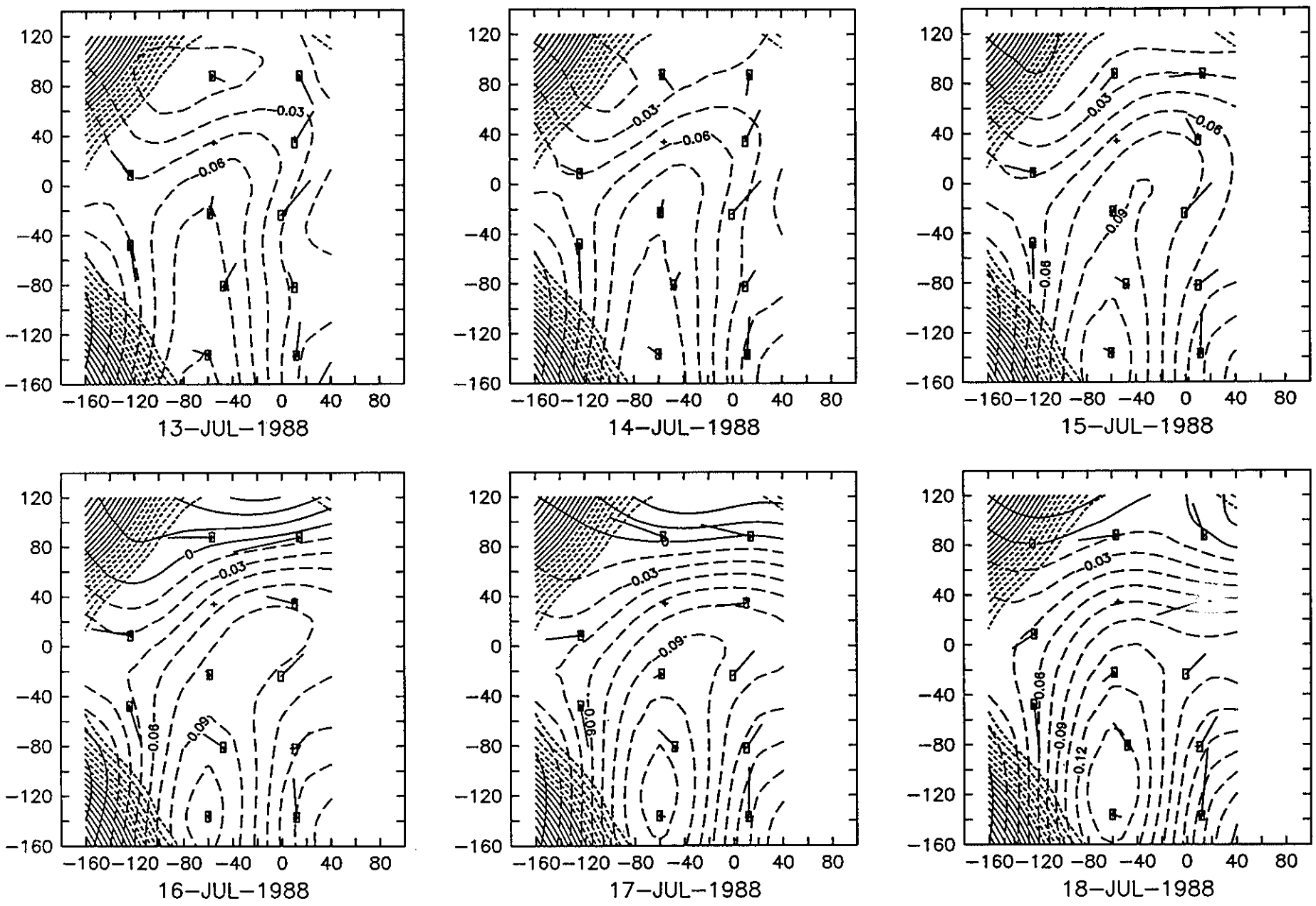
13-JUL-1988
14-JUL-1988
15-JUL-1988
16-JUL-1988
17-JUL-1988
18-JUL-1988

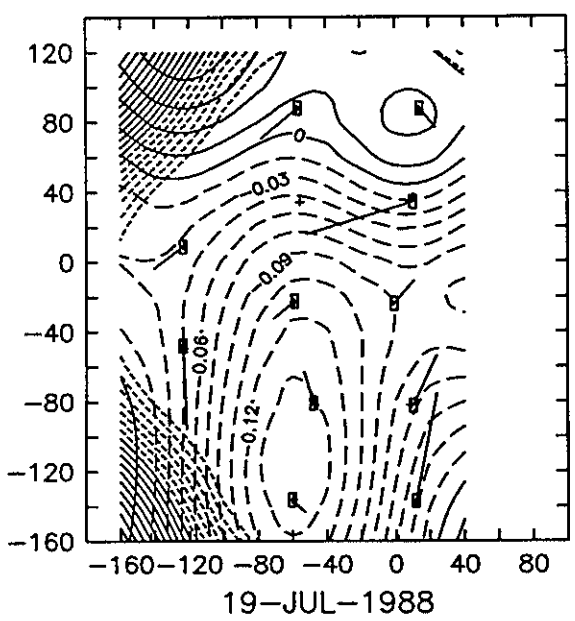
120
80
40
0
−40
−80
−120
−160
−160 −120 −80 −40 0 40 80
0
0.03
0.06
0.09
0.12
19−JUL−1988

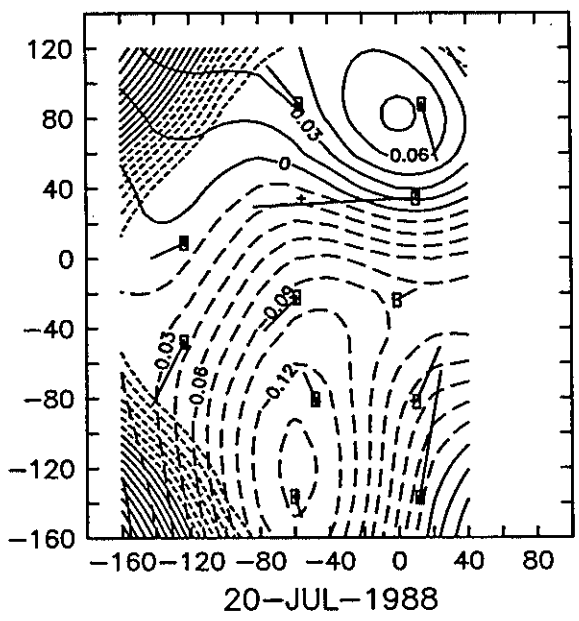
120
80
40
0
−40
−80
−120
−160
−160 −120 −80 −40 0 40 80
0
0.03
0.06
0.09
0.12
20−JUL−1988

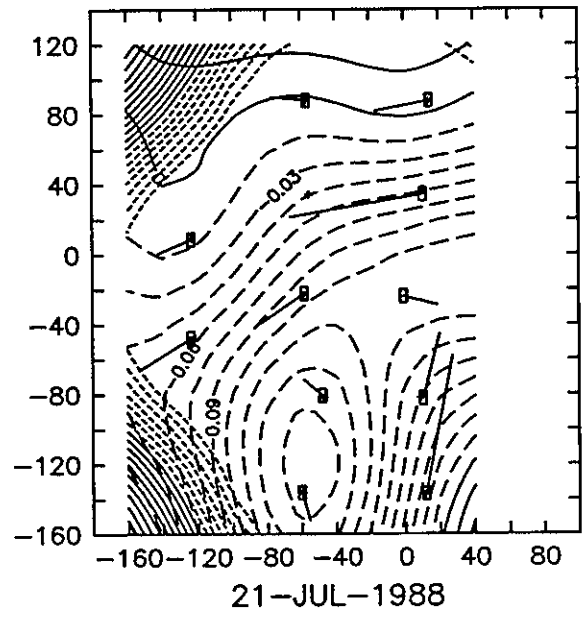
120
80
40
0
−40
−80
−120
−160
−160 −120 −80 −40 0 40 80
0.03
0.06
0.09
21−JUL−1988

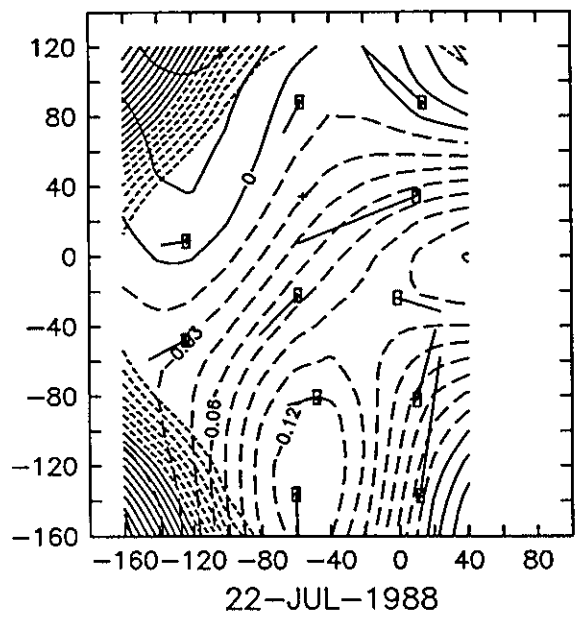
120
80
40
0
−40
−80
−120
−160
−160 −120 −80 −40 0 40 80
0
0.03
0.06
0.12
22−JUL−1988

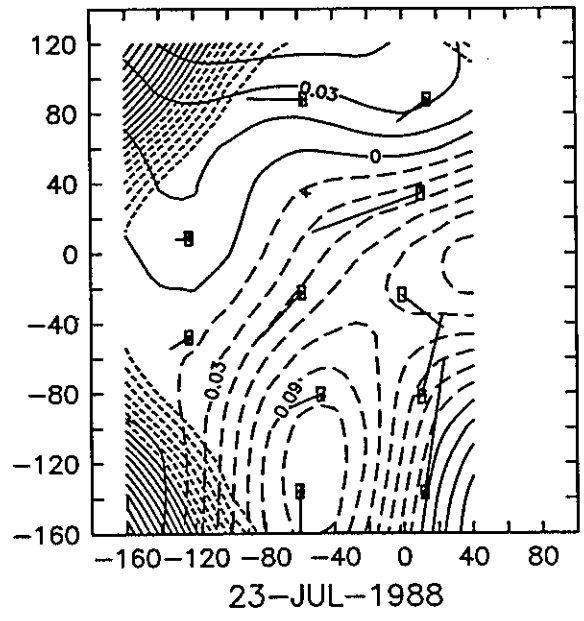
120
80
40
0
−40
−80
−120
−160
−160 −120 −80 −40 0 40 80
0.03
0
0.03
0.09
23−JUL−1988

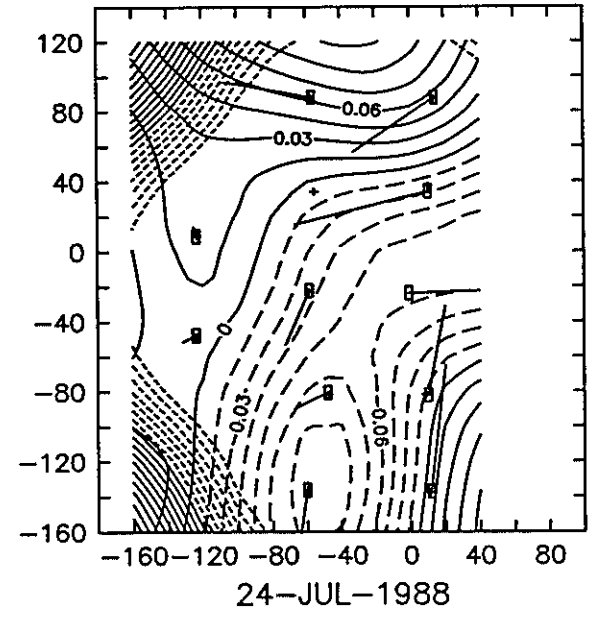
120
80
40
0
−40
−80
−120
−160
−160 −120 −80 −40 0 40 80
0.06
0.03
0
0.03
0.06
24−JUL−1988

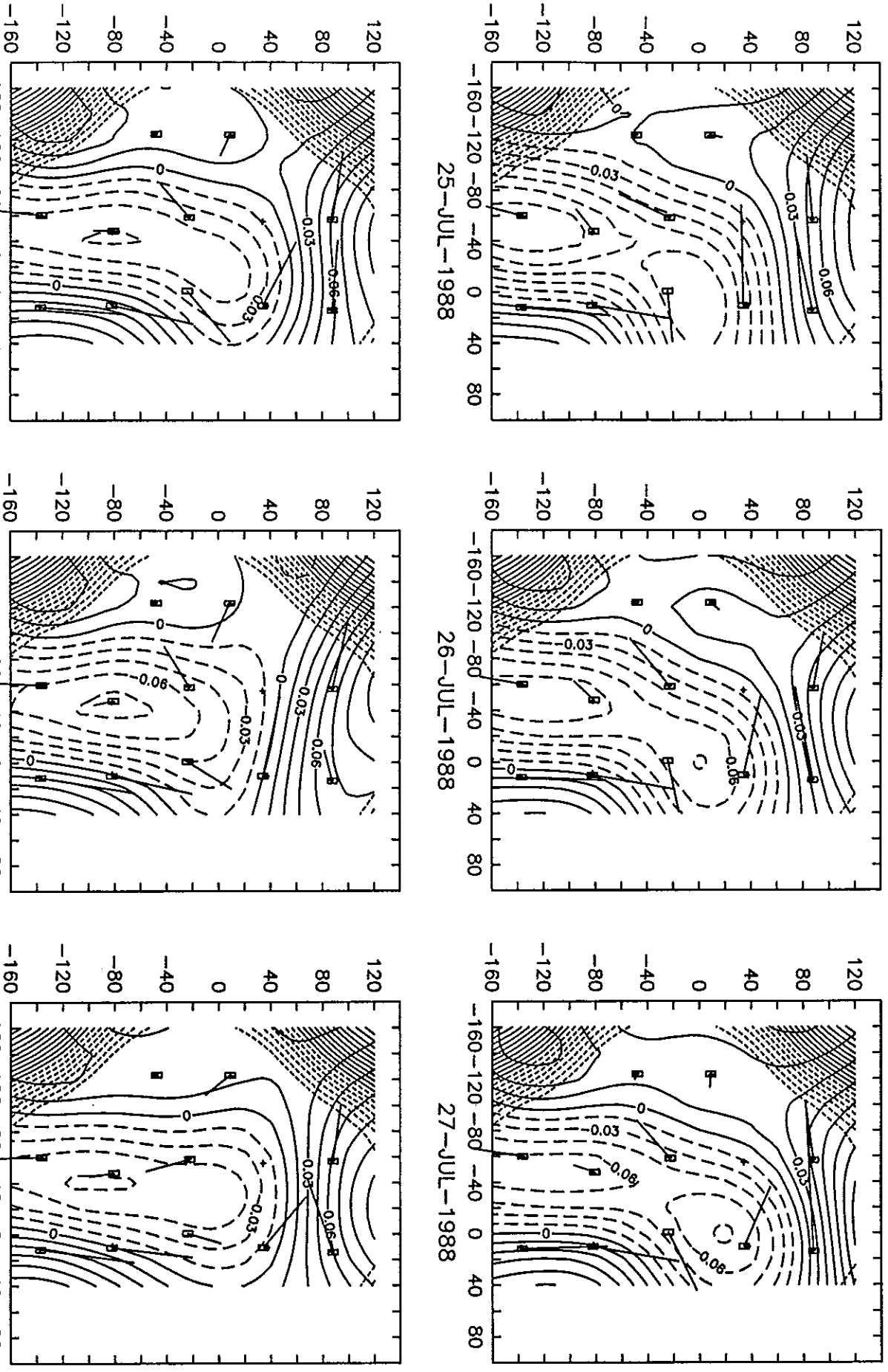
25-JUL-1988
26-JUL-1988
27-JUL-1988
28-JUL-1988
29-JUL-1988
30-JUL-1988

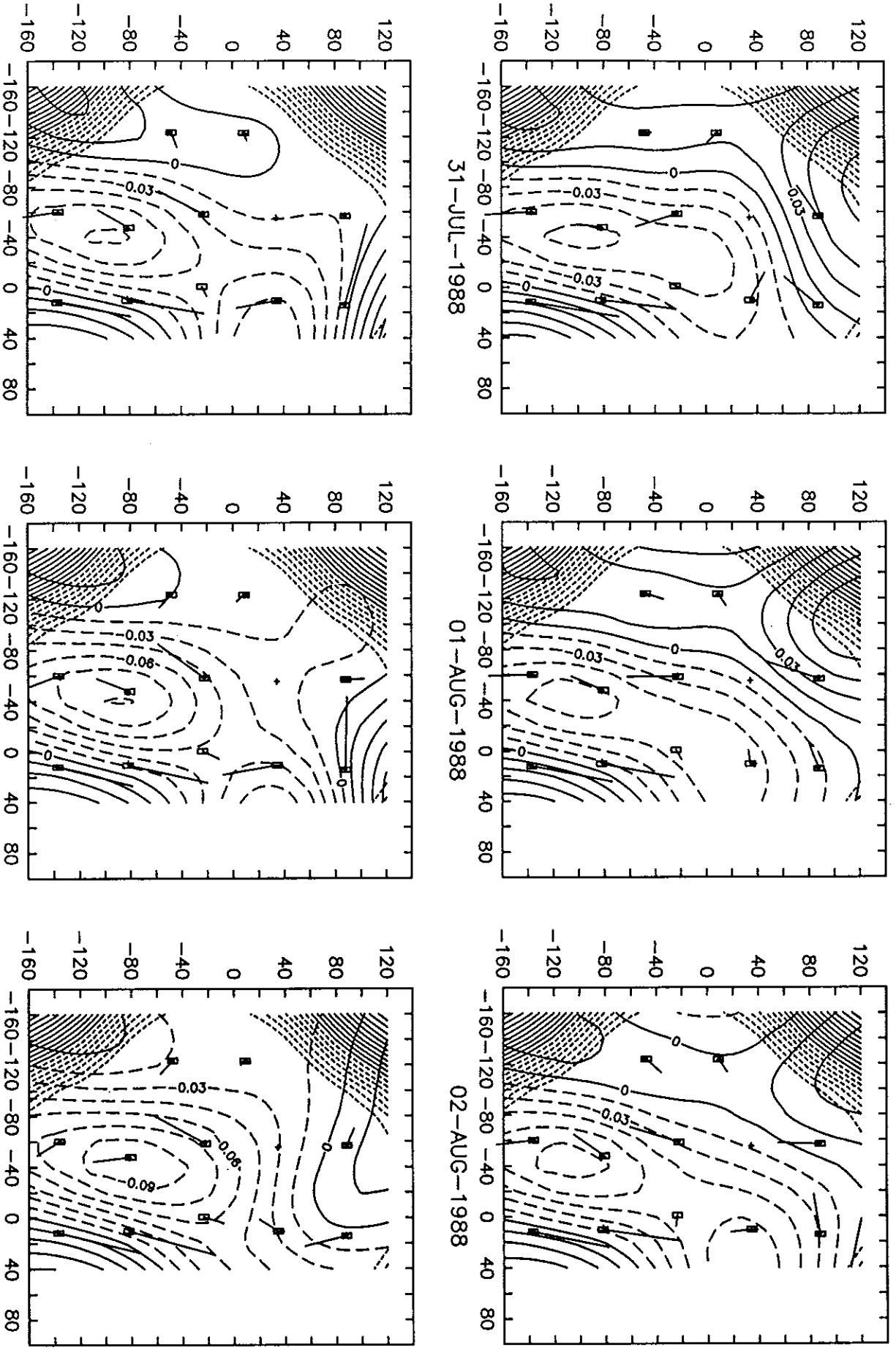
31-JUL-1988
01-AUG-1988
02-AUG-1988
03-AUG-1988
04-AUG-1988
05-AUG-1988

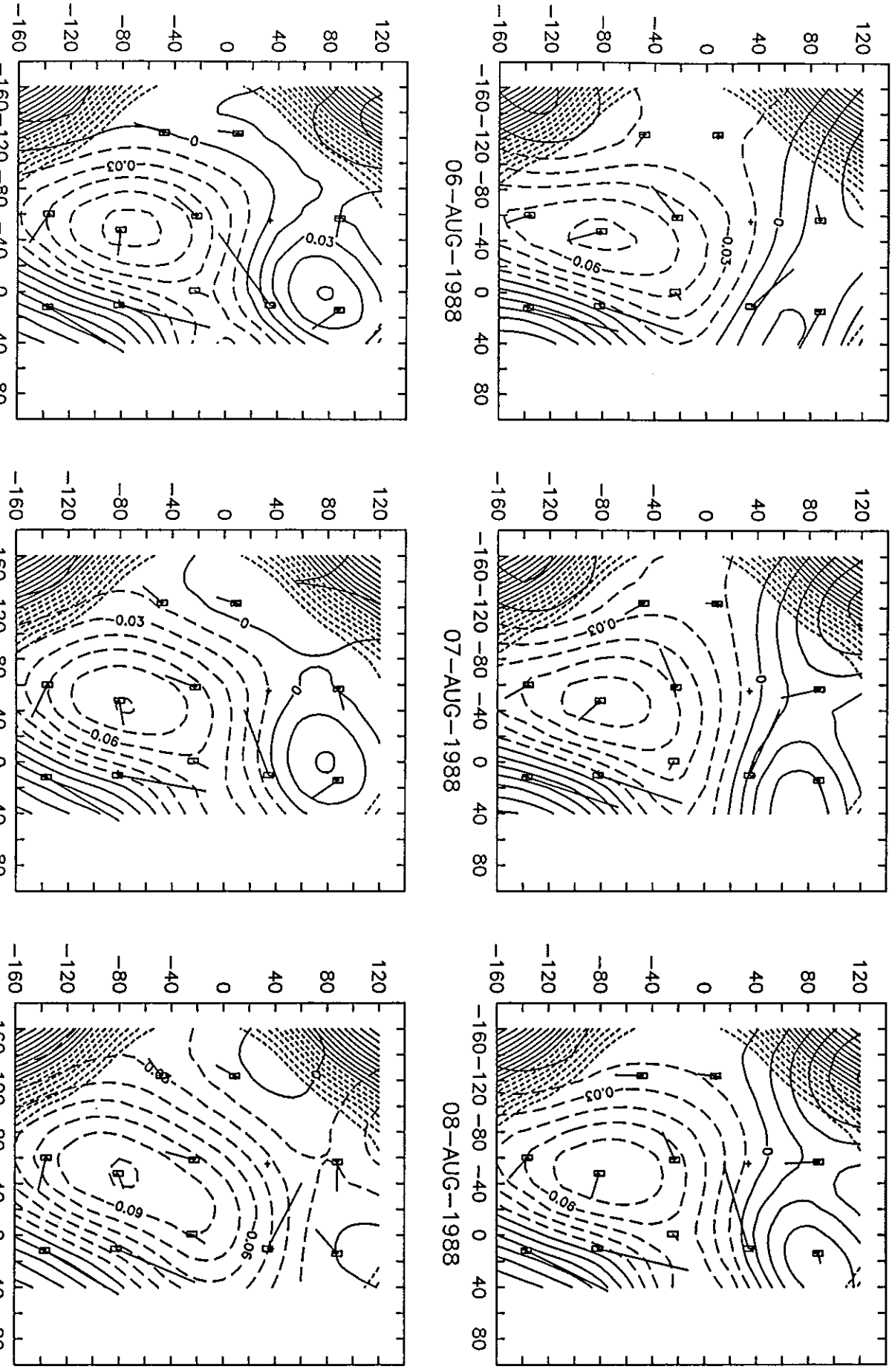
06-AUG-1988
07-AUG-1988
08-AUG-1988
09-AUG-1988
10-AUG-1988
11-AUG-1988

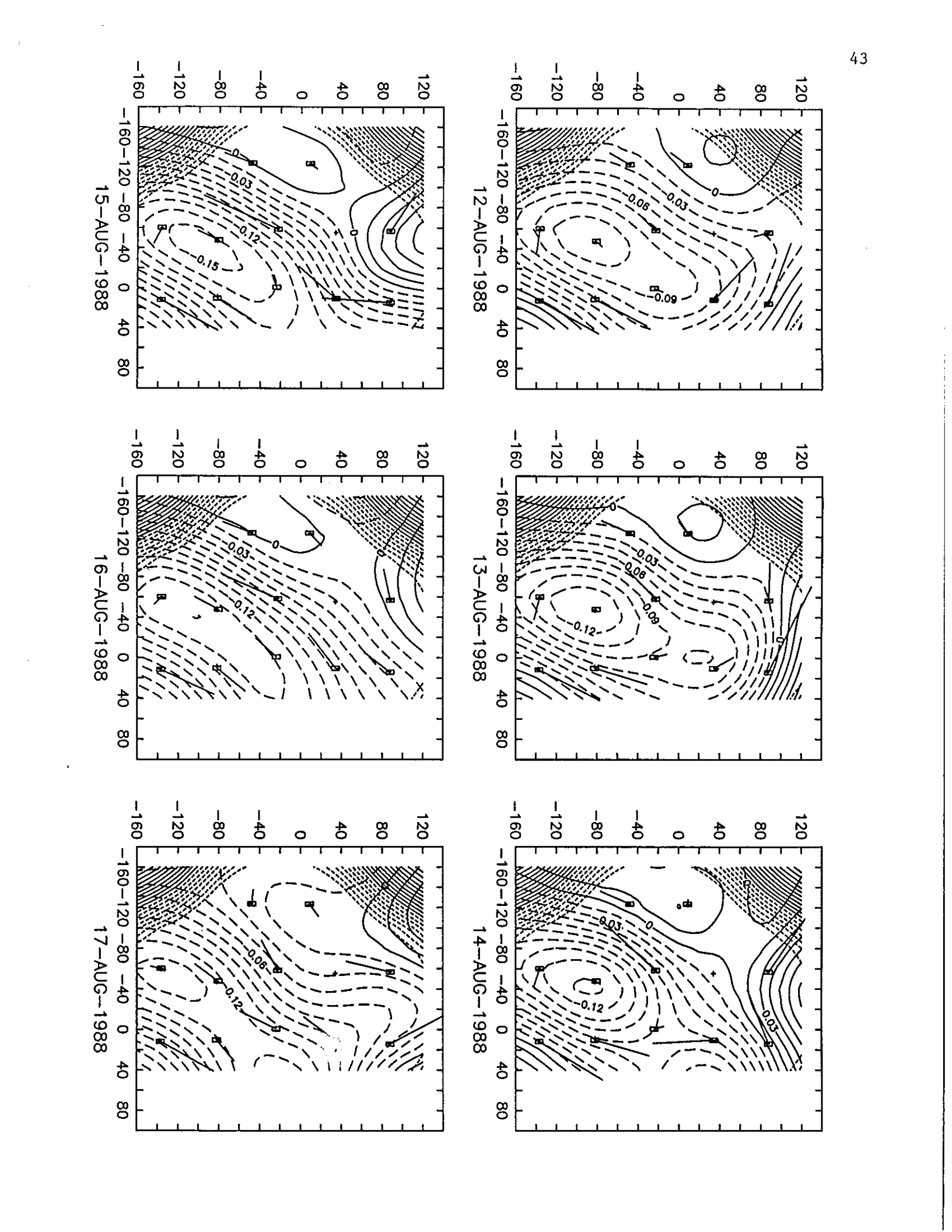
12-AUG-1988
13-AUG-1988
14-AUG-1988
15-AUG-1988
16-AUG-1988
17-AUG-1988

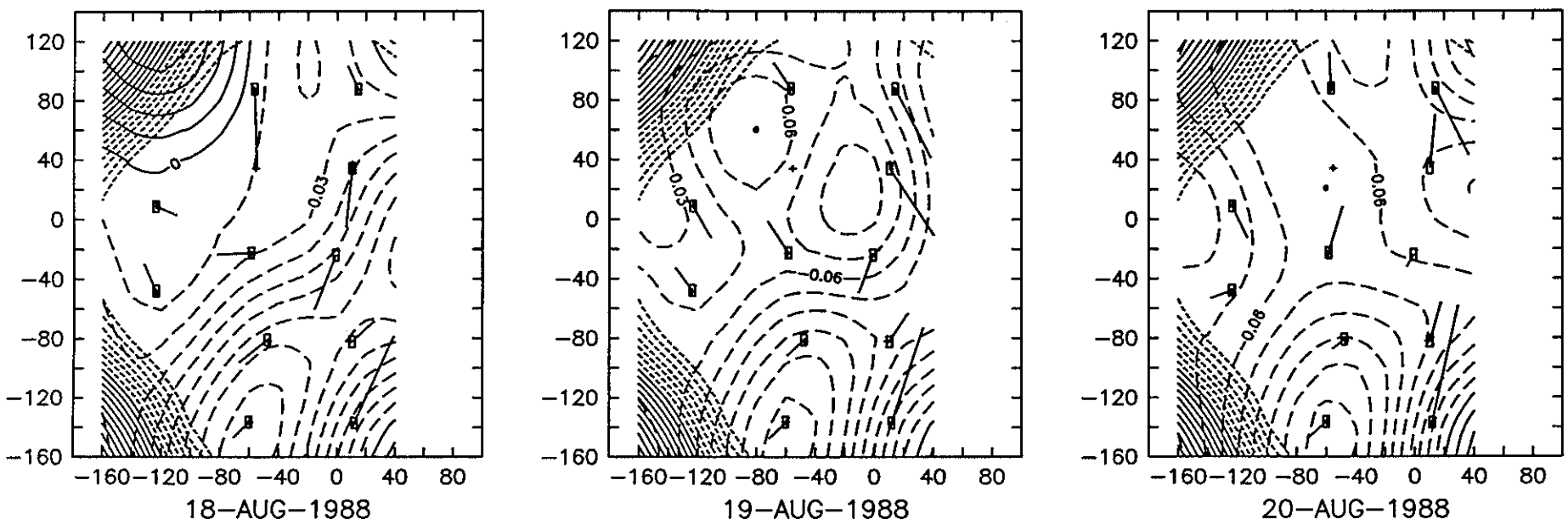
120
80
40
0
−40
−80
−120
−160
−160 −120 −80 −40 0 40 80
18−AUG−1988
19−AUG−1988
20−AUG−1988
21−AUG−1988
22−AUG−1988
23−AUG−1988

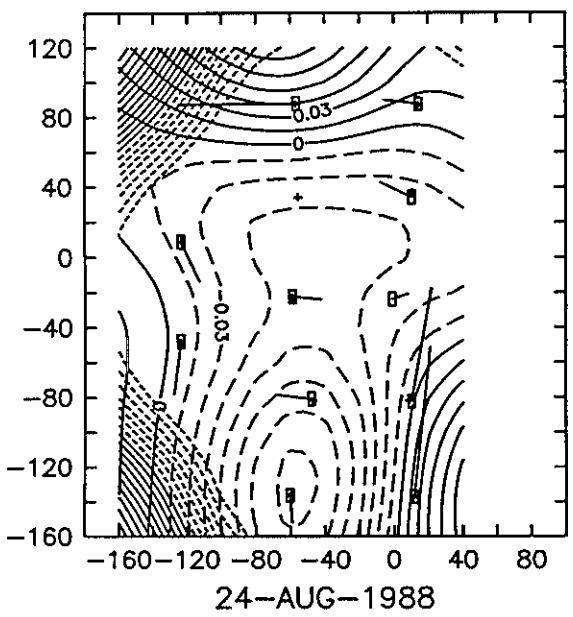
120
80
40
0
−40
−80
−120
−160
−160 −120 −80 −40 0 40 80
0.03
0
−0.03
24−AUG−1988

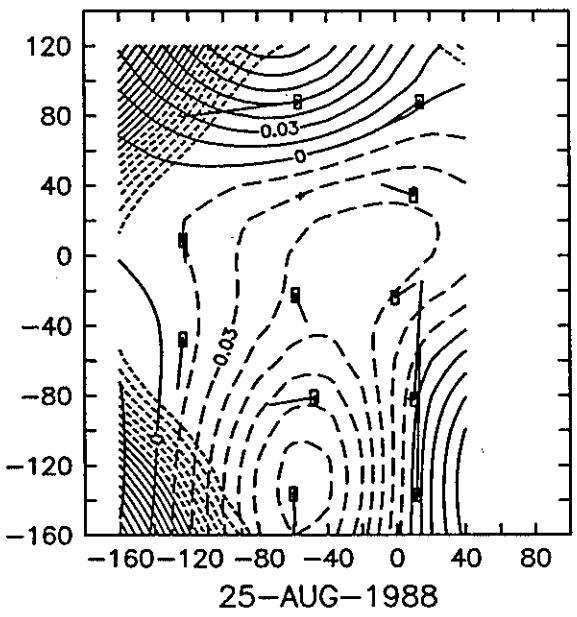
120
80
40
0
−40
−80
−120
−160
−160 −120 −80 −40 0 40 80
0.03
0
−0.03
25−AUG−1988

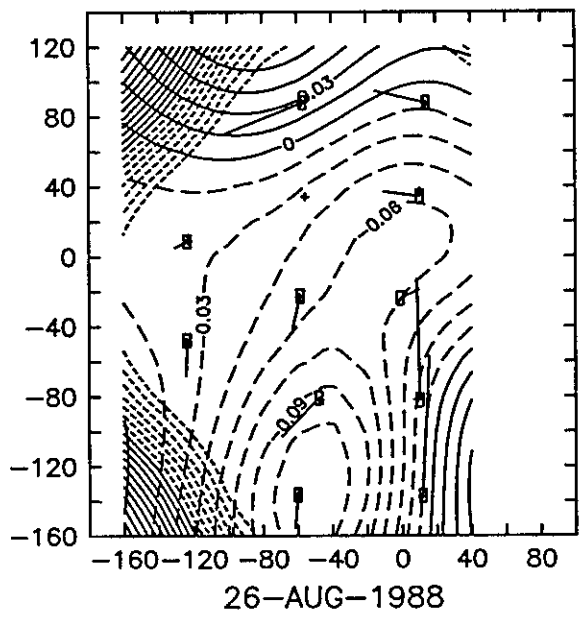
120
80
40
0
−40
−80
−120
−160
−160 −120 −80 −40 0 40 80
0.03
0
−0.03
0.06
0.09
26−AUG−1988

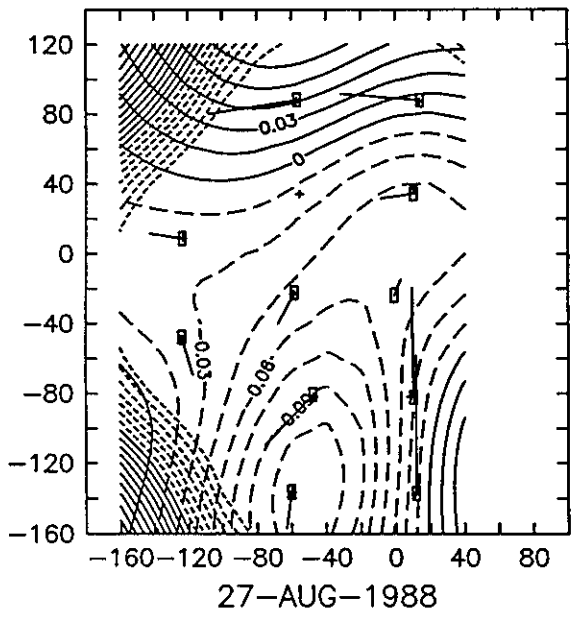
120
80
40
0
−40
−80
−120
−160
−160 −120 −80 −40 0 40 80
0.03
0
−0.03
0.06
0.09
27−AUG−1988

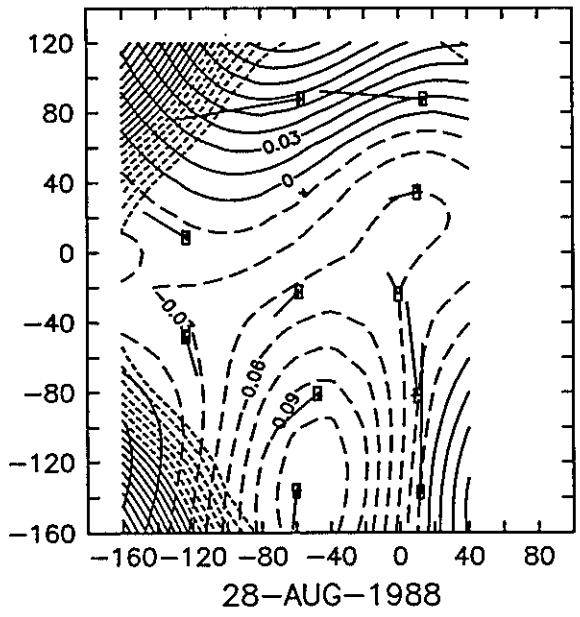
120
80
40
0
−40
−80
−120
−160
−160 −120 −80 −40 0 40 80
0.03
0
−0.03
0.06
0.09
28−AUG−1988

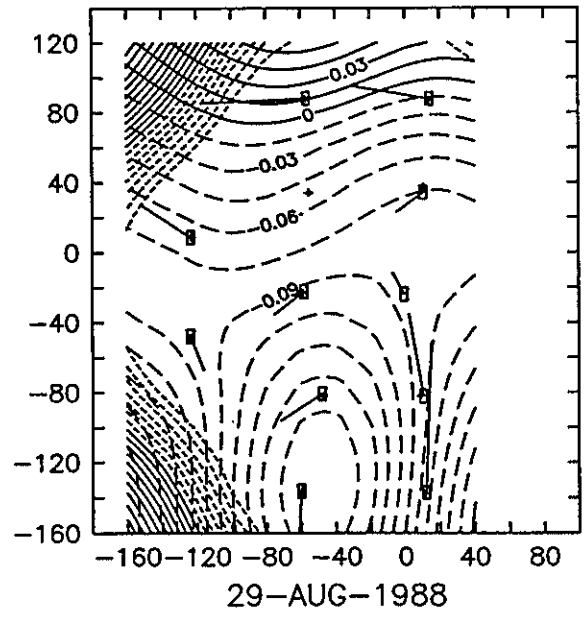
120
80
40
0
−40
−80
−120
−160
−160 −120 −80 −40 0 40 80
0.03
0
−0.03
0.06
0.09
29−AUG−1988

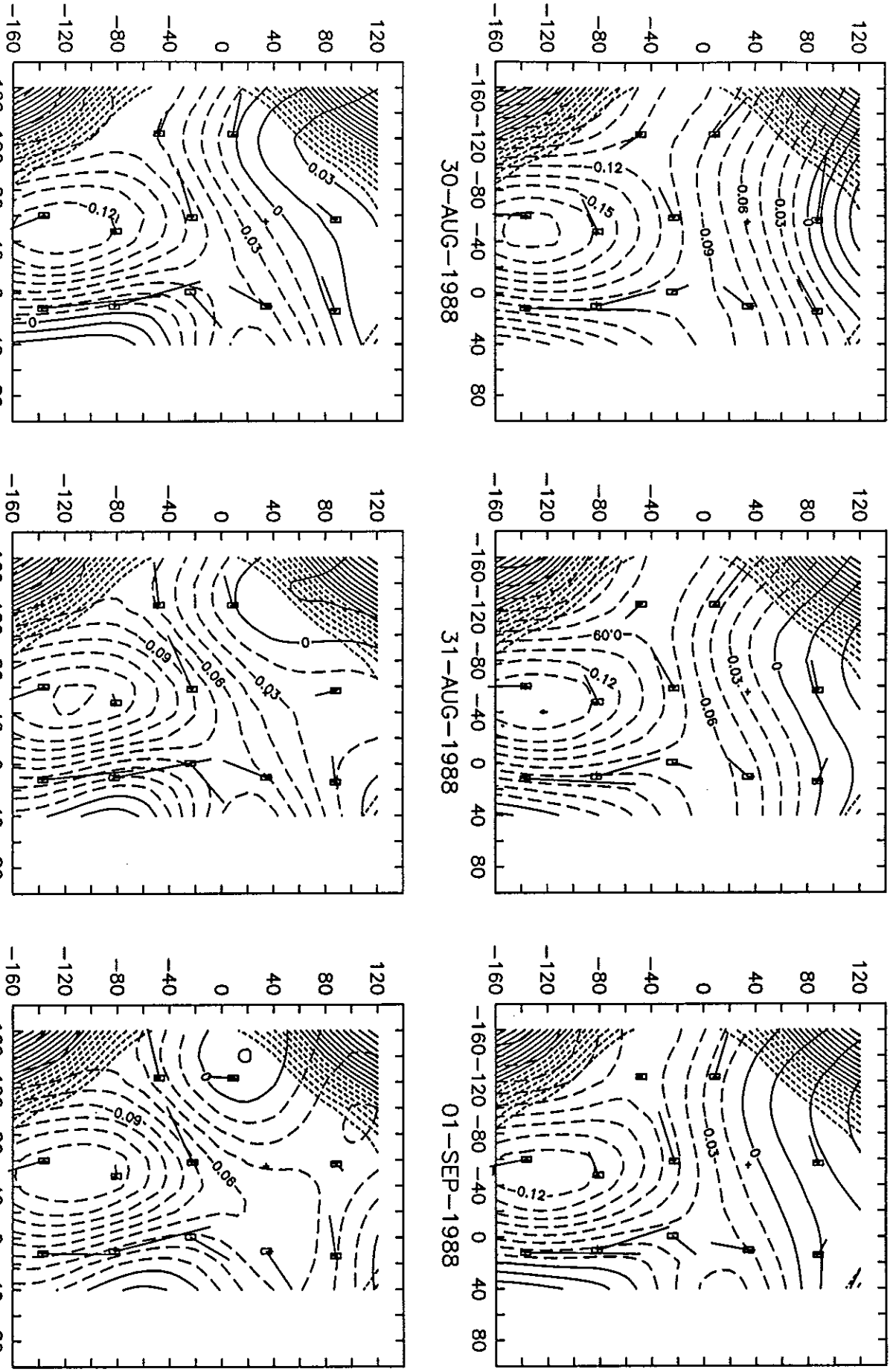
30-AUG-1988
31-AUG-1988
01-SEP-1988
02-SEP-1988
03-SEP-1988
04-SEP-1988

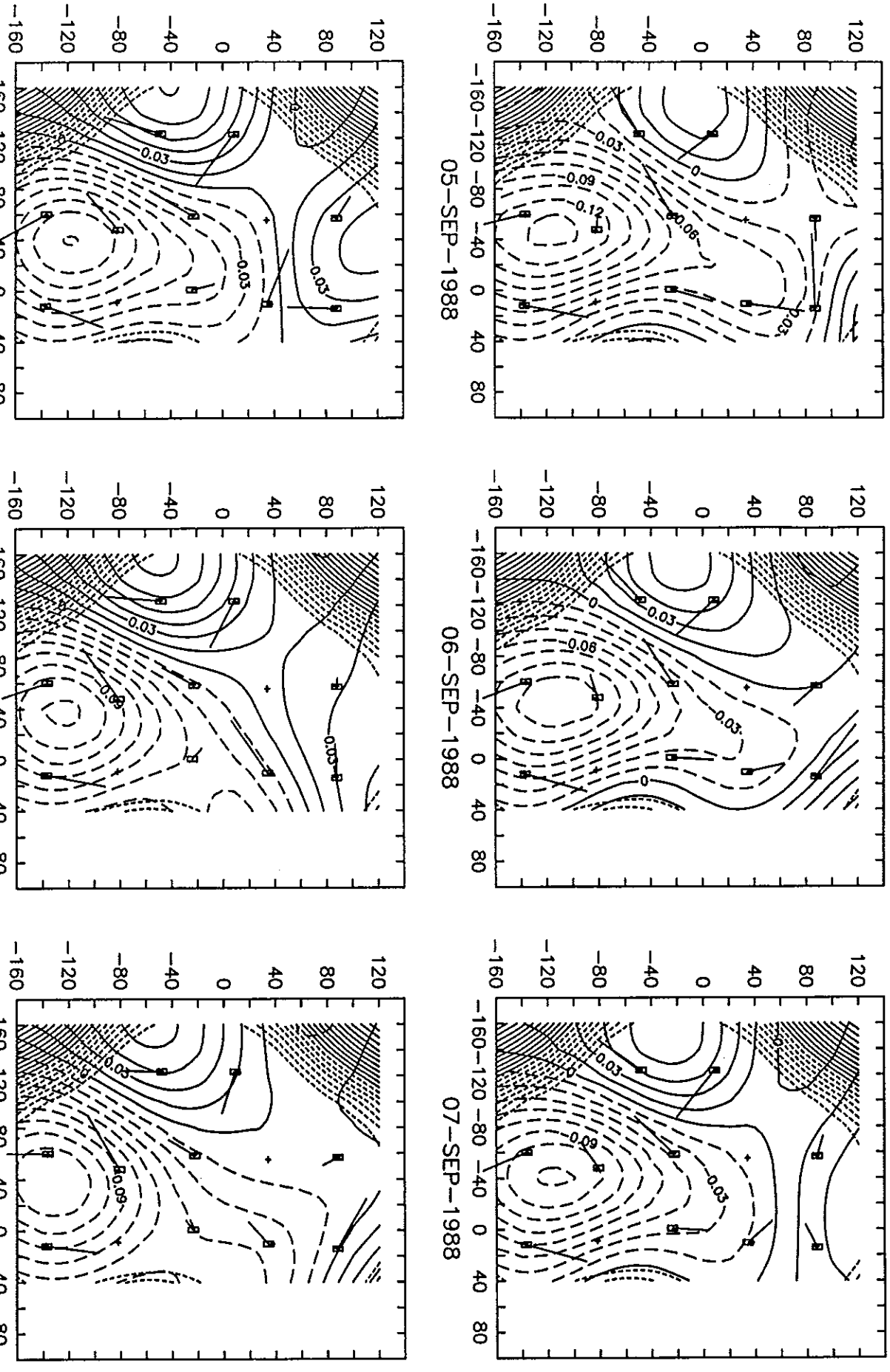
05-SEP-1988
06-SEP-1988
07-SEP-1988
08-SEP-1988
09-SEP-1988
10-SEP-1988

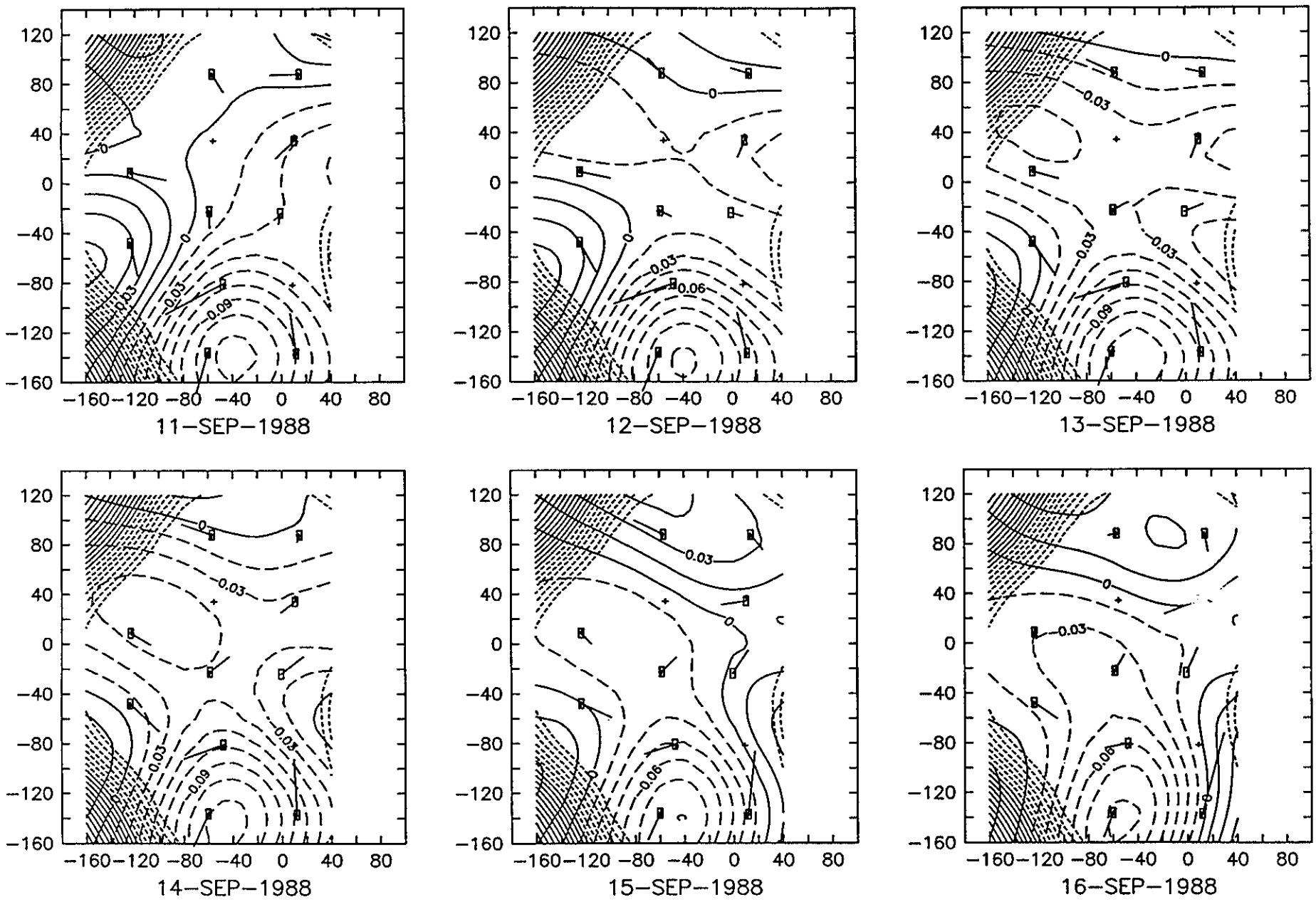
11-SEP-1988
12-SEP-1988
13-SEP-1988
14-SEP-1988
15-SEP-1988
16-SEP-1988

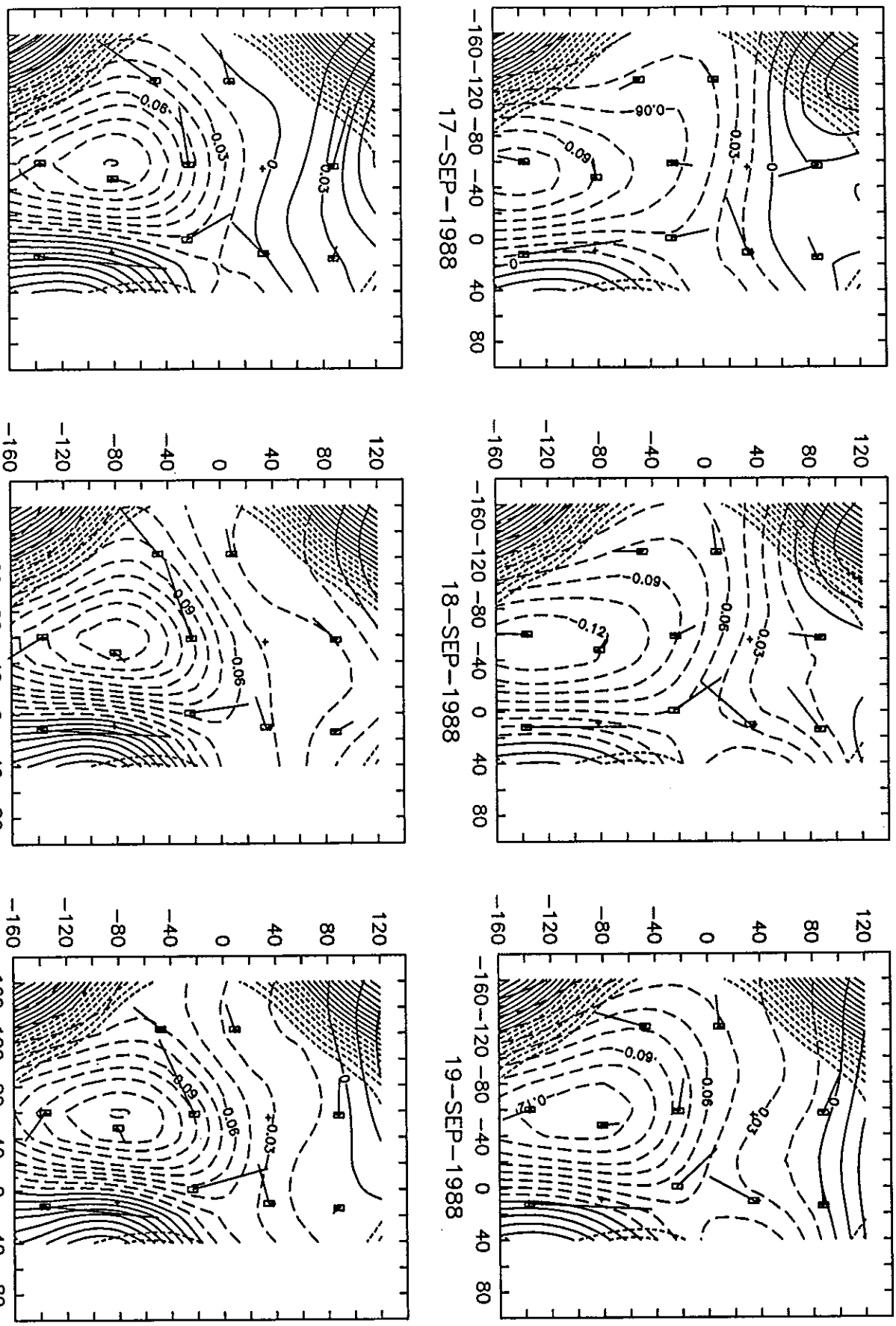
17-SEP-1988
18-SEP-1988
19-SEP-1988
20-SEP-1988
21-SEP-1988
22-SEP-1988

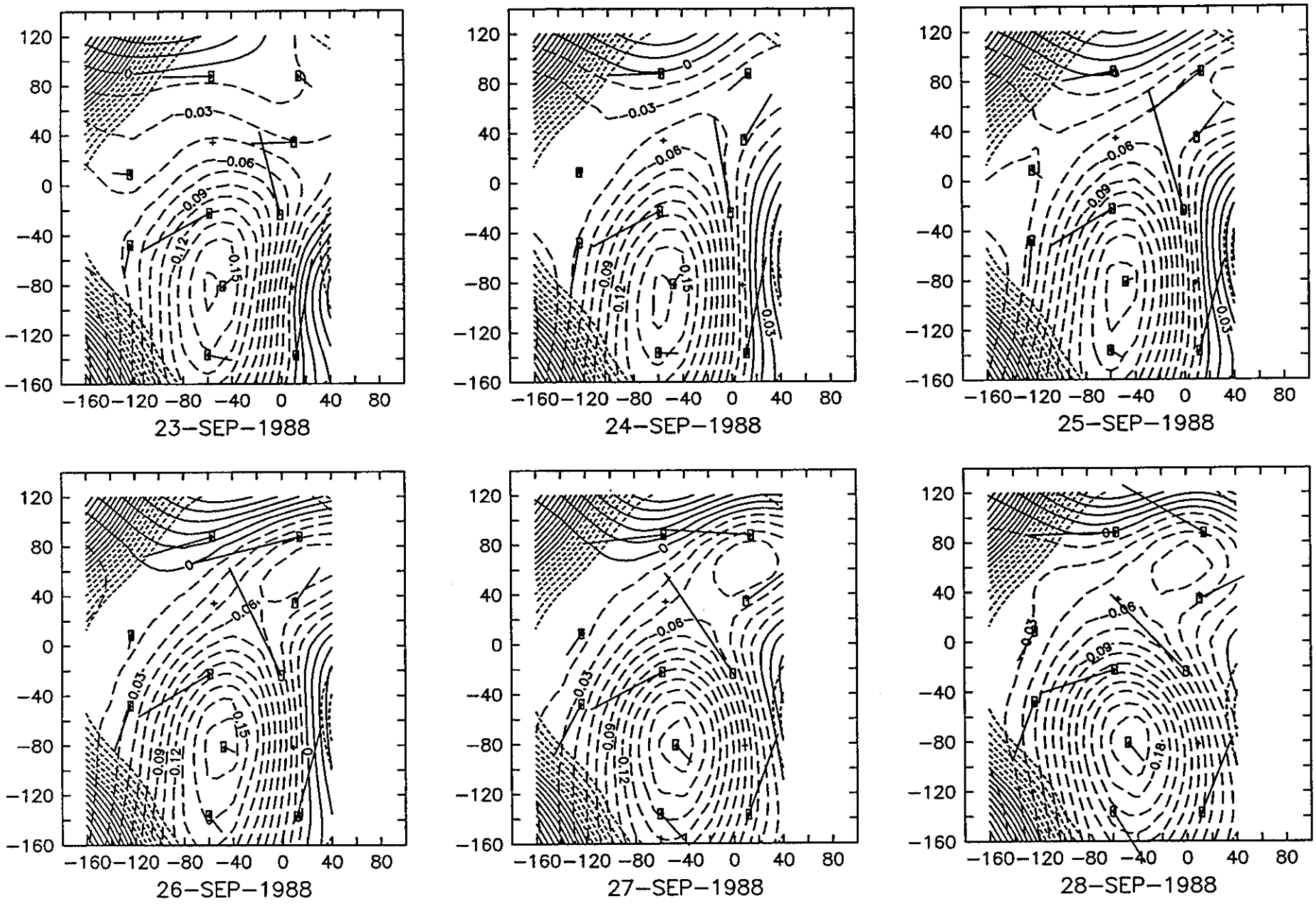
120
80
40
0
−40
−80
−120
−160
−160 −120 −80 −40 0 40 80
23−SEP−1988
24−SEP−1988
25−SEP−1988
26−SEP−1988
27−SEP−1988
28−SEP−1988

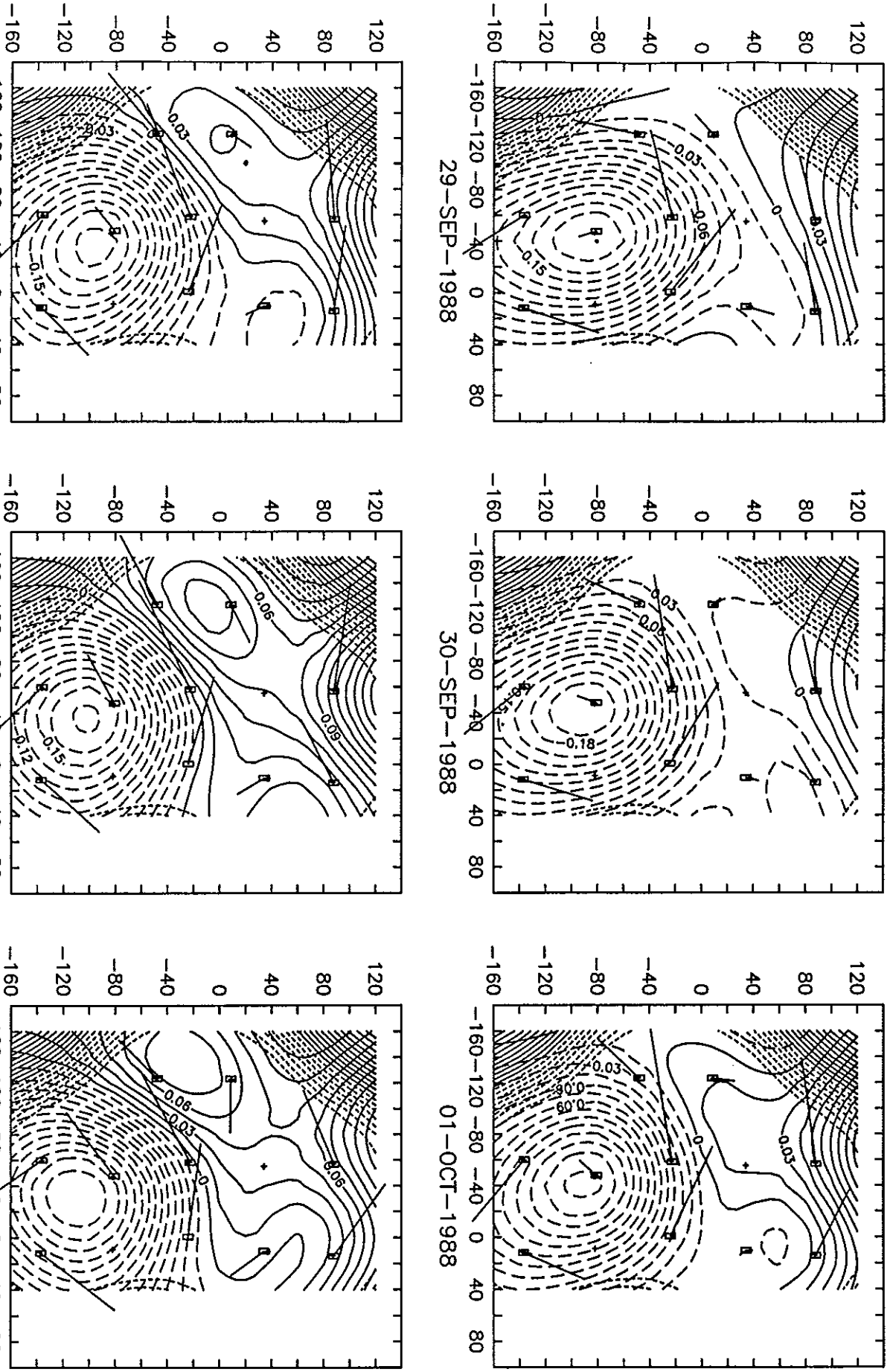
29-SEP-1988
30-SEP-1988
01-OCT-1988
02-OCT-1988
03-OCT-1988
04-OCT-1988

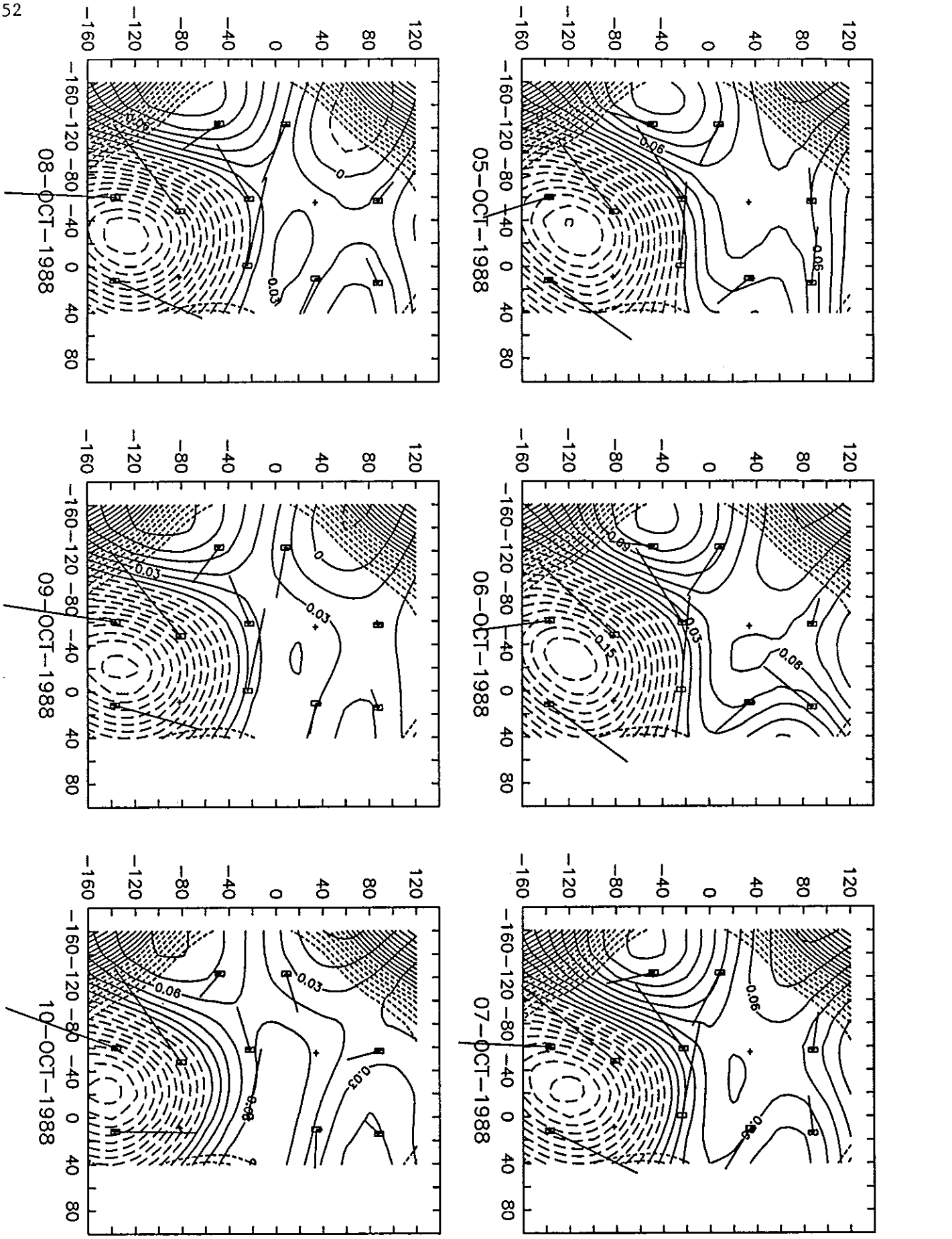
05-OCT-1988
06-OCT-1988
07-OCT-1988
08-OCT-1988
09-OCT-1988
10-OCT-1988

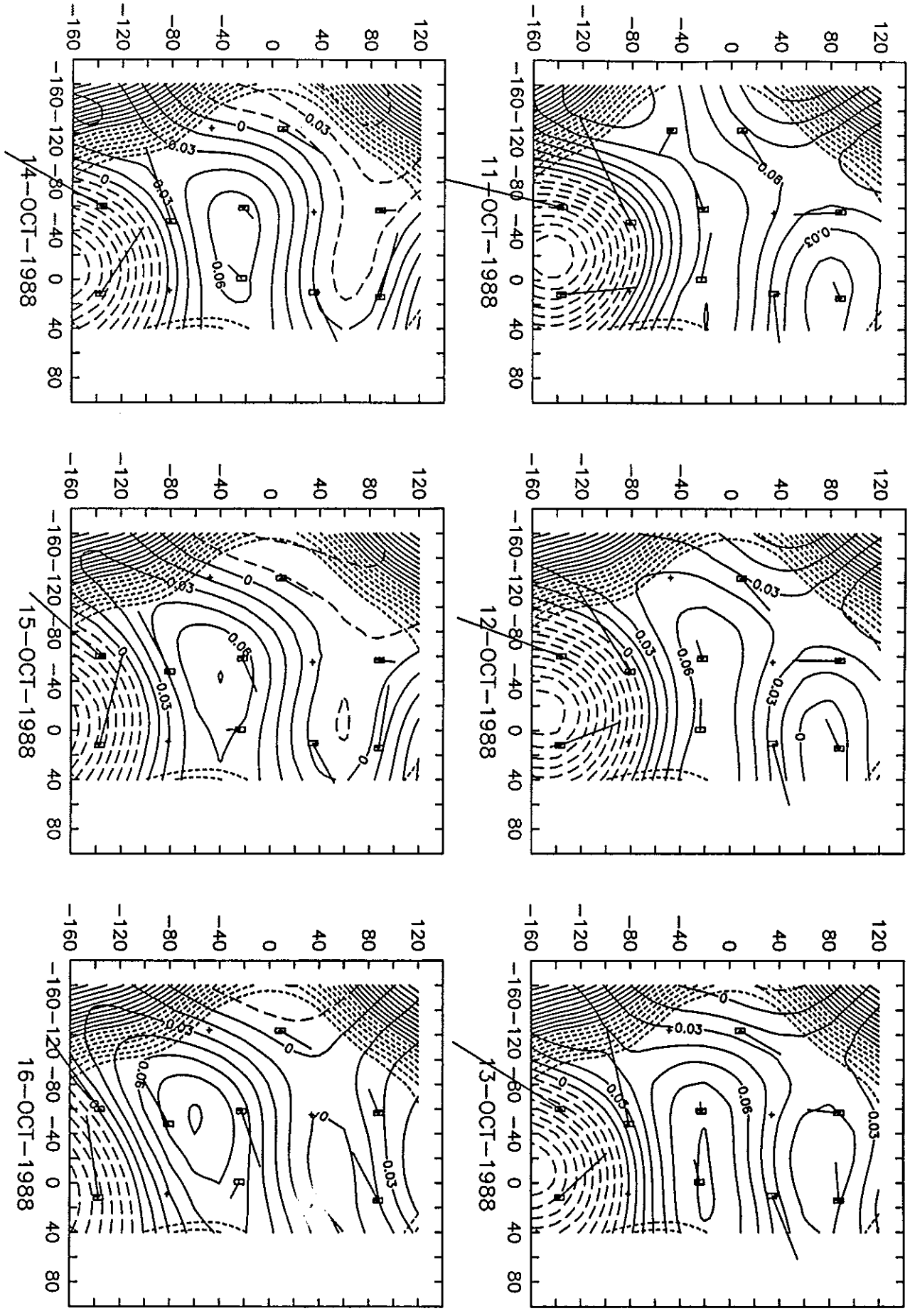
11-OCT-1988
12-OCT-1988
13-OCT-1988
14-OCT-1988
15-OCT-1988
16-OCT-1988

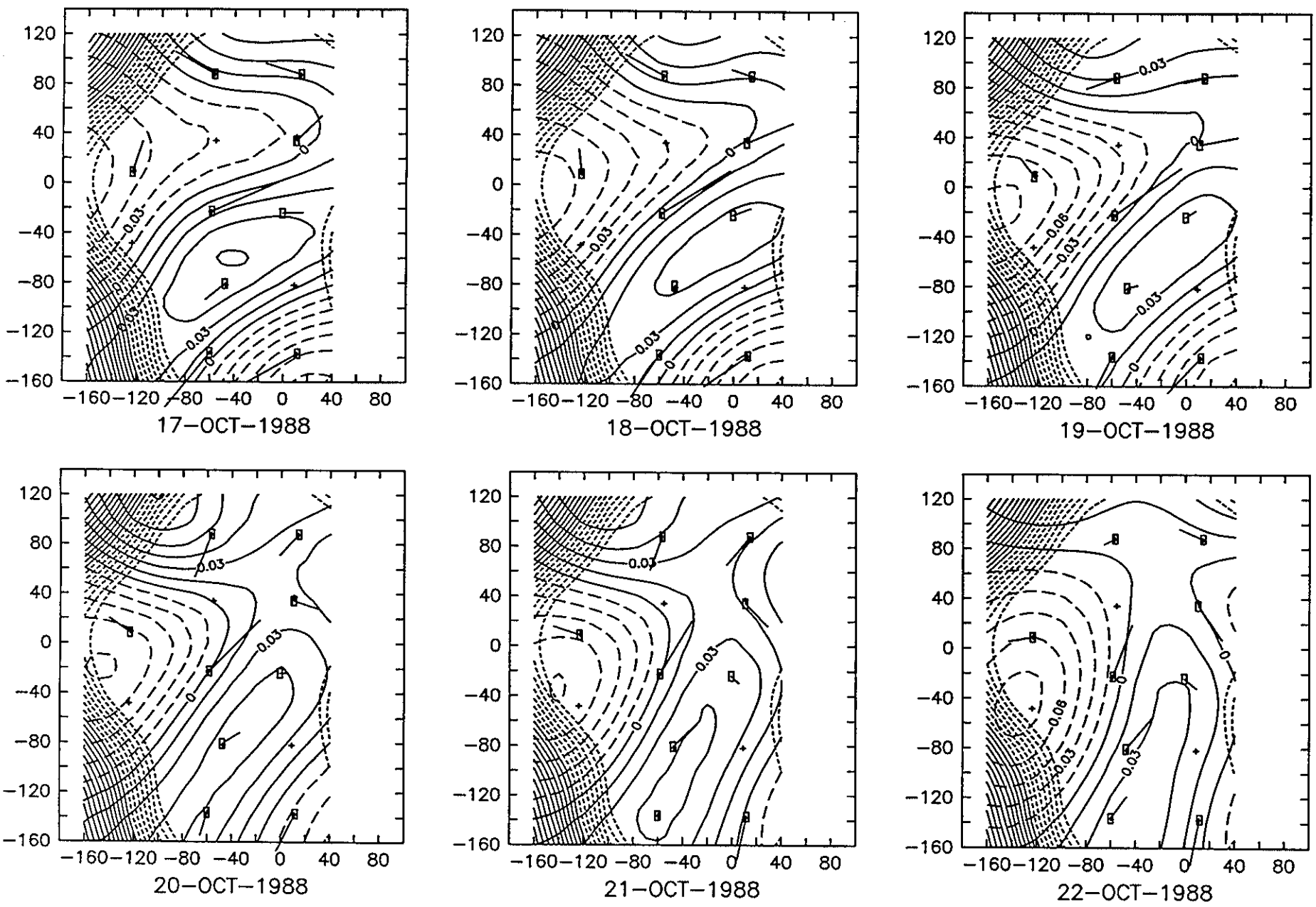
120
80
40
0
−40
−80
−120
−160
−160 −120 −80 −40 0 40 80
0.03
0
17−OCT−1988
18−OCT−1988
0.06
19−OCT−1988
20−OCT−1988
21−OCT−1988
22−OCT−1988

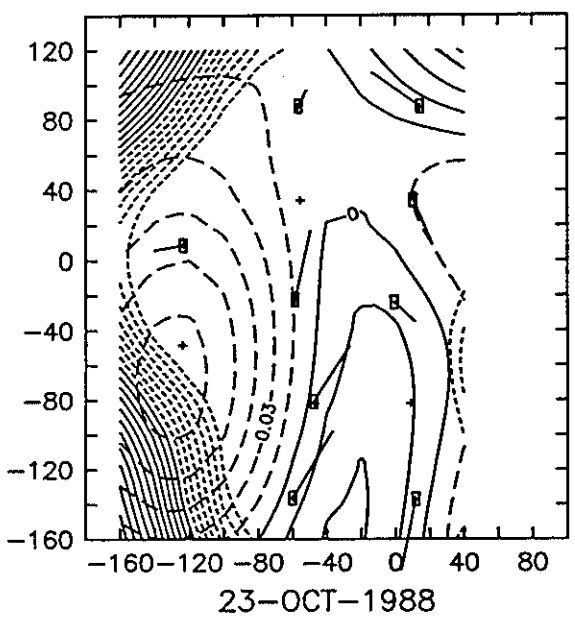
120
80
40
0
−40
−80
−120
−160
−160 −120 −80 −40 0 40 80
0.03
0
23−OCT−1988

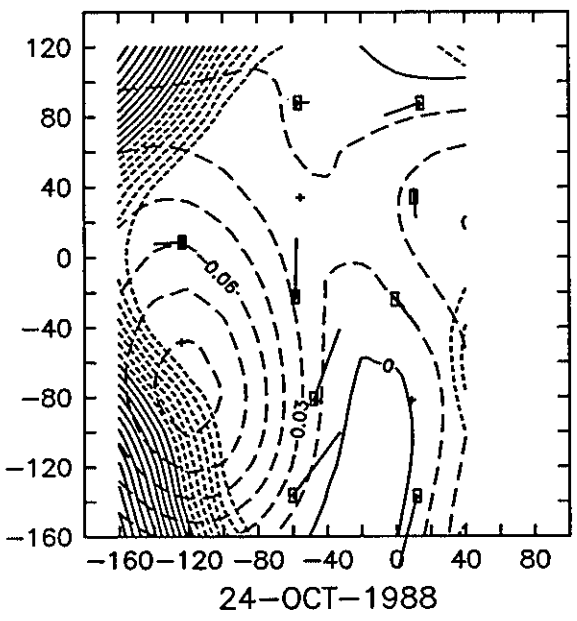
120
80
40
0
−40
−80
−120
−160
−160 −120 −80 −40 0 40 80
0.06
0.03
0
24−OCT−1988

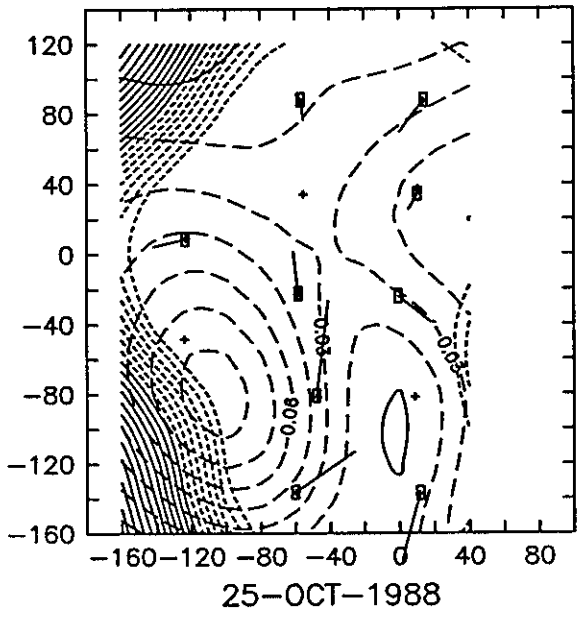
120
80
40
0
−40
−80
−120
−160
−160 −120 −80 −40 0 40 80
0.08
0.04
0.02
25−OCT−1988

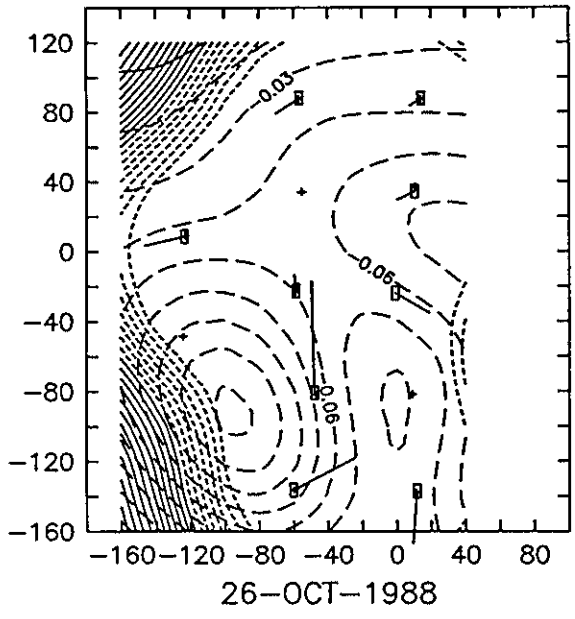
120
80
40
0
−40
−80
−120
−160
−160 −120 −80 −40 0 40 80
0.03
0.06
0.09
26−OCT−1988

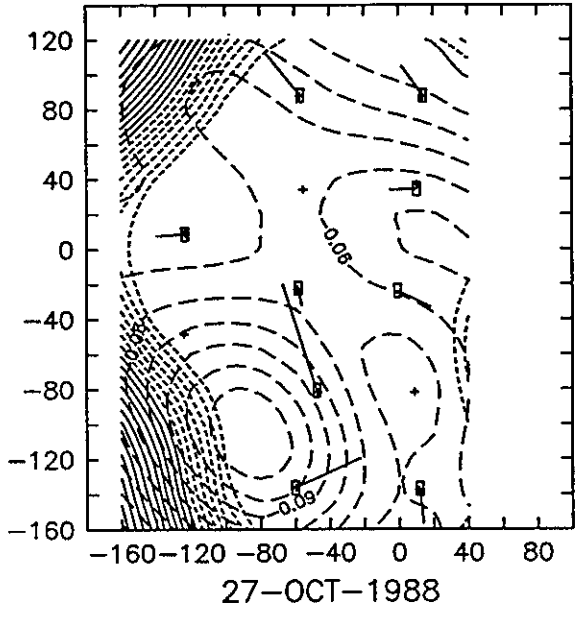
120
80
40
0
−40
−80
−120
−160
−160 −120 −80 −40 0 40 80
0.06
0.09
27−OCT−1988

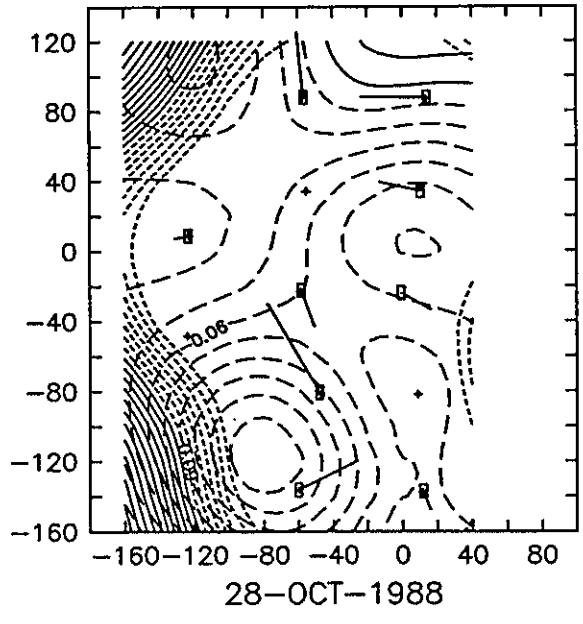
120
80
40
0
−40
−80
−120
−160
−160 −120 −80 −40 0 40 80
0.06
0.09
28−OCT−1988

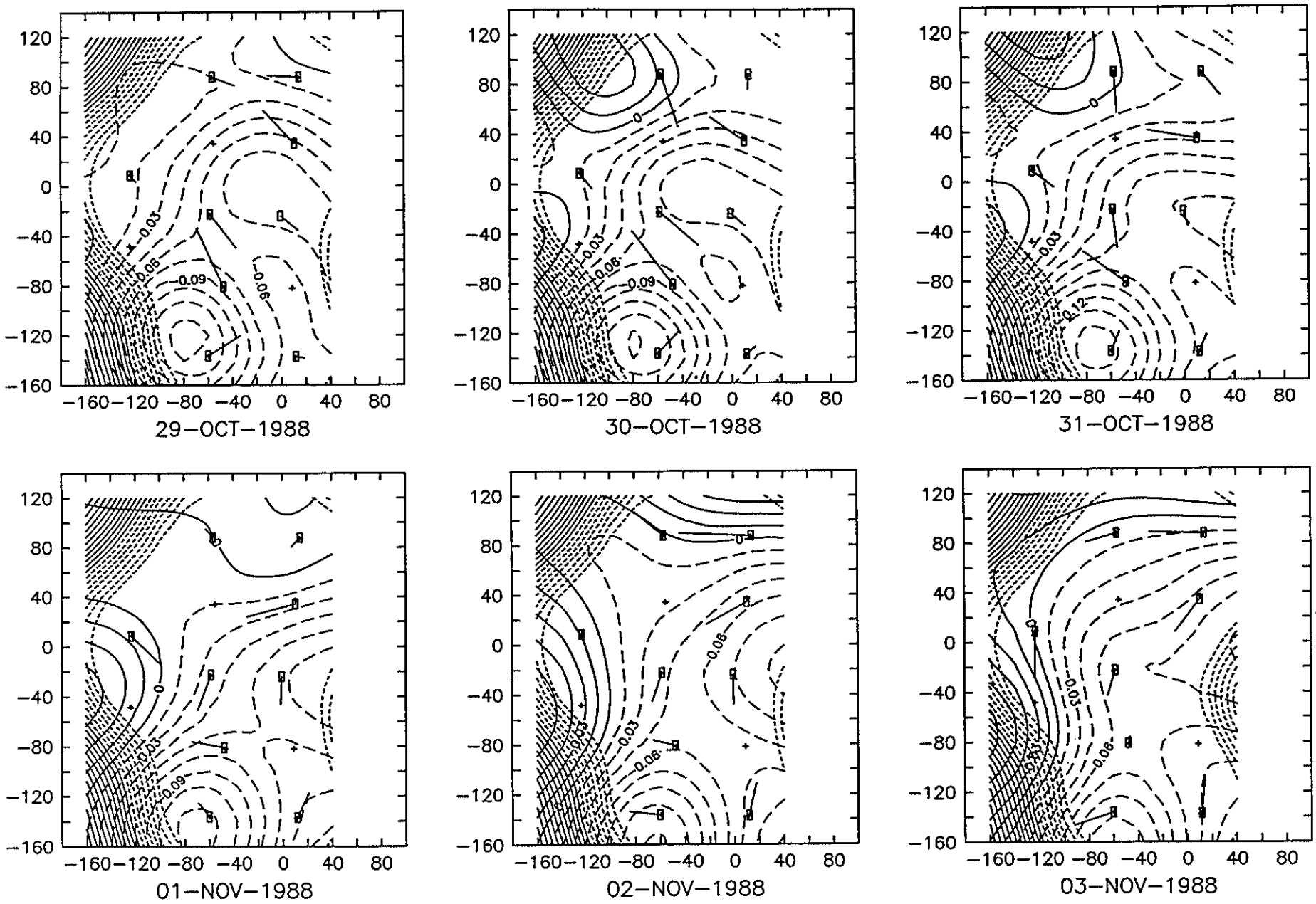
29-OCT-1988
30-OCT-1988
31-OCT-1988
01-NOV-1988
02-NOV-1988
03-NOV-1988

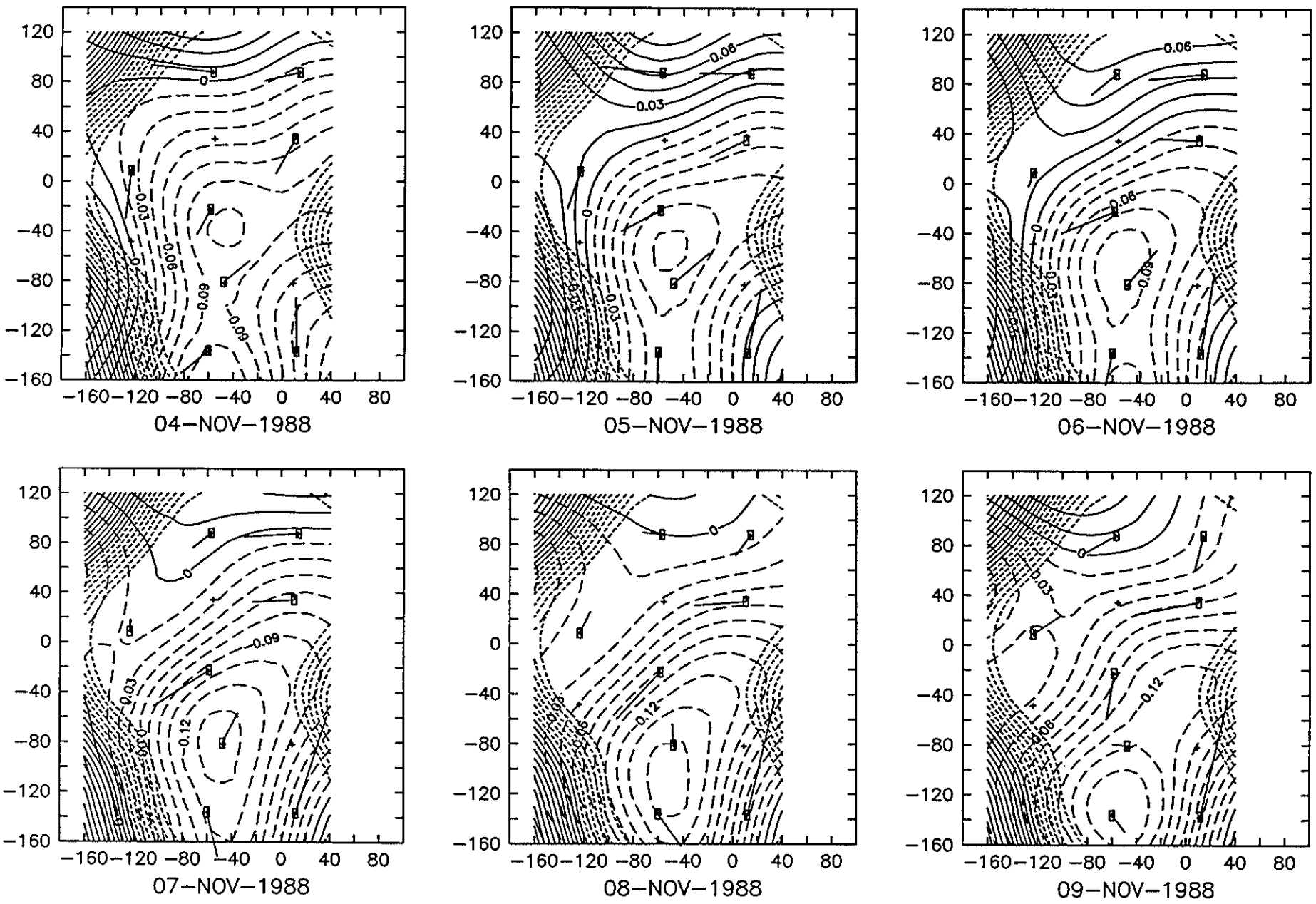
120
80
40
0
−40
−80
−120
−160
−160 −120 −80 −40 0 40 80
04−NOV−1988
05−NOV−1988
06−NOV−1988
07−NOV−1988
08−NOV−1988
09−NOV−1988

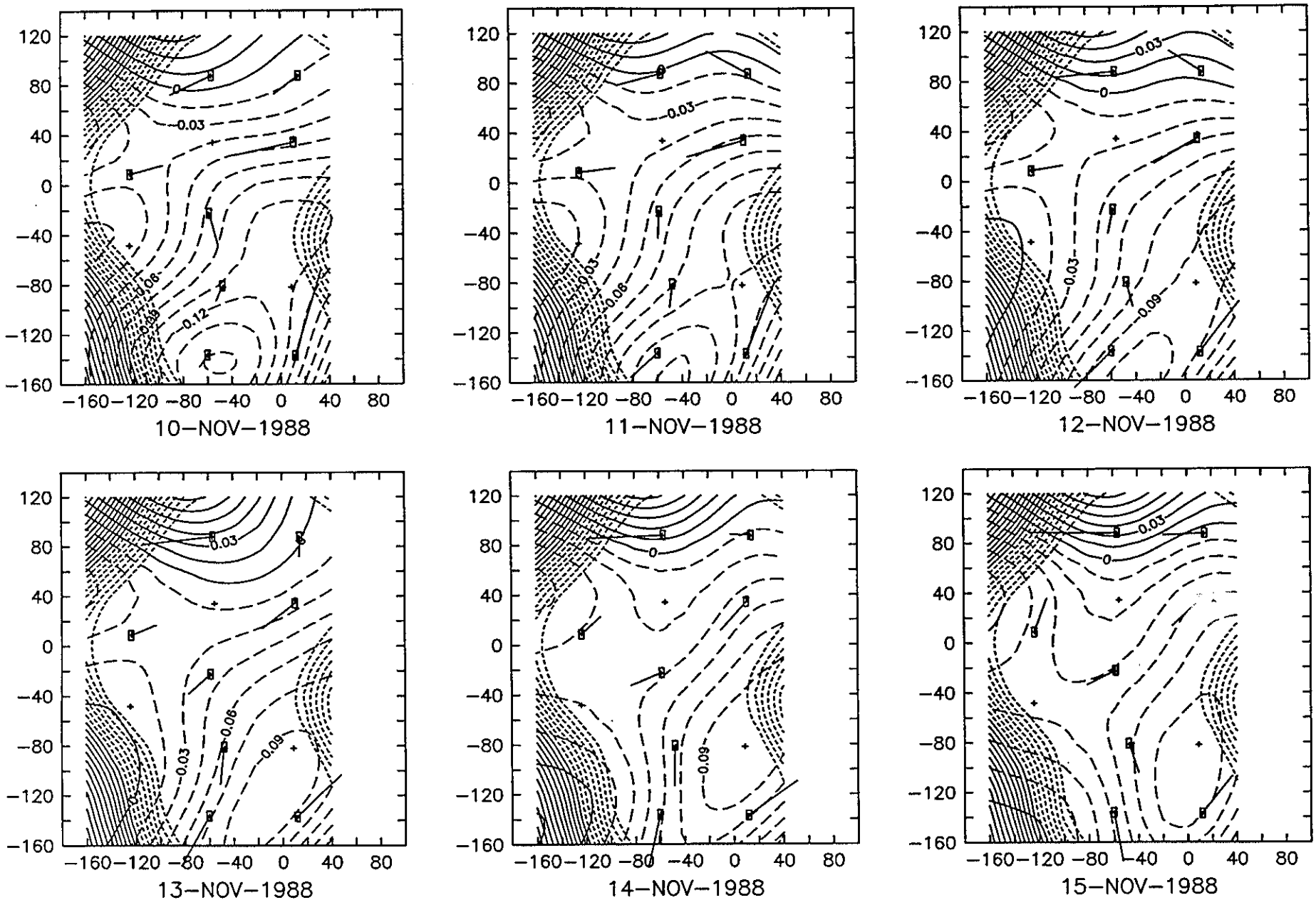
10-NOV-1988
11-NOV-1988
12-NOV-1988
13-NOV-1988
14-NOV-1988
15-NOV-1988

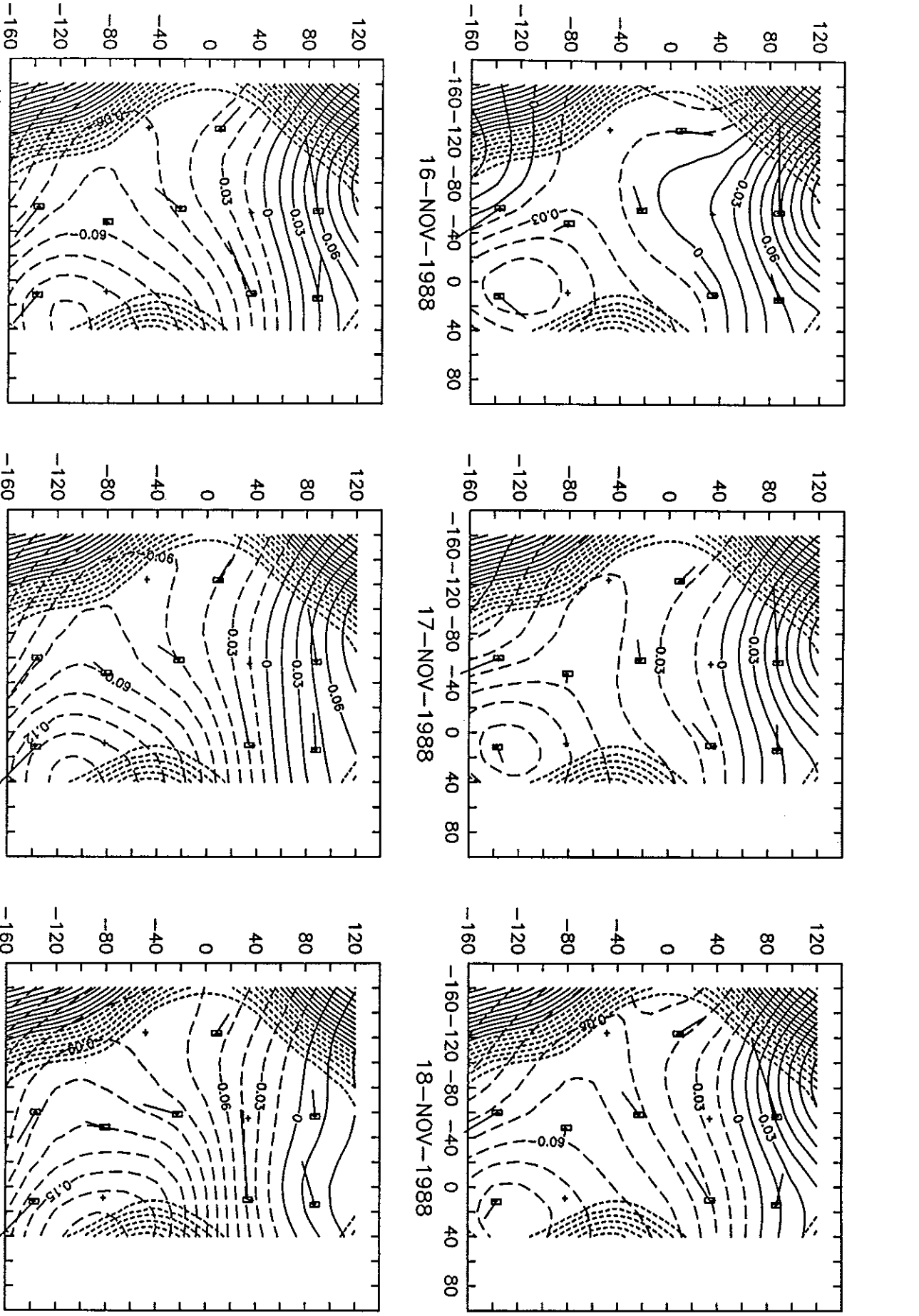
16-NOV-1988
17-NOV-1988
18-NOV-1988
19-NOV-1988
20-NOV-1988
21-NOV-1988

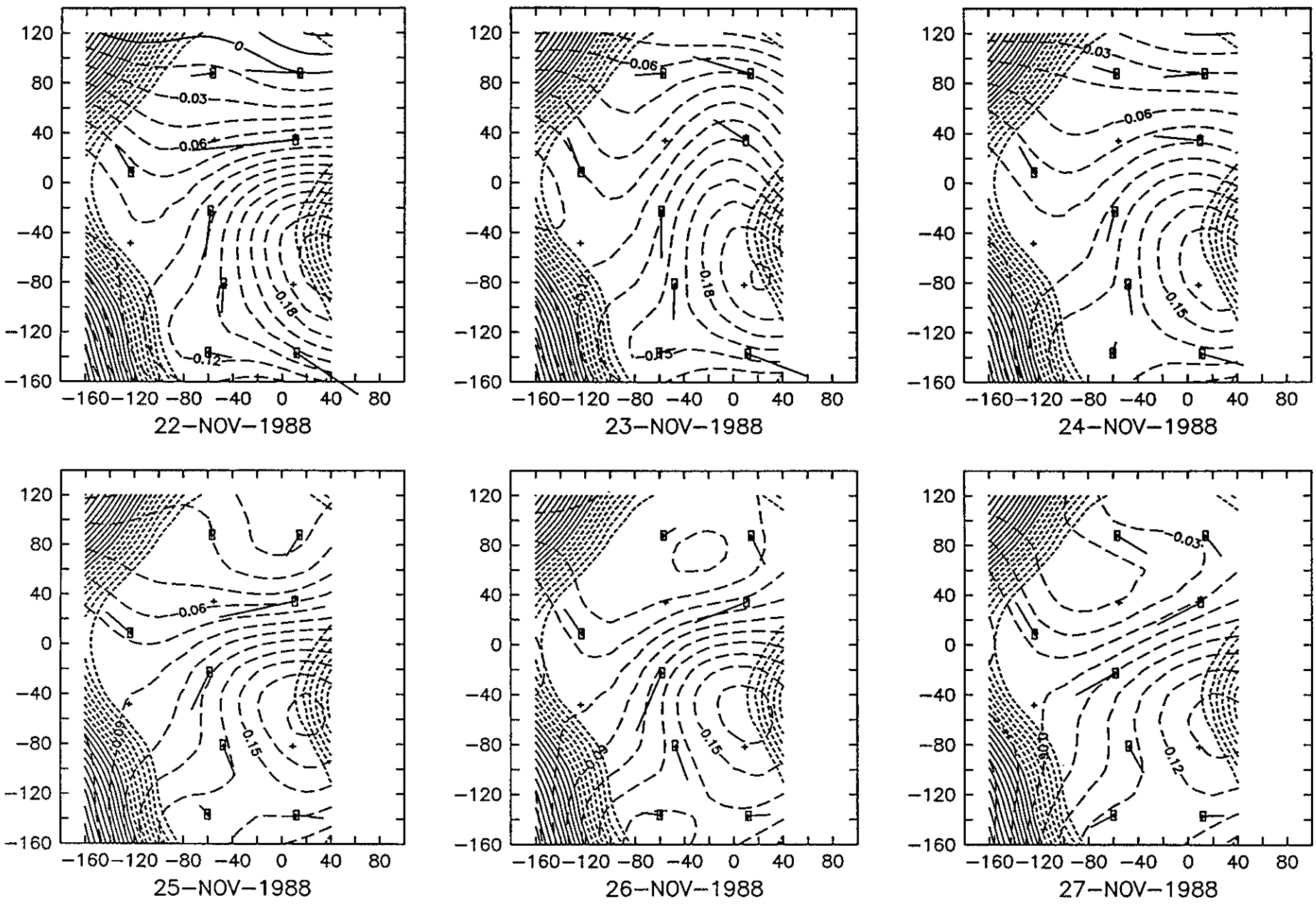
22-NOV-1988
23-NOV-1988
24-NOV-1988
25-NOV-1988
26-NOV-1988
27-NOV-1988

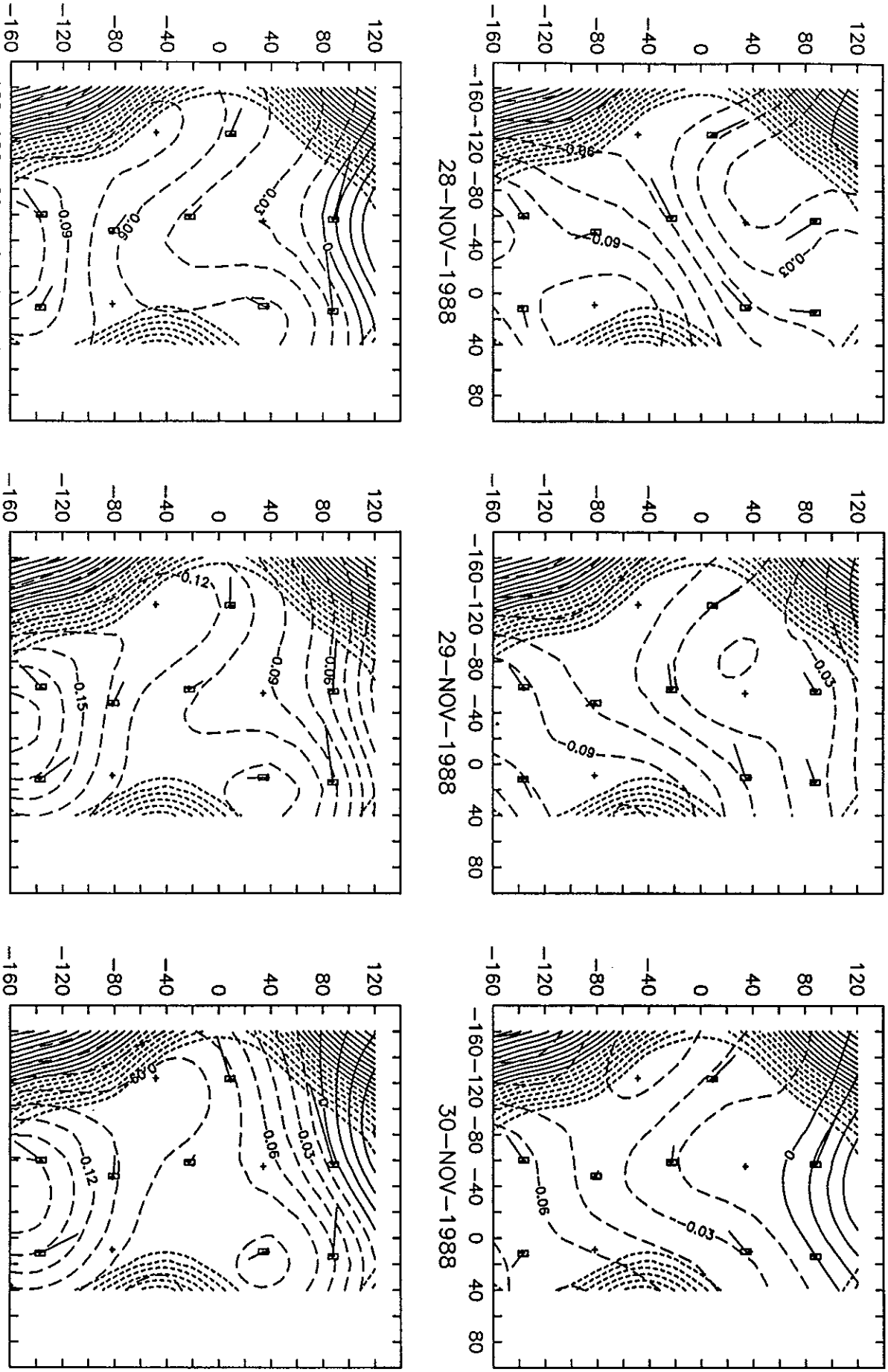
28-NOV-1988
29-NOV-1988
30-NOV-1988
01-DEC-1988
02-DEC-1988
03-DEC-1988

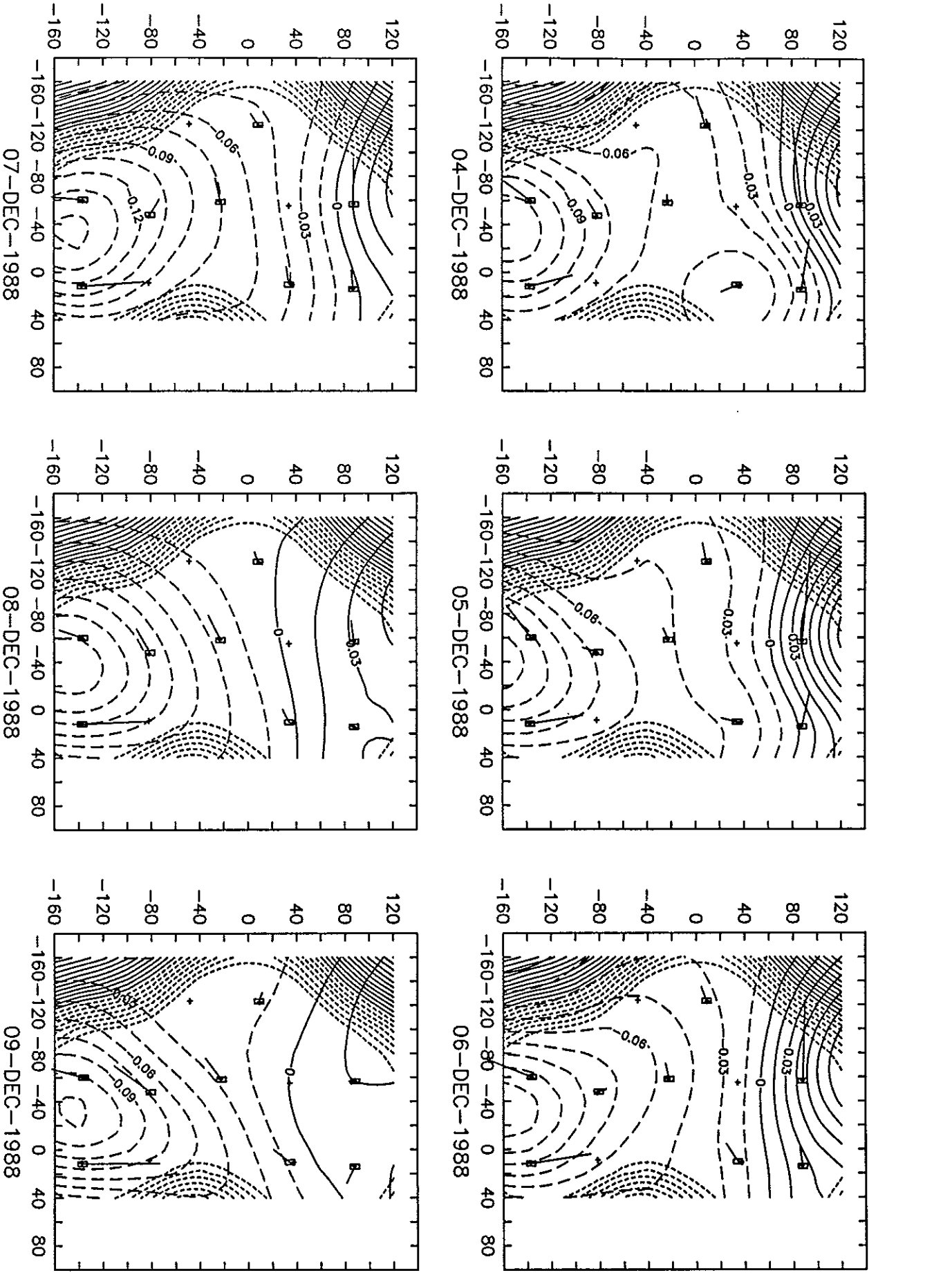
04-DEC-1988
05-DEC-1988
06-DEC-1988
07-DEC-1988
08-DEC-1988
09-DEC-1988

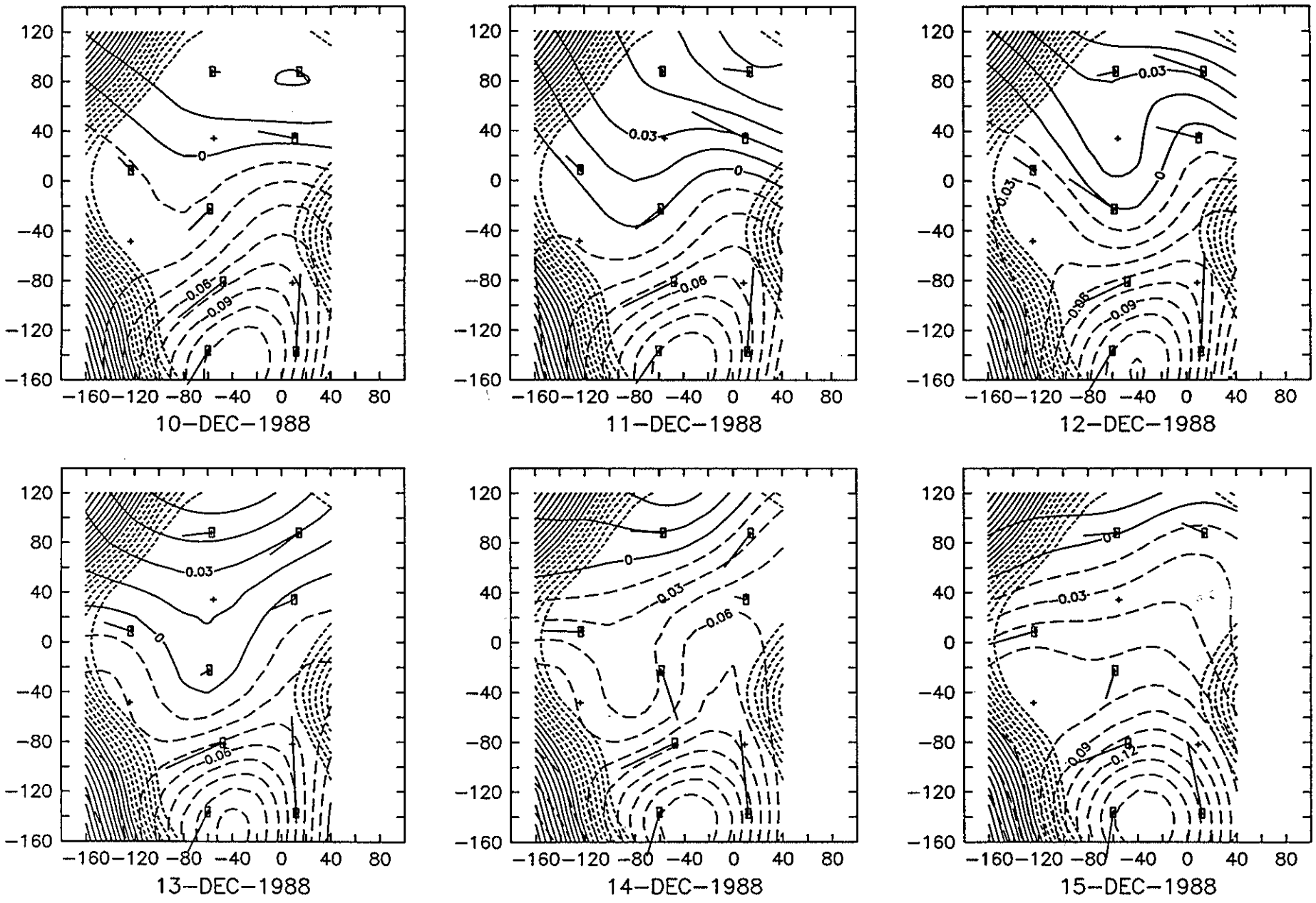
120
80
40
0
−40
−80
−120
−160
−160 −120 −80 −40 0 40 80
10−DEC−1988
11−DEC−1988
12−DEC−1988
13−DEC−1988
14−DEC−1988
15−DEC−1988
0
0.03
0.06
0.09
0.12

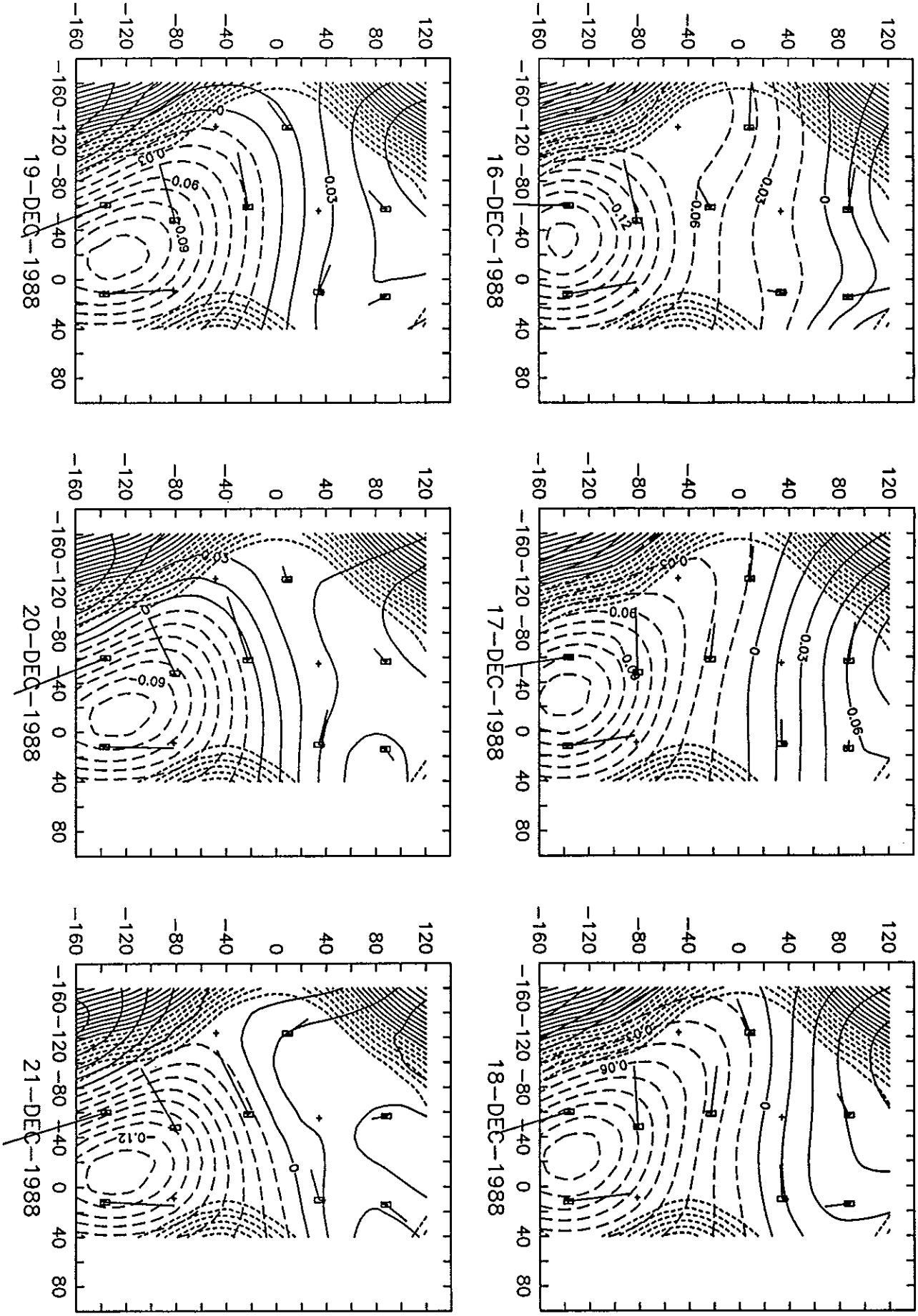
16-DEC-1988
17-DEC-1988
18-DEC-1988
19-DEC-1988
20-DEC-1988
21-DEC-1988

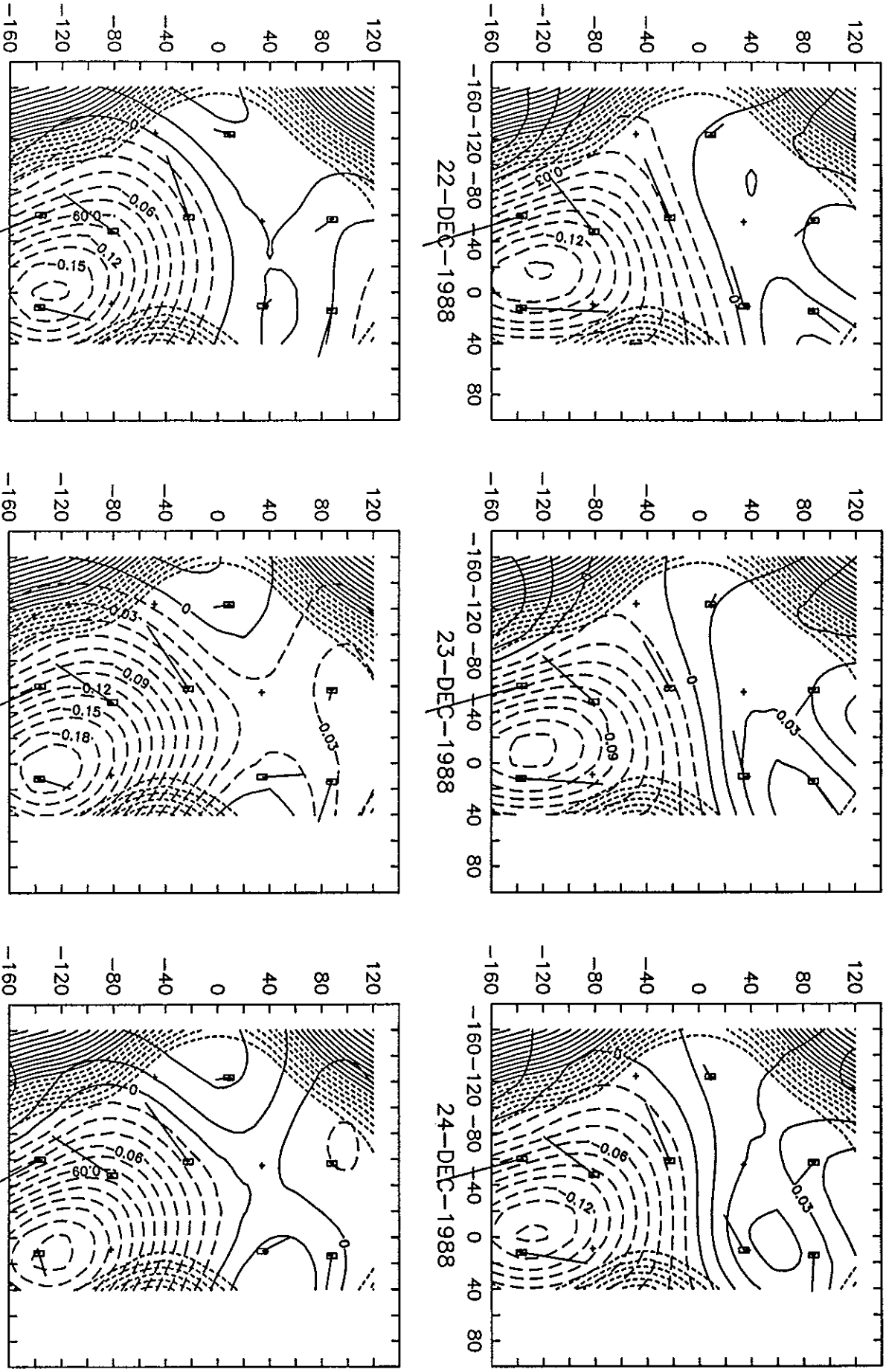
22-DEC-1988
23-DEC-1988
24-DEC-1988
25-DEC-1988
26-DEC-1988
27-DEC-1988

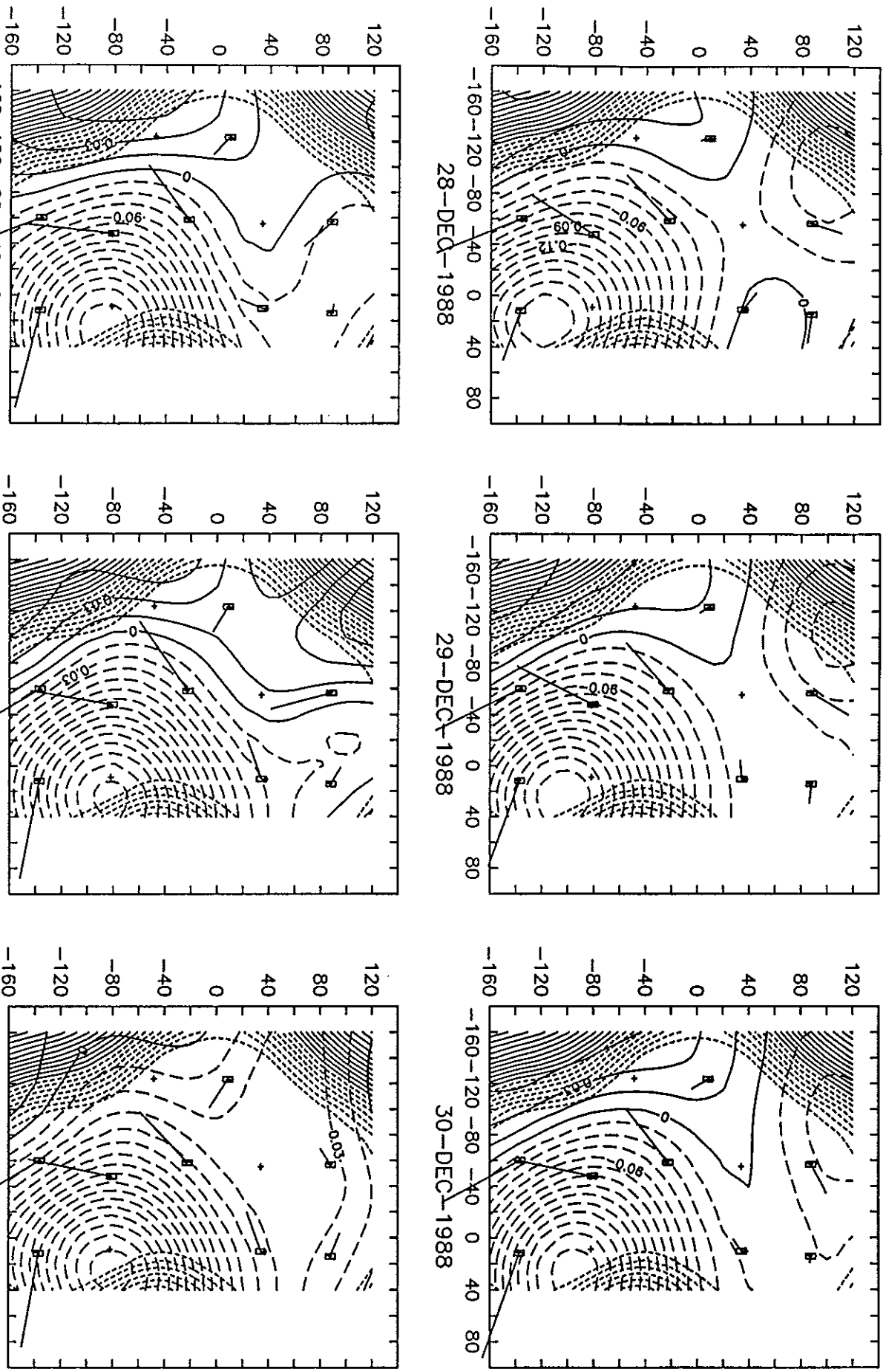
28-DEC-1988
29-DEC-1988
30-DEC-1988
31-DEC-1988
01-JAN-1989
02-JAN-1989

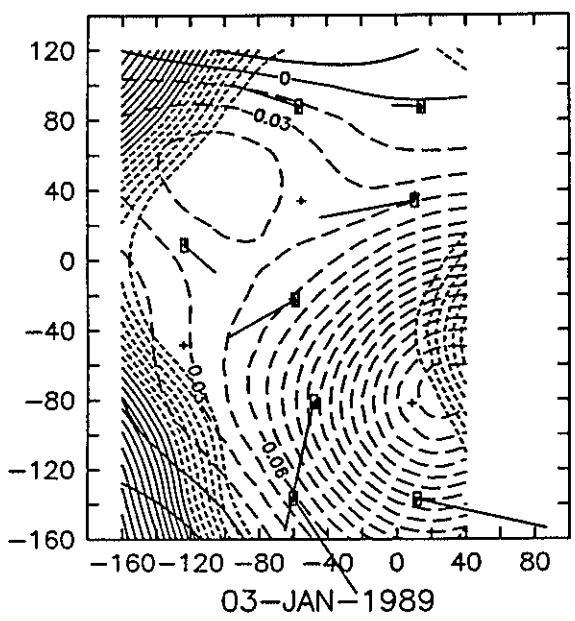
120
80
40
0
−40
−80
−120
−160
−160 −120 −80 −40 0 40 80
0
0.03
−0.03
−0.06
03−JAN−1989

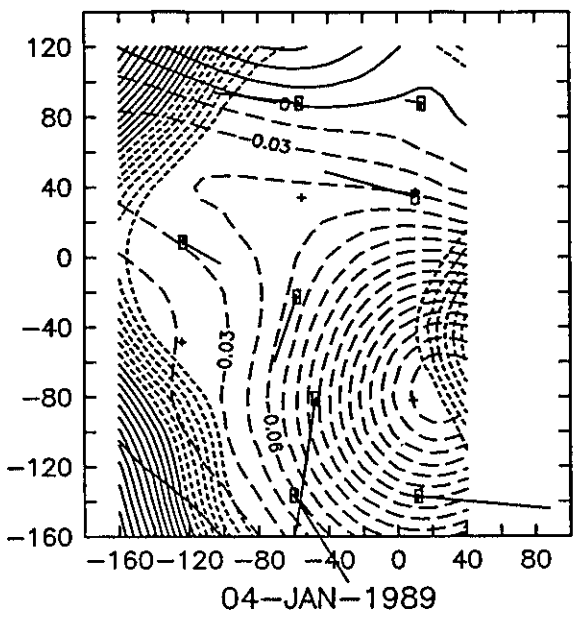
120
80
40
0
−40
−80
−120
−160
−160 −120 −80 −40 0 40 80
0
0.03
−0.03
−0.06
04−JAN−1989

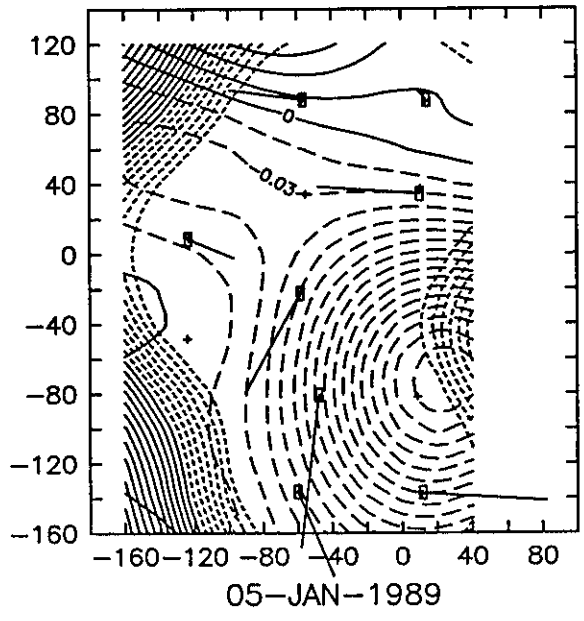
120
80
40
0
−40
−80
−120
−160
−160 −120 −80 −40 0 40 80
0
0.03
−0.03
−0.06
05−JAN−1989

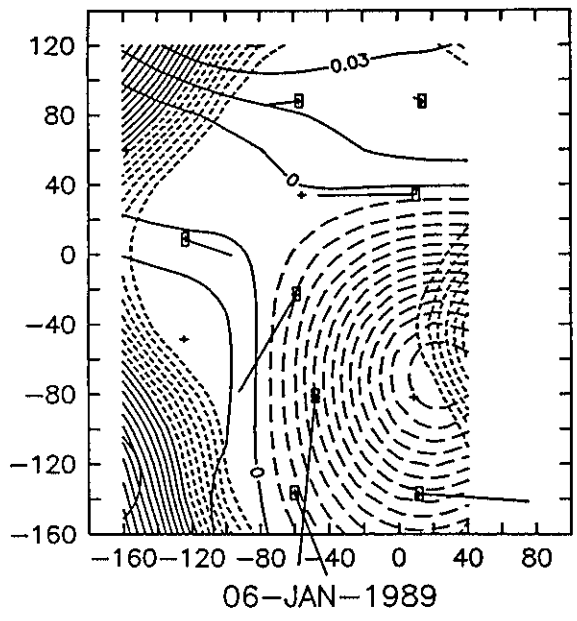
120
80
40
0
−40
−80
−120
−160
−160 −120 −80 −40 0 40 80
0.03
0
−0.03
−0.06
06−JAN−1989

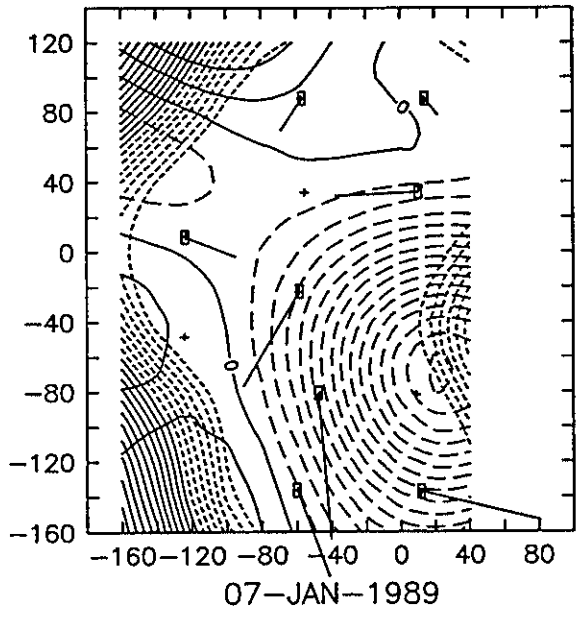
120
80
40
0
−40
−80
−120
−160
−160 −120 −80 −40 0 40 80
0
−0.03
−0.06
07−JAN−1989

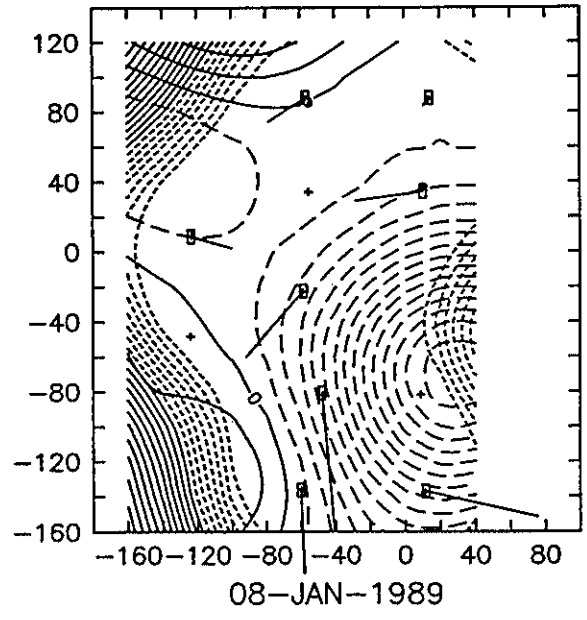
120
80
40
0
−40
−80
−120
−160
−160 −120 −80 −40 0 40 80
0
−0.03
−0.06
08−JAN−1989

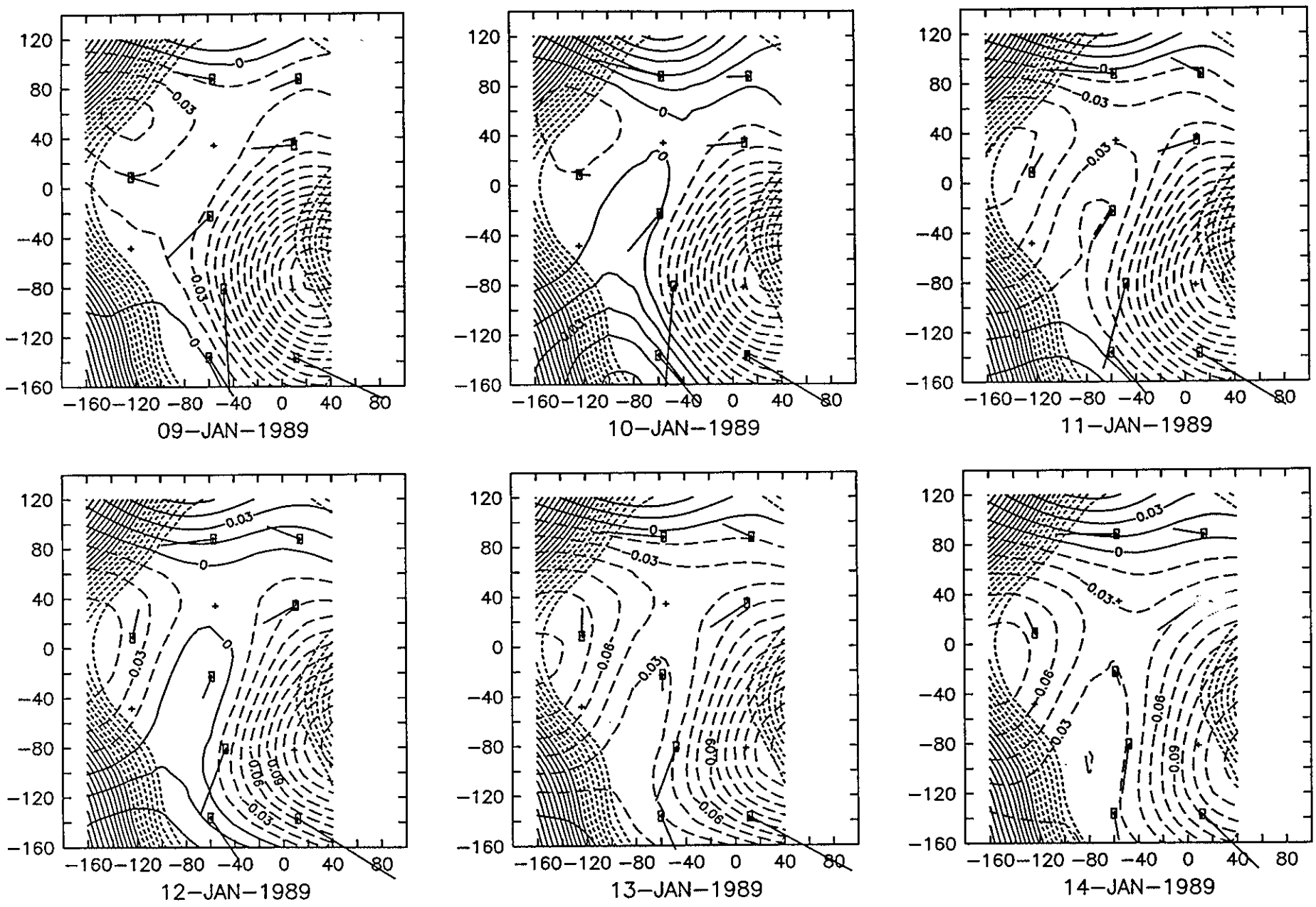
09-JAN-1989
10-JAN-1989
11-JAN-1989
12-JAN-1989
13-JAN-1989
14-JAN-1989

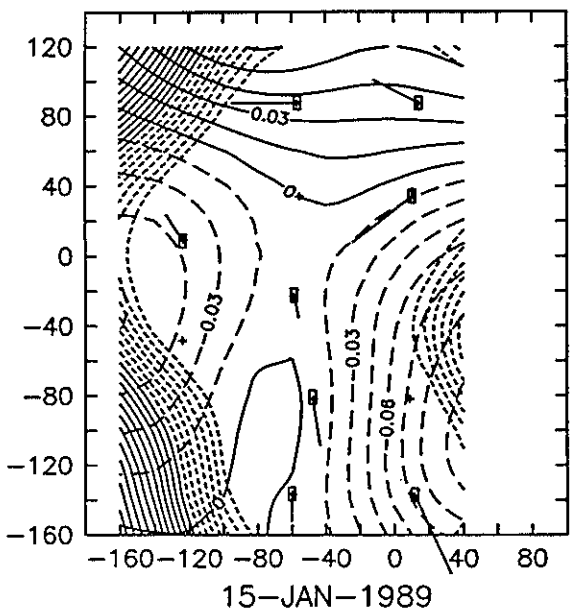
120
80
40
0
−40
−80
−120
−160
−160 −120 −80 −40 0 40 80
0.03
0
0.03
0.06
15−JAN−1989

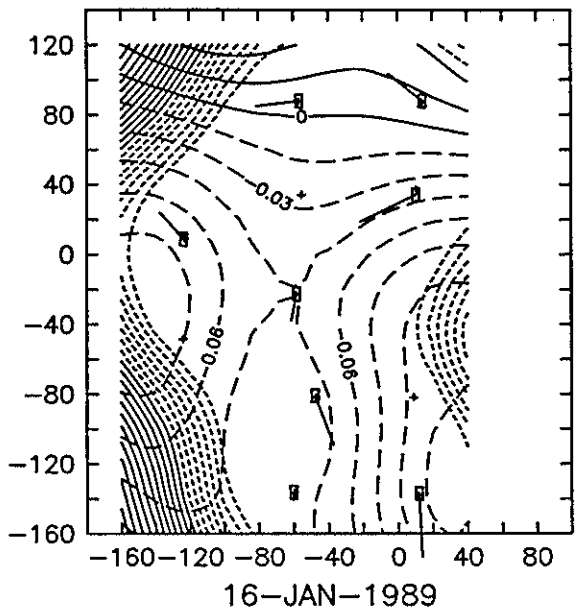
120
80
40
0
−40
−80
−120
−160
−160 −120 −80 −40 0 40 80
0
0.03
0.06
0.09
16−JAN−1989

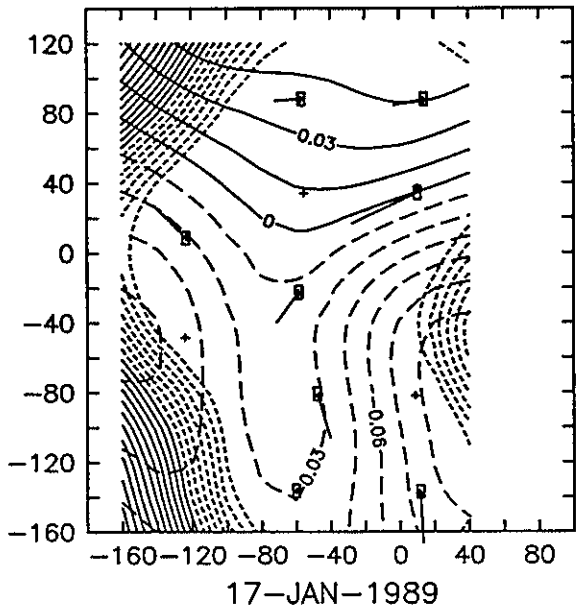
120
80
40
0
−40
−80
−120
−160
−160 −120 −80 −40 0 40 80
0.03
0
0.06
0.09
0.03
17−JAN−1989

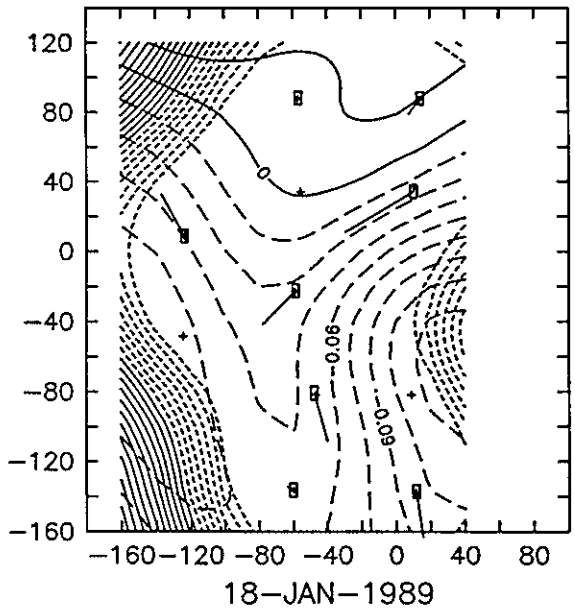
120
80
40
0
−40
−80
−120
−160
−160 −120 −80 −40 0 40 80
0
0.06
0.09
18−JAN−1989

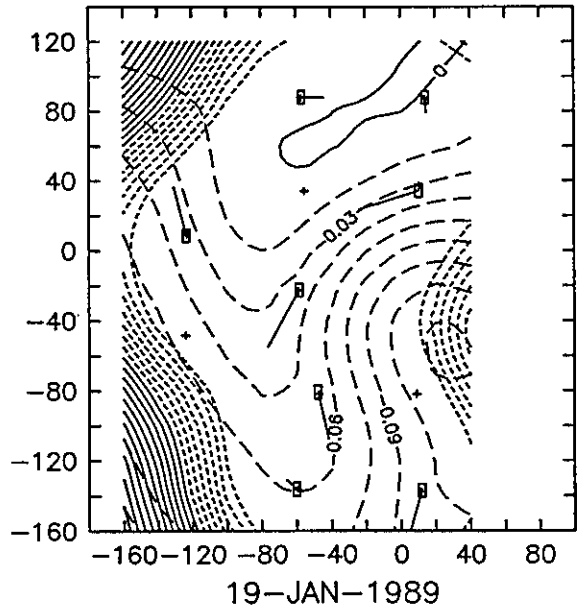
120
80
40
0
−40
−80
−120
−160
−160 −120 −80 −40 0 40 80
0
0.03
0.09
0.06
19−JAN−1989

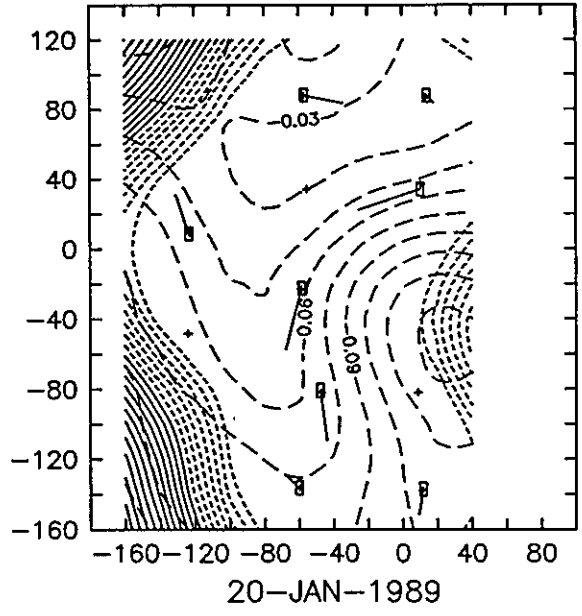
120
80
40
0
−40
−80
−120
−160
−160 −120 −80 −40 0 40 80
0.03
0.09
0.06
20−JAN−1989

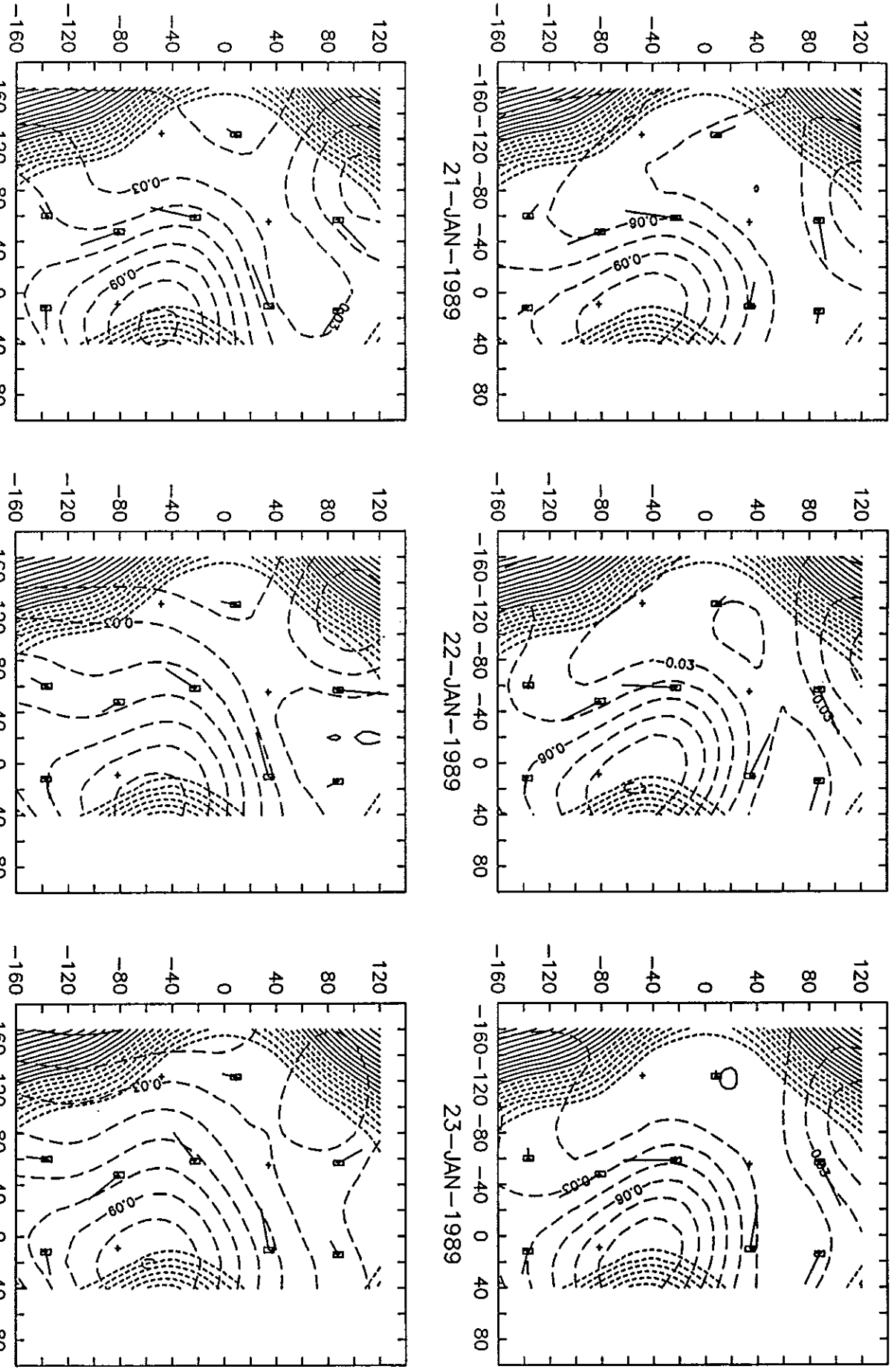
21-JAN-1989
22-JAN-1989
23-JAN-1989
24-JAN-1989
25-JAN-1989
26-JAN-1989

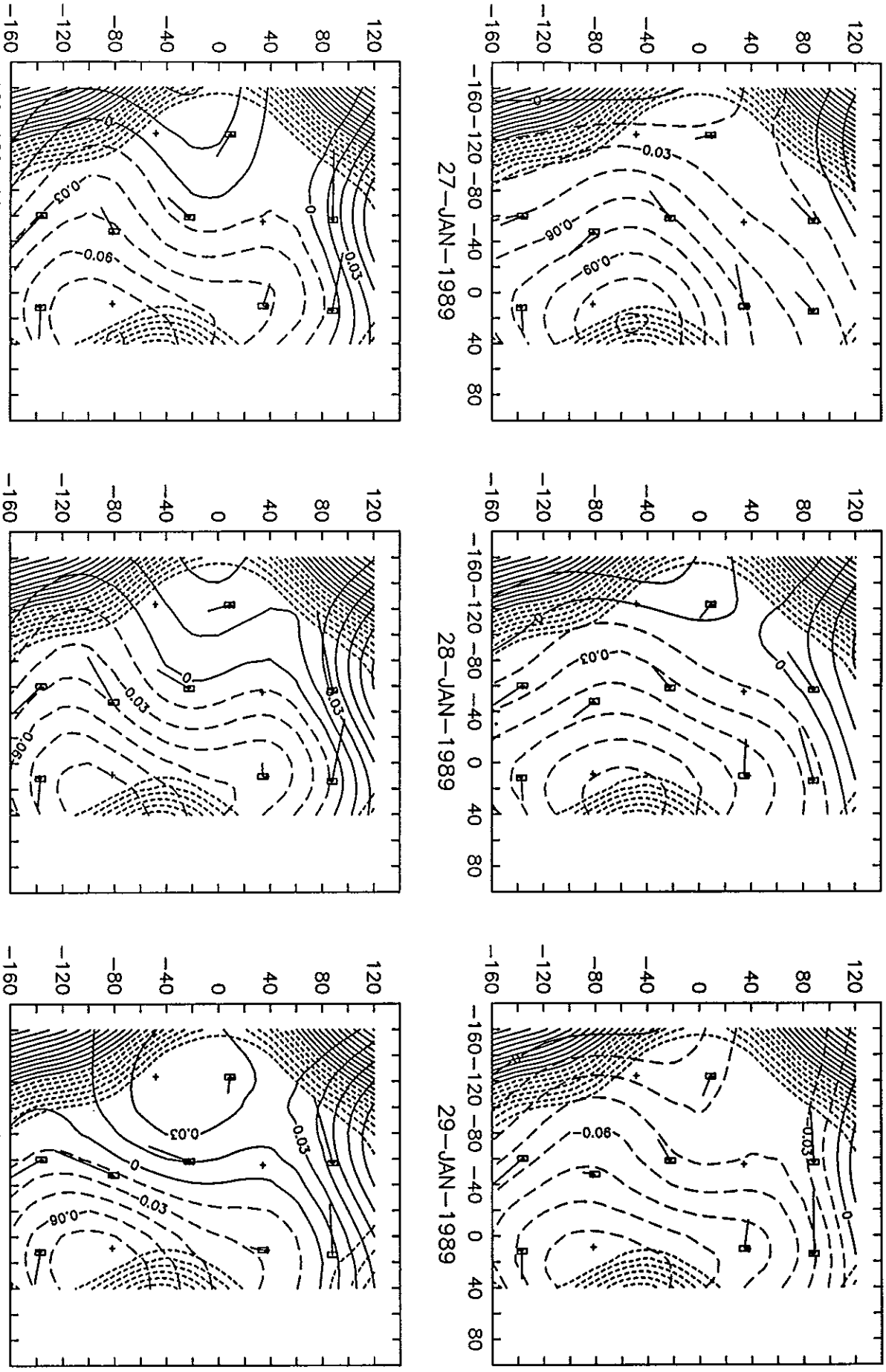
27-JAN-1989
28-JAN-1989
29-JAN-1989
30-JAN-1989
31-JAN-1989
01-FEB-1989

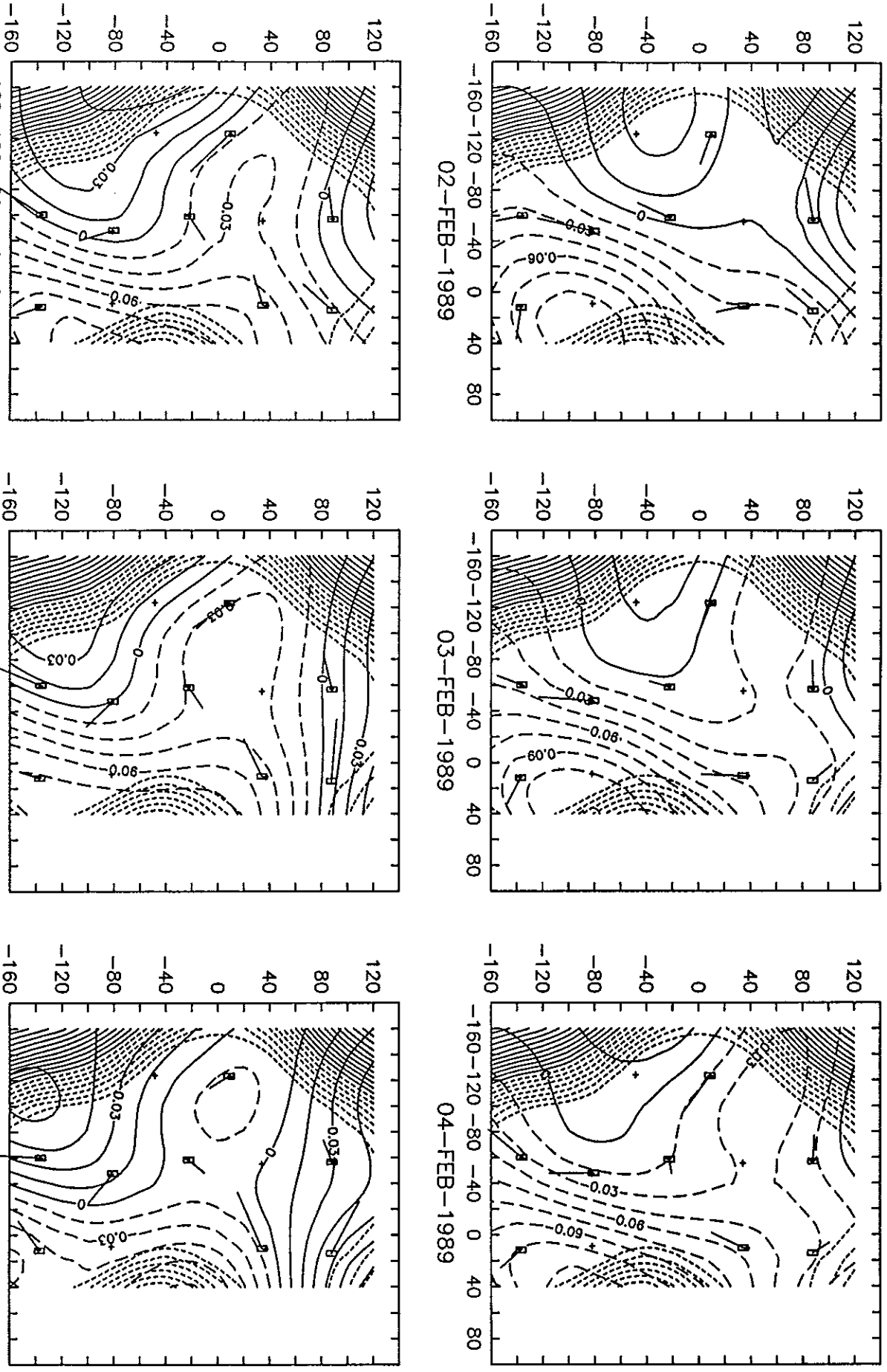
02-FEB-1989
03-FEB-1989
04-FEB-1989
05-FEB-1989
06-FEB-1989
07-FEB-1989

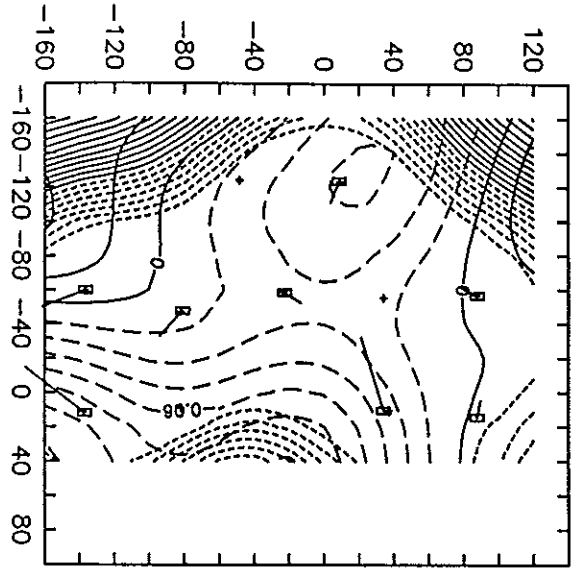
08-FEB-1989
-0.06
0

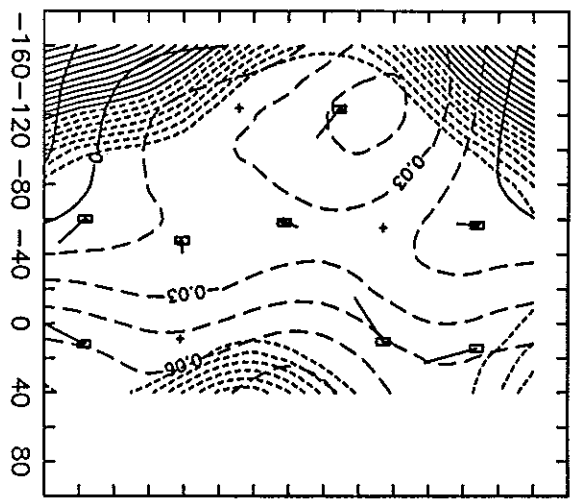
09-FEB-1989
0.03
-0.03
-0.06
0

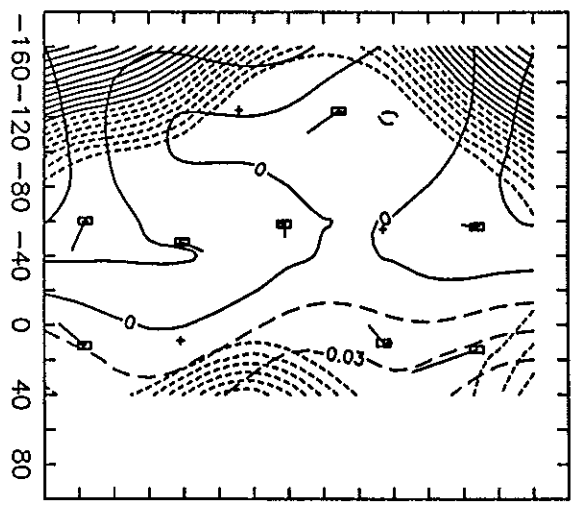
10-FEB-1989
0.03
0

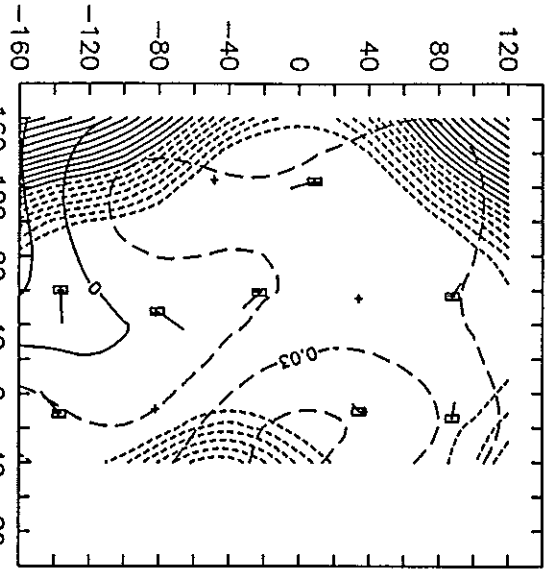
11-FEB-1989
-0.03
0

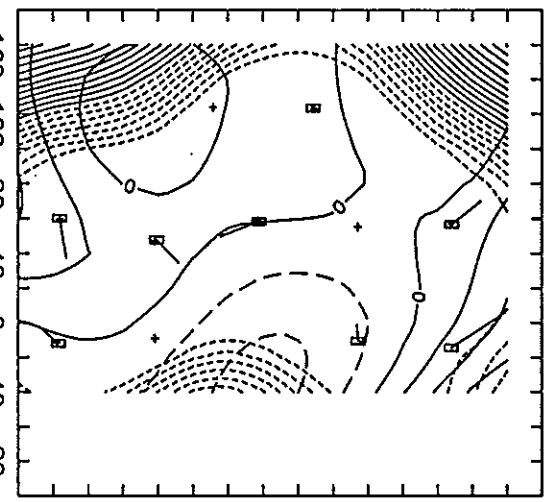
12-FEB-1989
0

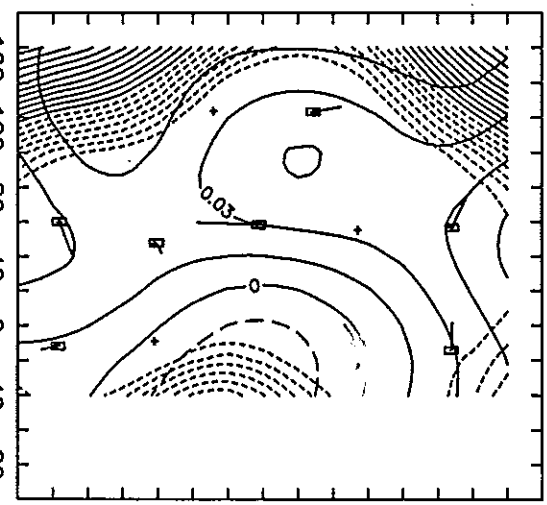
13-FEB-1989
0.03
0

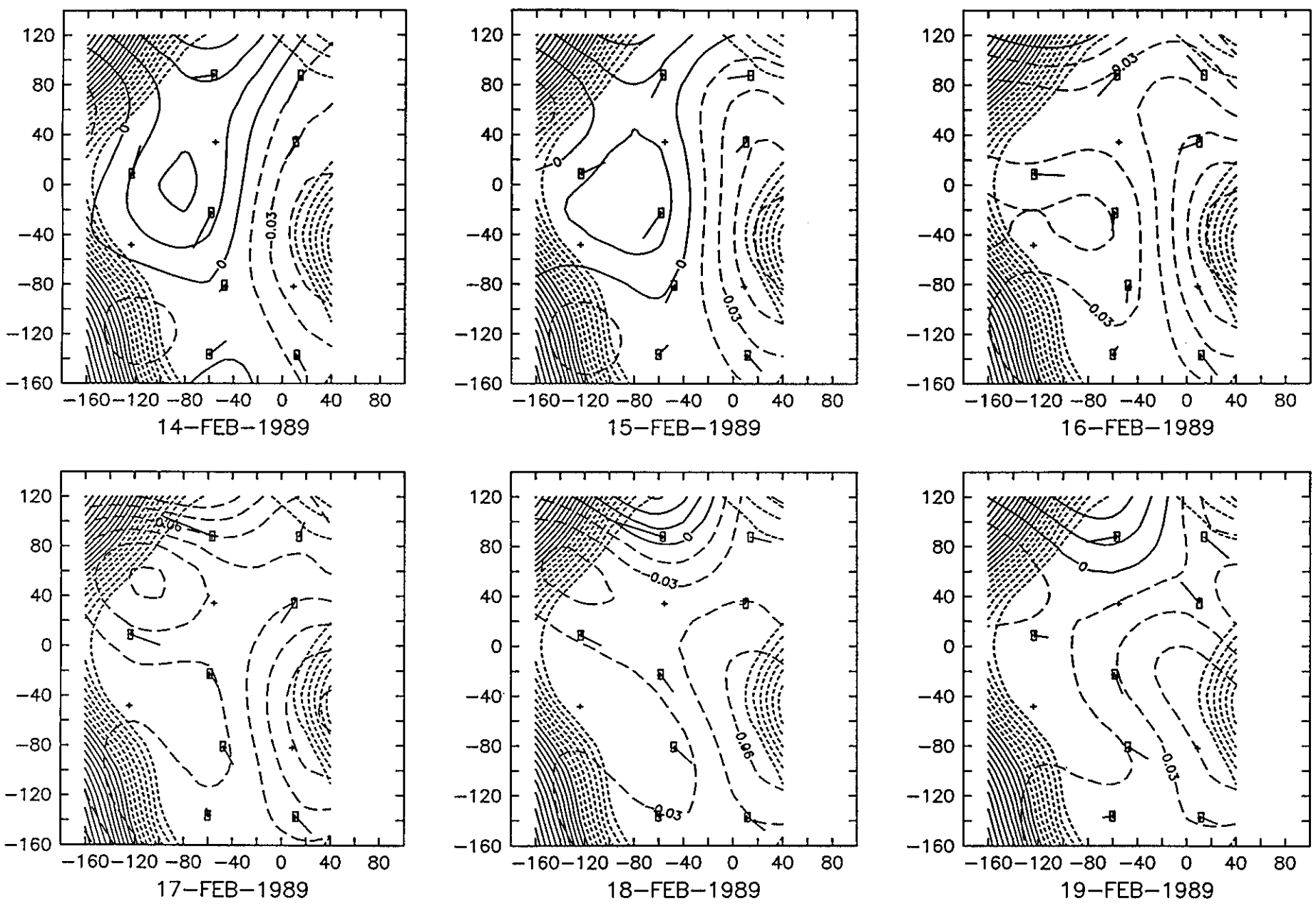
14-FEB-1989
15-FEB-1989
16-FEB-1989
17-FEB-1989
18-FEB-1989
19-FEB-1989

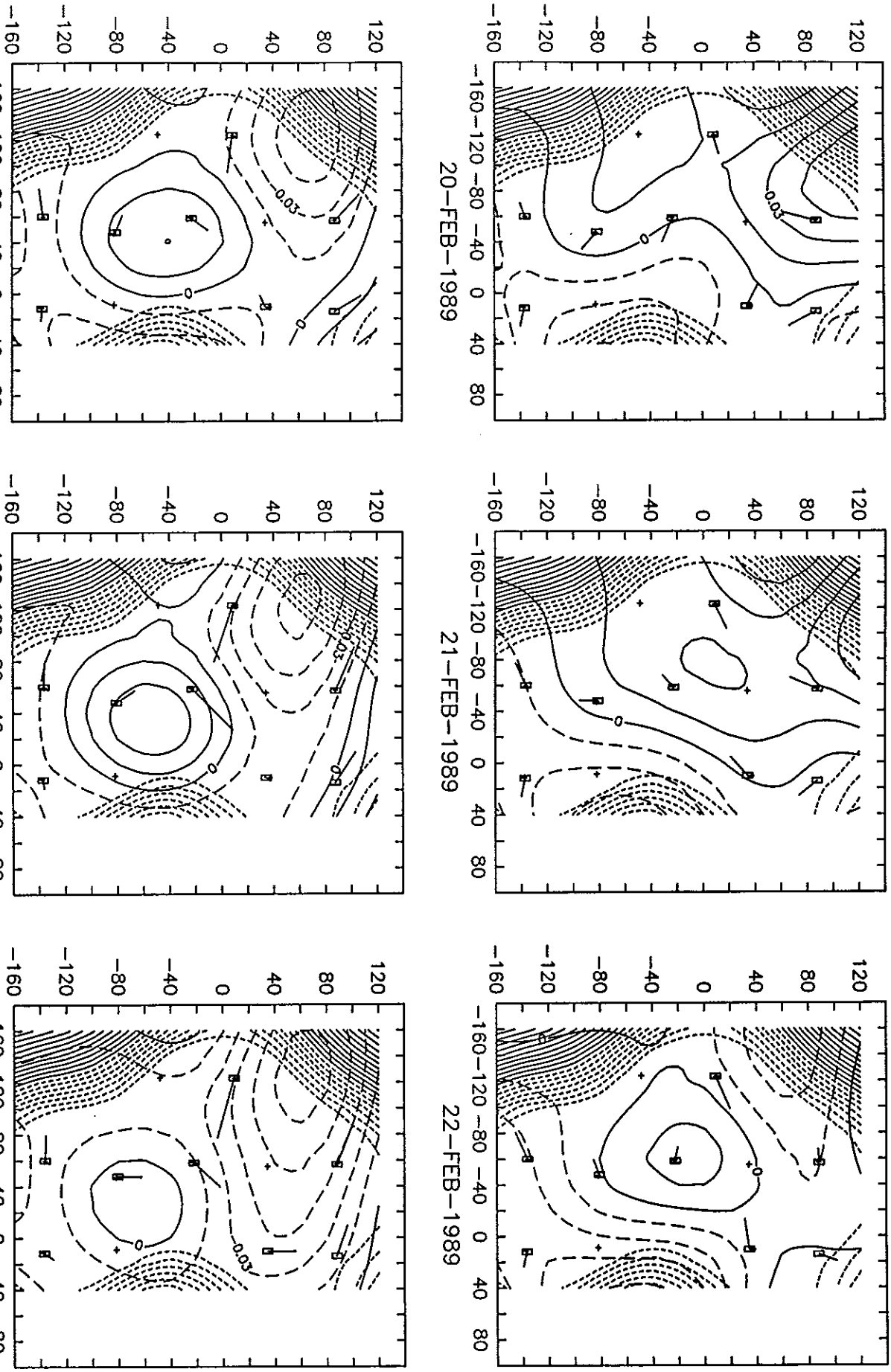
20-FEB-1989
21-FEB-1989
22-FEB-1989
23-FEB-1989
24-FEB-1989
25-FEB-1989

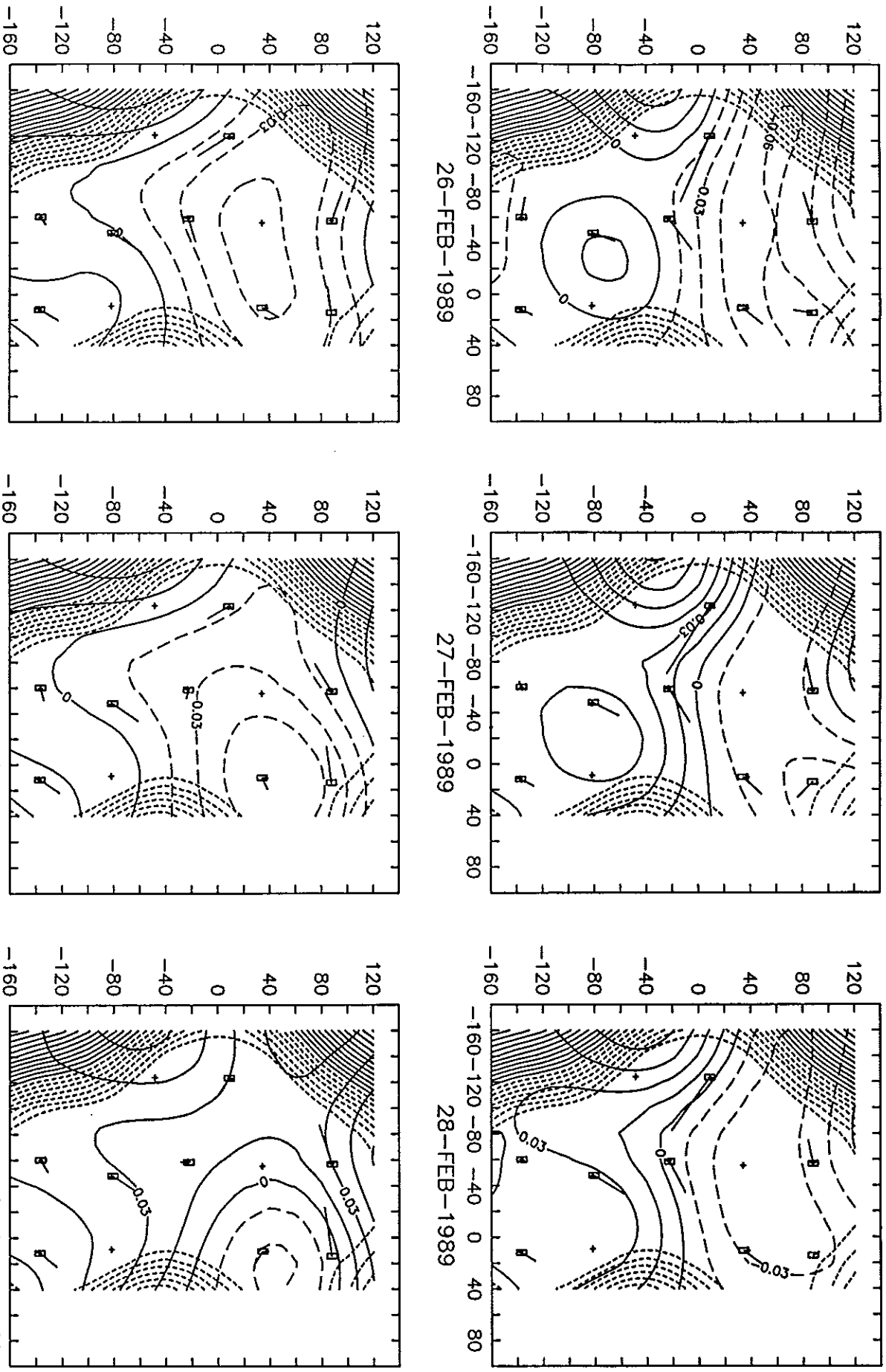
26-FEB-1989
27-FEB-1989
28-FEB-1989
01-MAR-1989
02-MAR-1989
03-MAR-1989

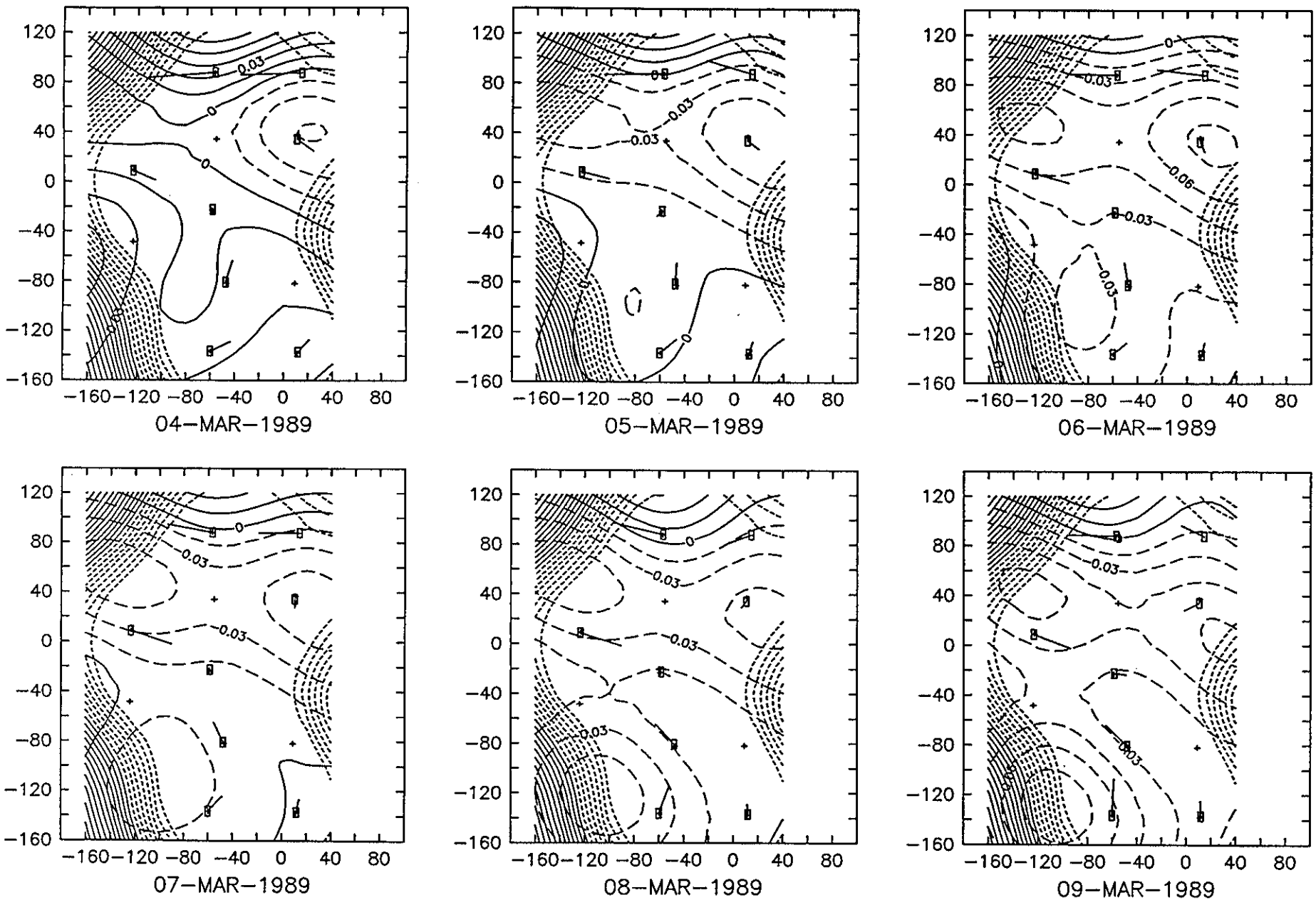
120
80
40
0
−40
−80
−120
−160
−160 −120 −80 −40 0 40 80
0.03
0
−0.03
0.06
04−MAR−1989
05−MAR−1989
06−MAR−1989
07−MAR−1989
08−MAR−1989
09−MAR−1989

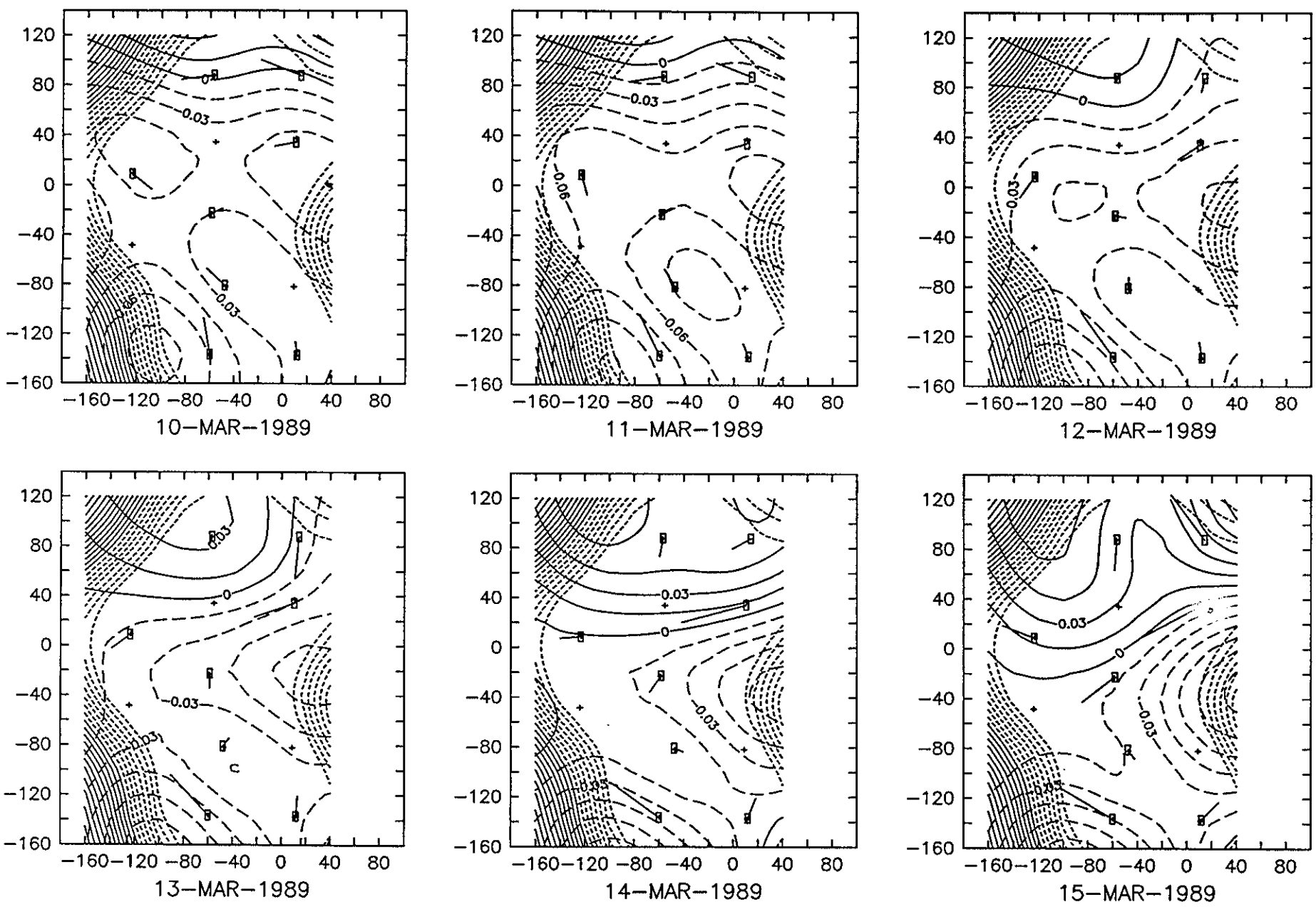
10−MAR−1989
11−MAR−1989
12−MAR−1989
13−MAR−1989
14−MAR−1989
15−MAR−1989

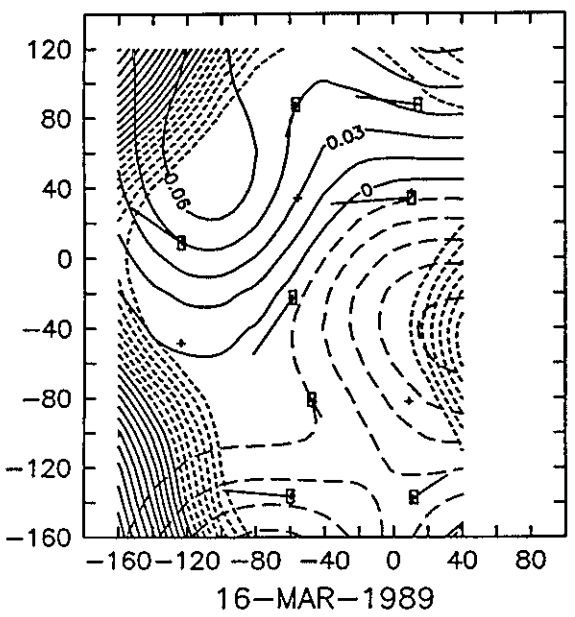
120
80
40
0
−40
−80
−120
−160
−160 −120 −80 −40 0 40 80
0.03
0
0.06
16−MAR−1989

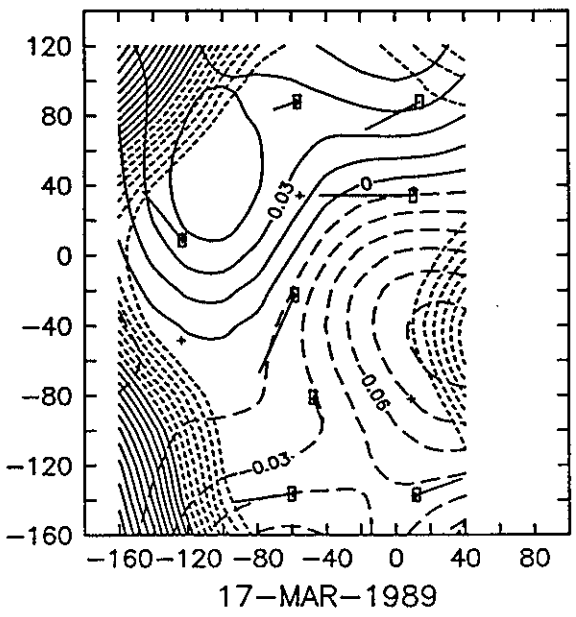
120
80
40
0
−40
−80
−120
−160
−160 −120 −80 −40 0 40 80
0.03
0
0.06
17−MAR−1989

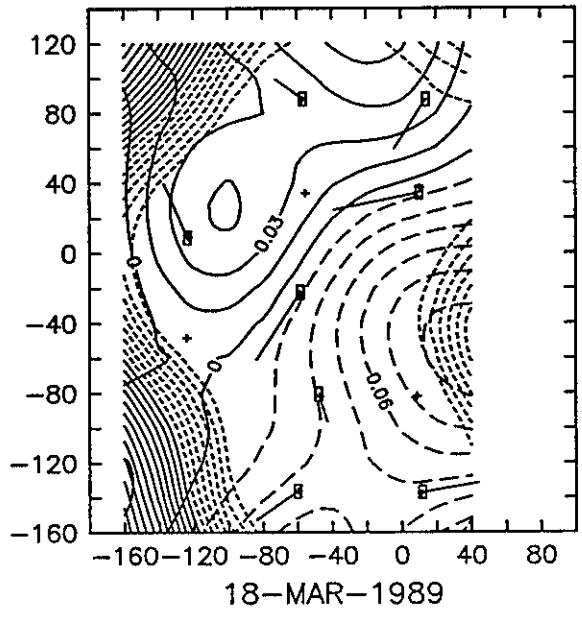
120
80
40
0
−40
−80
−120
−160
−160 −120 −80 −40 0 40 80
0.03
0
0.06
18−MAR−1989

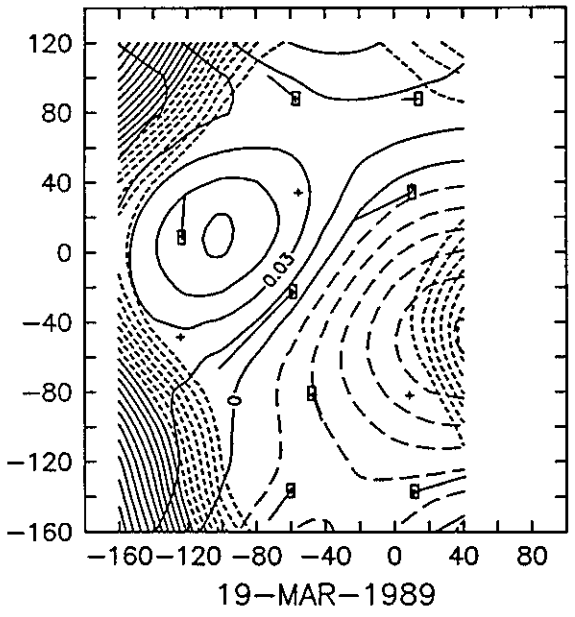
120
80
40
0
−40
−80
−120
−160
−160 −120 −80 −40 0 40 80
0.03
0
19−MAR−1989

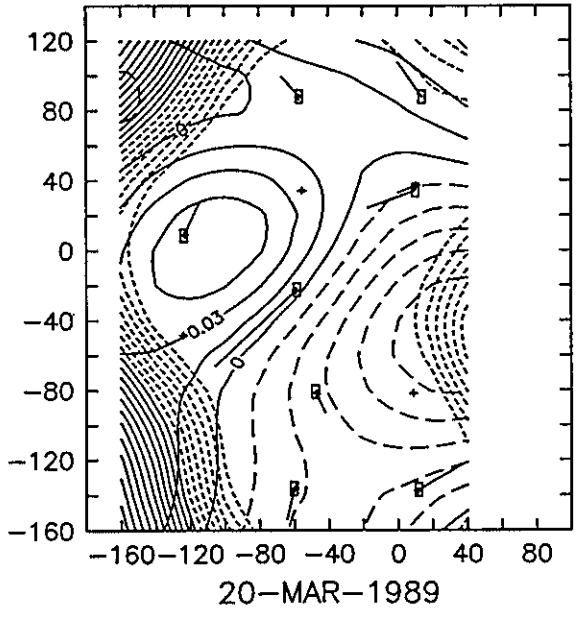
120
80
40
0
−40
−80
−120
−160
−160 −120 −80 −40 0 40 80
0.03
0
20−MAR−1989

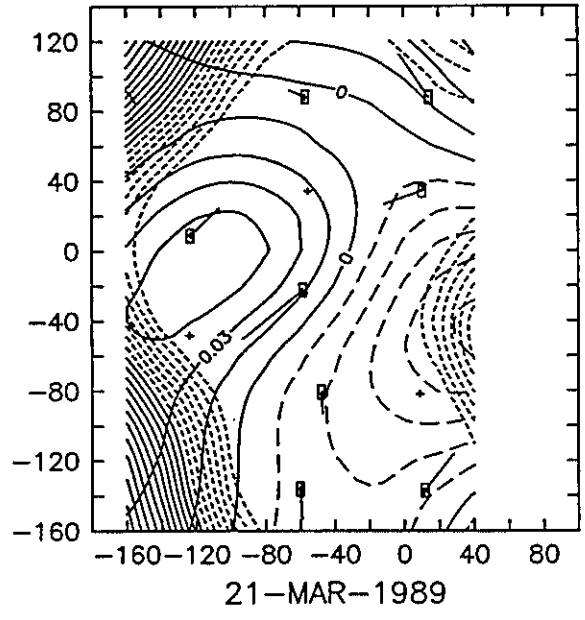
120
80
40
0
−40
−80
−120
−160
−160 −120 −80 −40 0 40 80
0
0.03
21−MAR−1989

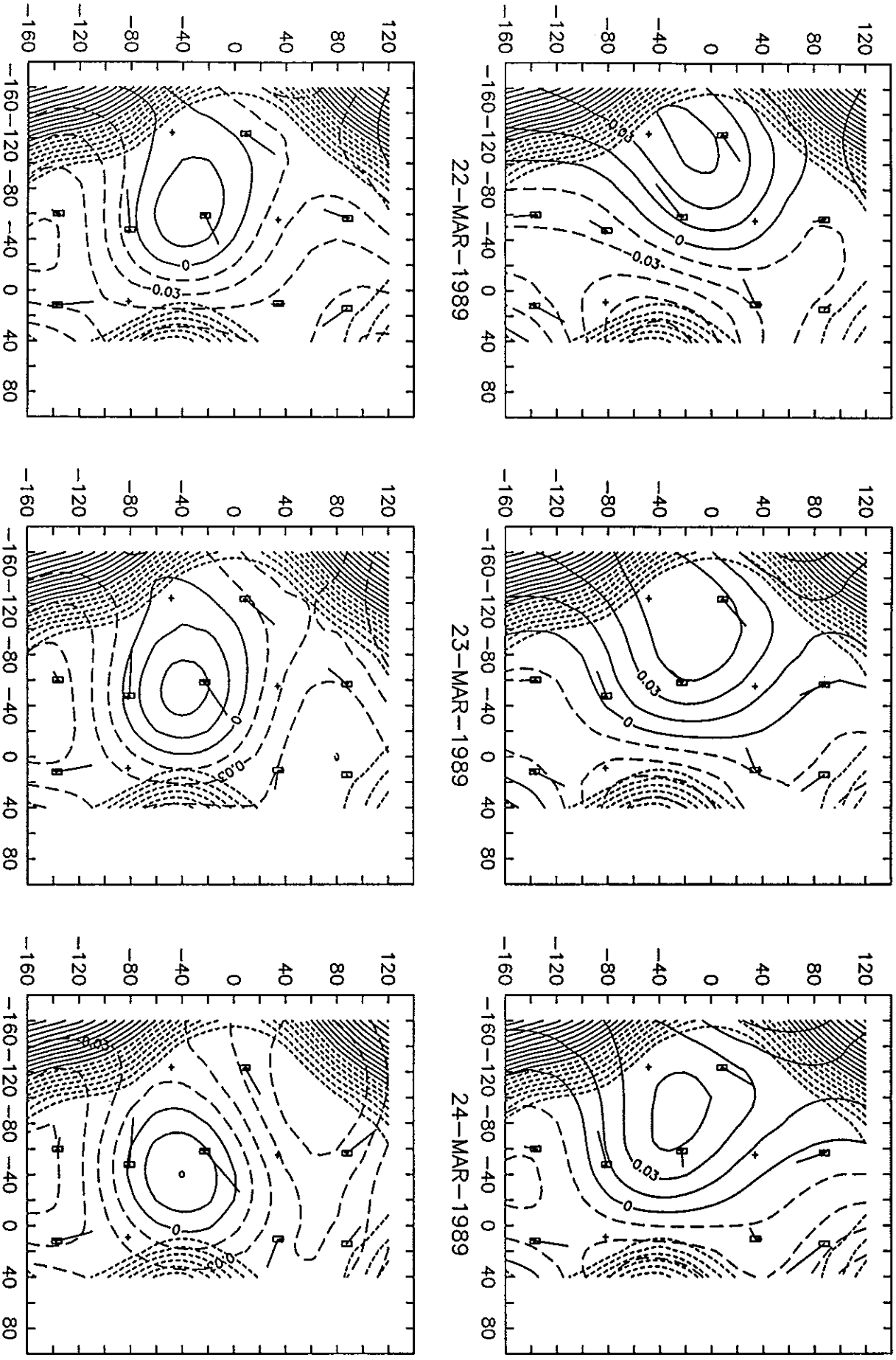
22-MAR-1989
23-MAR-1989
24-MAR-1989
25-MAR-1989
26-MAR-1989
27-MAR-1989
0.03
0
-0.03

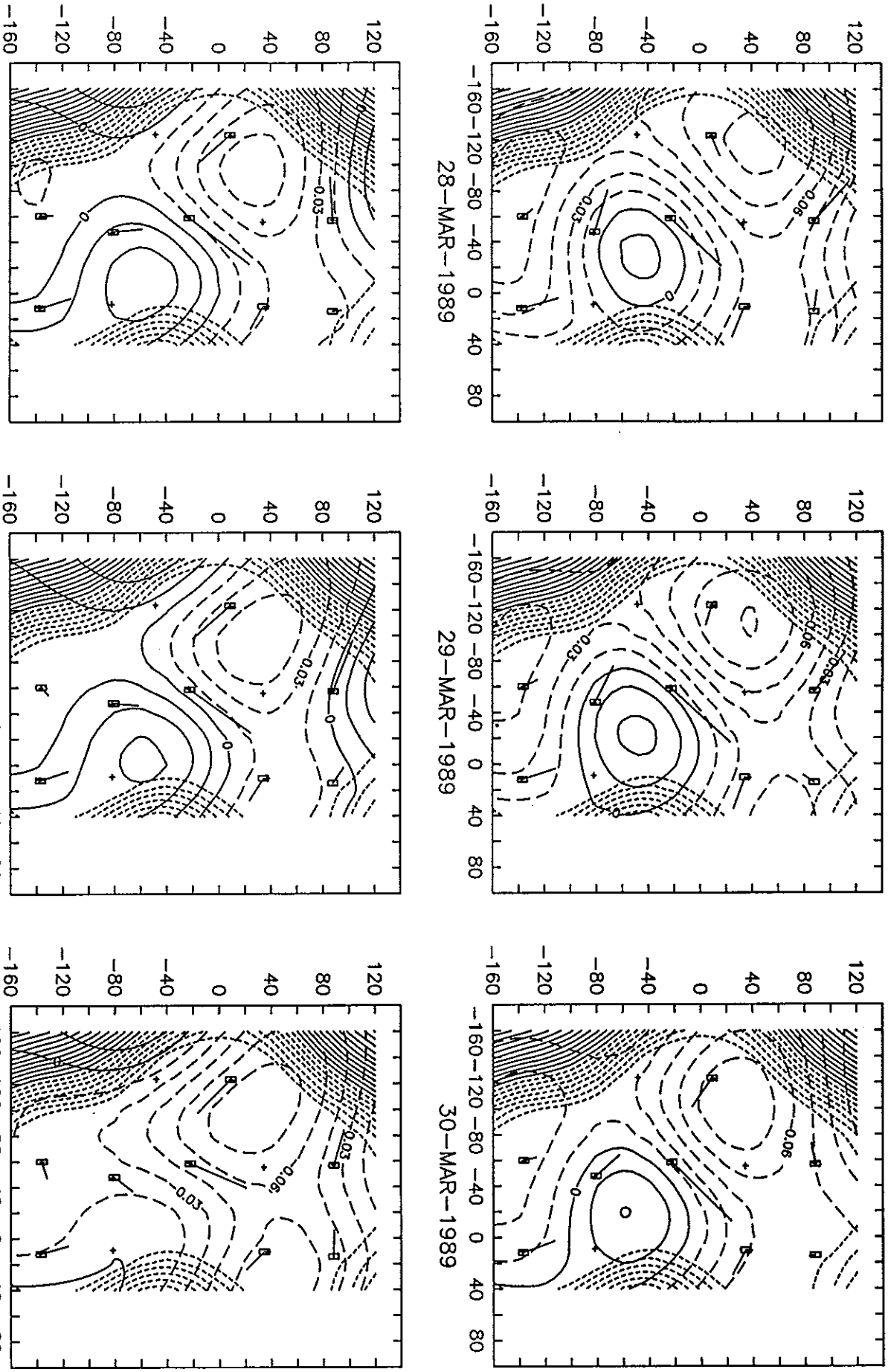
28-MAR-1989
29-MAR-1989
30-MAR-1989
31-MAR-1989
01-APR-1989
02-APR-1989

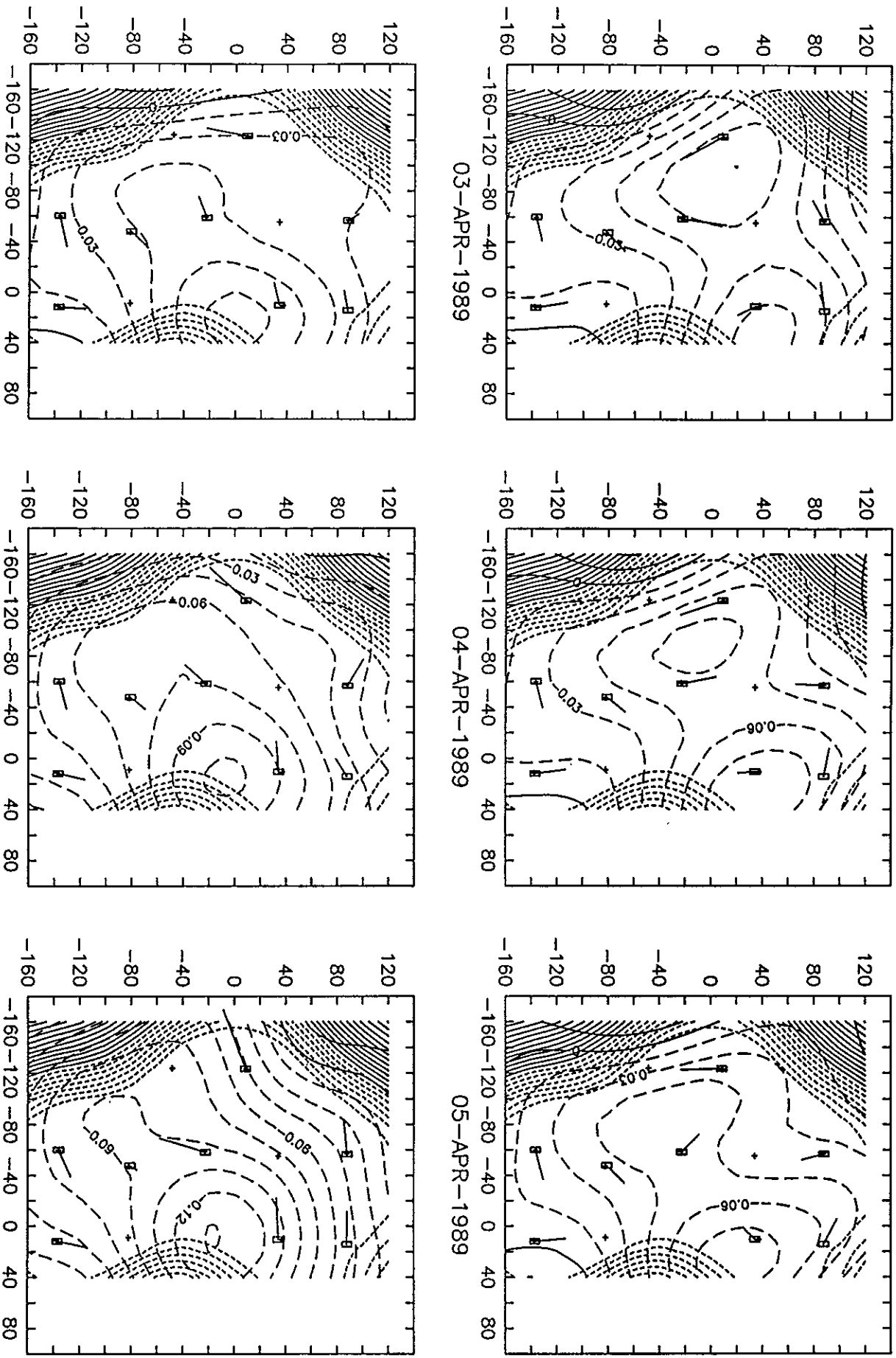
03-APR-1989
04-APR-1989
05-APR-1989
06-APR-1989
07-APR-1989
08-APR-1989

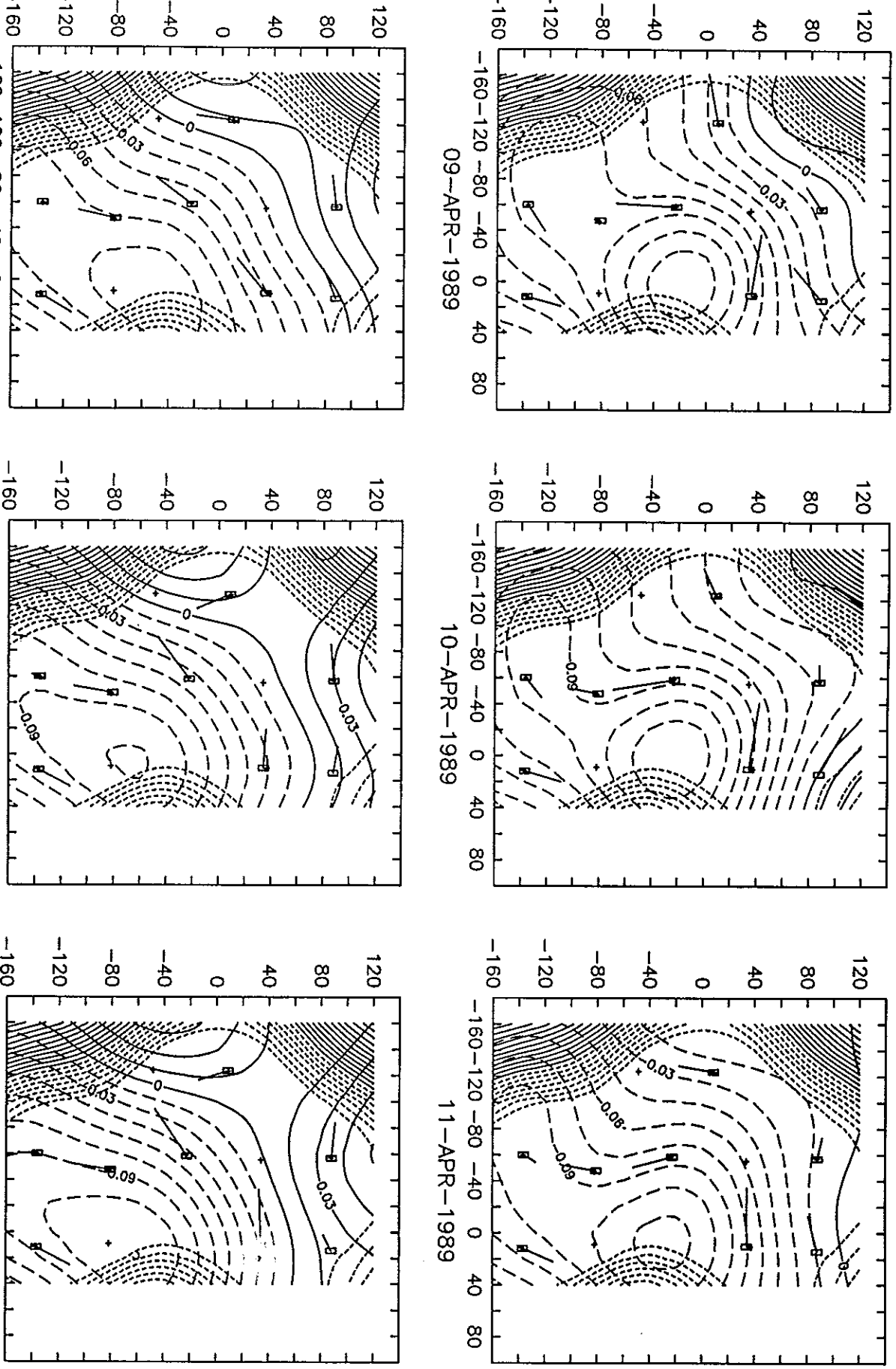
09-APR-1989
10-APR-1989
11-APR-1989
12-APR-1989
13-APR-1989
14-APR-1989

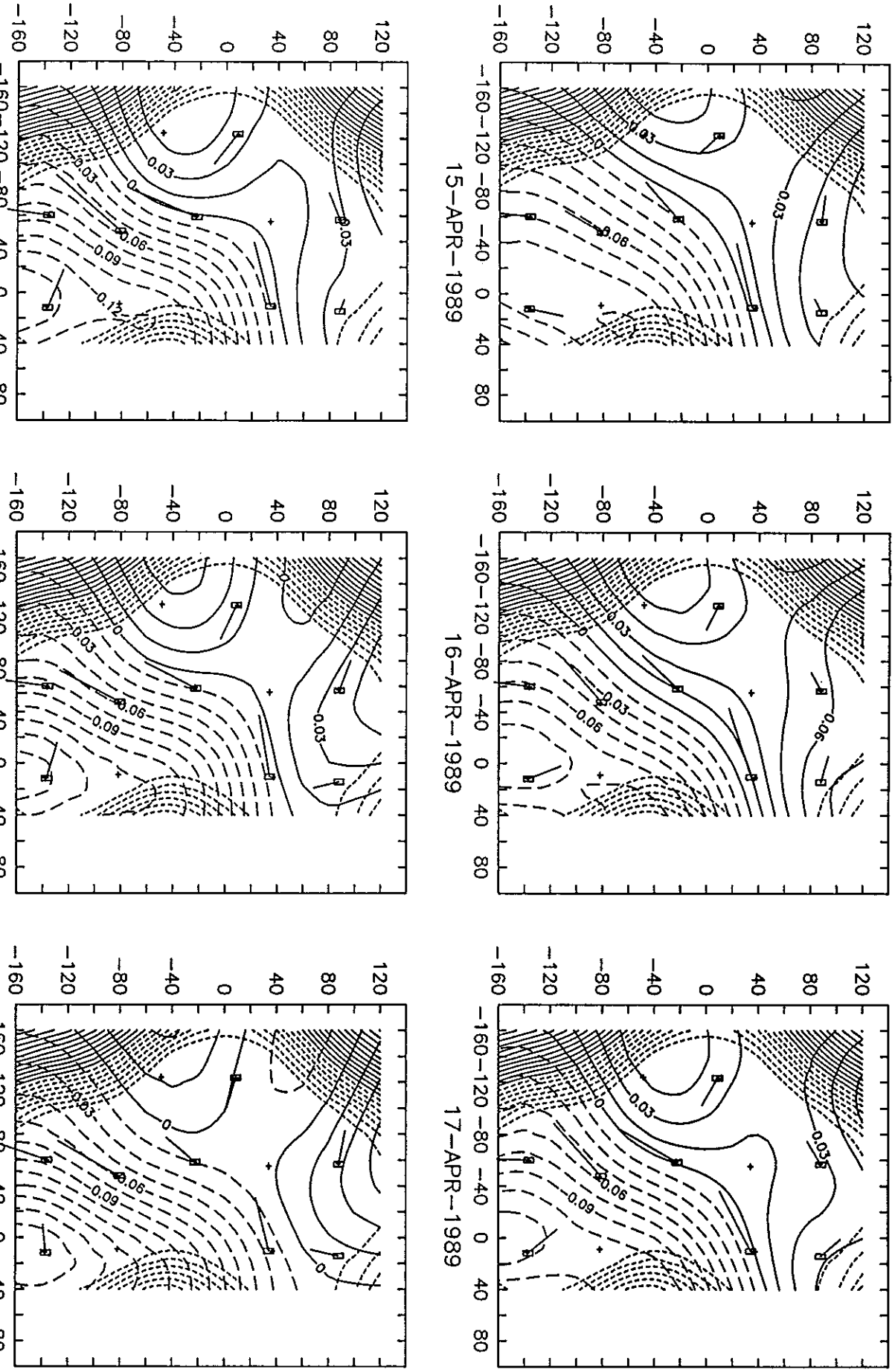
15-APR-1989
16-APR-1989
17-APR-1989
18-APR-1989
19-APR-1989
20-APR-1989

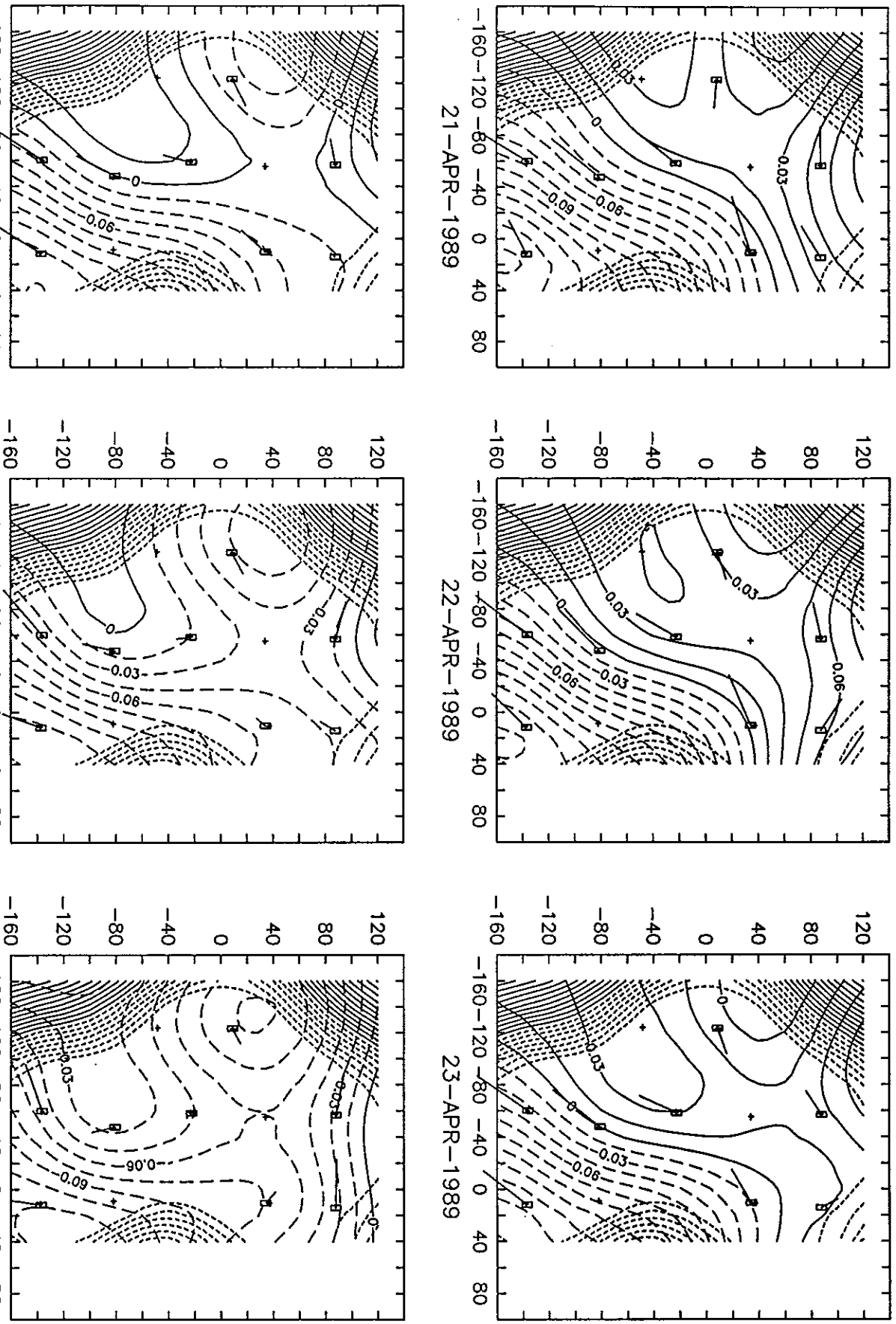
21-APR-1989
22-APR-1989
23-APR-1989
24-APR-1989
25-APR-1989
26-APR-1989

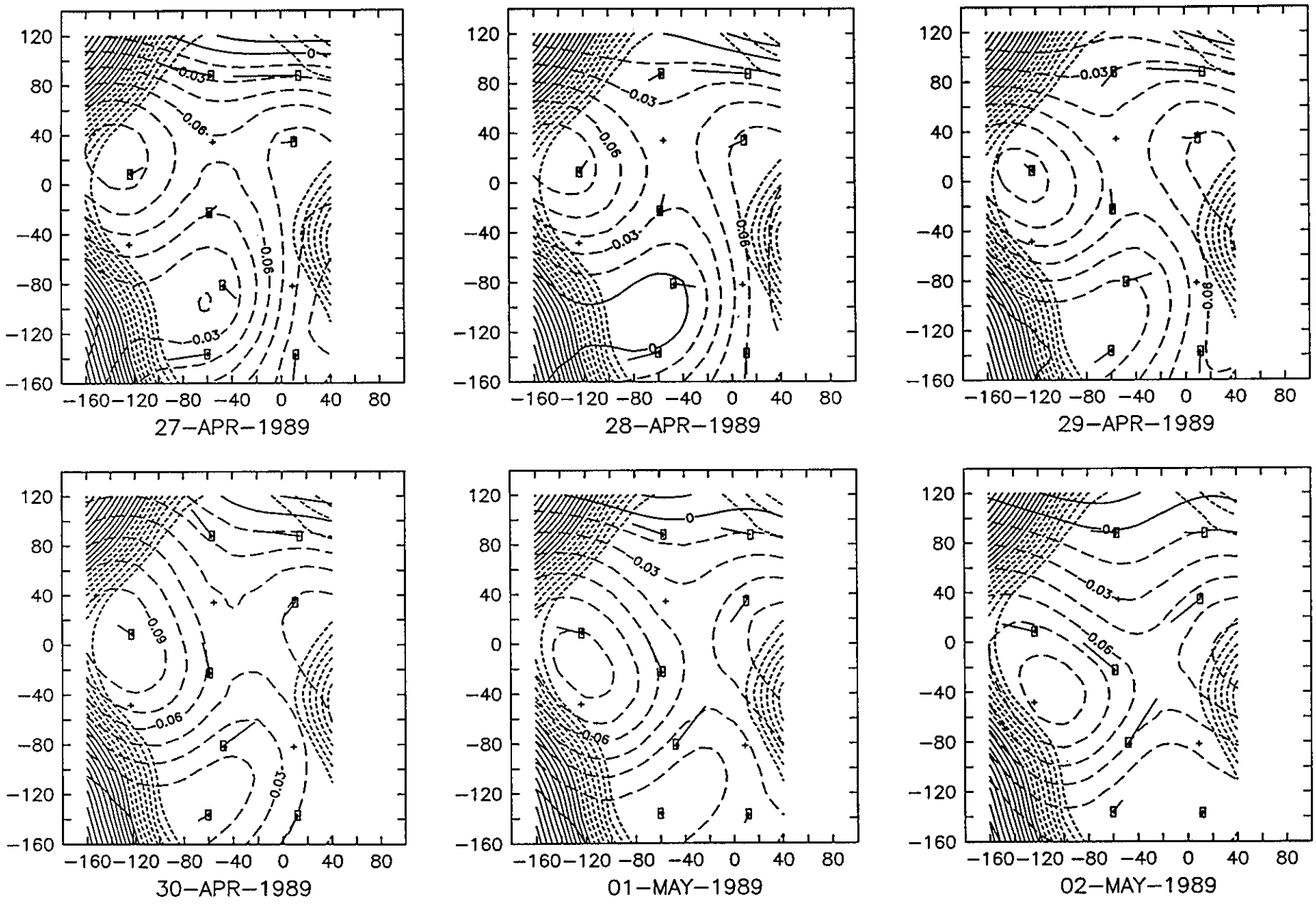
120
80
40
0
−40
−80
−120
−160
−160 −120 −80 −40 0 40 80
0
0.03
0.06
0.09
27−APR−1989
28−APR−1989
29−APR−1989
30−APR−1989
01−MAY−1989
02−MAY−1989

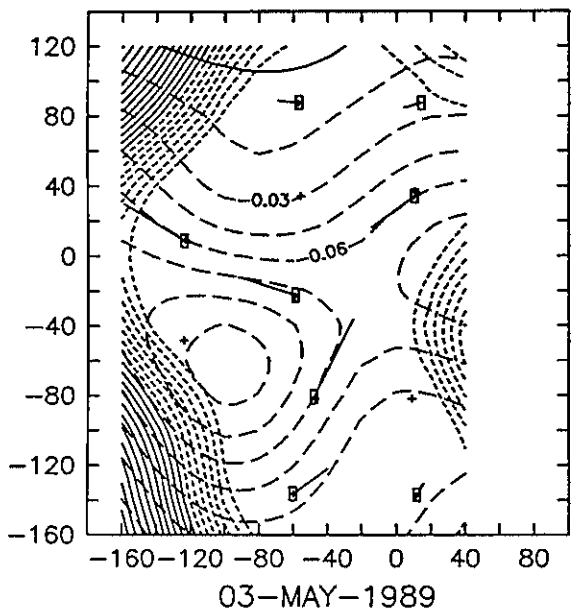
120
80
40
0
−40
−80
−120
−160
−160 −120 −80 −40 0 40 80
0.03
0.06
03−MAY−1989

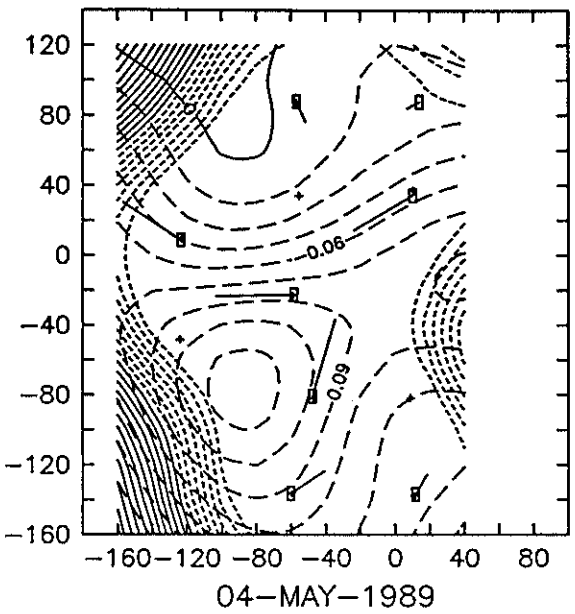
120
80
40
0
−40
−80
−120
−160
−160 −120 −80 −40 0 40 80
0.06
0.09
04−MAY−1989

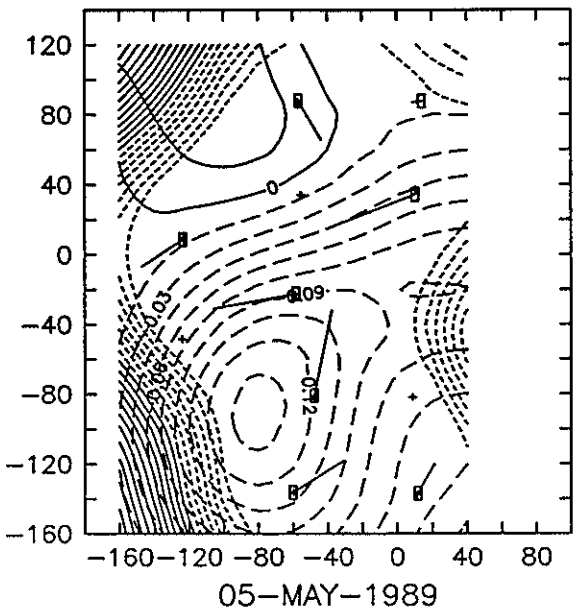
120
80
40
0
−40
−80
−120
−160
−160 −120 −80 −40 0 40 80
0
0.03
0.09
0.12
05−MAY−1989

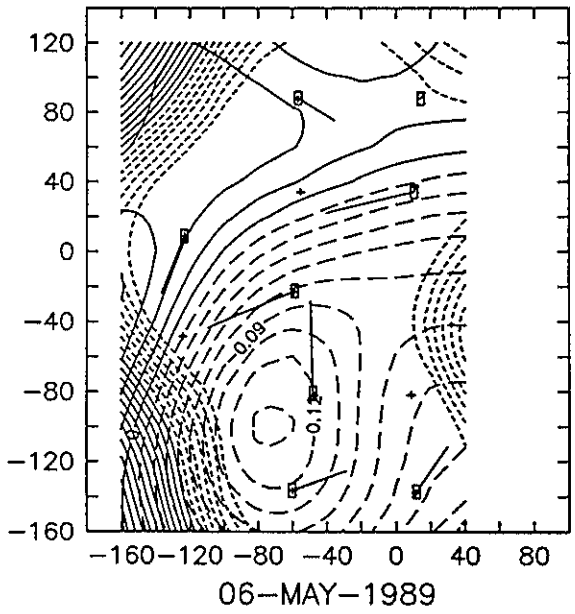
120
80
40
0
−40
−80
−120
−160
−160 −120 −80 −40 0 40 80
0.09
0.12
06−MAY−1989

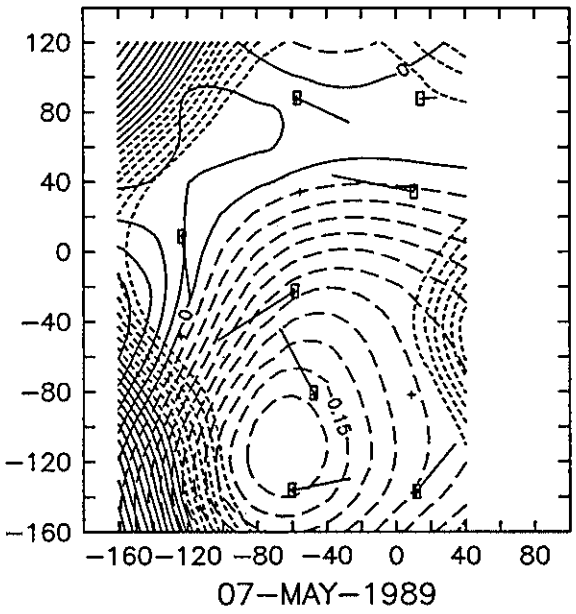
120
80
40
0
−40
−80
−120
−160
−160 −120 −80 −40 0 40 80
0
0.15
07−MAY−1989

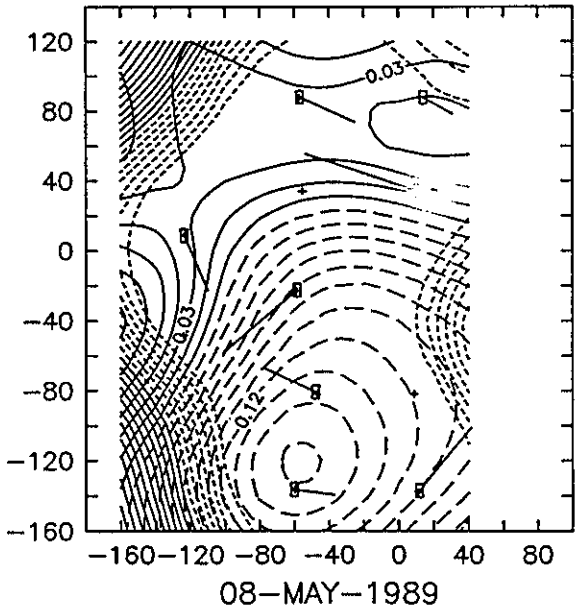
120
80
40
0
−40
−80
−120
−160
−160 −120 −80 −40 0 40 80
0.03
0.12
08−MAY−1989

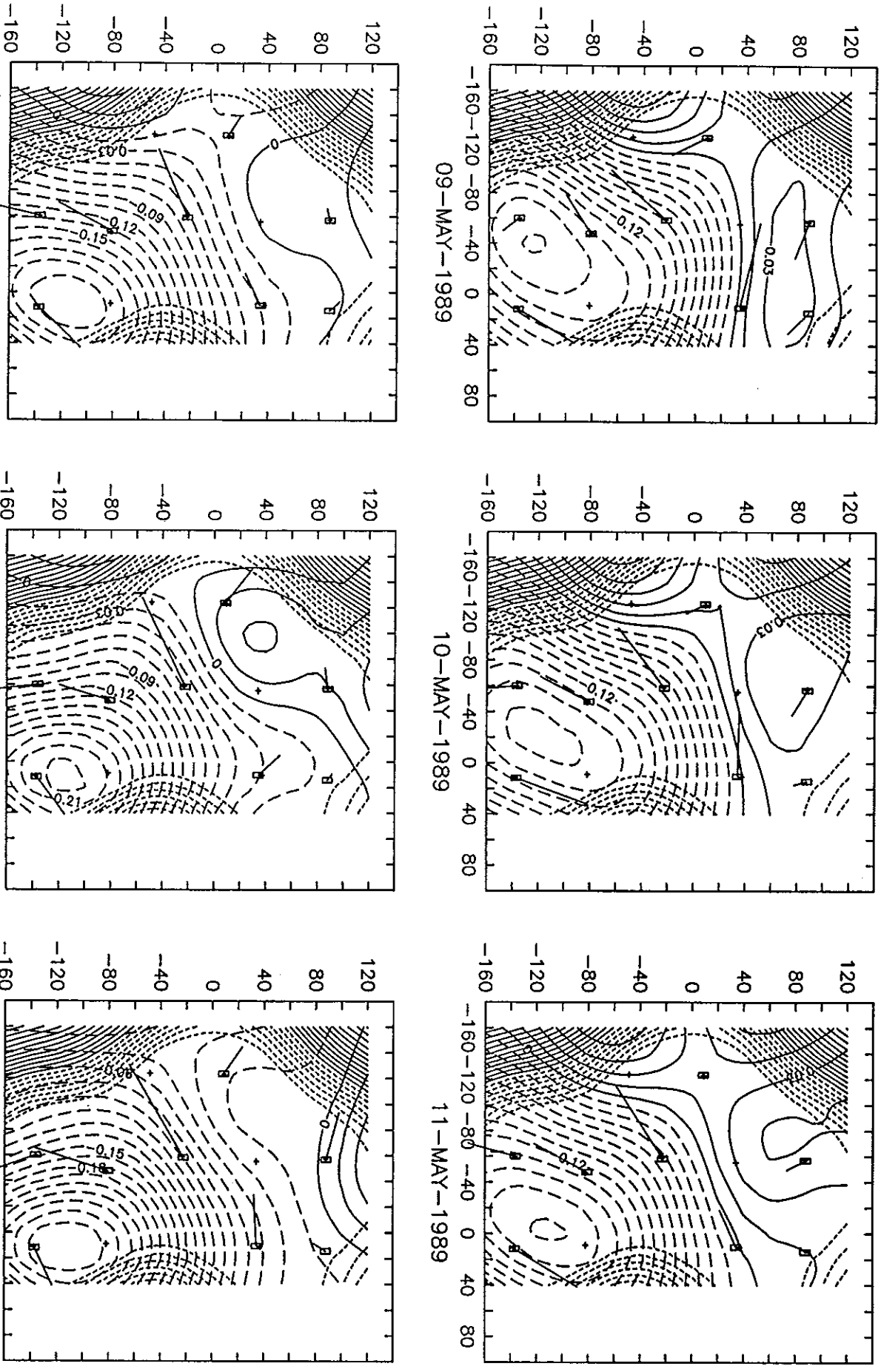
09-MAY-1989
10-MAY-1989
11-MAY-1989
12-MAY-1989
13-MAY-1989
14-MAY-1989

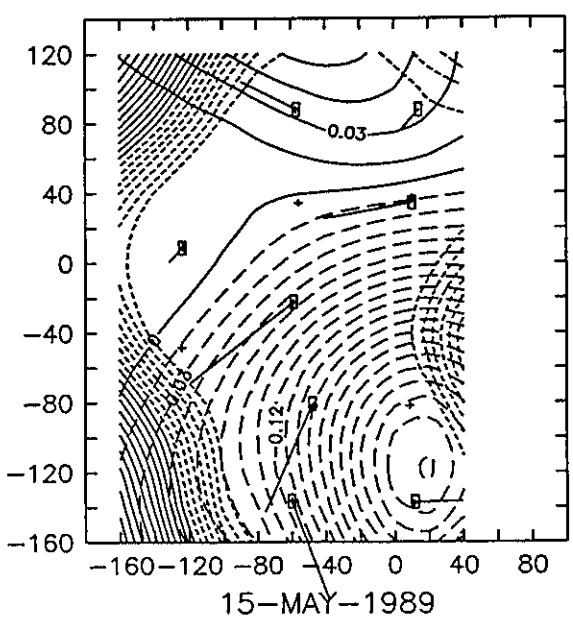
120
80
40
0
−40
−80
−120
−160
−160 −120 −80 −40 0 40 80
0.03
0.12
15−MAY−1989

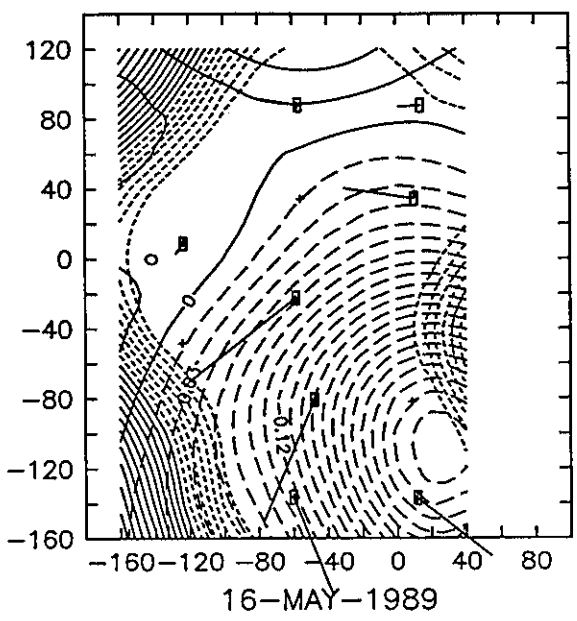
120
80
40
0
−40
−80
−120
−160
−160 −120 −80 −40 0 40 80
0
0.03
0.12
16−MAY−1989

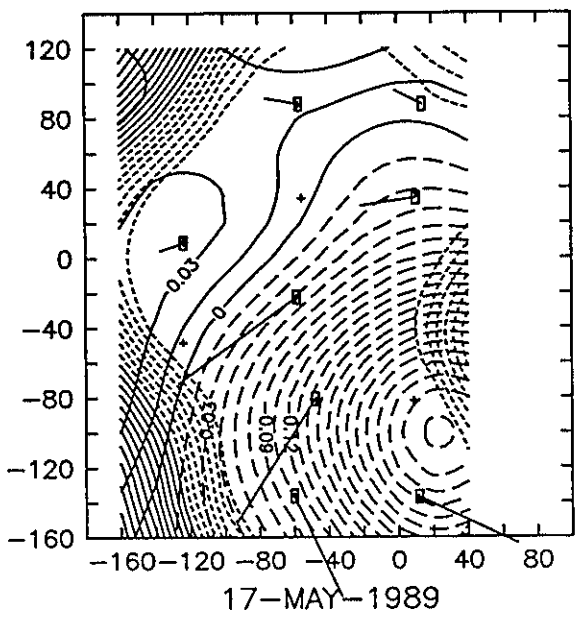
120
80
40
0
−40
−80
−120
−160
−160 −120 −80 −40 0 40 80
0.03
0
0.06
0.09
17−MAY−1989

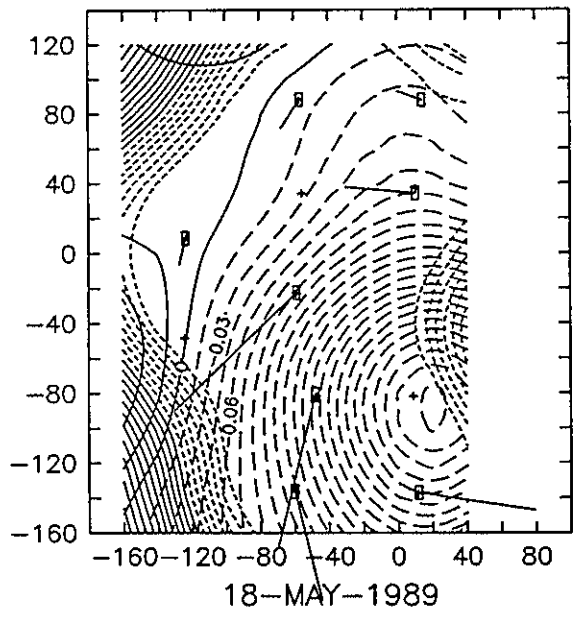
120
80
40
0
−40
−80
−120
−160
−160 −120 −80 −40 0 40 80
0.03
0.06
18−MAY−1989

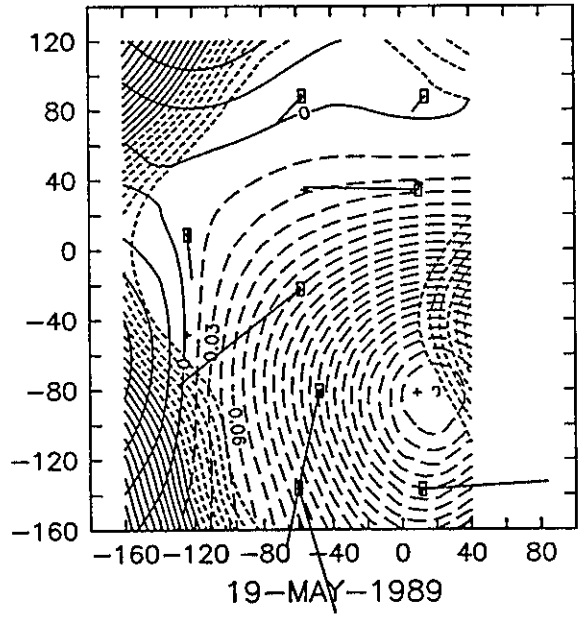
120
80
40
0
−40
−80
−120
−160
−160 −120 −80 −40 0 40 80
0
0.03
0.06
19−MAY−1989

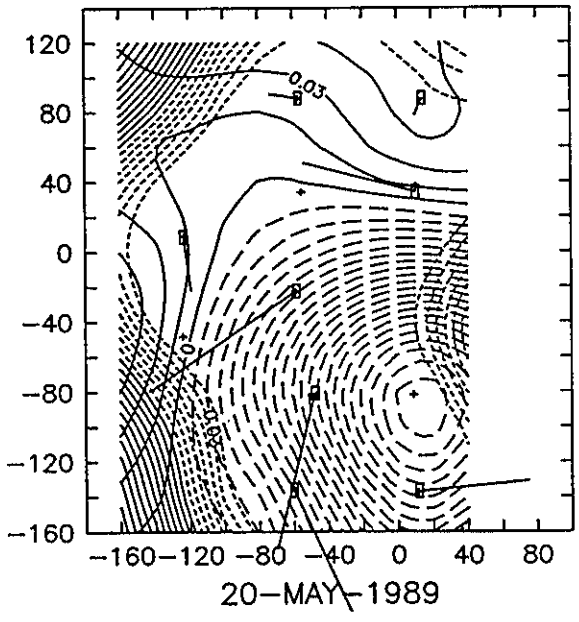
120
80
40
0
−40
−80
−120
−160
−160 −120 −80 −40 0 40 80
0.03
0
0.03
20−MAY−1989

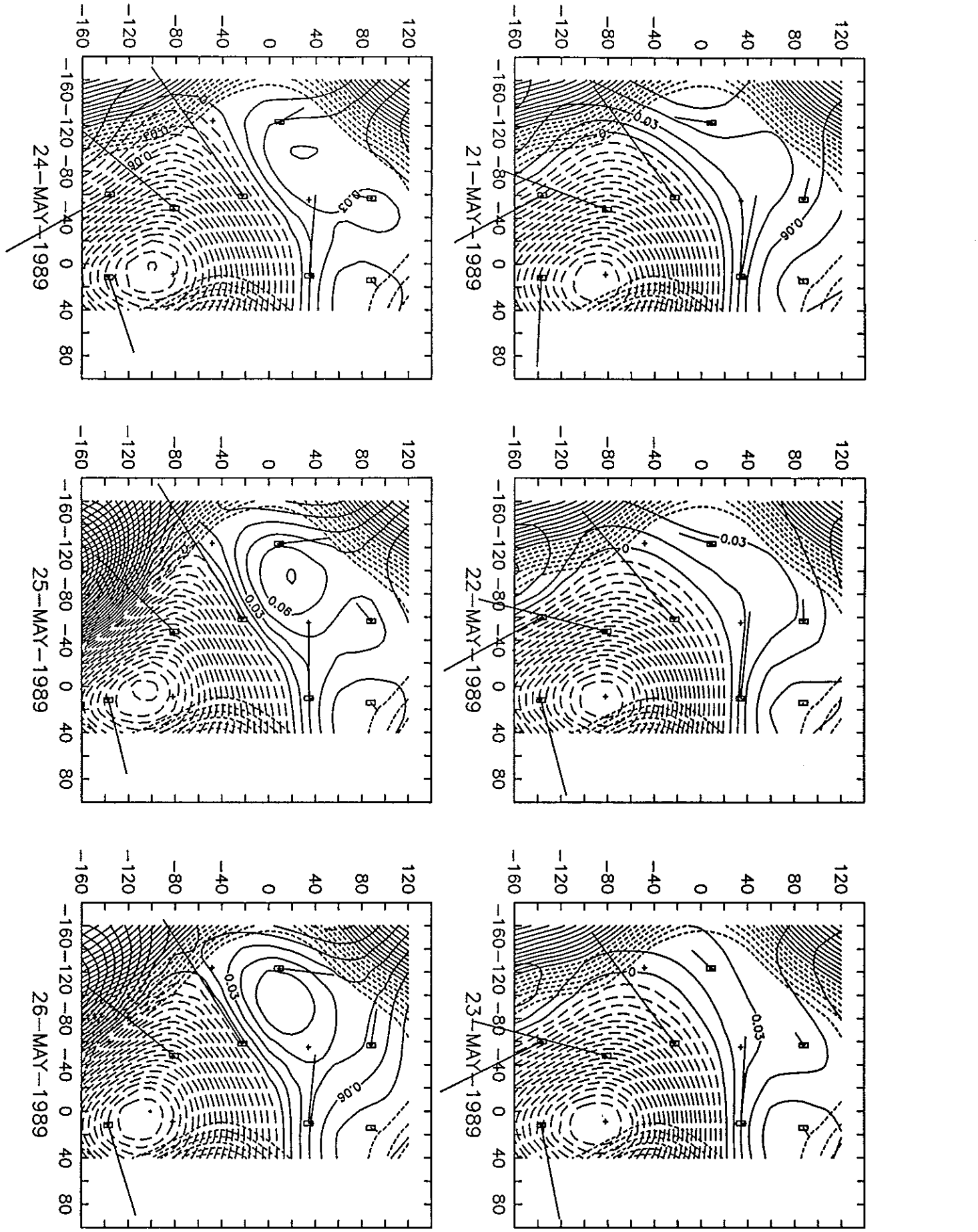
21-MAY-1989
22-MAY-1989
23-MAY-1989
24-MAY-1989
25-MAY-1989
26-MAY-1989
0.03
0.06
0
120
80
40
0
-40
-80
-120
-160
-160 -120 -80 -40 0 40 80

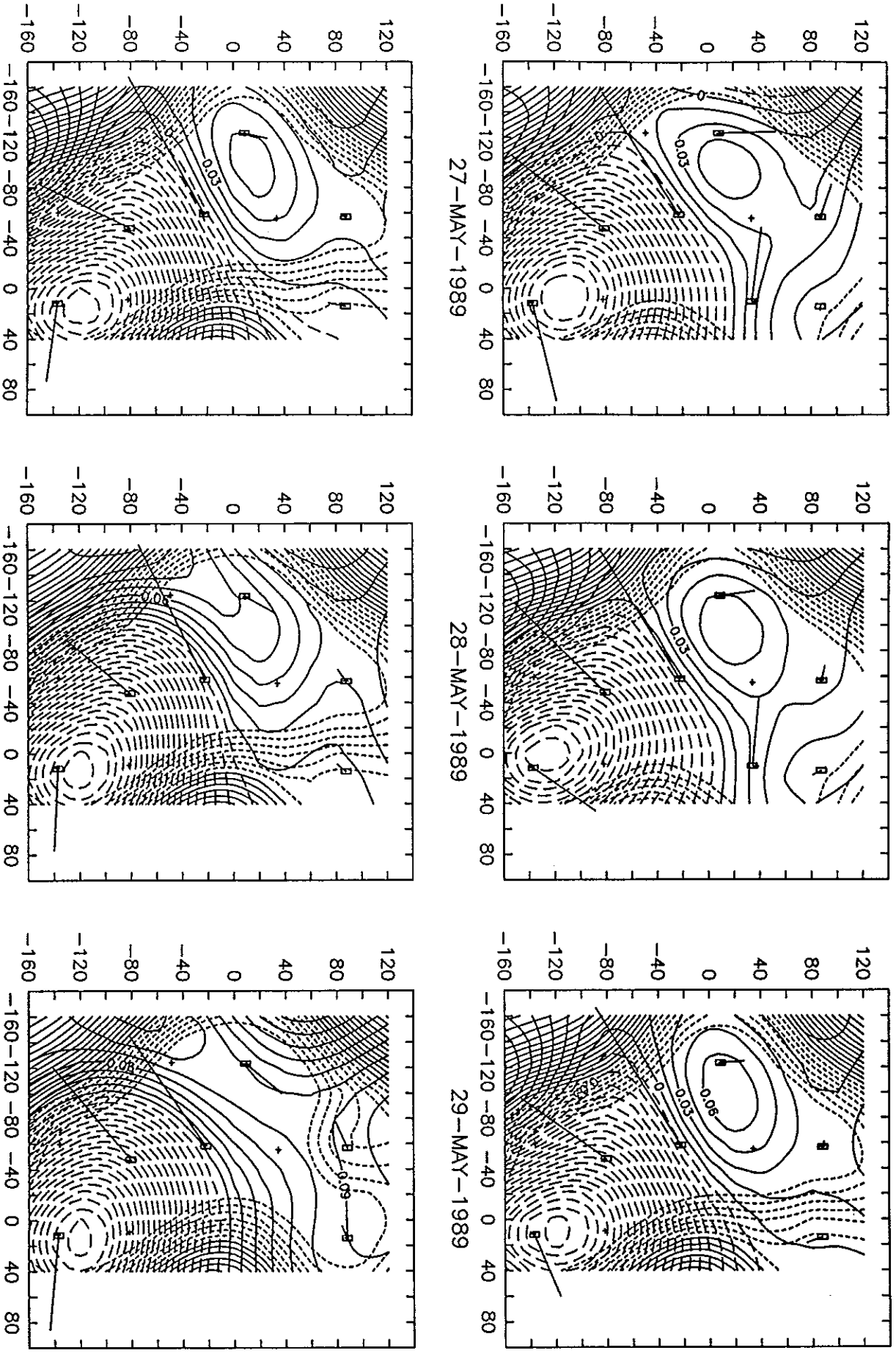
27-MAY-1989
28-MAY-1989
29-MAY-1989
30-MAY-1989
31-MAY-1989
01-JUN-1989

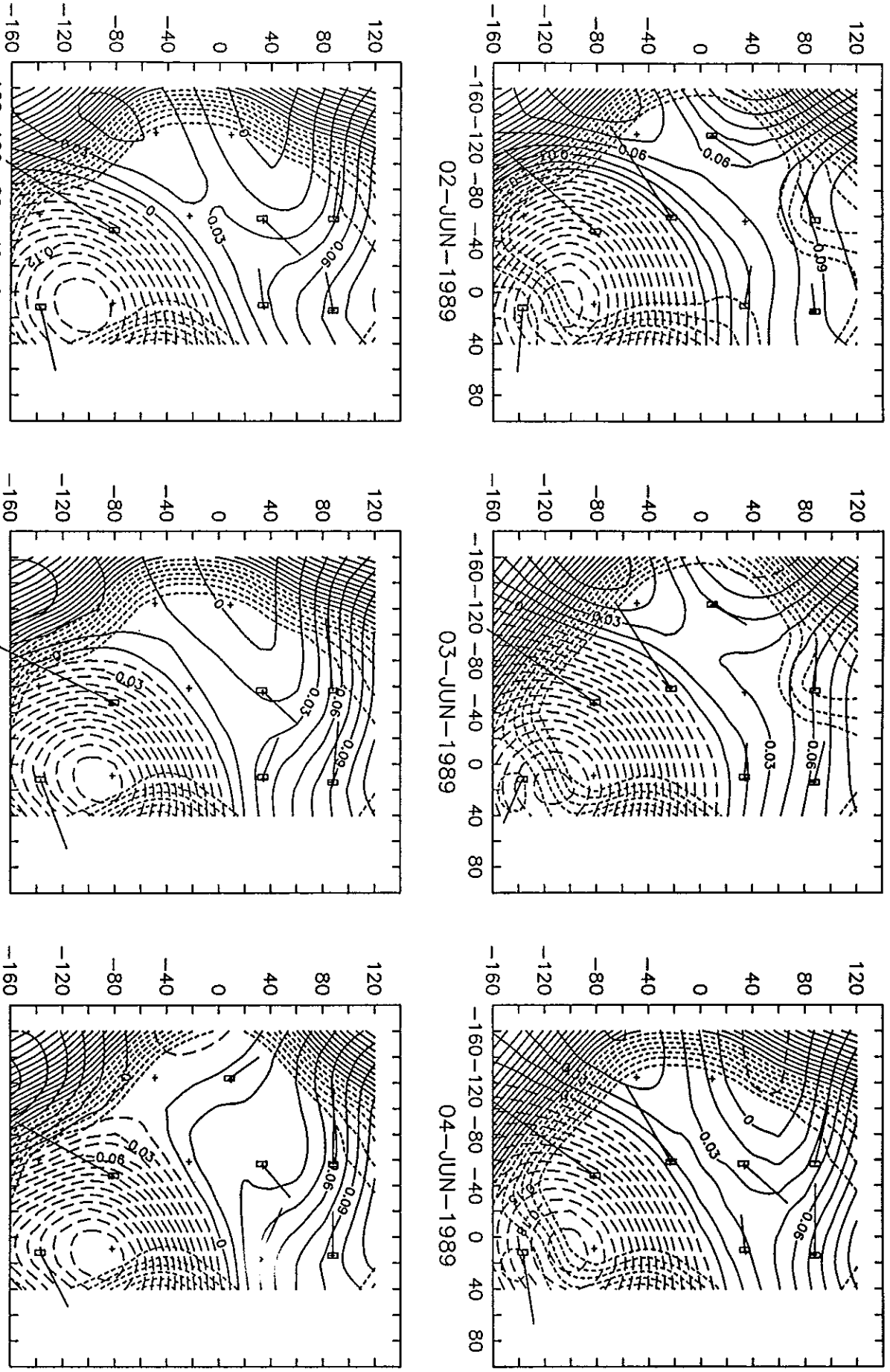
02-JUN-1989
03-JUN-1989
04-JUN-1989
05-JUN-1989
06-JUN-1989
07-JUN-1989

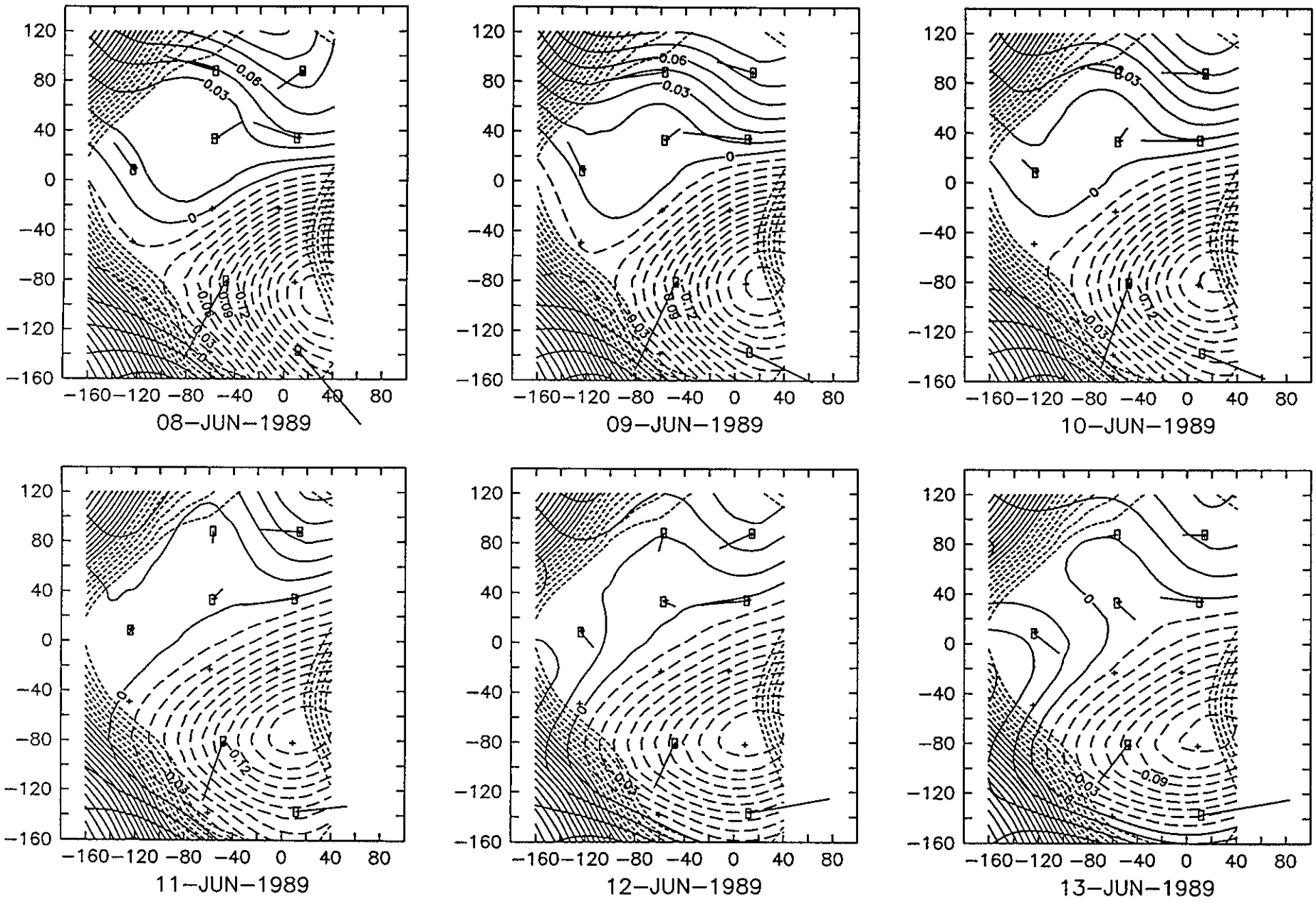
08–JUN–1989
09–JUN–1989
10–JUN–1989
11–JUN–1989
12–JUN–1989
13–JUN–1989

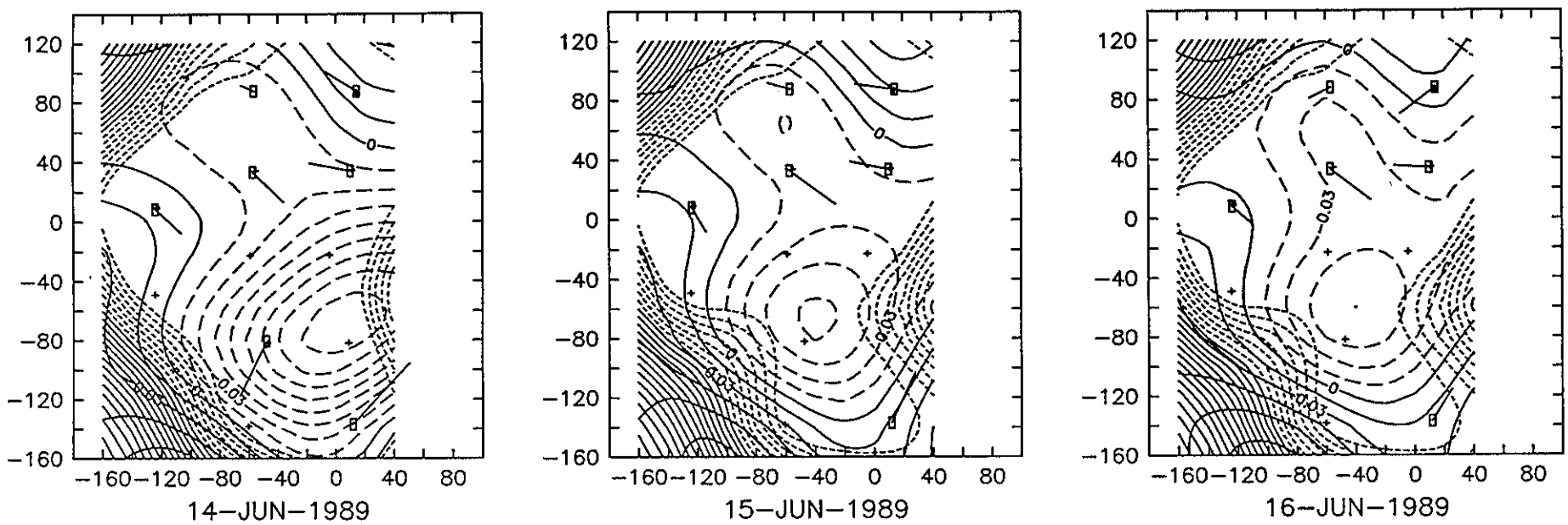
120
80
40
0
−40
−80
−120
−160
−160 −120 −80 −40 0 40 80
14−JUN−1989
15−JUN−1989
16−JUN−1989
17−JUN−1989
18−JUN−1989
19−JUN−1989
0
0.03
0.06

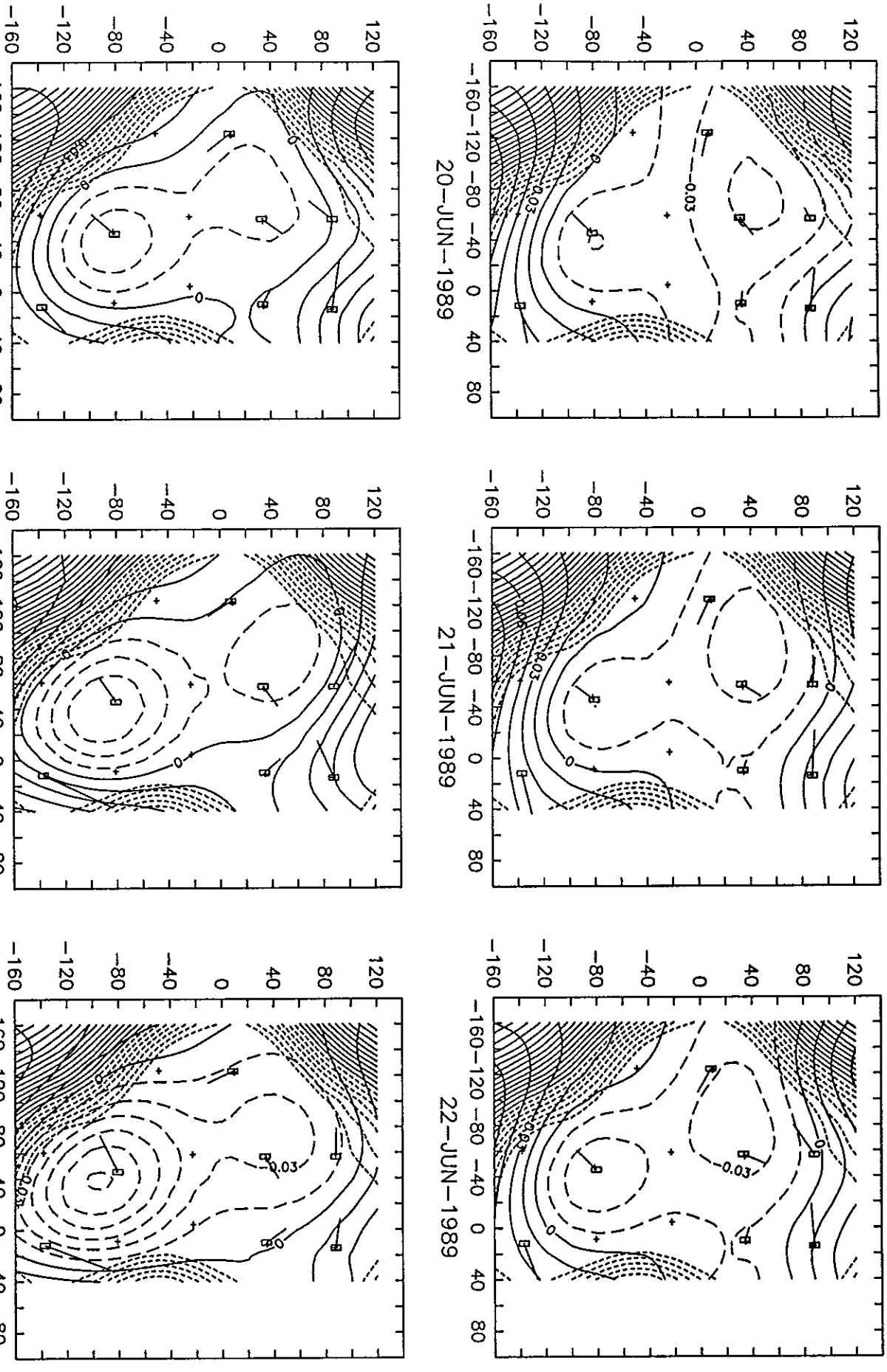
20-JUN-1989
21-JUN-1989
22-JUN-1989
23-JUN-1989
24-JUN-1989
25-JUN-1989

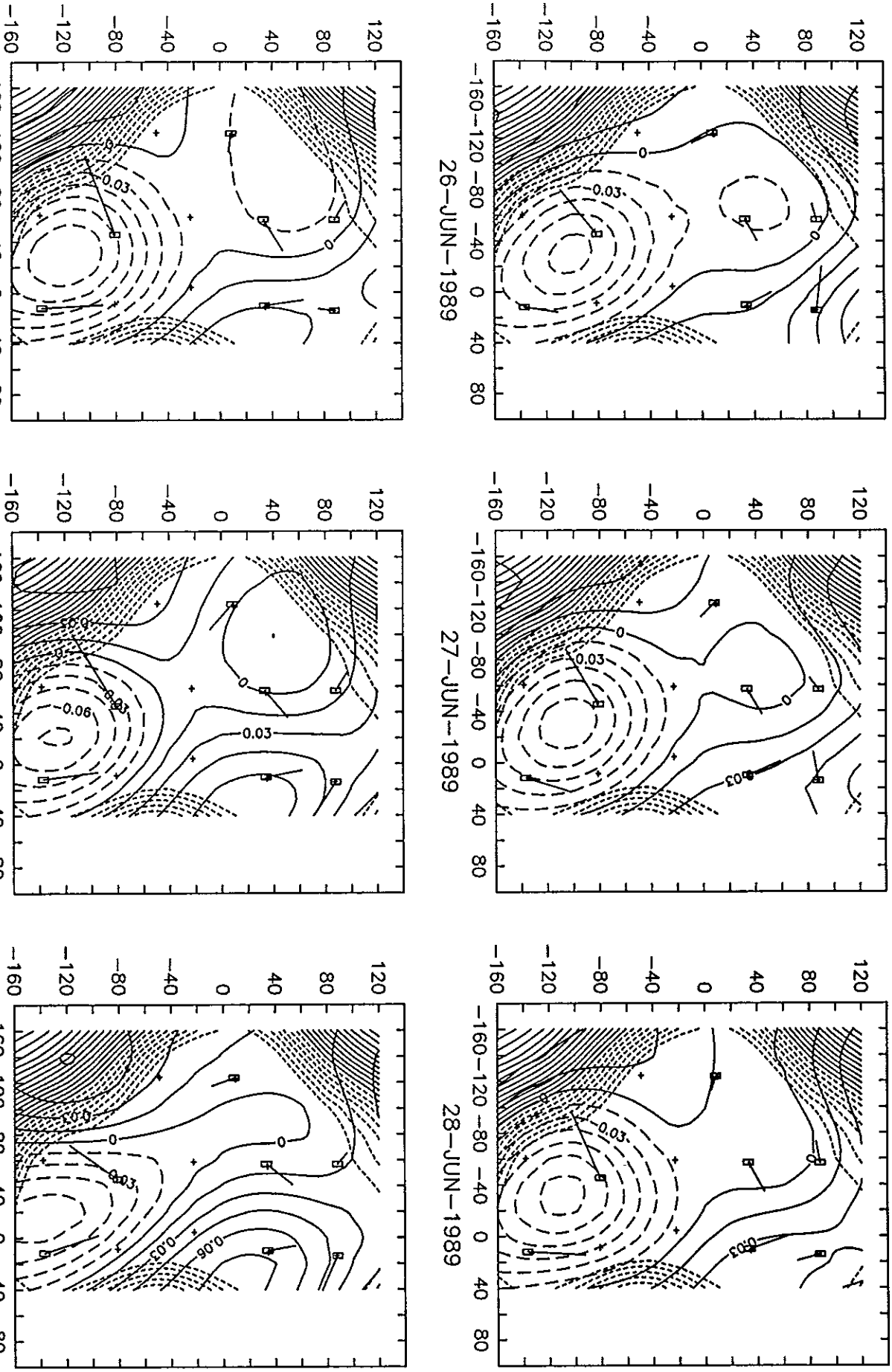
26-JUN-1989
27-JUN-1989
28-JUN-1989
29-JUN-1989
30-JUN-1989
01-JUL-1989

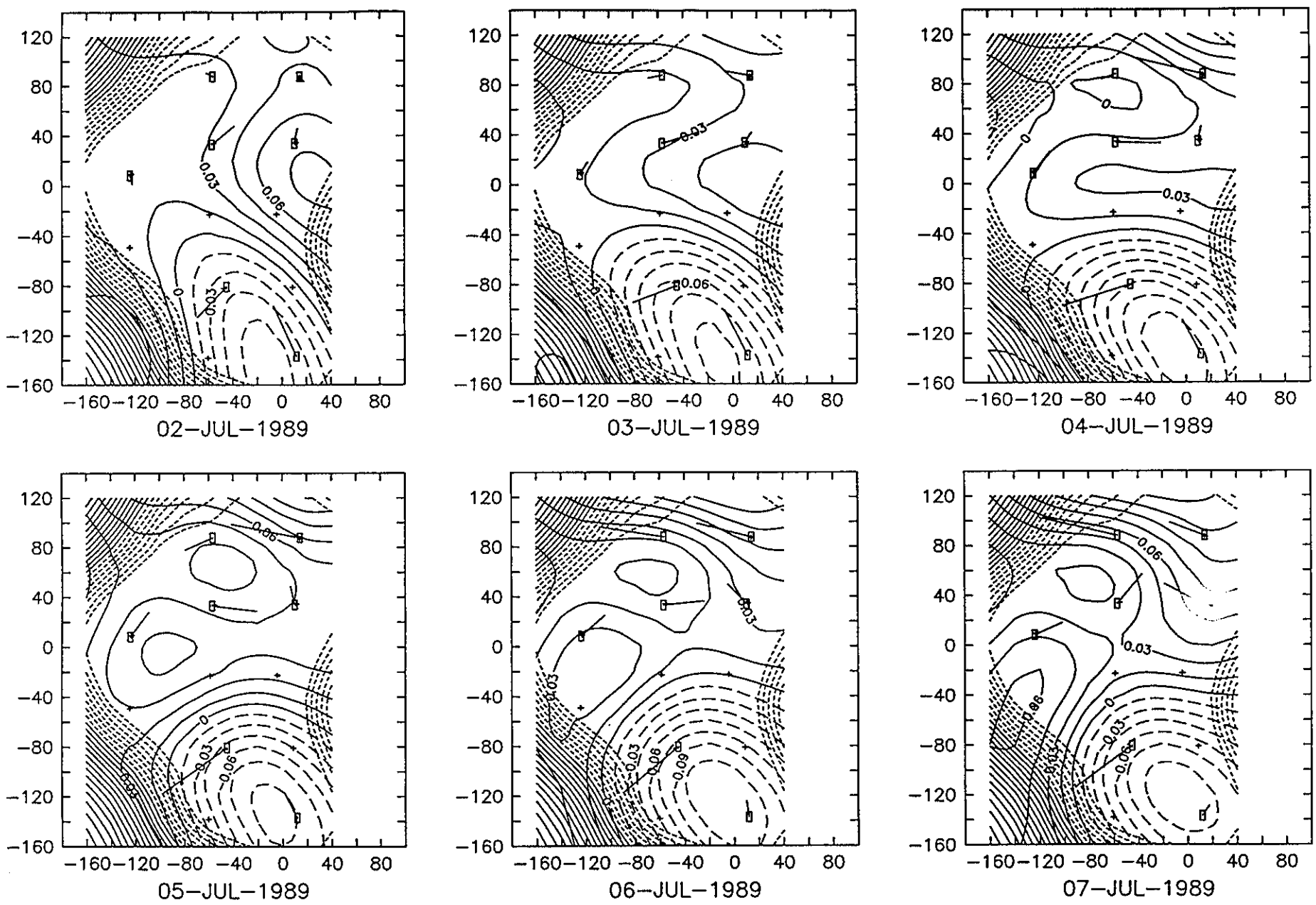
120
80
40
0
−40
−80
−120
−160
−160 −120 −80 −40 0 40 80
02−JUL−1989
03−JUL−1989
04−JUL−1989
05−JUL−1989
06−JUL−1989
07−JUL−1989

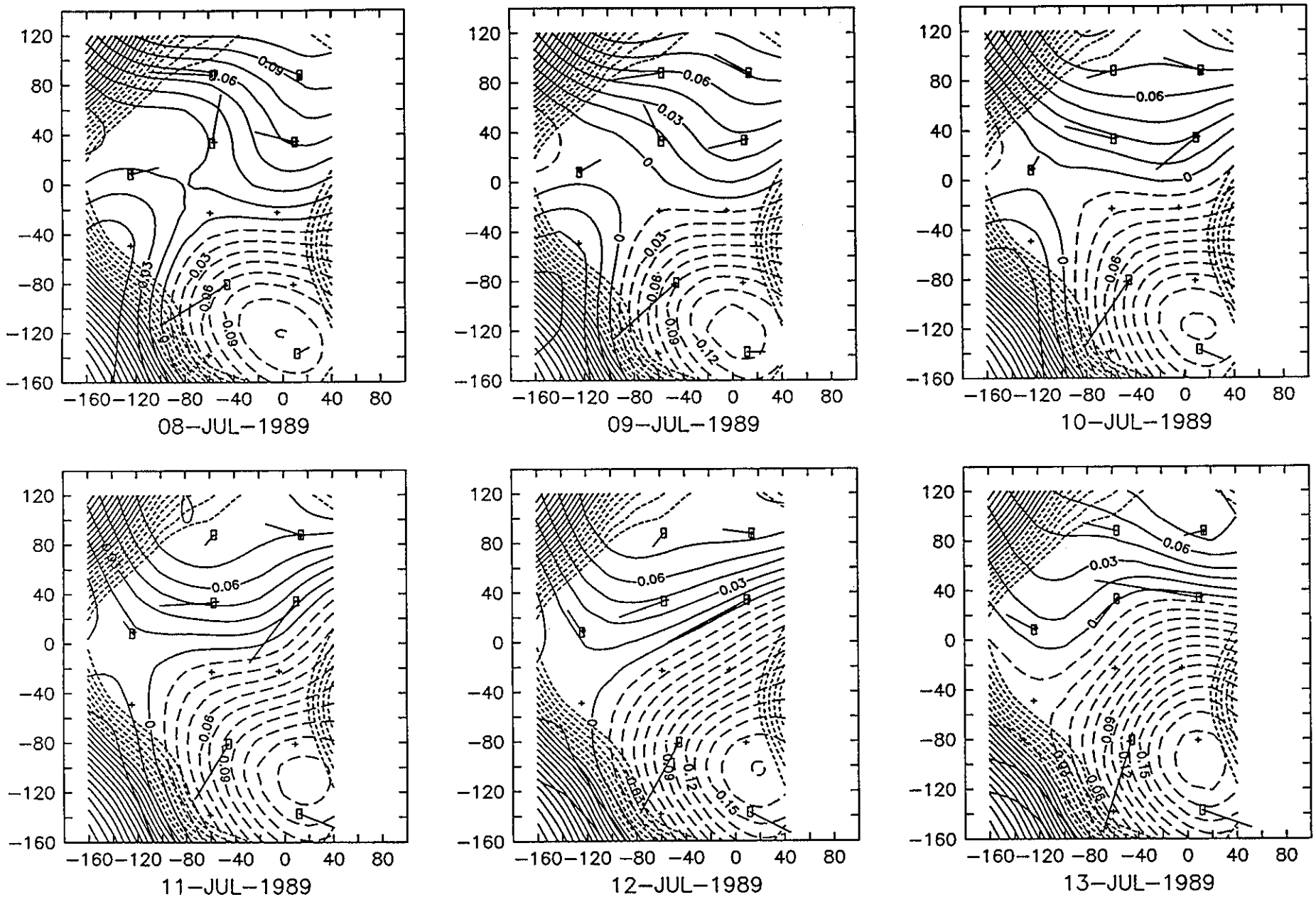
08-JUL-1989
09-JUL-1989
10-JUL-1989
11-JUL-1989
12-JUL-1989
13-JUL-1989

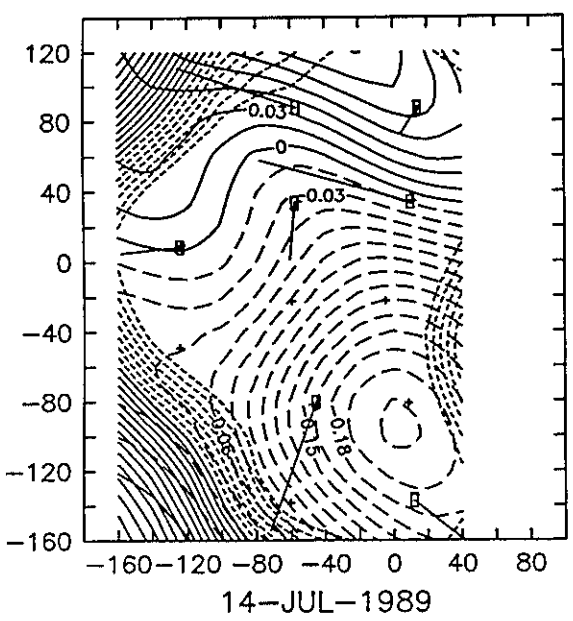
120
80
40
0
−40
−80
−120
−160
−160 −120 −80 −40 0 40 80
0.03
0
0.03
0.06
0.18
14−JUL−1989

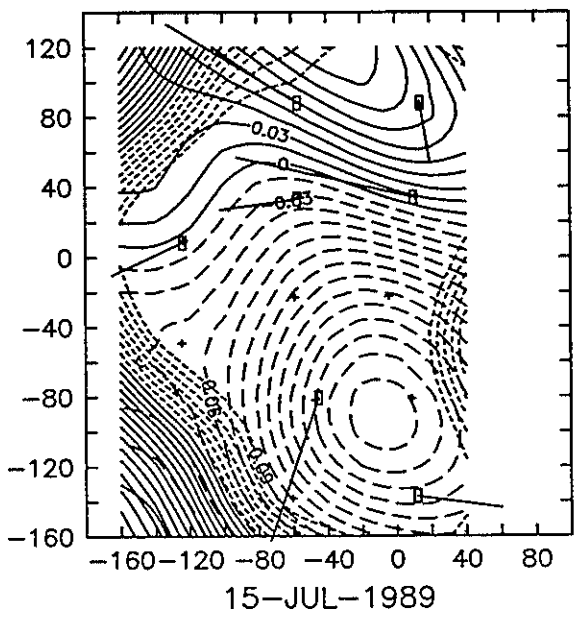
120
80
40
0
−40
−80
−120
−160
−160 −120 −80 −40 0 40 80
0.03
0
0.03
0.06
15−JUL−1989

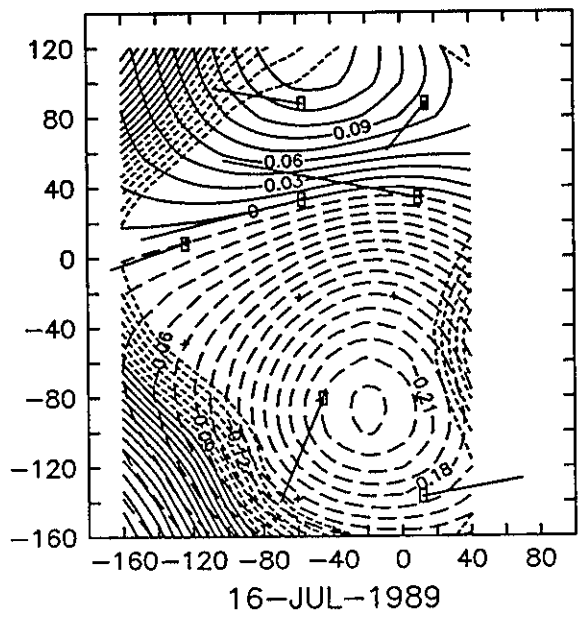
120
80
40
0
−40
−80
−120
−160
−160 −120 −80 −40 0 40 80
0.09
0.06
0.03
0
0.06
0.12
0.21
0.18
16−JUL−1989

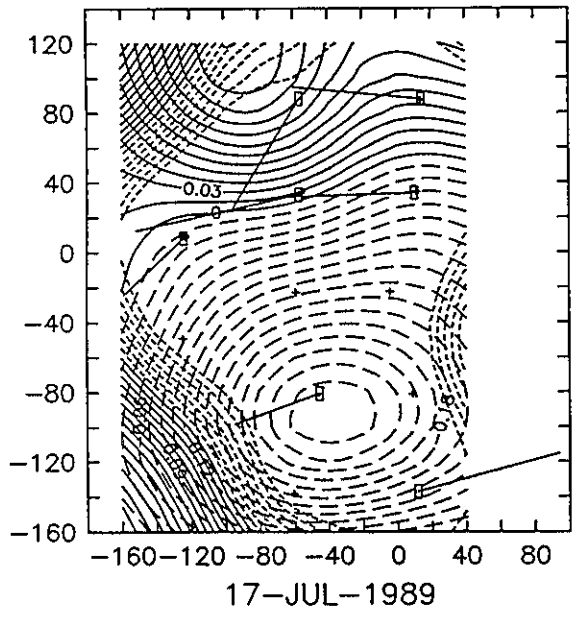
120
80
40
0
−40
−80
−120
−160
−160 −120 −80 −40 0 40 80
0.03
0
0.06
17−JUL−1989

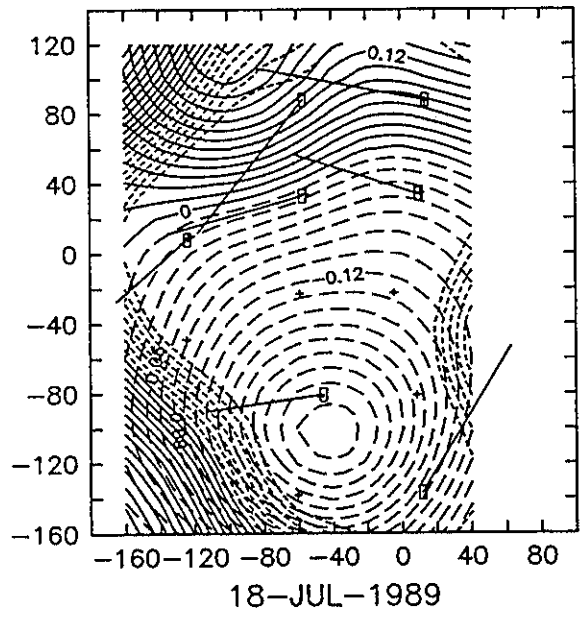
120
80
40
0
−40
−80
−120
−160
−160 −120 −80 −40 0 40 80
0.12
0
0.12
0.06
18−JUL−1989

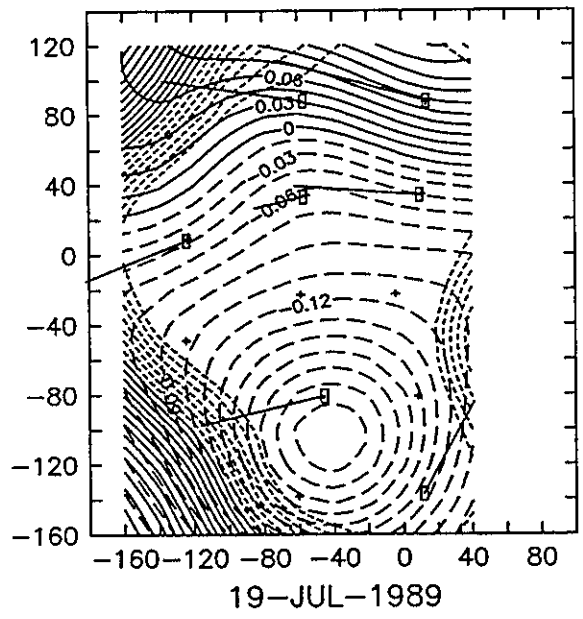
120
80
40
0
−40
−80
−120
−160
−160 −120 −80 −40 0 40 80
0.06
0.03
0
0.03
0.06
0.12
19−JUL−1989

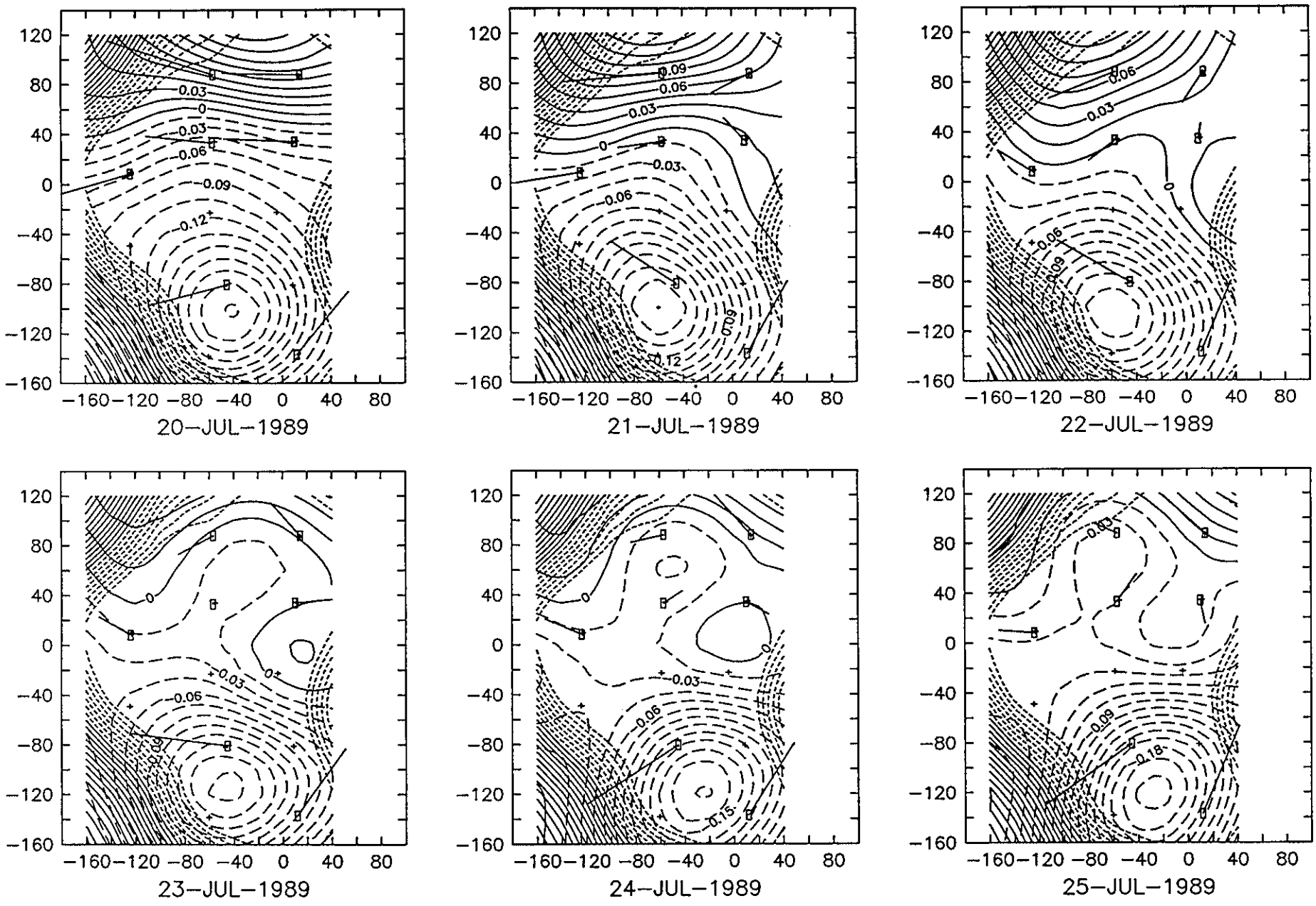
120
80
40
0
−40
−80
−120
−160
−160 −120 −80 −40 0 40 80
20−JUL−1989
21−JUL−1989
22−JUL−1989
23−JUL−1989
24−JUL−1989
25−JUL−1989

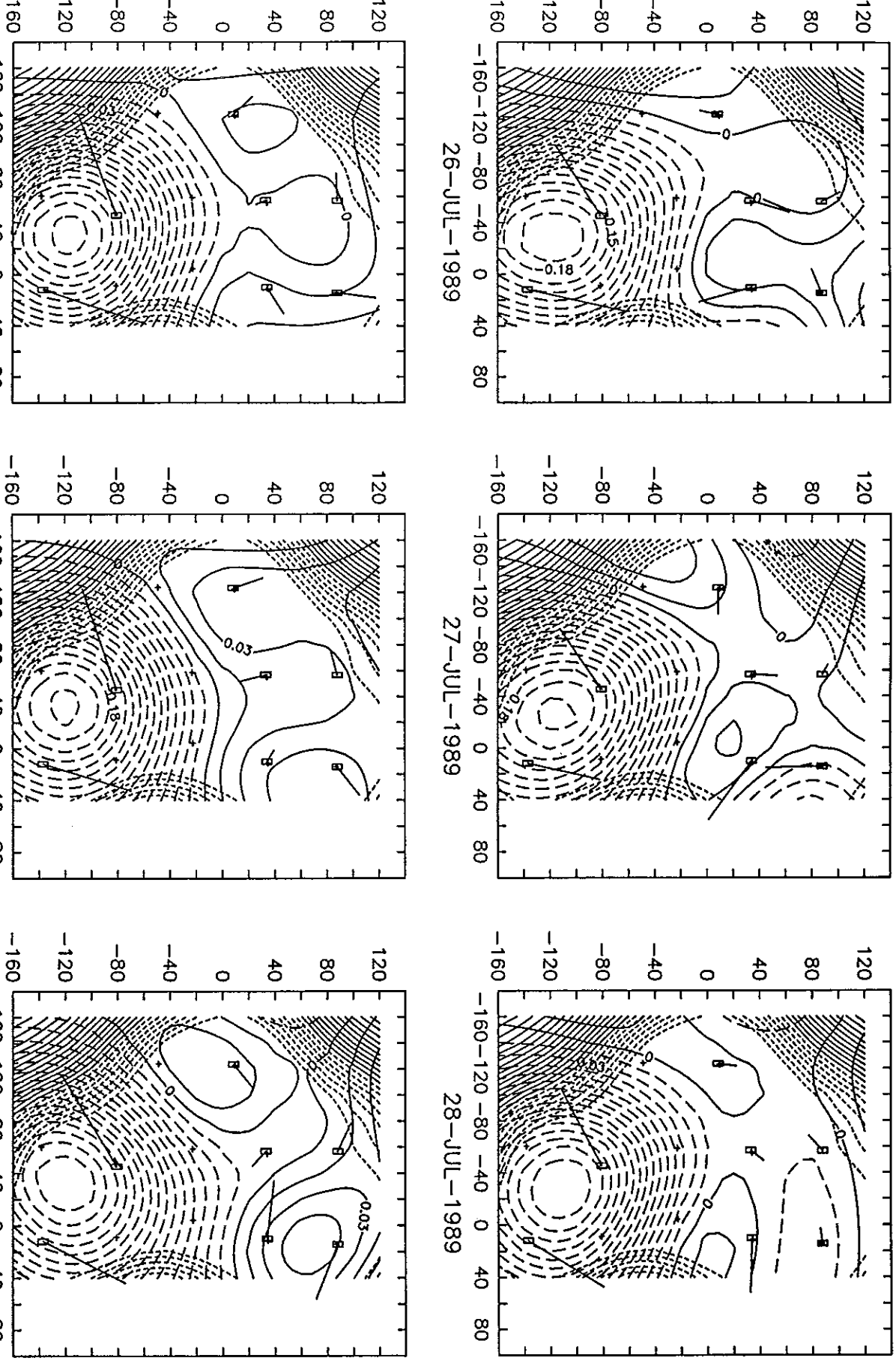
26-JUL-1989
27-JUL-1989
28-JUL-1989
29-JUL-1989
30-JUL-1989
31-JUL-1989

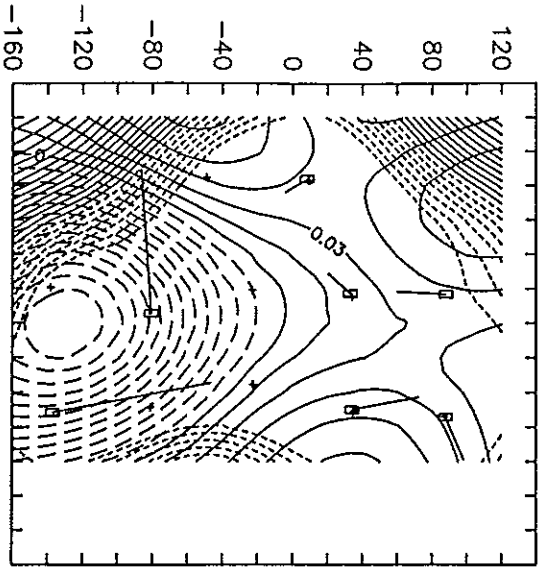
01-AUG-1989

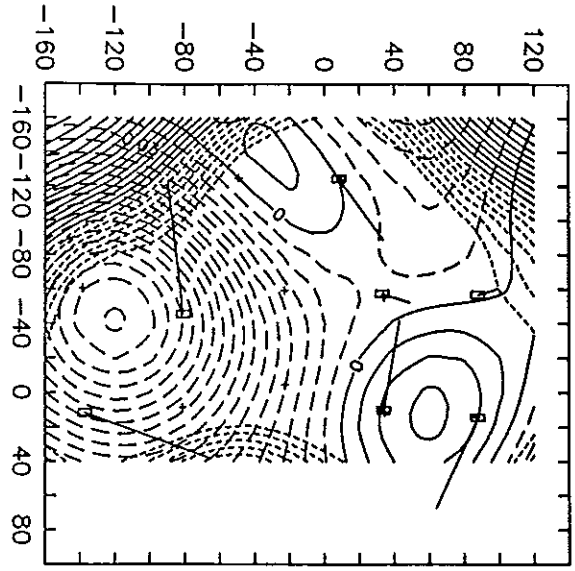
02-AUG-1989

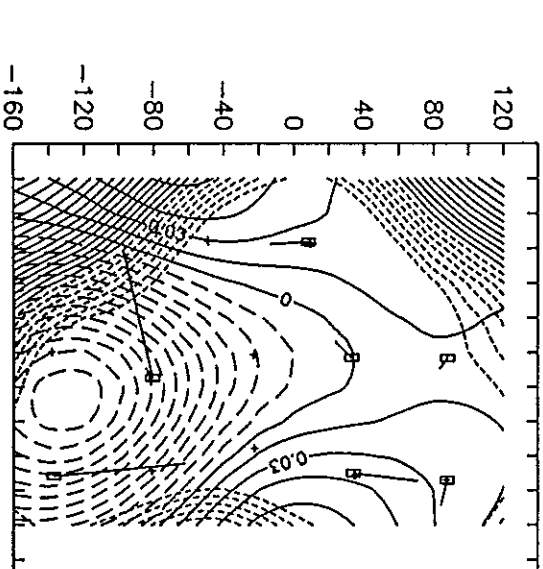
03-AUG-1989

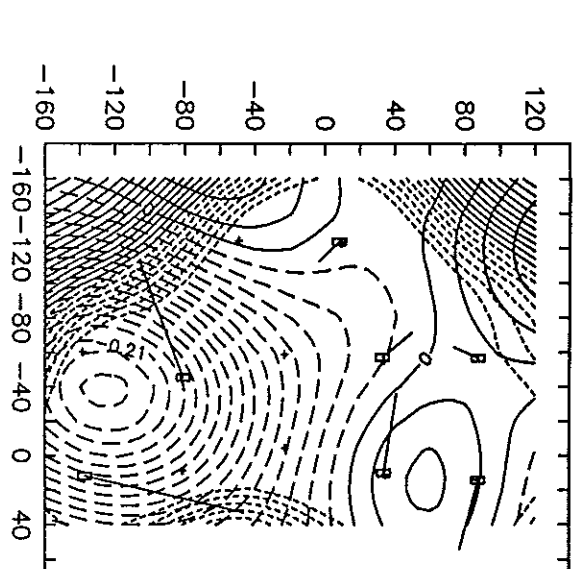
04-AUG-1989

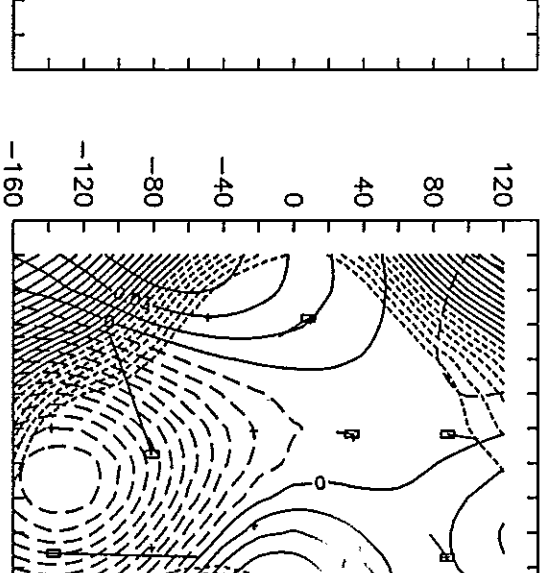
05-AUG-1989

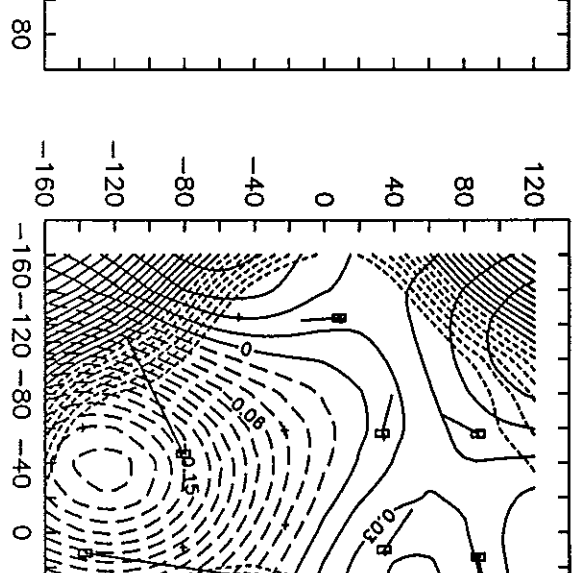
06-AUG-1989

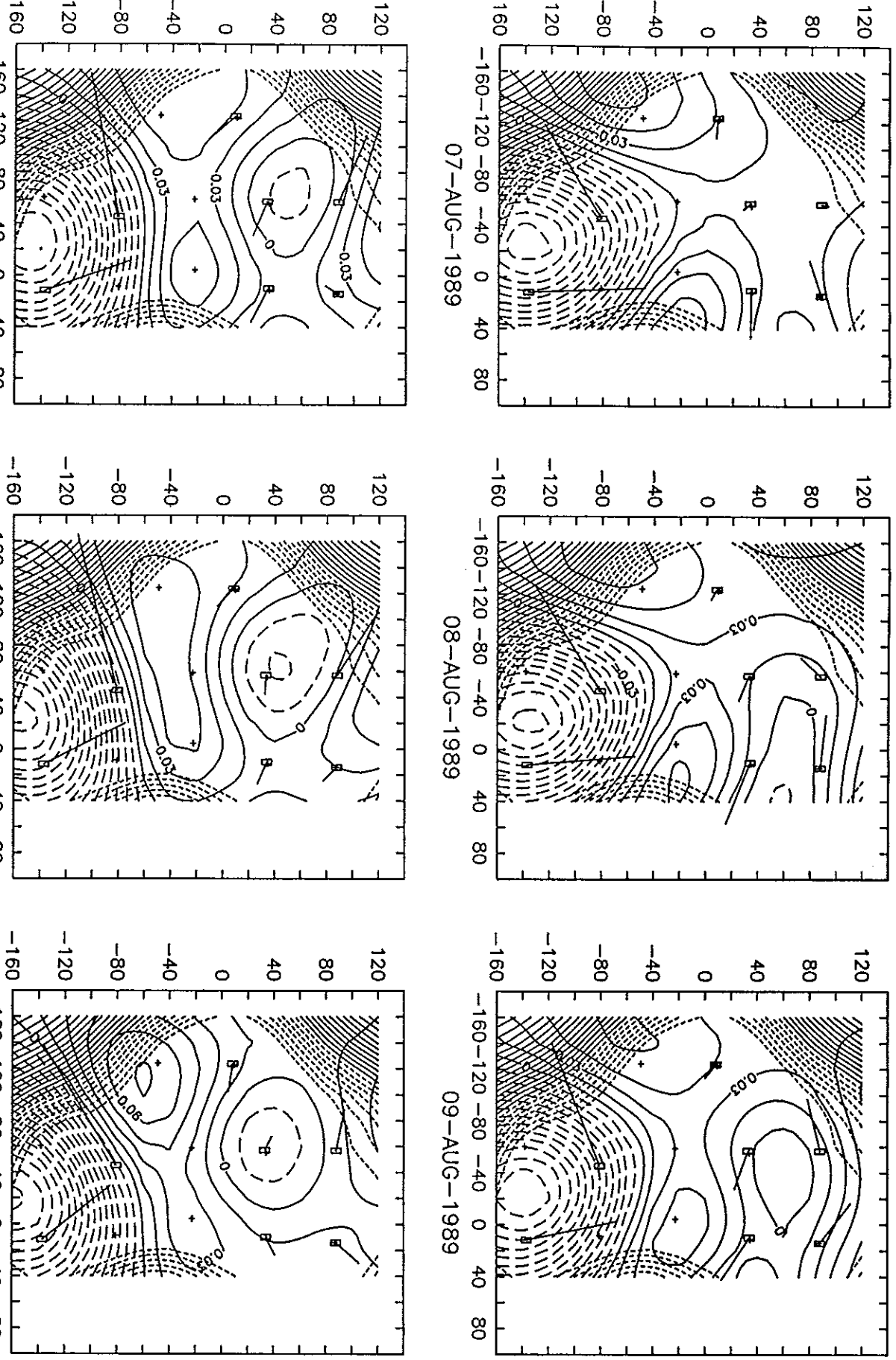
07-AUG-1989
08-AUG-1989
09-AUG-1989
10-AUG-1989
11-AUG-1989
12-AUG-1989

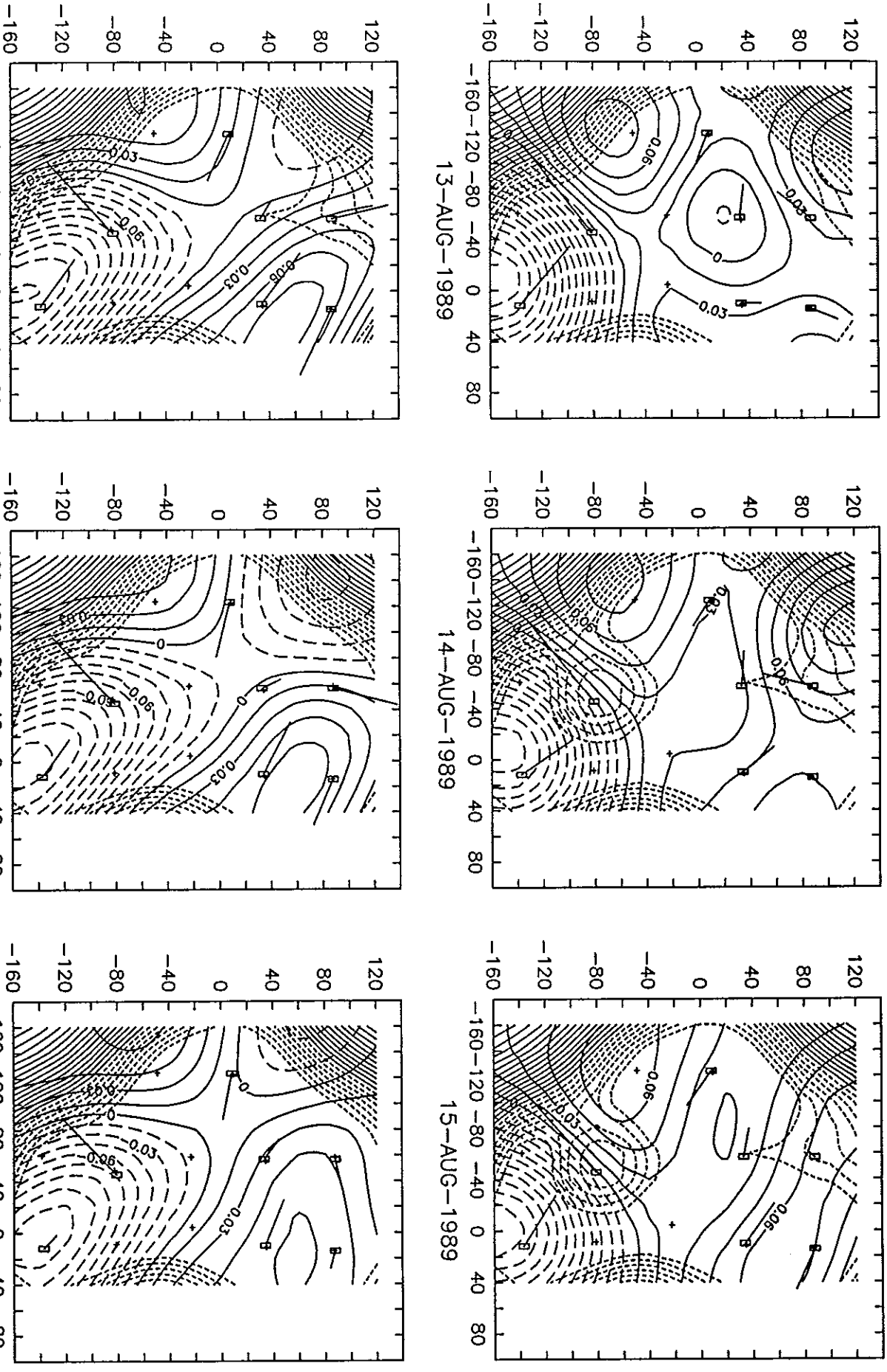
13-AUG-1989
14-AUG-1989
15-AUG-1989
16-AUG-1989
17-AUG-1989
18-AUG-1989

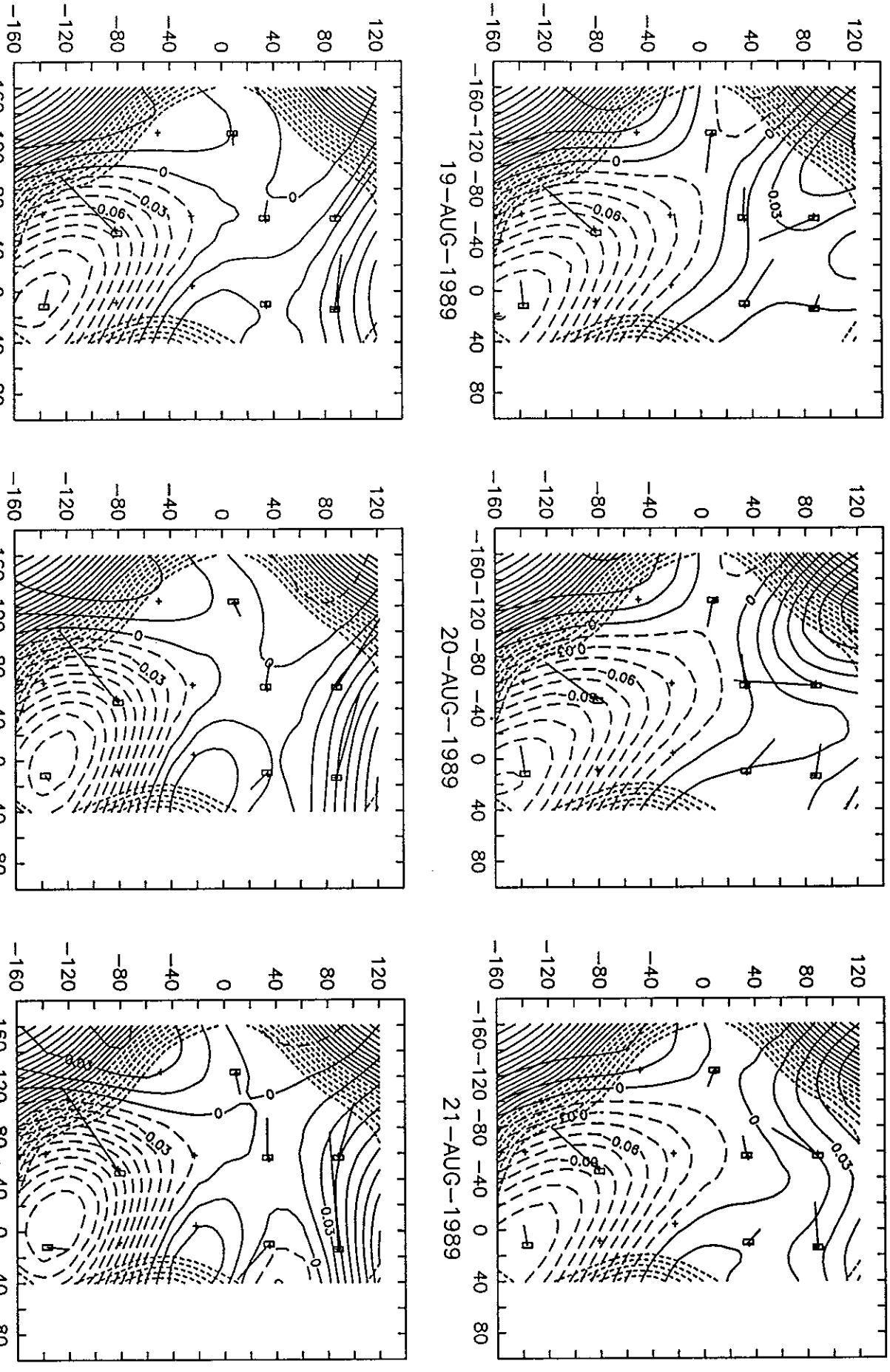
19-AUG-1989
20-AUG-1989
21-AUG-1989
22-AUG-1989
23-AUG-1989
24-AUG-1989

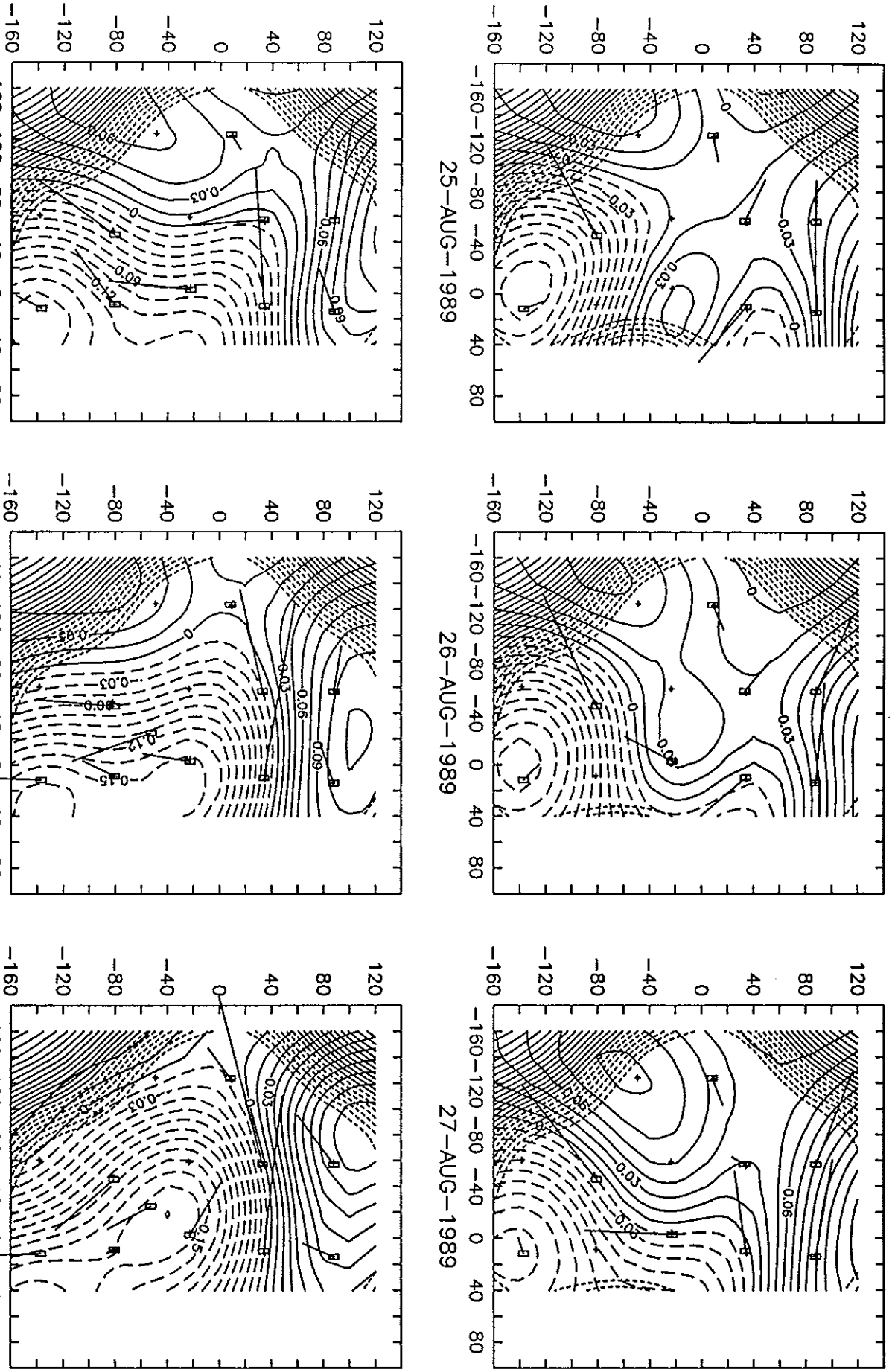
25-AUG-1989
26-AUG-1989
27-AUG-1989
28-AUG-1989
29-AUG-1989
30-AUG-1989

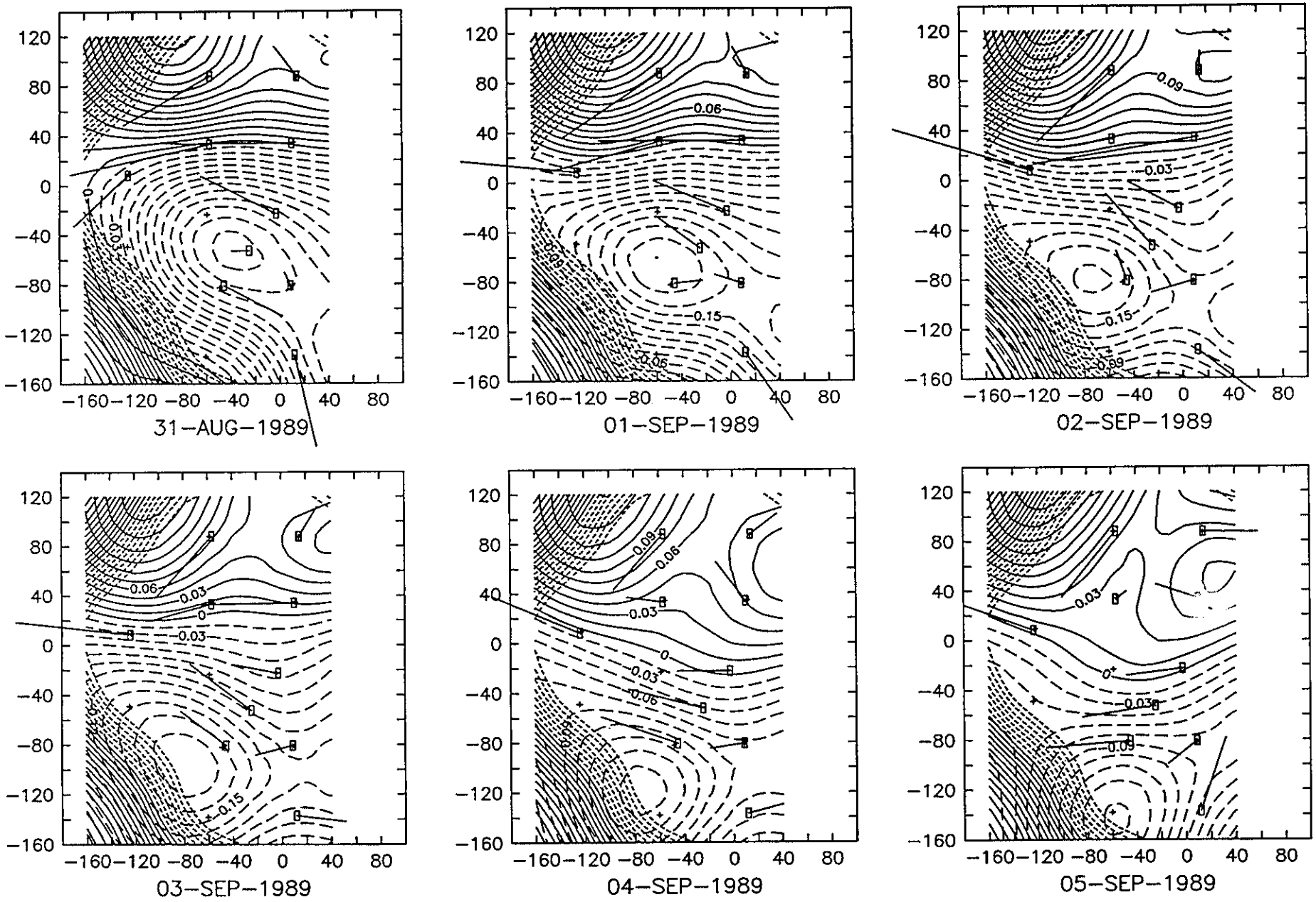
31-AUG-1989
01-SEP-1989
02-SEP-1989
03-SEP-1989
04-SEP-1989
05-SEP-1989

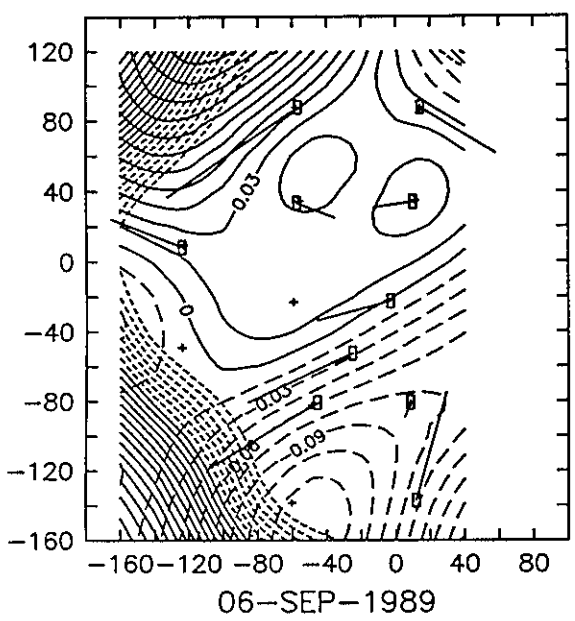
120
80
40
0
−40
−80
−120
−160
−160 −120 −80 −40 0 40 80
0.03
0
−0.03
−0.09
06−SEP−1989

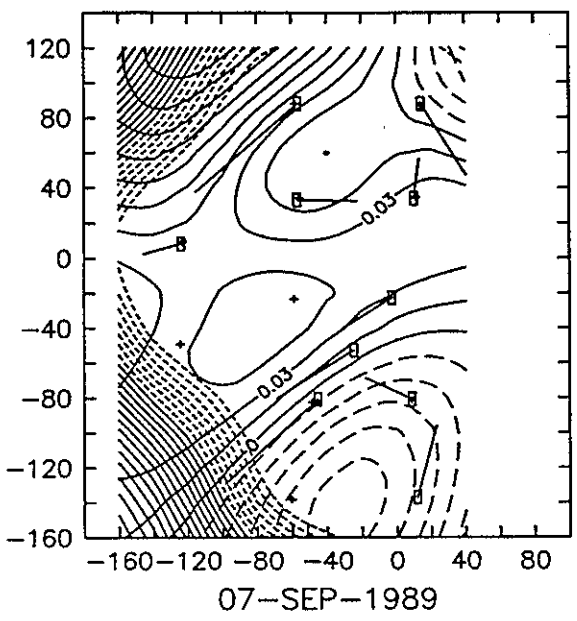
120
80
40
0
−40
−80
−120
−160
−160 −120 −80 −40 0 40 80
0.03
0
−0.03
07−SEP−1989

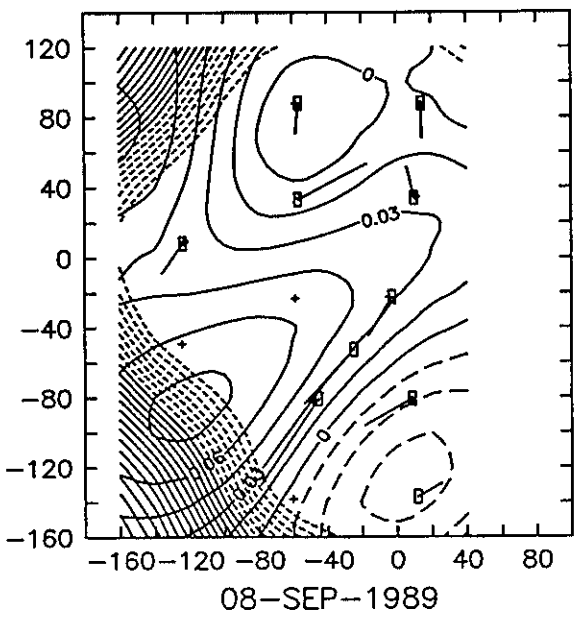
120
80
40
0
−40
−80
−120
−160
−160 −120 −80 −40 0 40 80
0
0.03
−0.06
−0.03
08−SEP−1989

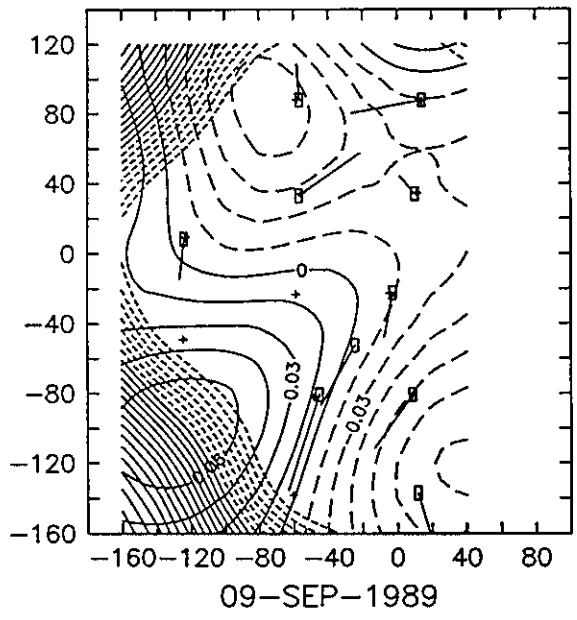
120
80
40
0
−40
−80
−120
−160
−160 −120 −80 −40 0 40 80
0
0.03
−0.03
−0.06
09−SEP−1989

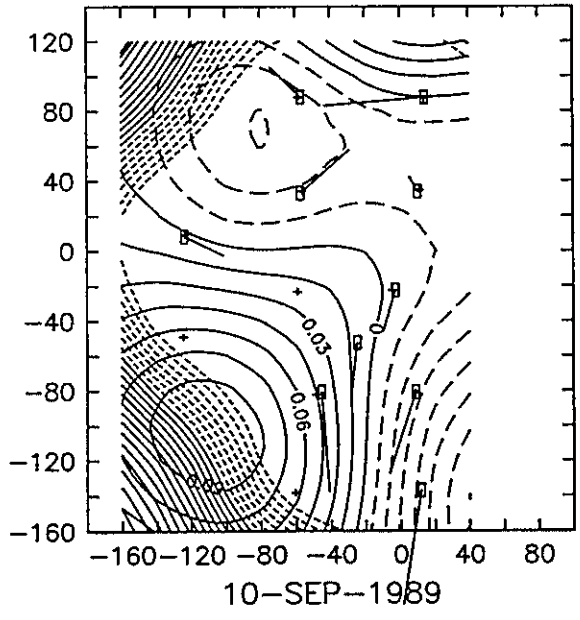
120
80
40
0
−40
−80
−120
−160
−160 −120 −80 −40 0 40 80
0.03
0
−0.03
−0.06
10−SEP−1989

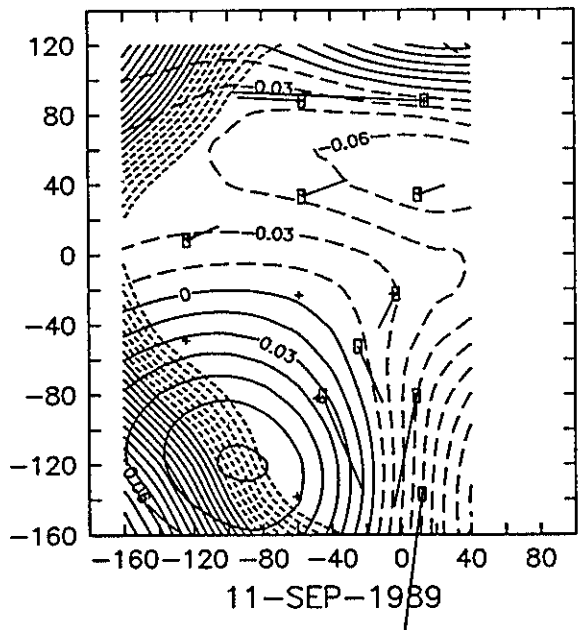
120
80
40
0
−40
−80
−120
−160
−160 −120 −80 −40 0 40 80
0.03
−0.06
0.03
0
0.03
−0.06
11−SEP−1989

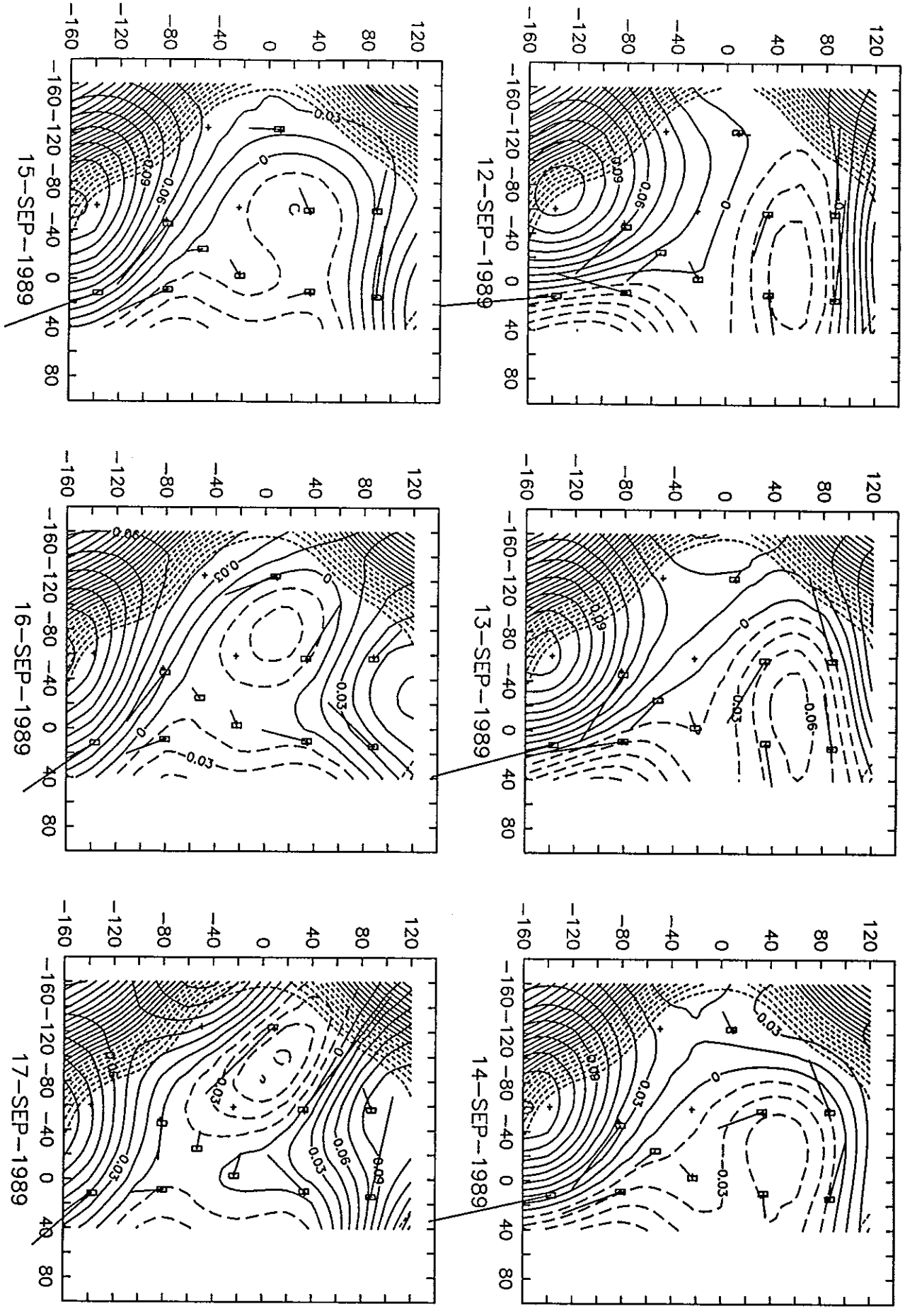
12-SEP-1989
13-SEP-1989
14-SEP-1989
15-SEP-1989
16-SEP-1989
17-SEP-1989

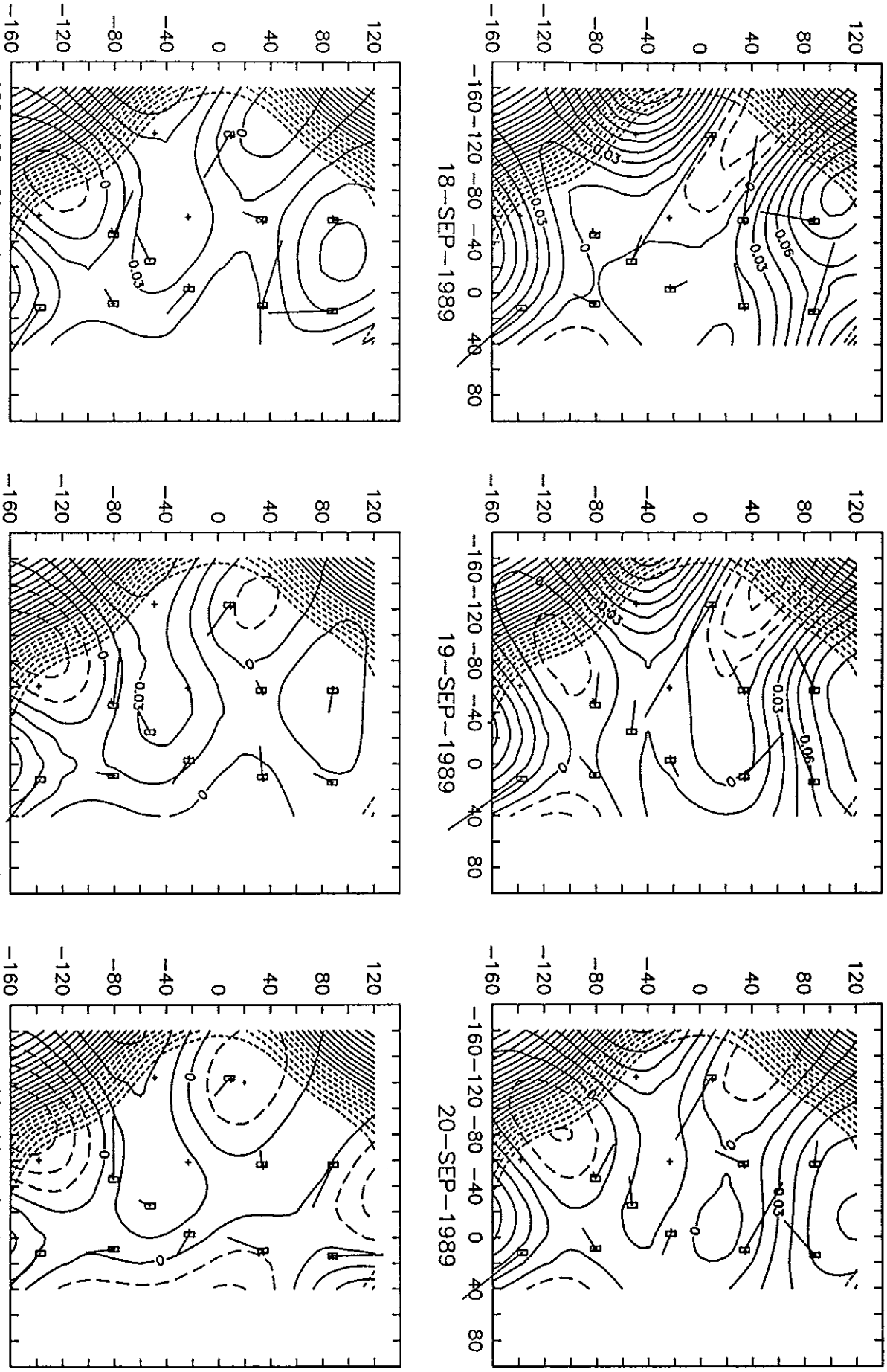
18-SEP-1989
19-SEP-1989
20-SEP-1989
21-SEP-1989
22-SEP-1989
23-SEP-1989

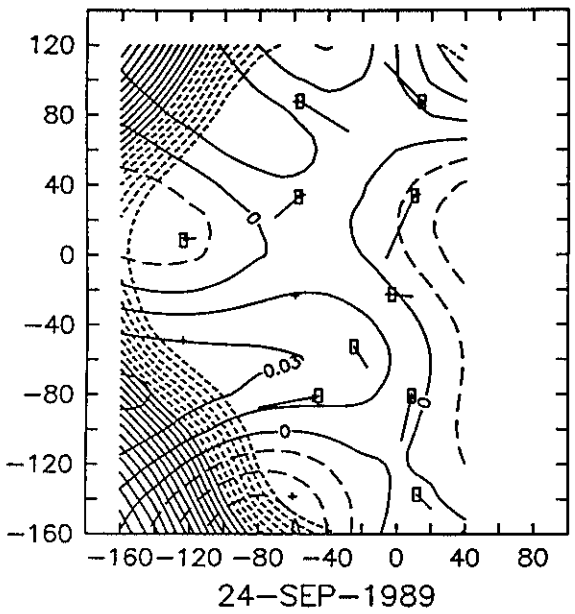
120
80
40
0
−40
−80
−120
−160
−160 −120 −80 −40 0 40 80
0
0.03
24−SEP−1989

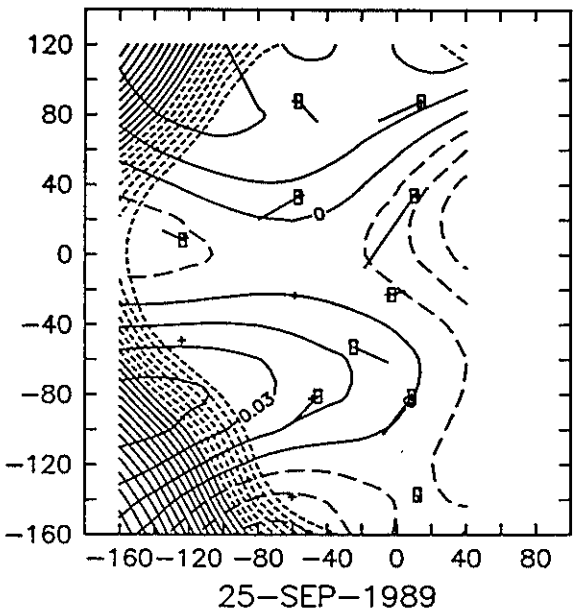
120
80
40
0
−40
−80
−120
−160
−160 −120 −80 −40 0 40 80
0
0.03
25−SEP−1989

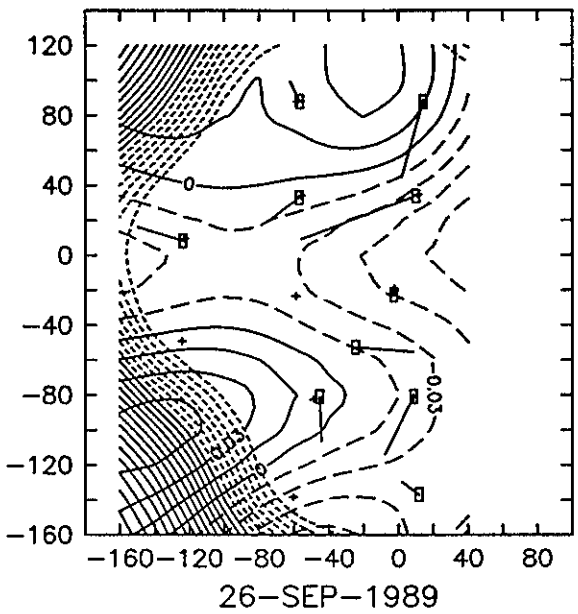
120
80
40
0
−40
−80
−120
−160
−160 −120 −80 −40 0 40 80
0
0.03
26−SEP−1989

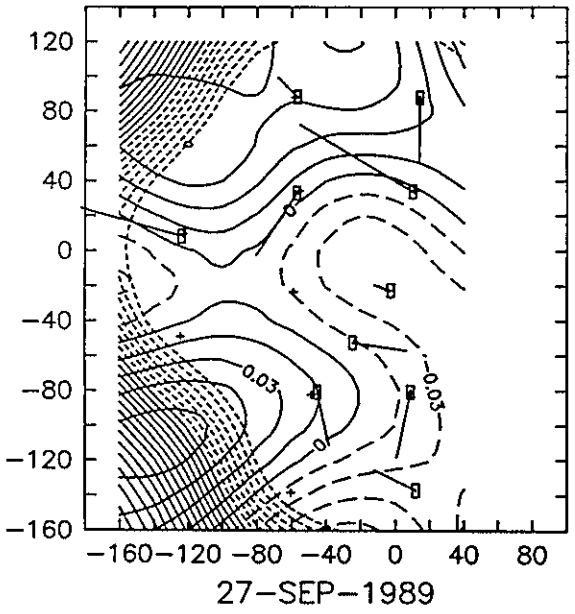
120
80
40
0
−40
−80
−120
−160
−160 −120 −80 −40 0 40 80
0
0.03
27−SEP−1989

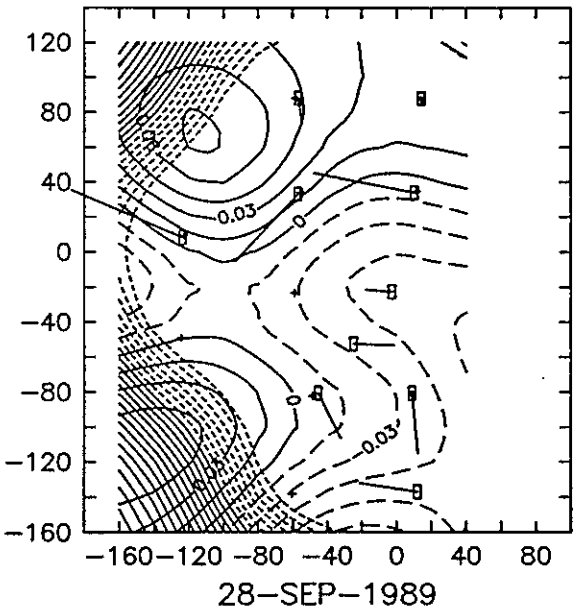
120
80
40
0
−40
−80
−120
−160
−160 −120 −80 −40 0 40 80
0
0.03
28−SEP−1989

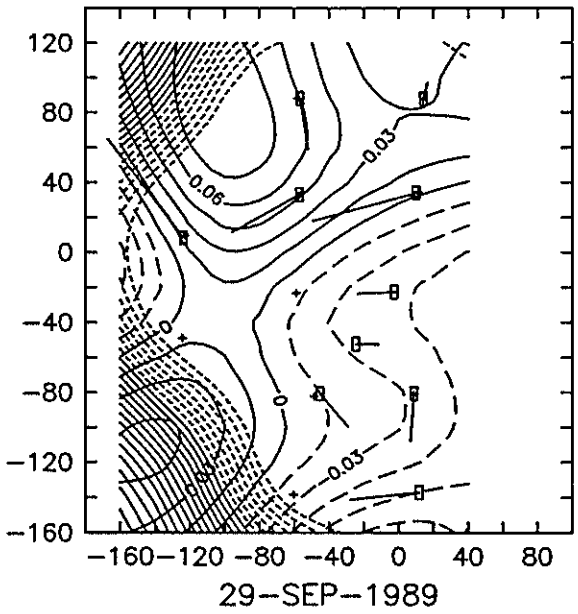
120
80
40
0
−40
−80
−120
−160
−160 −120 −80 −40 0 40 80
0
0.03
0.06
29−SEP−1989

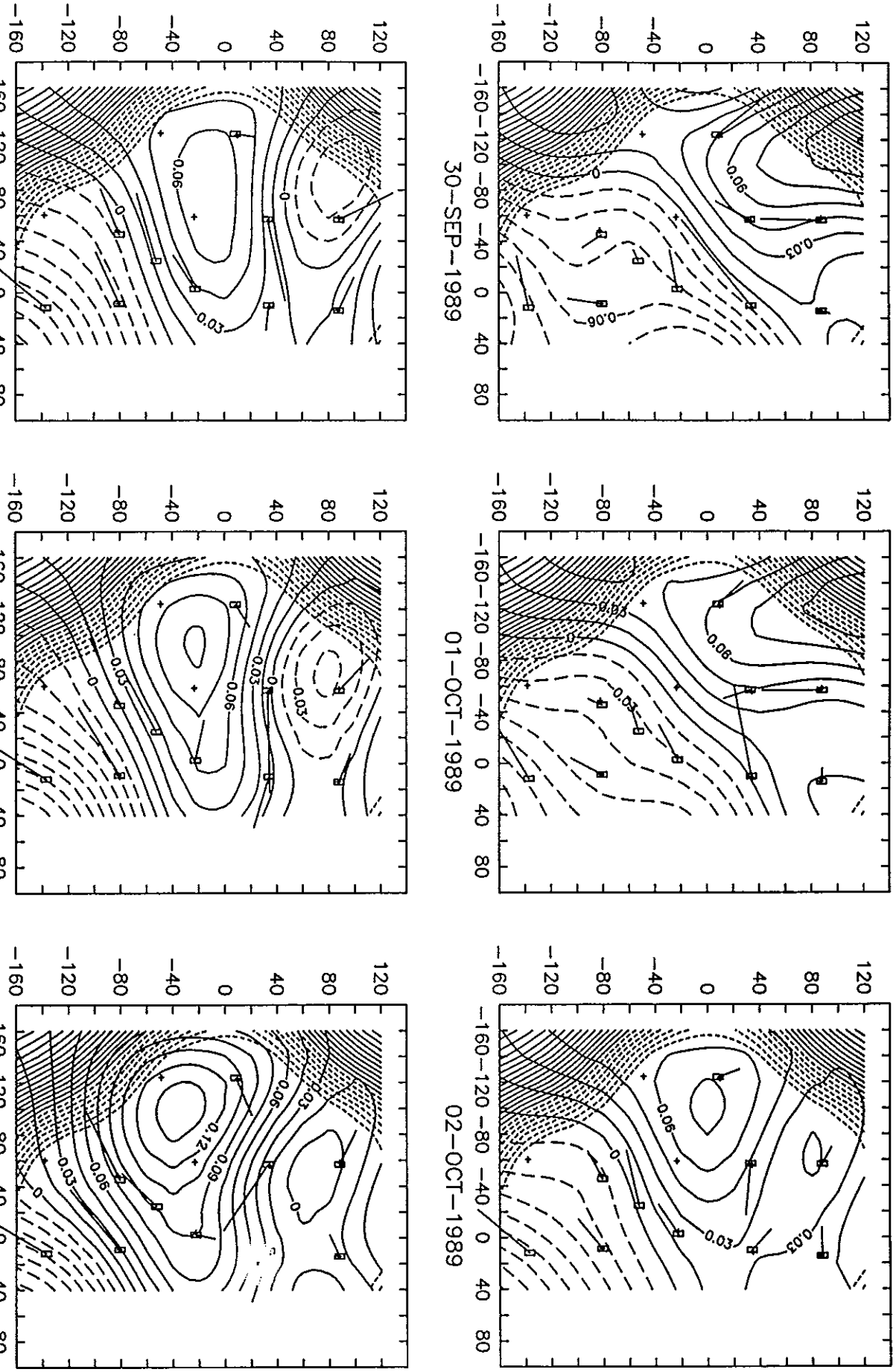
30-SEP-1989
01-OCT-1989
02-OCT-1989
03-OCT-1989
04-OCT-1989
05-OCT-1989

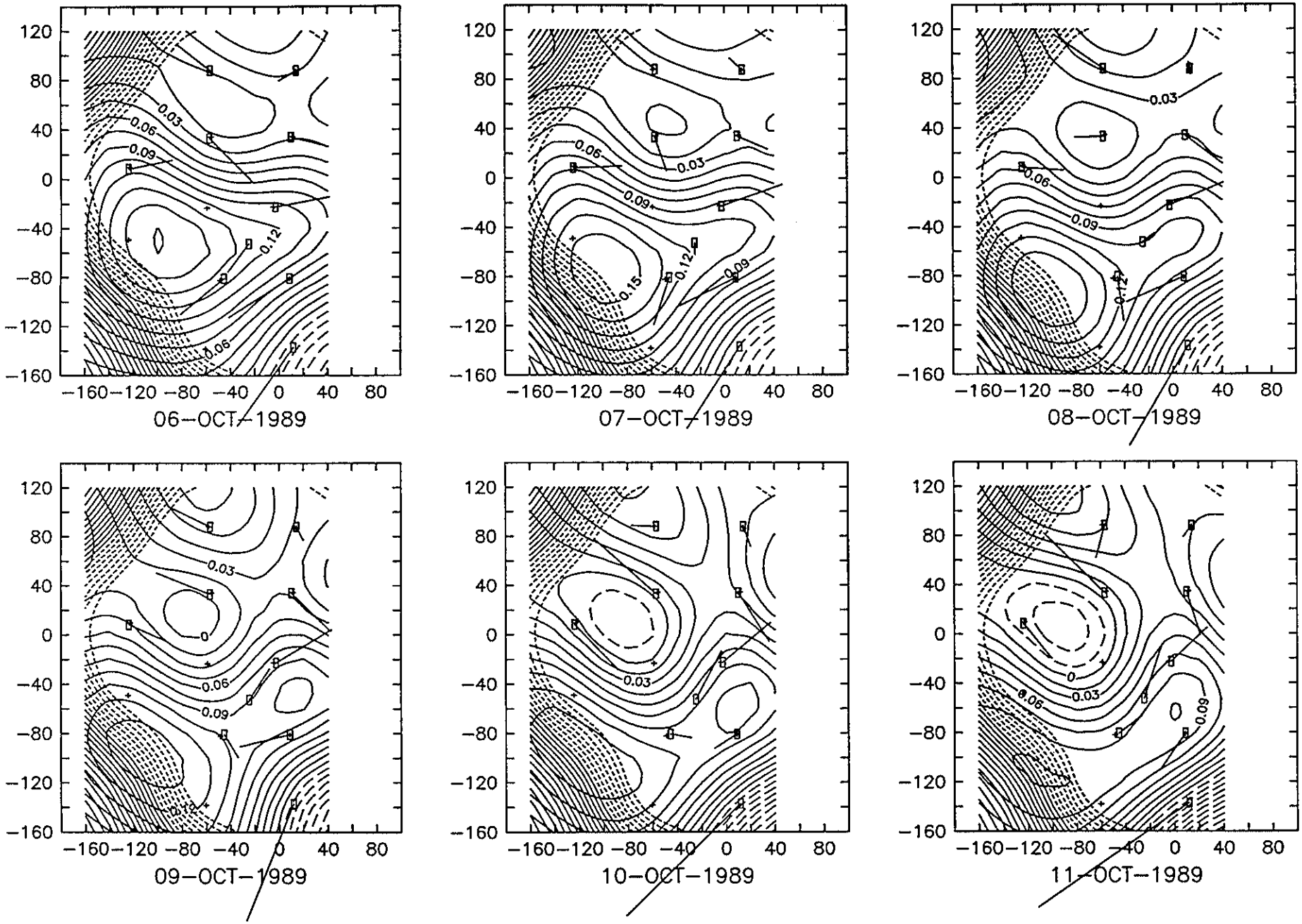
06-OCT-1989
07-OCT-1989
08-OCT-1989
09-OCT-1989
10-OCT-1989
11-OCT-1989

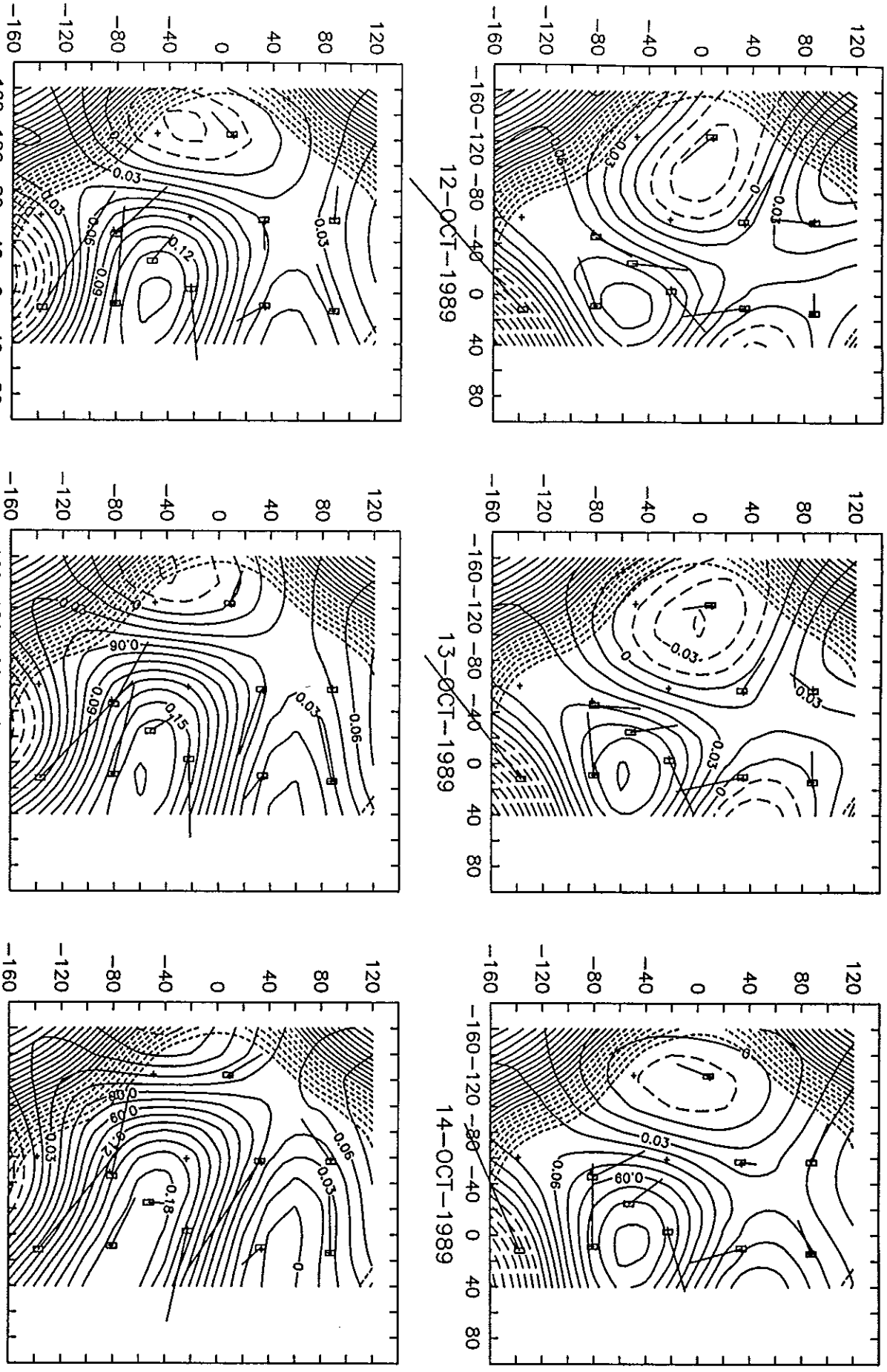
12-OCT-1989
13-OCT-1989
14-OCT-1989
15-OCT-1989
16-OCT-1989
17-OCT-1989

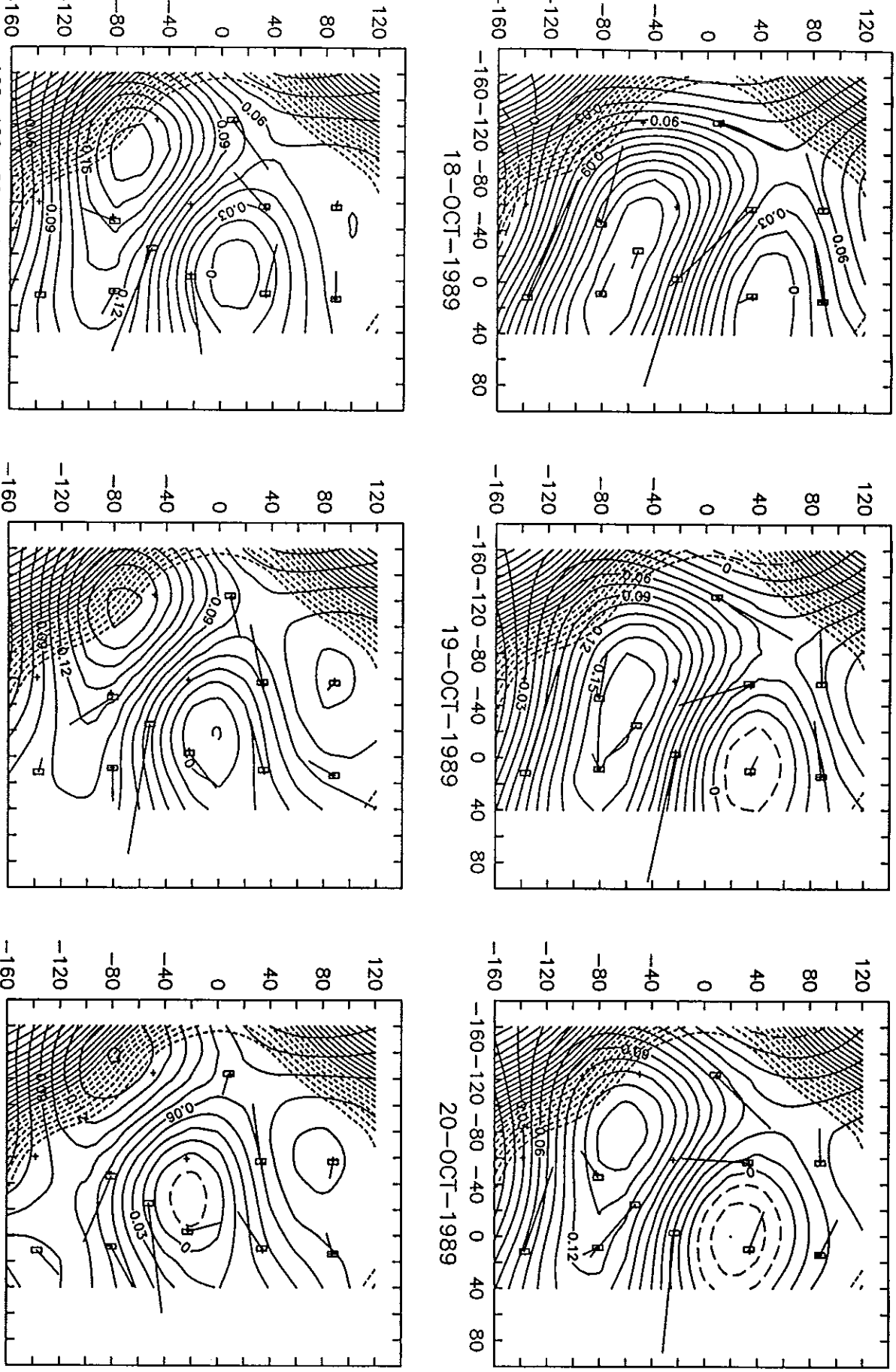
18-OCT-1989
19-OCT-1989
20-OCT-1989
21-OCT-1989
22-OCT-1989
23-OCT-1989

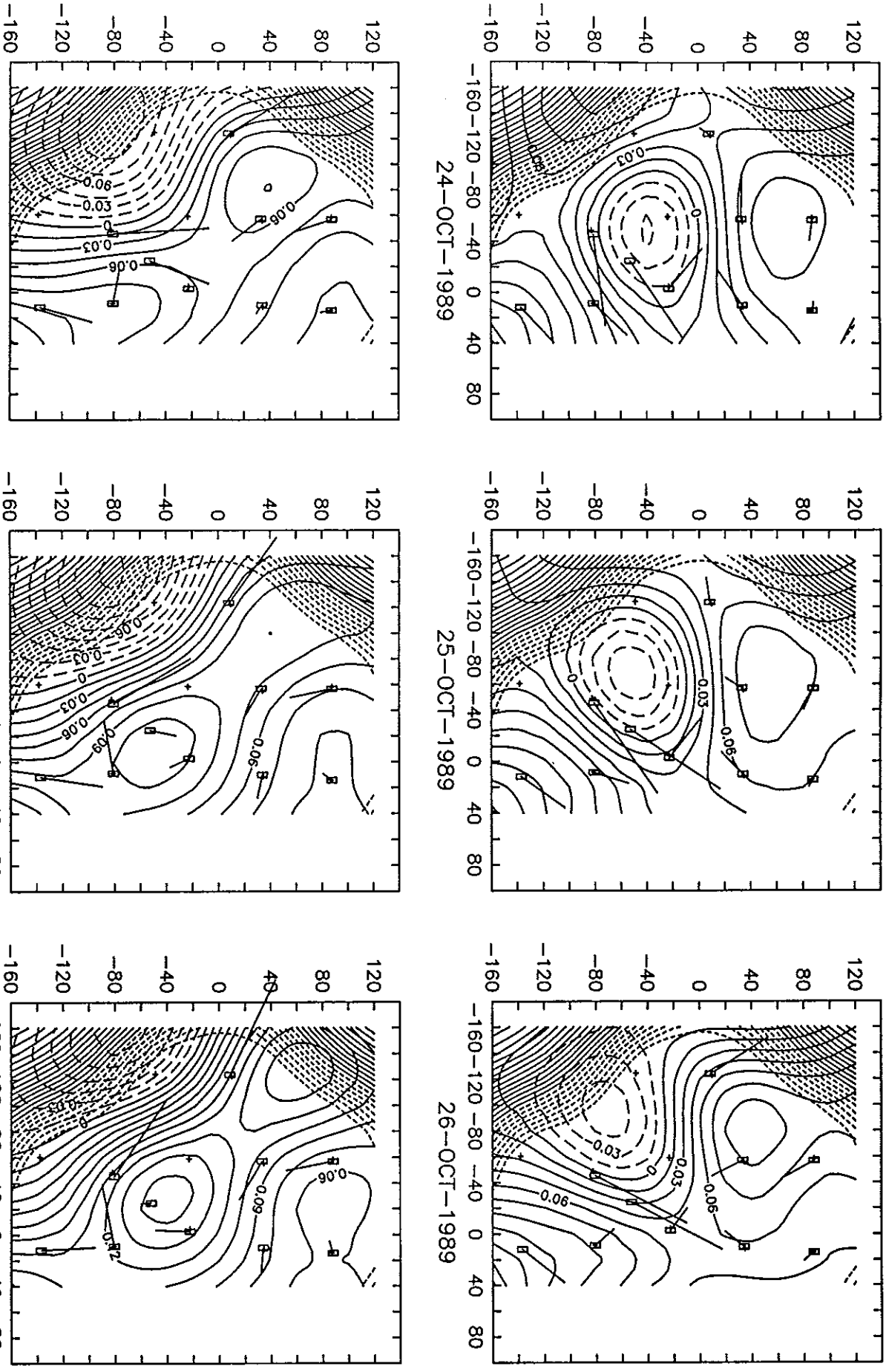
24-OCT-1989
25-OCT-1989
26-OCT-1989
27-OCT-1989
28-OCT-1989
29-OCT-1989

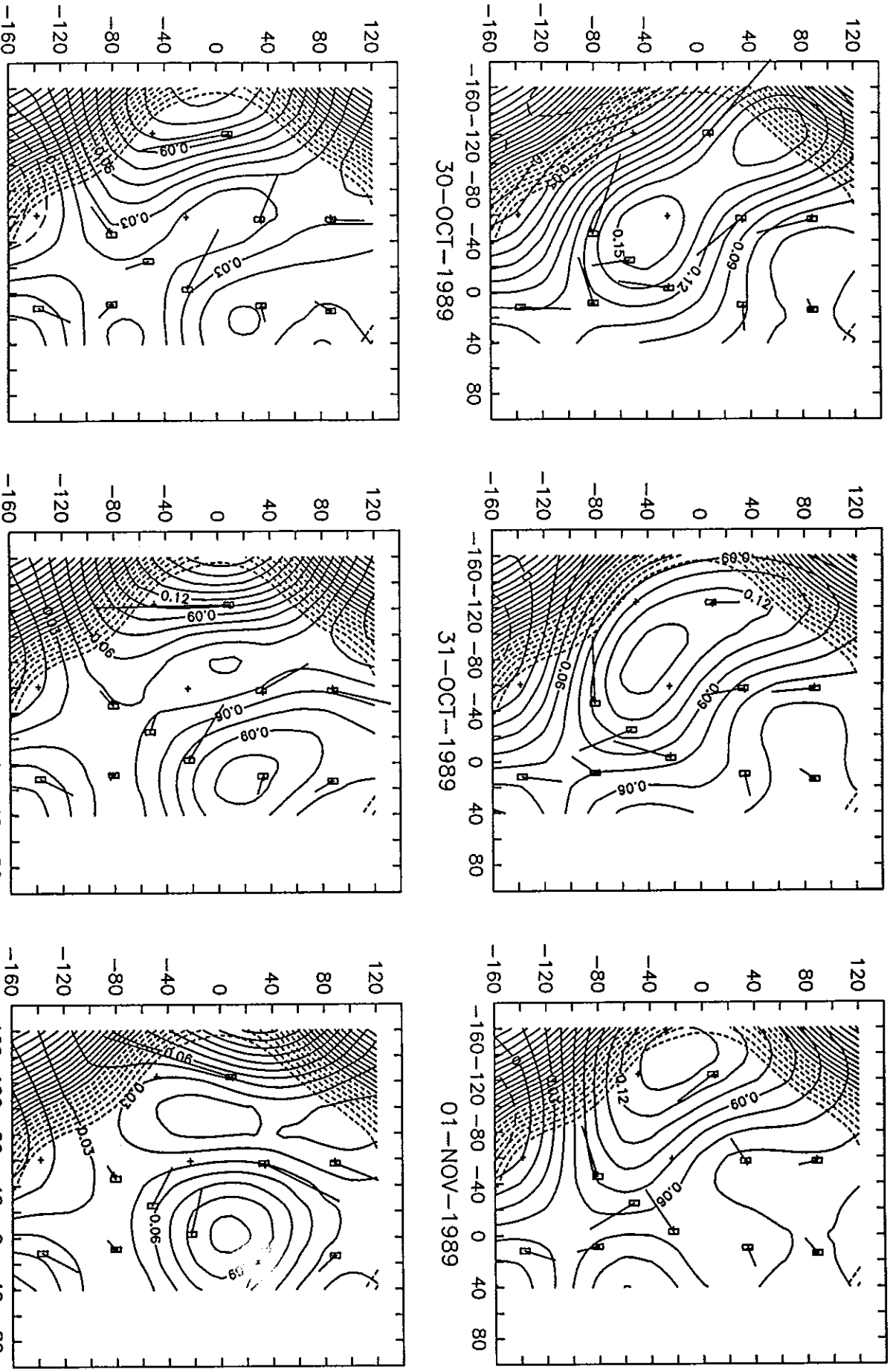
30-OCT-1989
31-OCT-1989
01-NOV-1989
02-NOV-1989
03-NOV-1989
04-NOV-1989

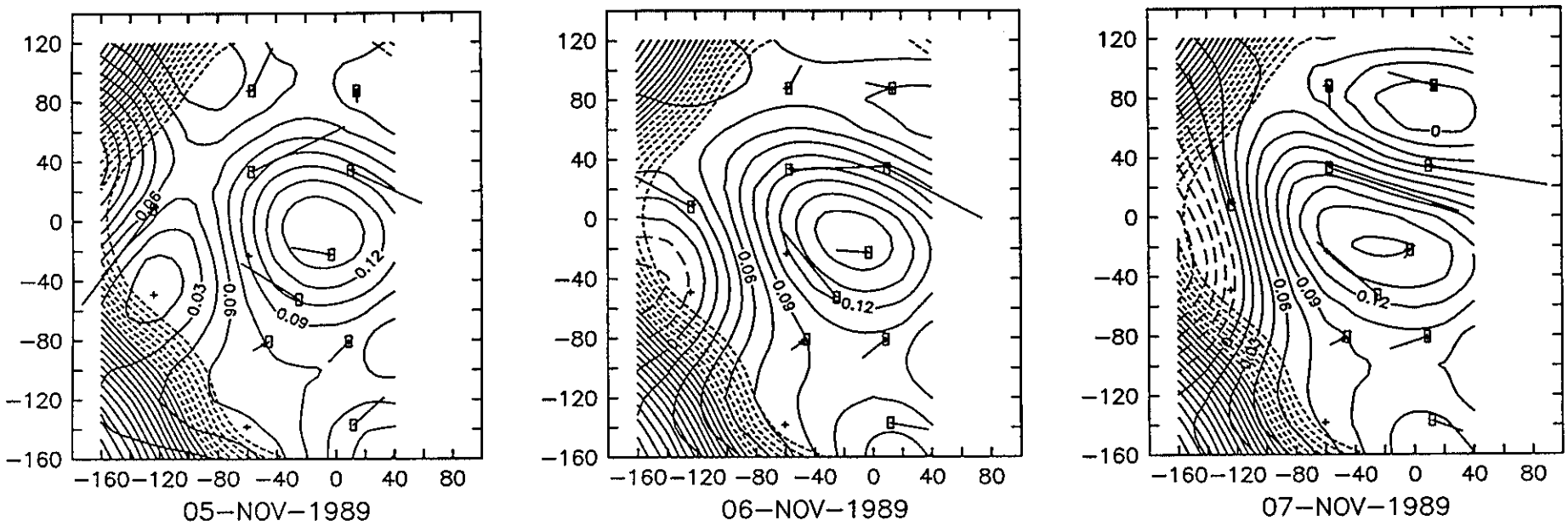
120
80
40
0
−40
−80
−120
−160
−160 −120 −80 −40 0 40 80
0.06
0.03
0.09
0.12
05−NOV−1989
06−NOV−1989
07−NOV−1989

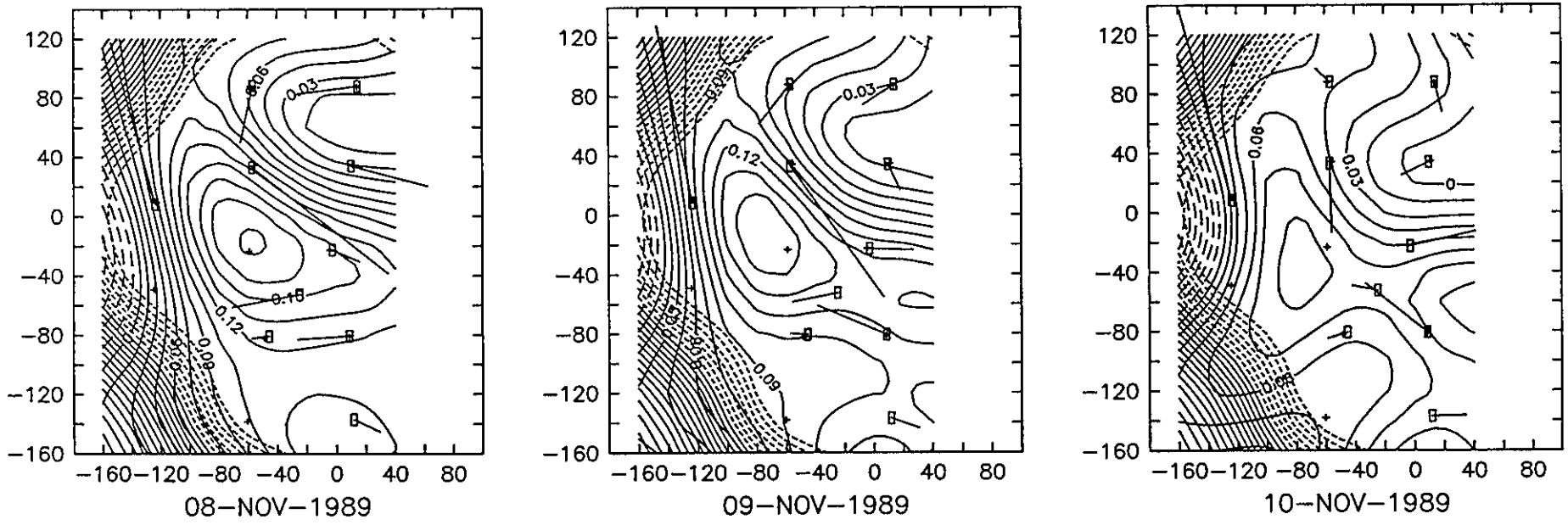
120
80
40
0
−40
−80
−120
−160
−160 −120 −80 −40 0 40 80
0.06
0.03
0.15
0.12
0.09
08−NOV−1989
09−NOV−1989
10−NOV−1989

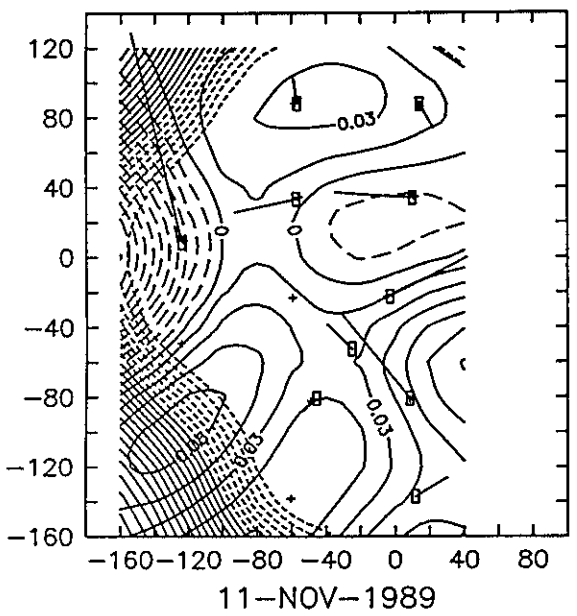
120
80
40
0
−40
−80
−120
−160
−160 −120 −80 −40 0 40 80
0.03
0
11−NOV−1989

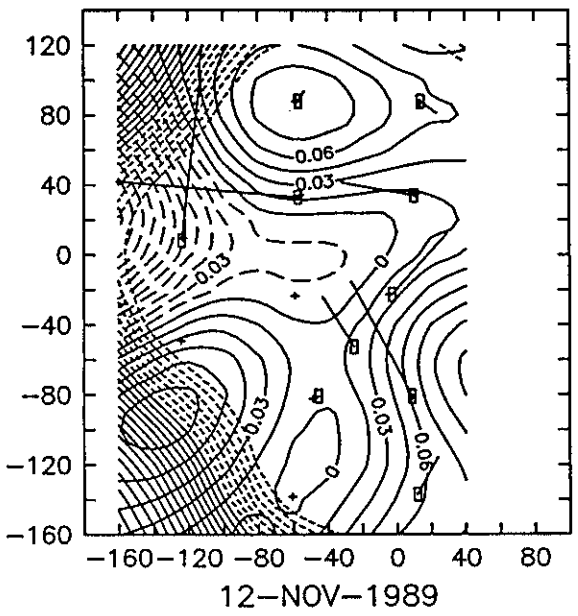
120
80
40
0
−40
−80
−120
−160
−160 −120 −80 −40 0 40 80
0.06
0.03
0
12−NOV−1989

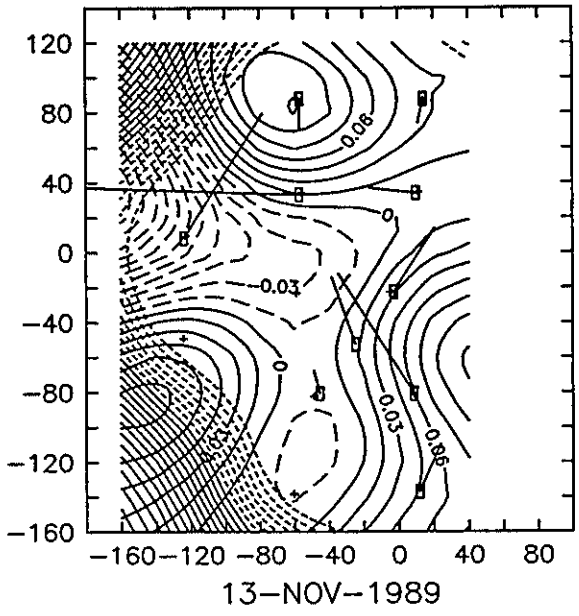
120
80
40
0
−40
−80
−120
−160
−160 −120 −80 −40 0 40 80
0.06
0.03
0
13−NOV−1989

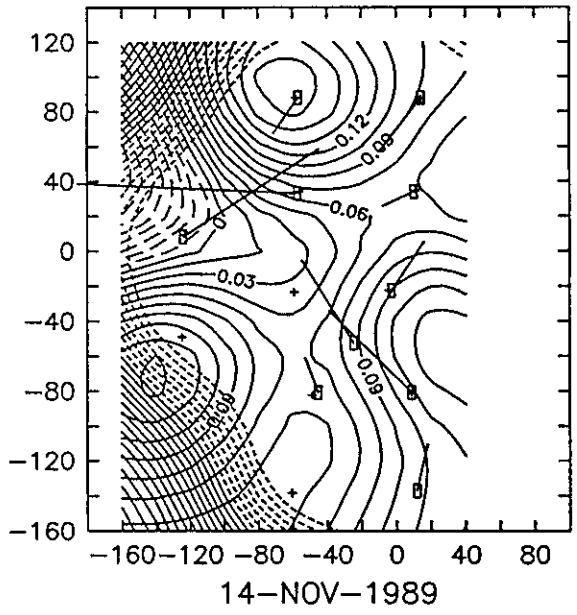
120
80
40
0
−40
−80
−120
−160
−160 −120 −80 −40 0 40 80
0.12
0.09
0.06
0.03
0
14−NOV−1989

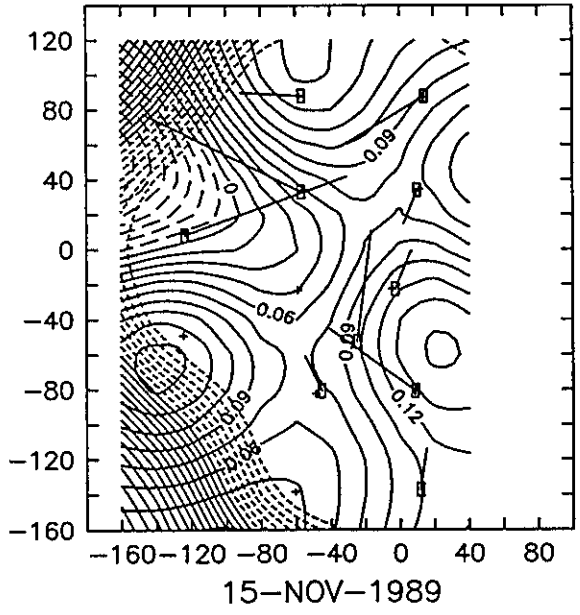
120
80
40
0
−40
−80
−120
−160
−160 −120 −80 −40 0 40 80
0.09
0.06
0.12
0
15−NOV−1989

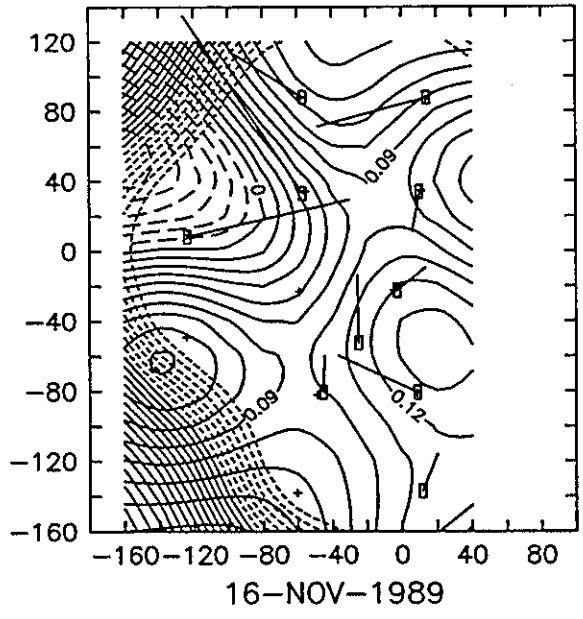
120
80
40
0
−40
−80
−120
−160
−160 −120 −80 −40 0 40 80
0.09
0.12
0
16−NOV−1989

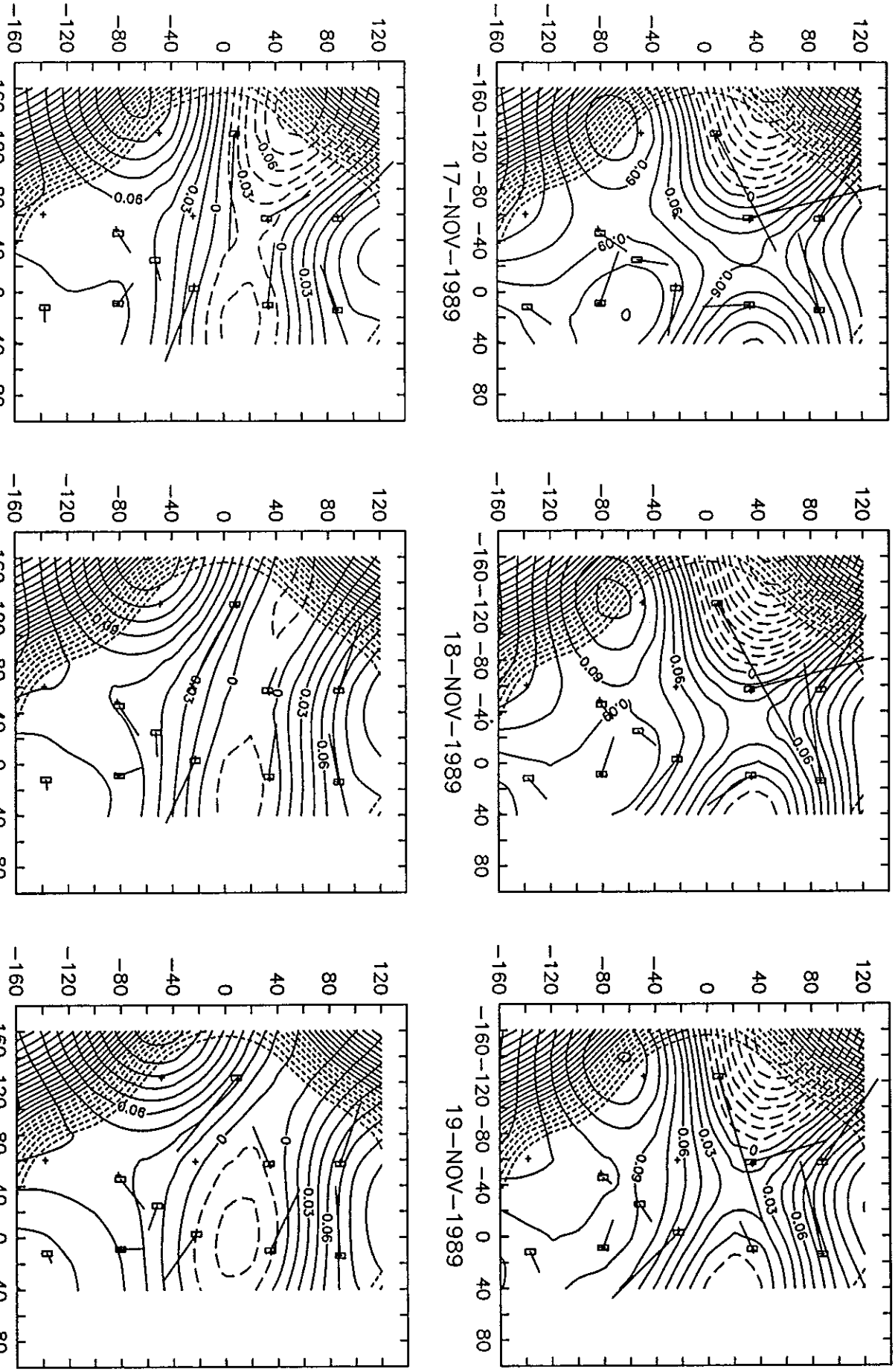
17-NOV-1989
18-NOV-1989
19-NOV-1989
20-NOV-1989
21-NOV-1989
22-NOV-1989

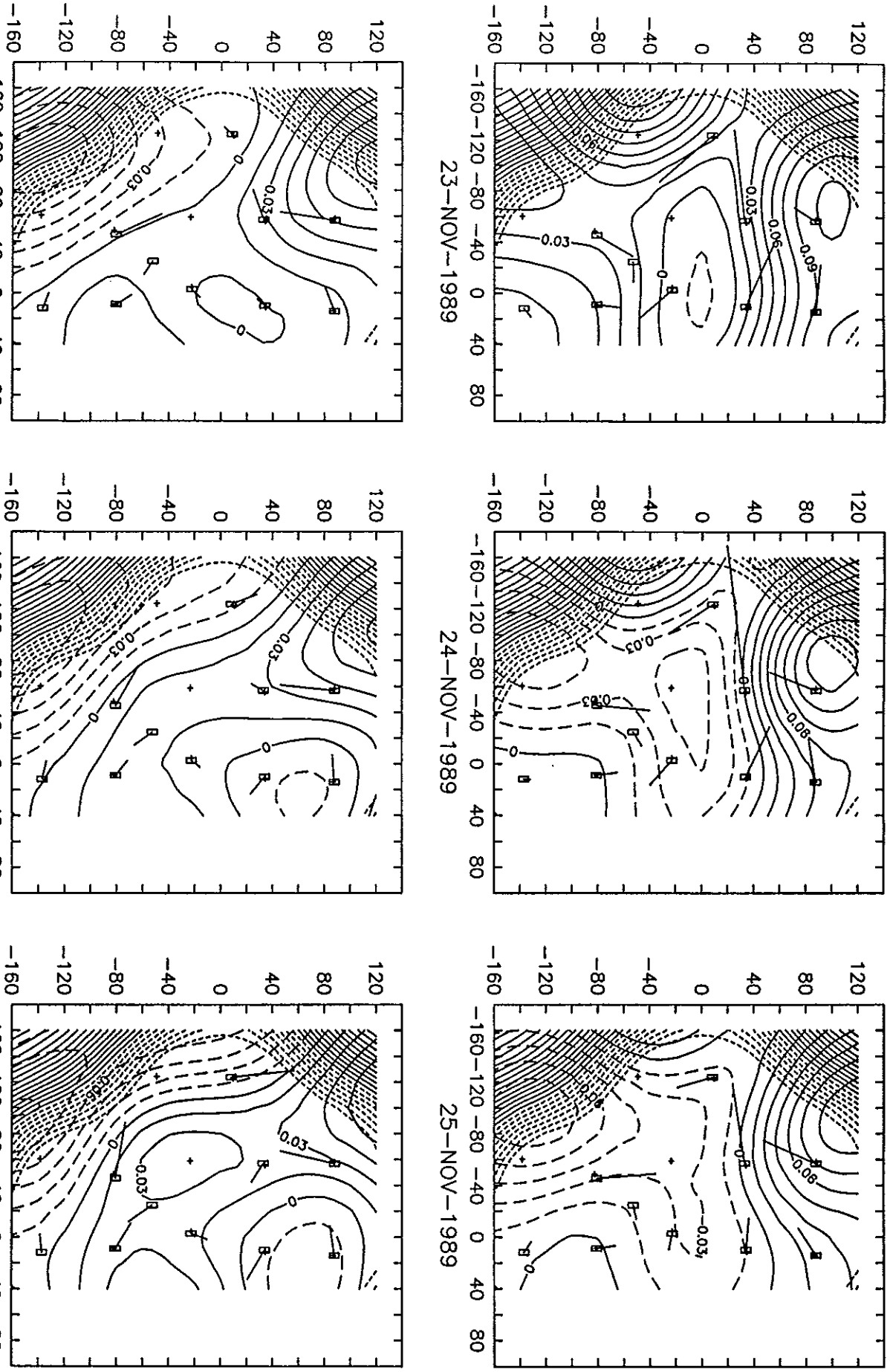
23-NOV-1989
24-NOV-1989
25-NOV-1989
26-NOV-1989
27-NOV-1989
28-NOV-1989

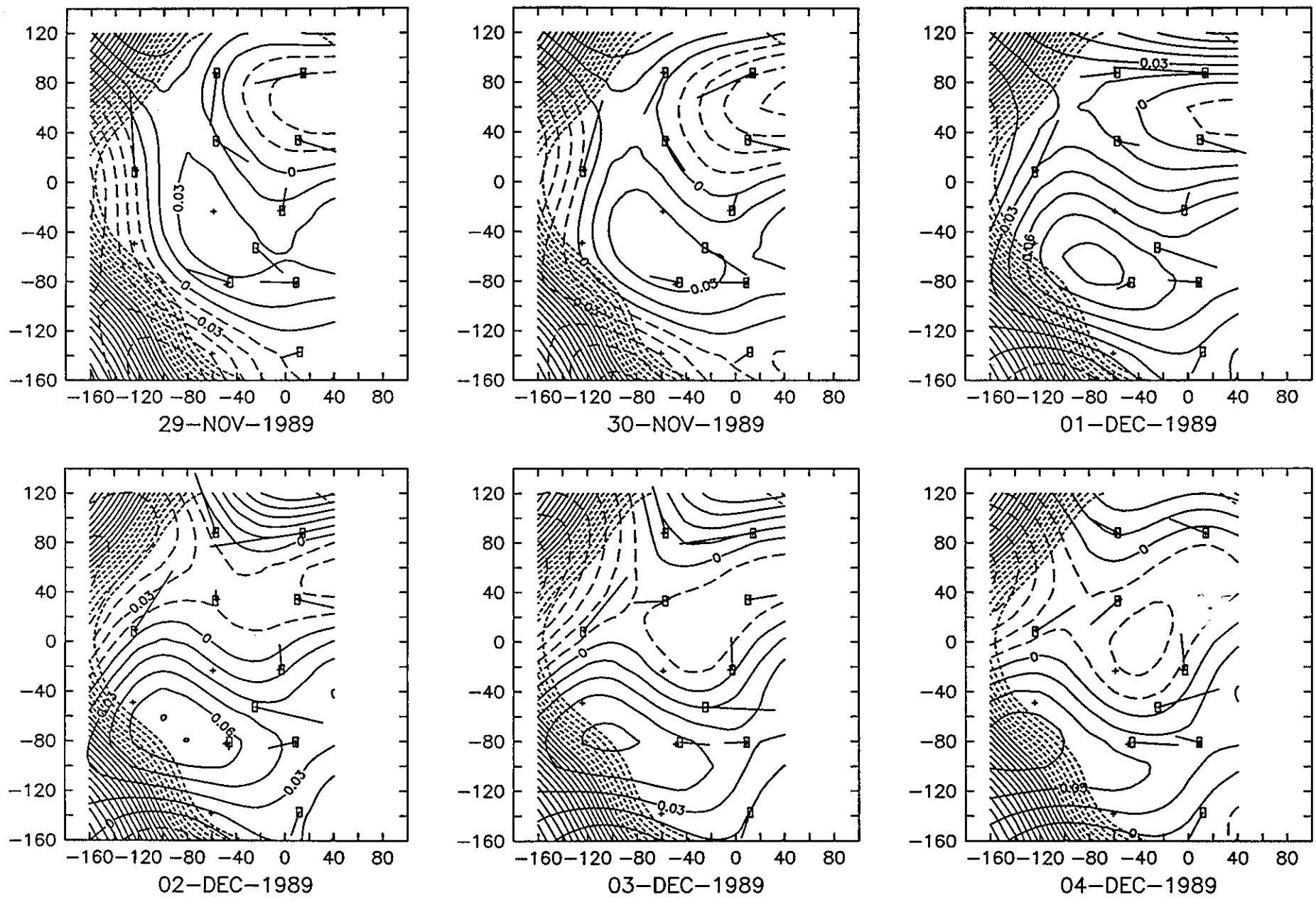
29-NOV-1989
30-NOV-1989
01-DEC-1989
02-DEC-1989
03-DEC-1989
04-DEC-1989

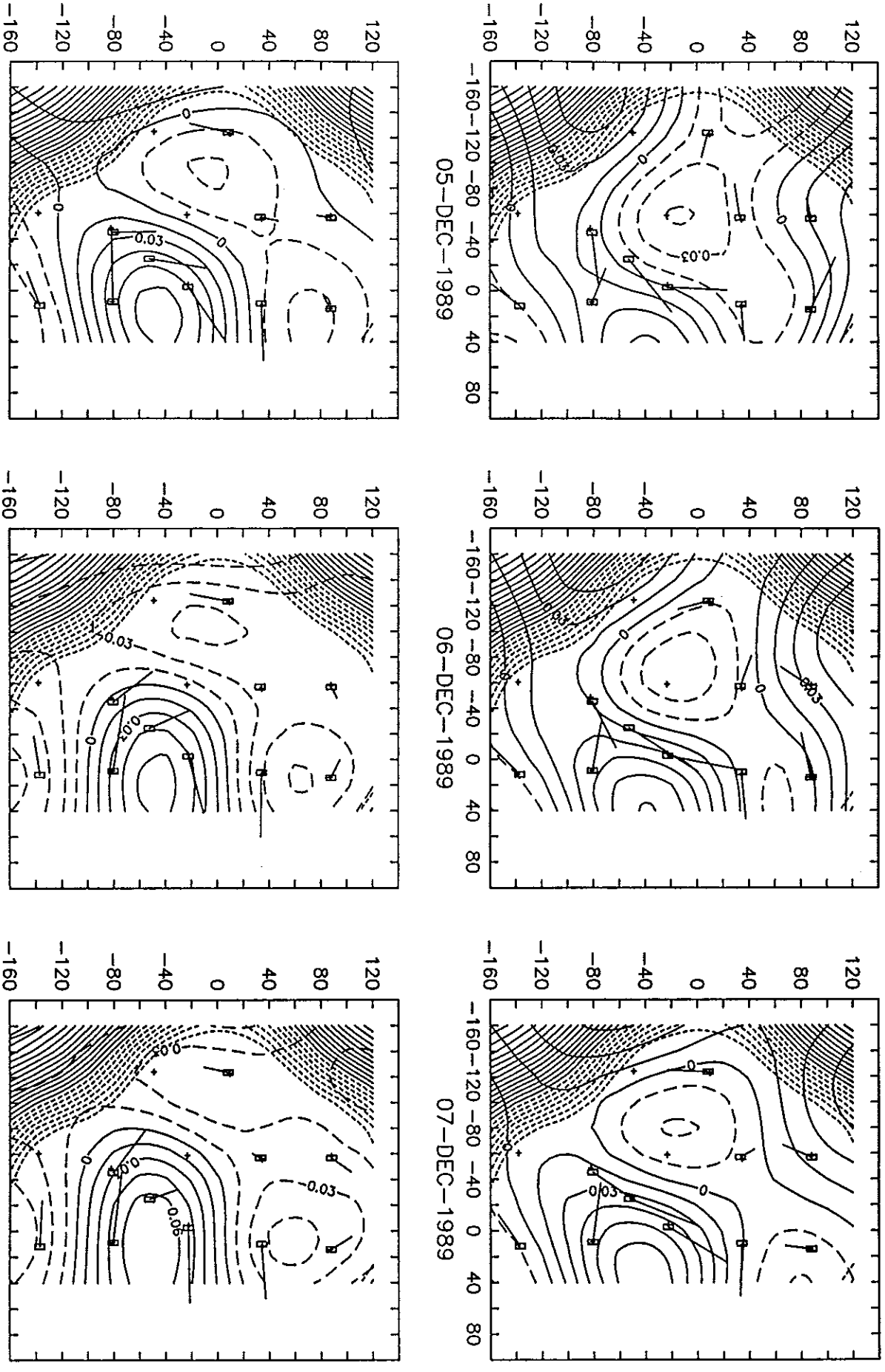
05-DEC-1989
06-DEC-1989
07-DEC-1989
08-DEC-1989
09-DEC-1989
10-DEC-1989

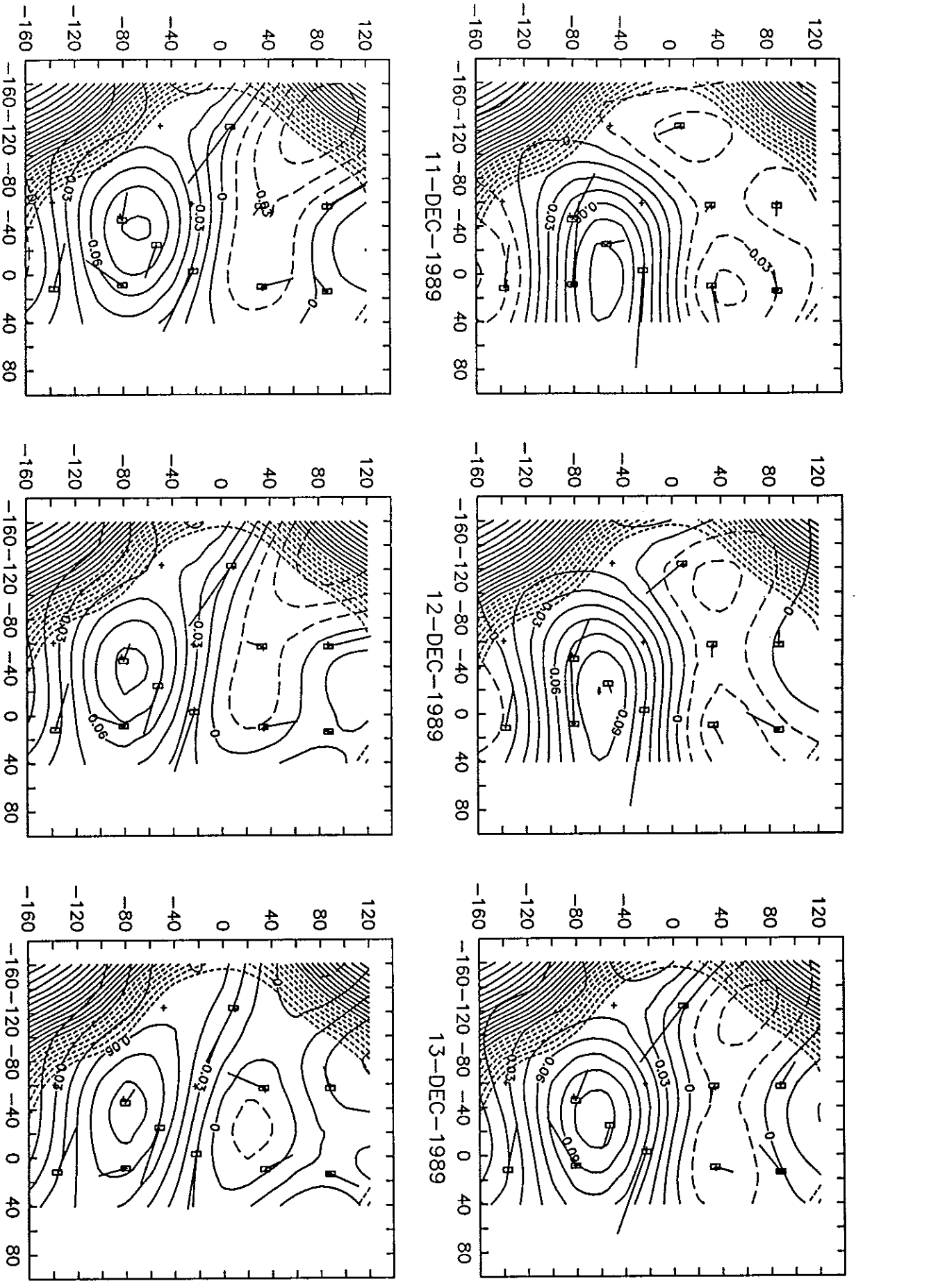
11-DEC-1989
12-DEC-1989
13-DEC-1989
14-DEC-1989
15-DEC-1989
16-DEC-1989

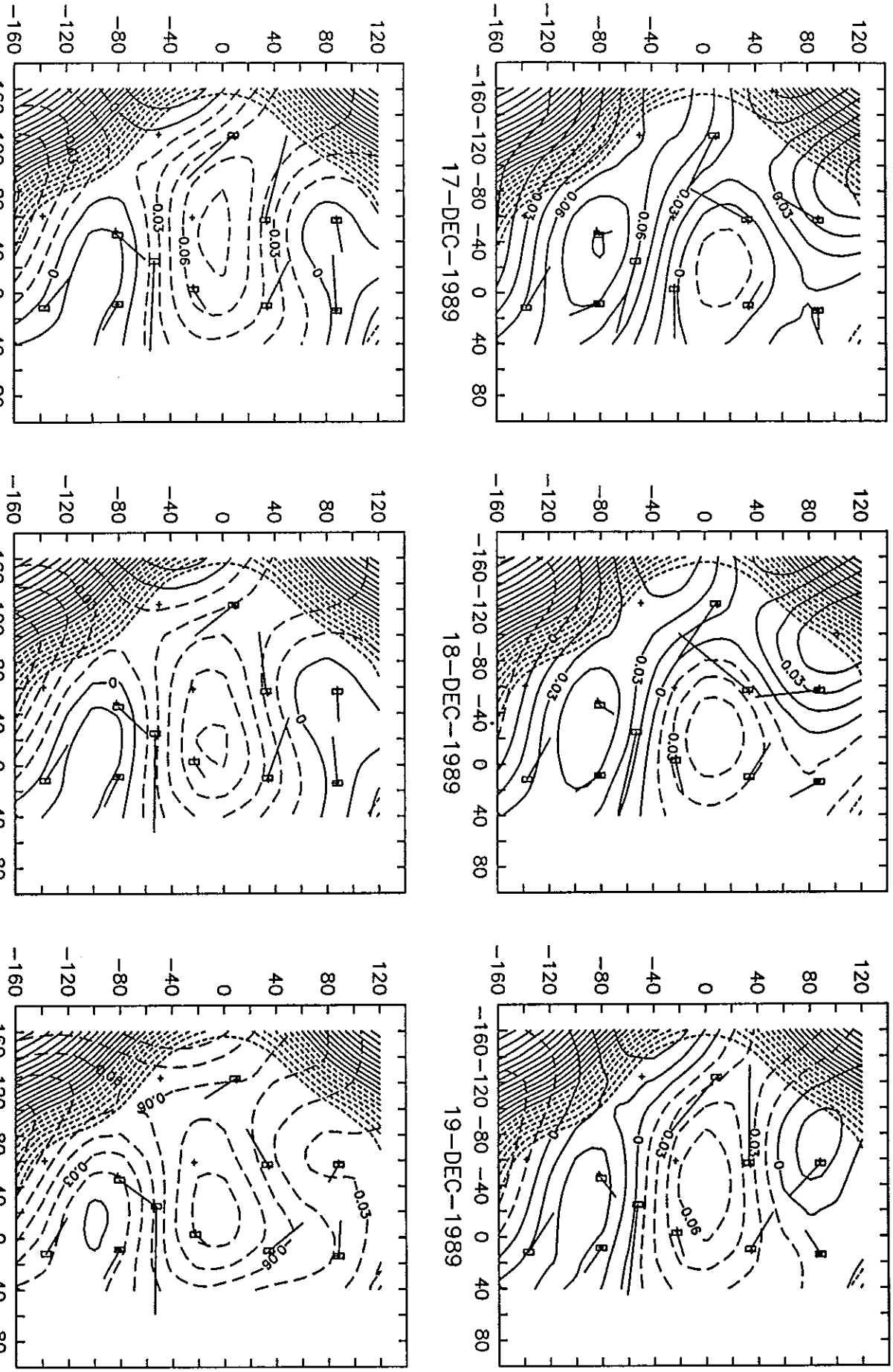
17-DEC-1989
18-DEC-1989
19-DEC-1989
20-DEC-1989
21-DEC-1989
22-DEC-1989

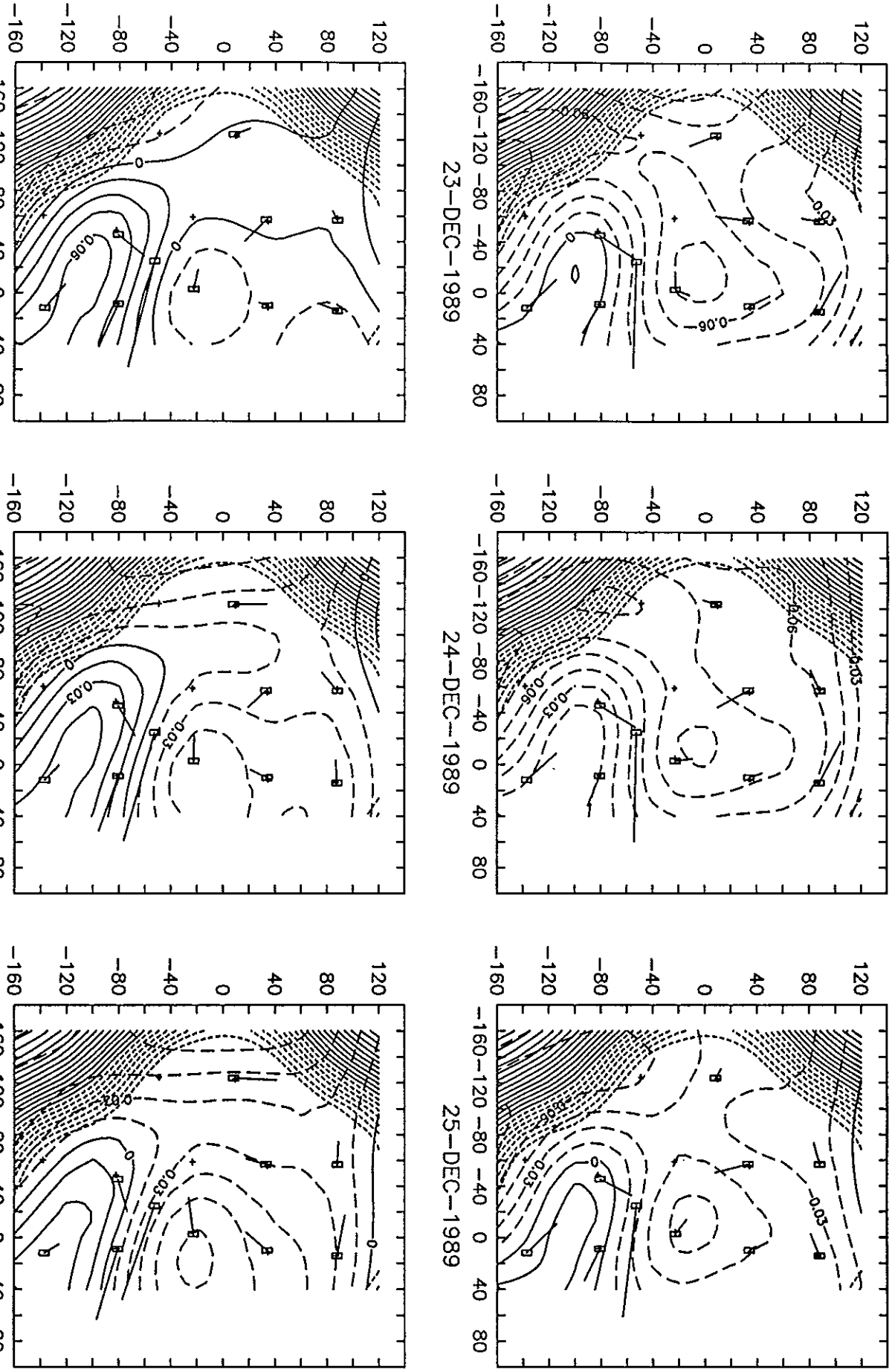
23-DEC-1989
24-DEC-1989
25-DEC-1989
26-DEC-1989
27-DEC-1989
28-DEC-1989

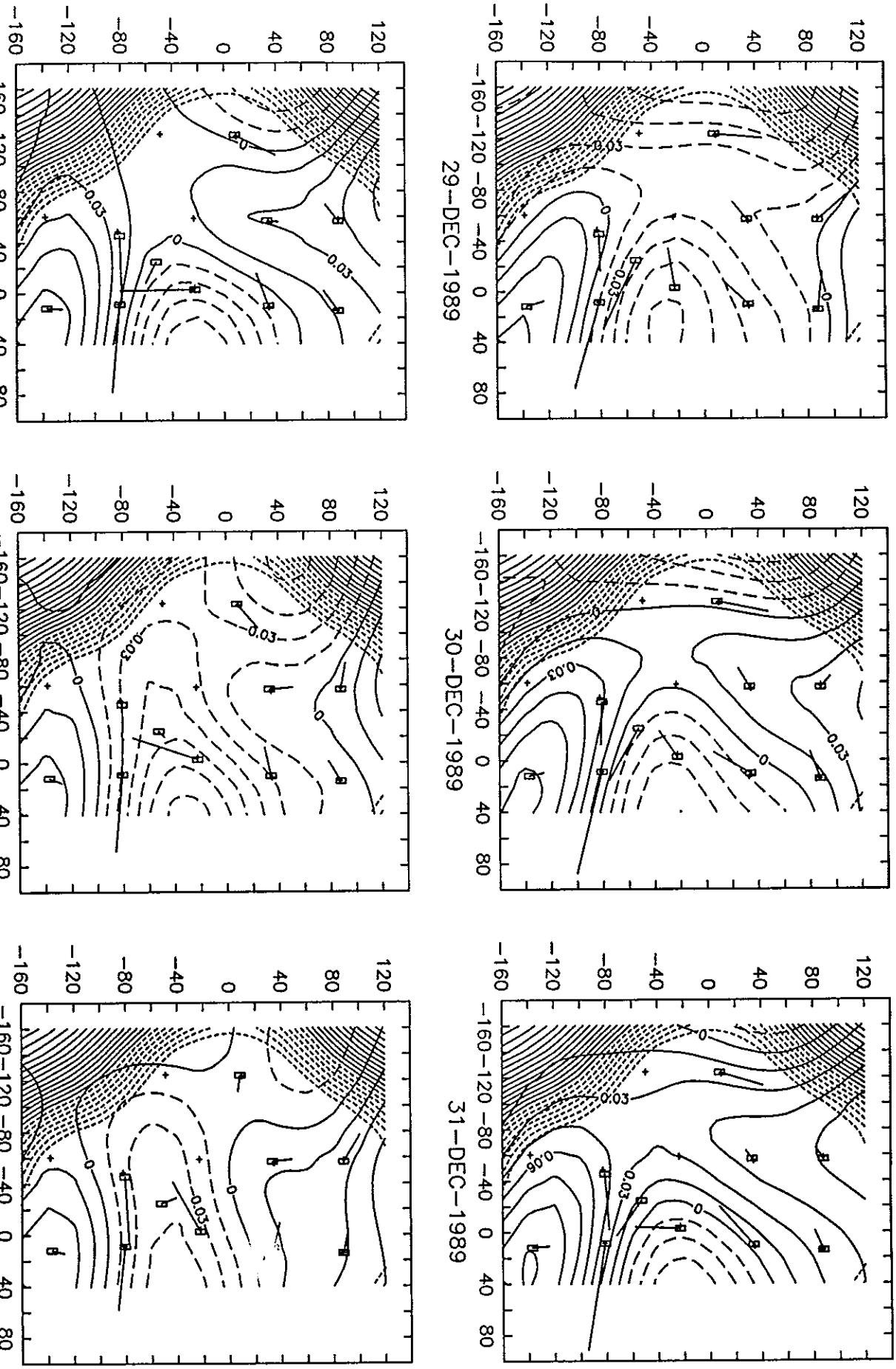
29--DEC--1989
30--DEC--1989
31--DEC--1989
01--JAN--1990
02--JAN--1990
03--JAN--1990

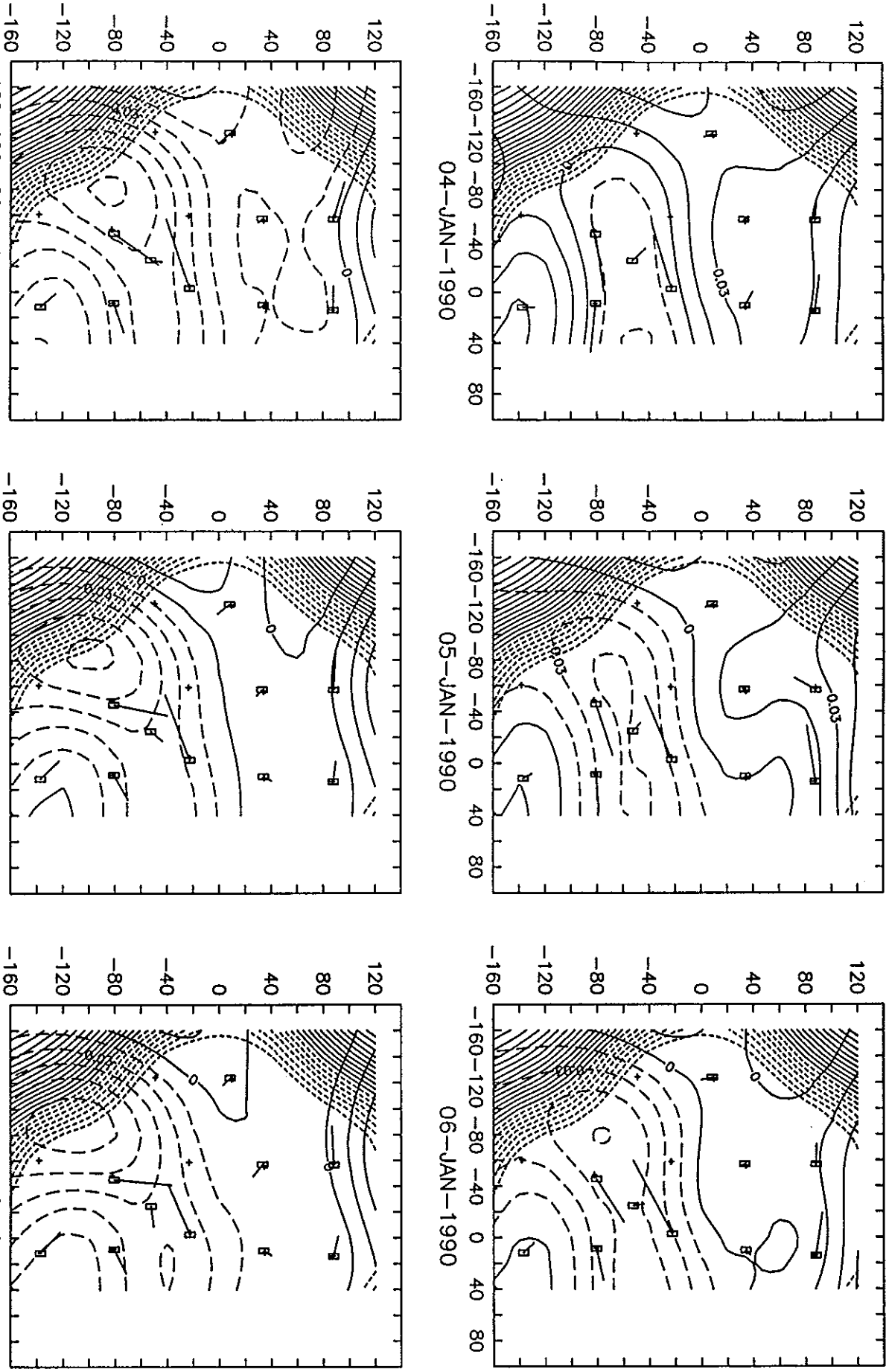
04-JAN-1990
05-JAN-1990
06-JAN-1990
07-JAN-1990
08-JAN-1990
09-JAN-1990

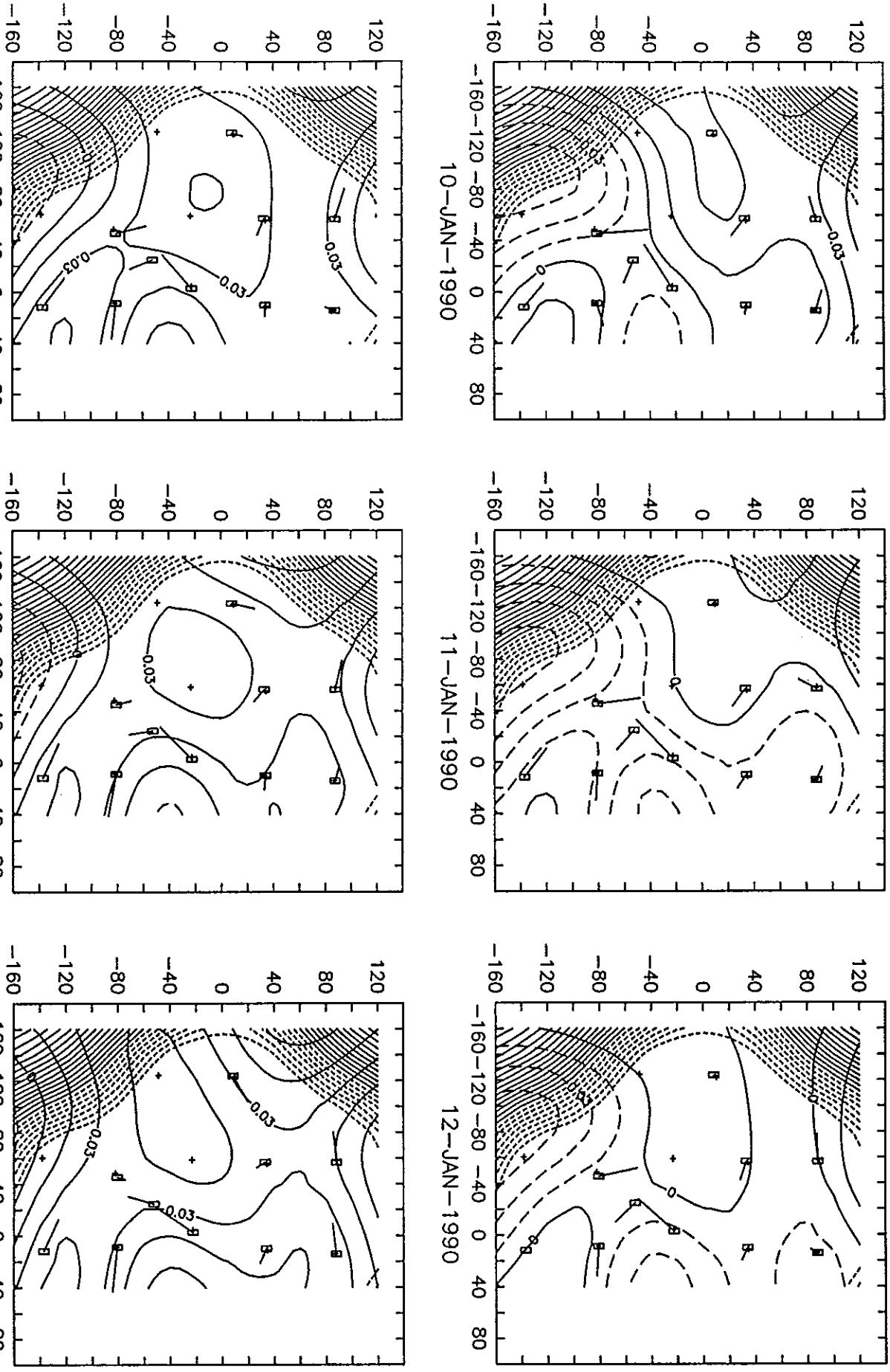
10-JAN-1990
11-JAN-1990
12-JAN-1990
13-JAN-1990
14-JAN-1990
15-JAN-1990
0.03
0
-0.03

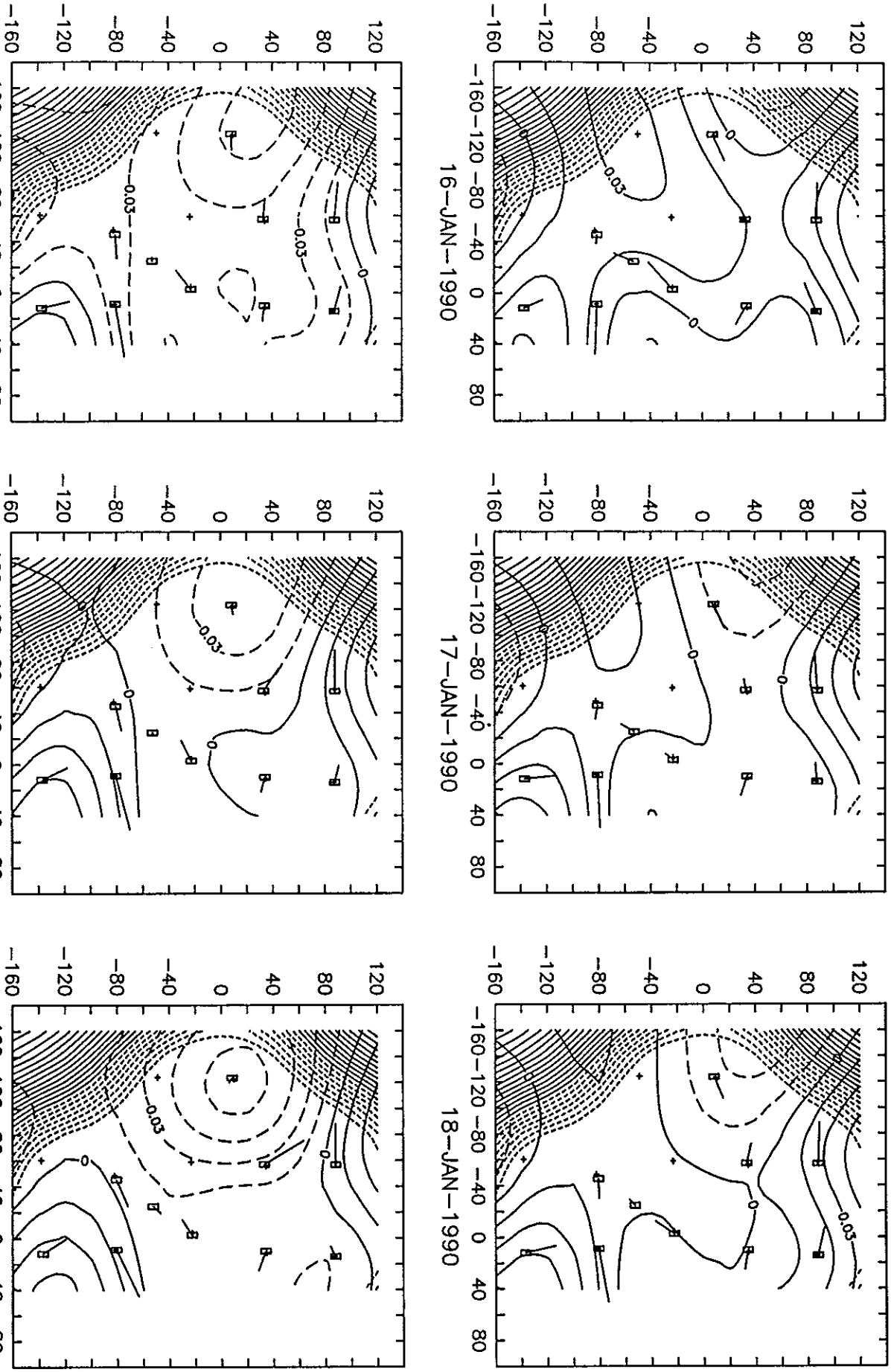
16-JAN-1990
17-JAN-1990
18-JAN-1990
19-JAN-1990
20-JAN-1990
21-JAN-1990

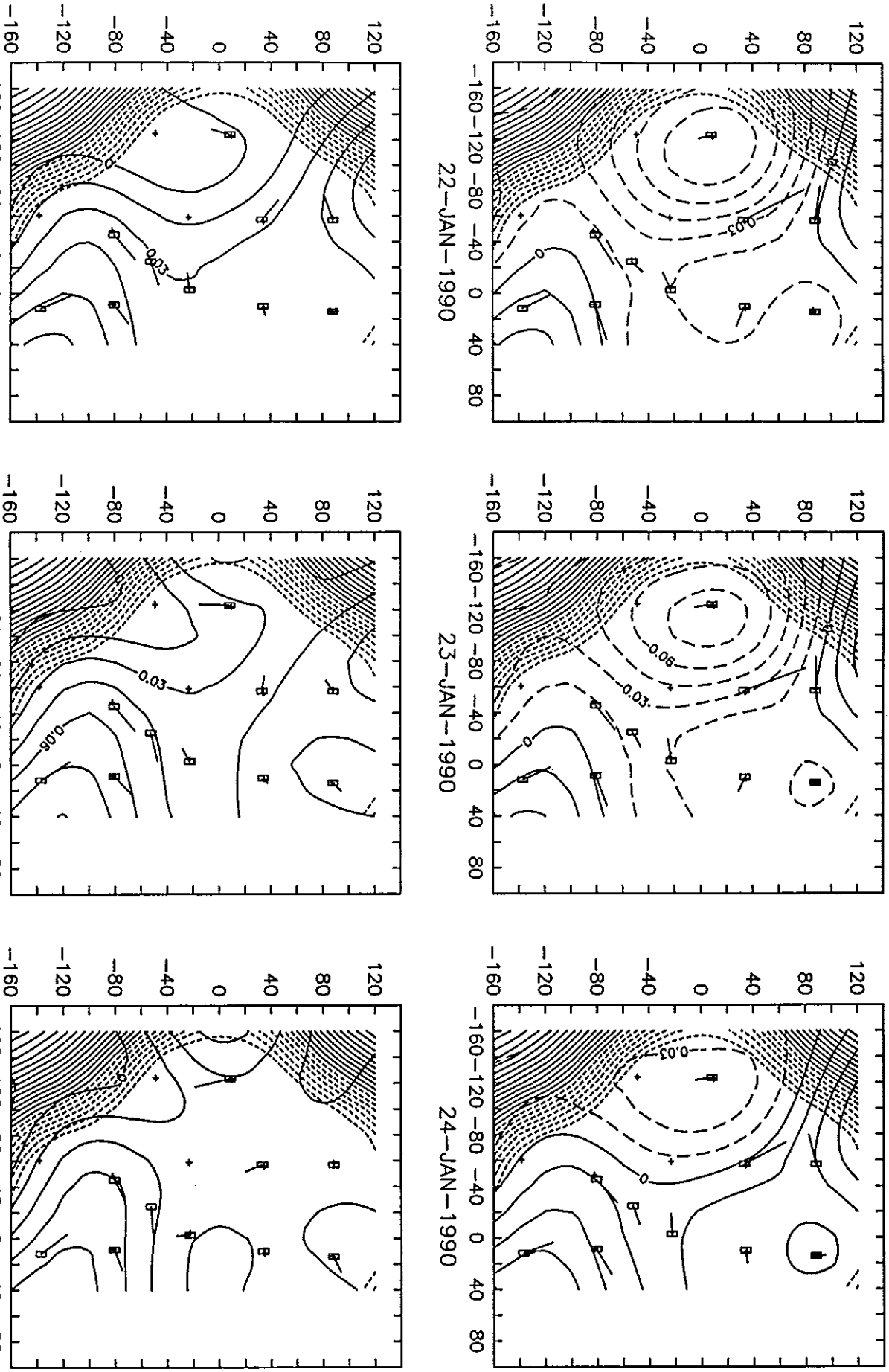
22-JAN-1990
23-JAN-1990
24-JAN-1990
25-JAN-1990
26-JAN-1990
27-JAN-1990

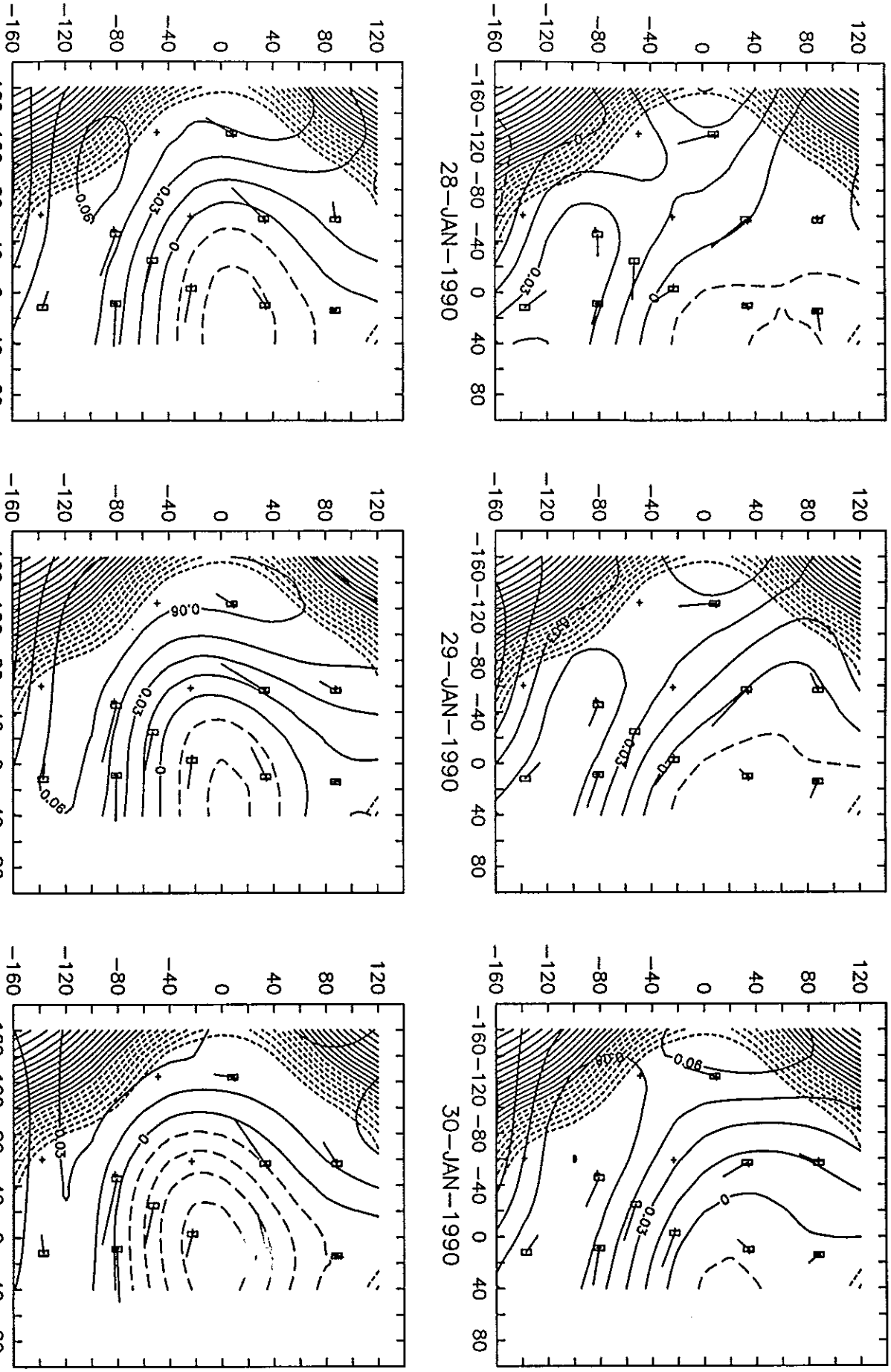
28-JAN-1990
29-JAN-1990
30-JAN-1990
31-JAN-1990
01-FEB-1990
02-FEB-1990

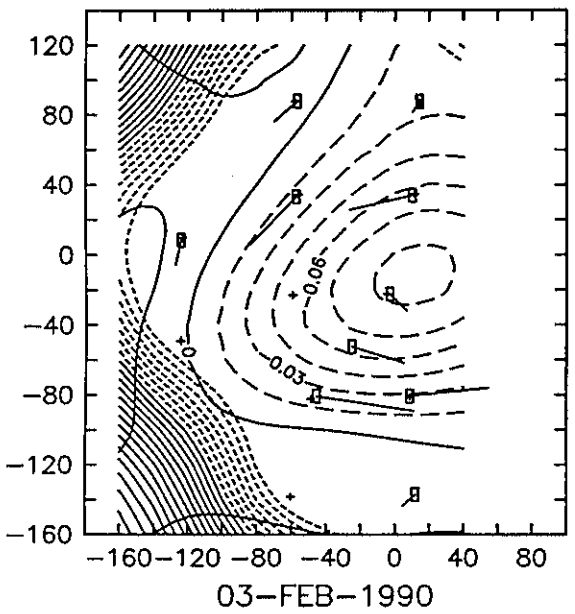
120
80
40
0
−40
−80
−120
−160
−160 −120 −80 −40 0 40 80
0.06
0.03
0
03−FEB−1990

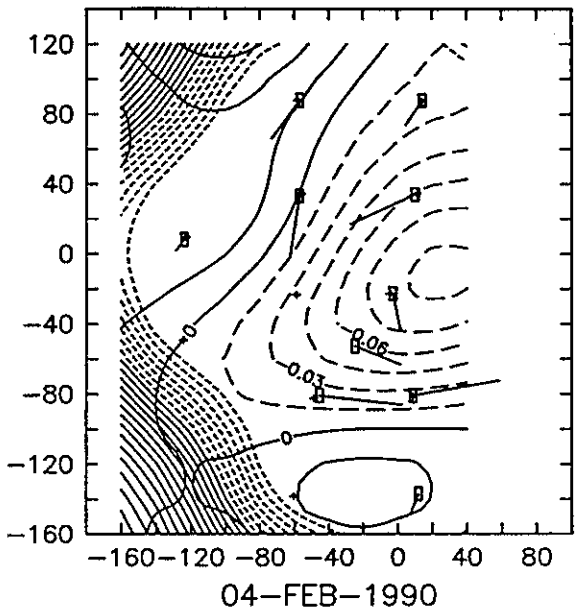
120
80
40
0
−40
−80
−120
−160
−160 −120 −80 −40 0 40 80
0.06
0.03
0
04−FEB−1990

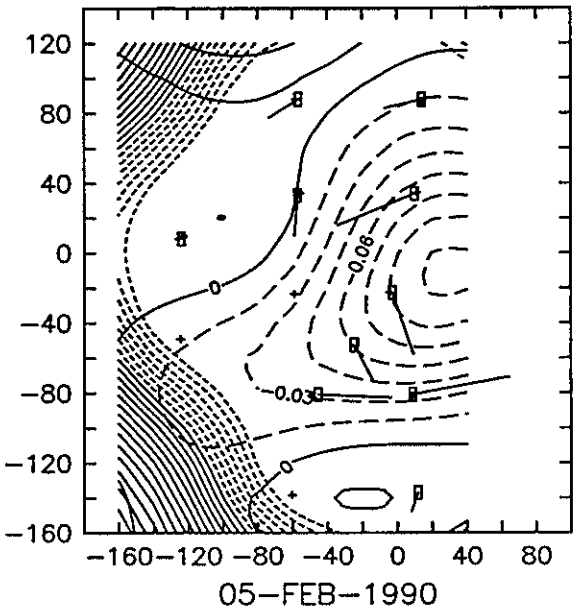
120
80
40
0
−40
−80
−120
−160
−160 −120 −80 −40 0 40 80
0.06
0.03
0
05−FEB−1990

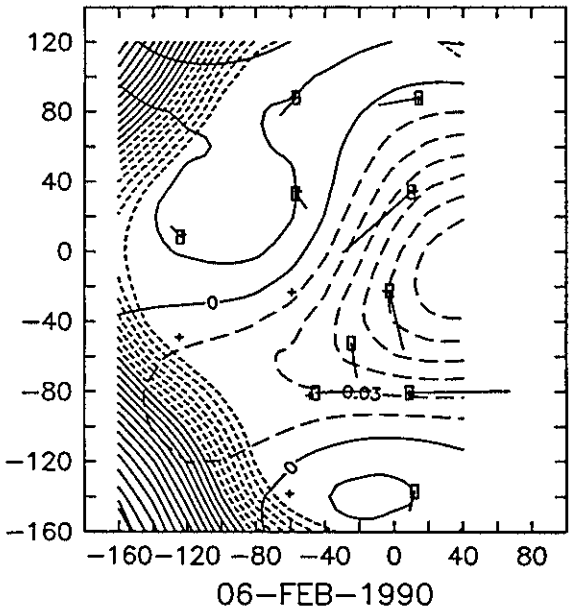
120
80
40
0
−40
−80
−120
−160
−160 −120 −80 −40 0 40 80
0.03
0
06−FEB−1990

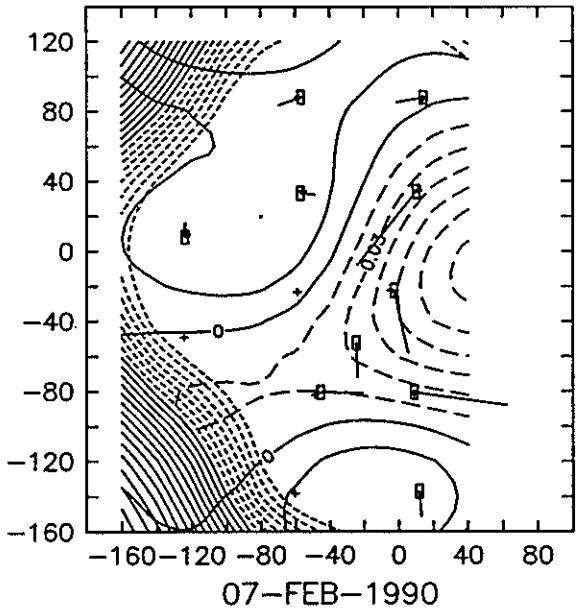
120
80
40
0
−40
−80
−120
−160
−160 −120 −80 −40 0 40 80
0.03
0
07−FEB−1990

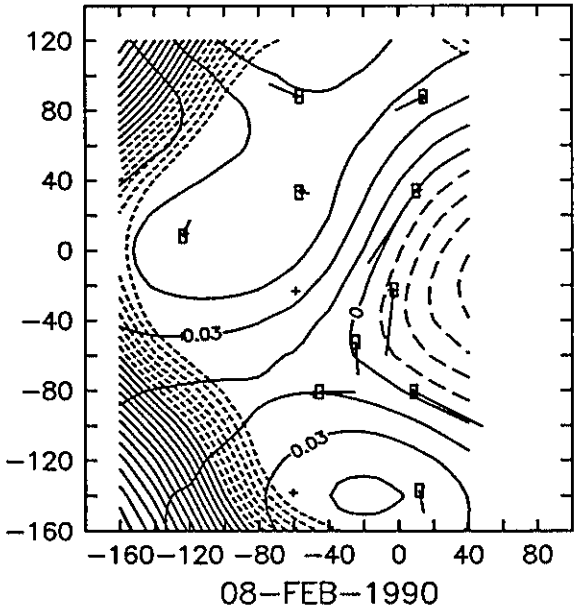
120
80
40
0
−40
−80
−120
−160
−160 −120 −80 −40 0 40 80
0.03
0
08−FEB−1990

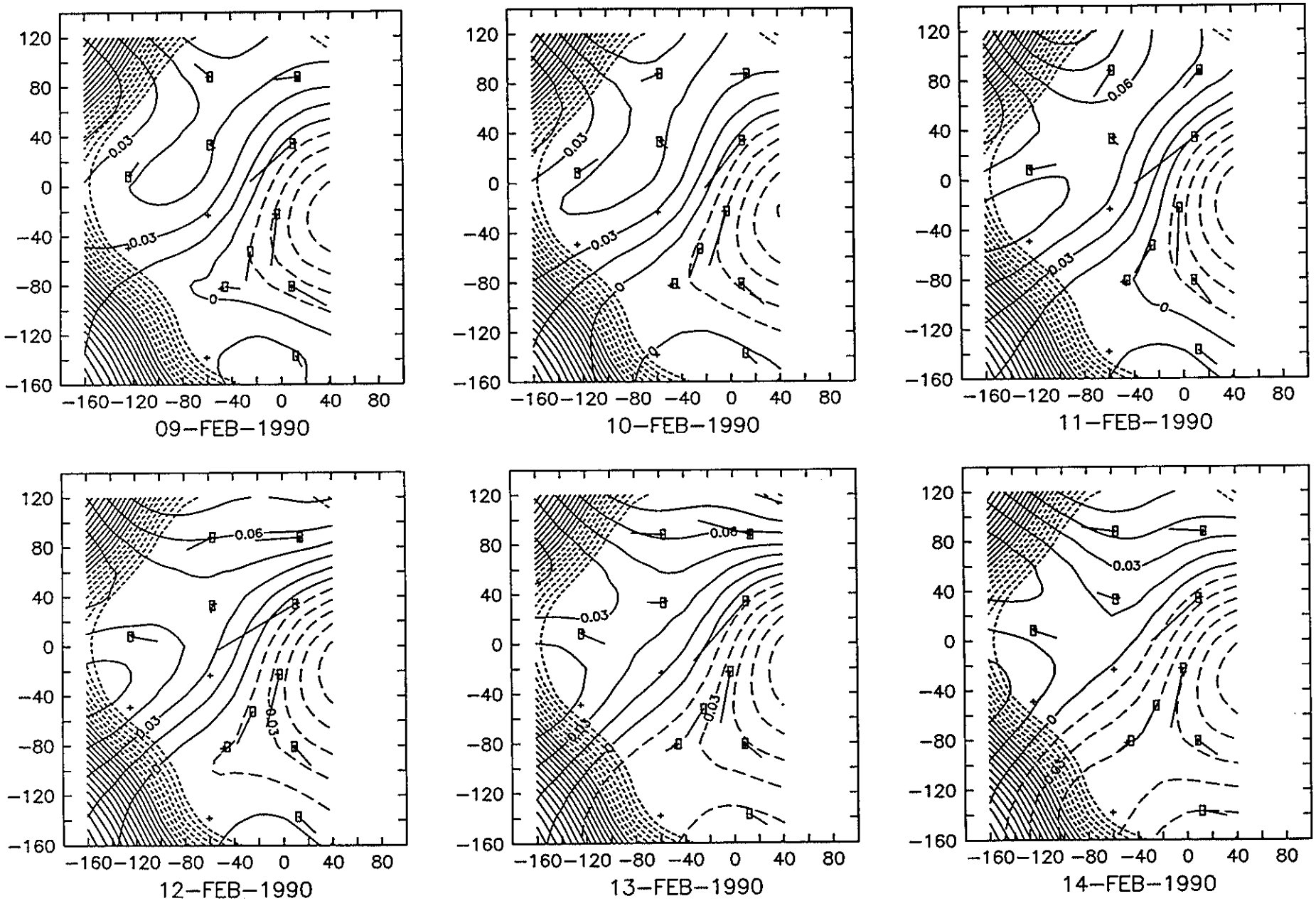
09-FEB-1990
10-FEB-1990
11-FEB-1990
12-FEB-1990
13-FEB-1990
14-FEB-1990

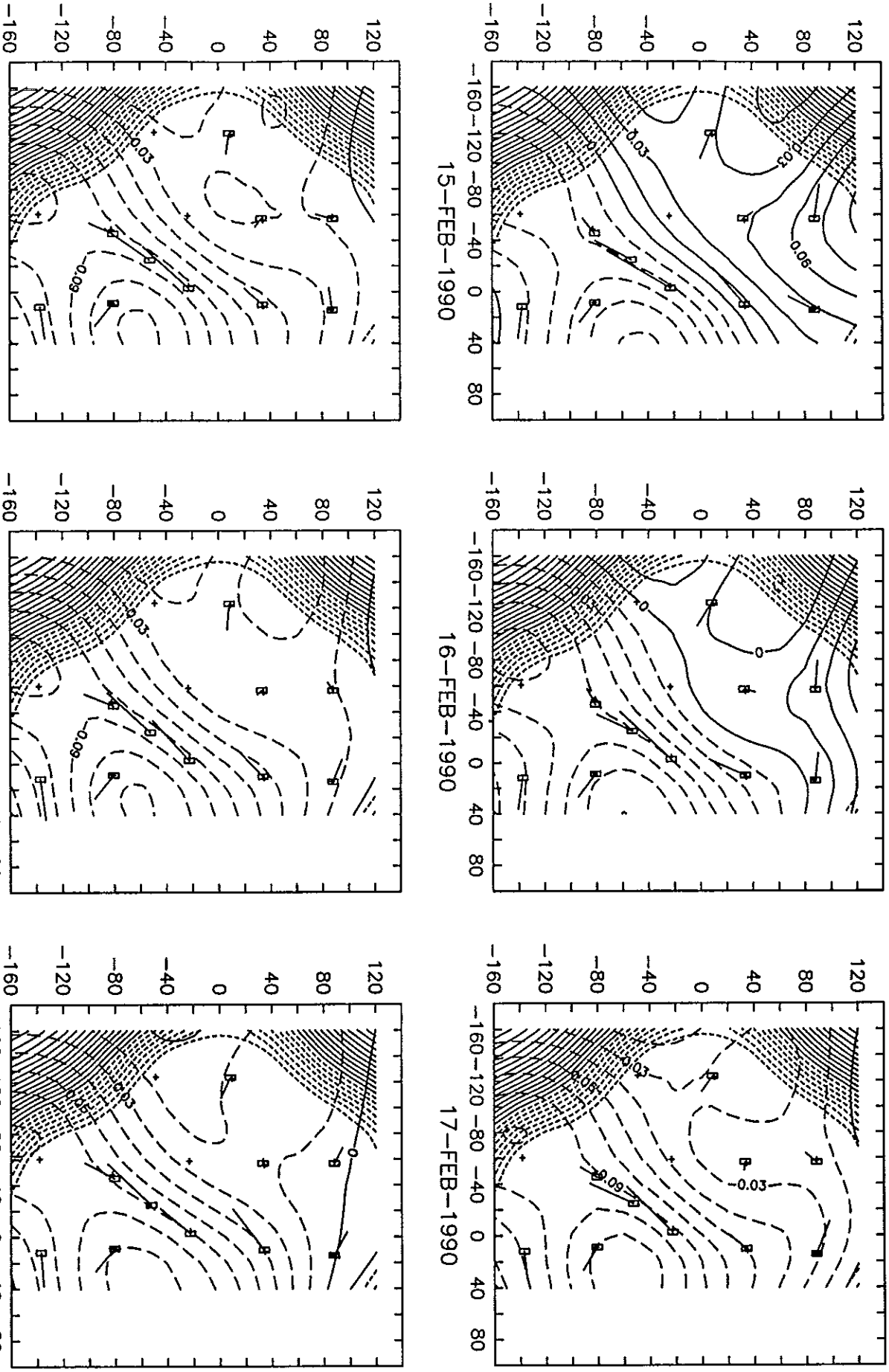
15-FEB-1990
16-FEB-1990
17-FEB-1990
18-FEB-1990
19-FEB-1990
20-FEB-1990

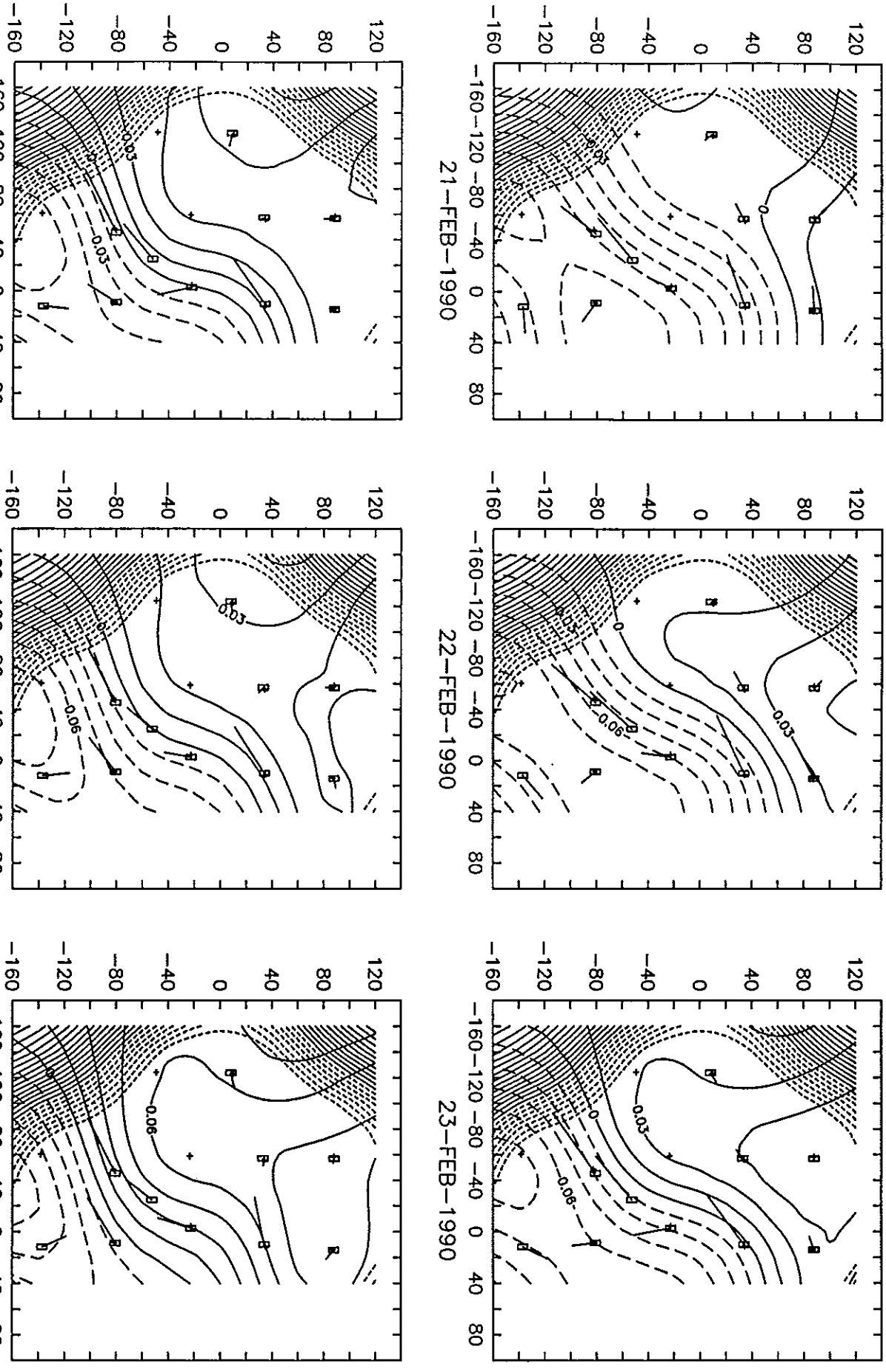
21-FEB-1990
22-FEB-1990
23-FEB-1990
24-FEB-1990
25-FEB-1990
26-FEB-1990

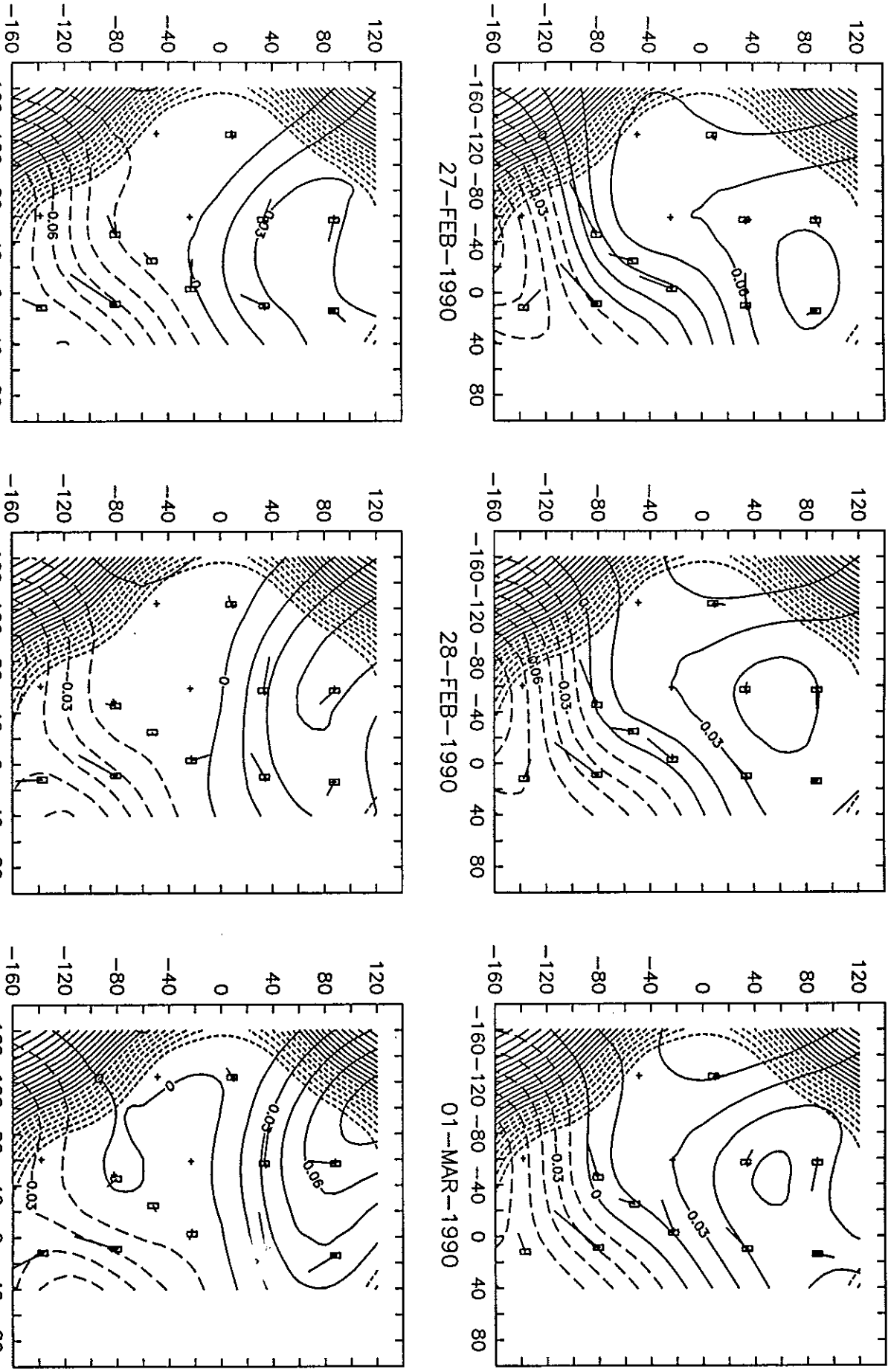
27-FEB-1990
28-FEB-1990
01-MAR-1990
02-MAR-1990
03-MAR-1990
04-MAR-1990

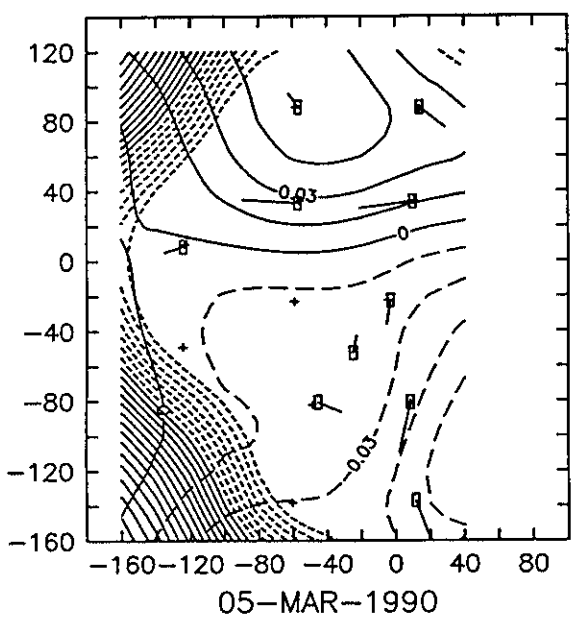
120
80
40
0
−40
−80
−120
−160
−160 −120 −80 −40 0 40 80
0.03
0
0.03
05−MAR−1990

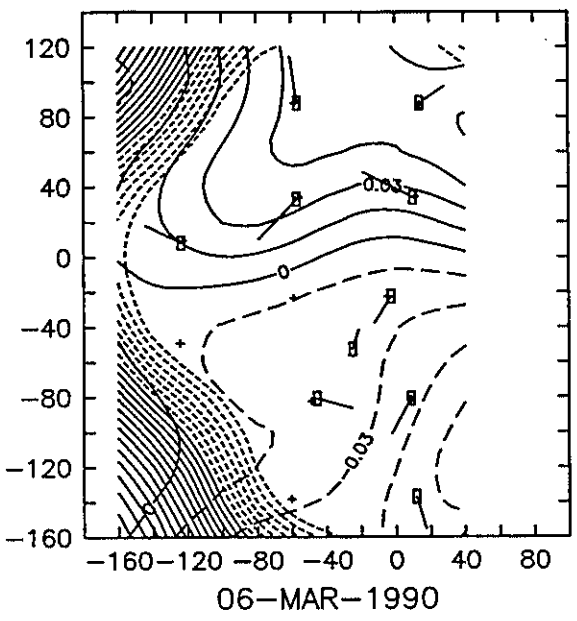
120
80
40
0
−40
−80
−120
−160
−160 −120 −80 −40 0 40 80
0.03
0
0.03
06−MAR−1990

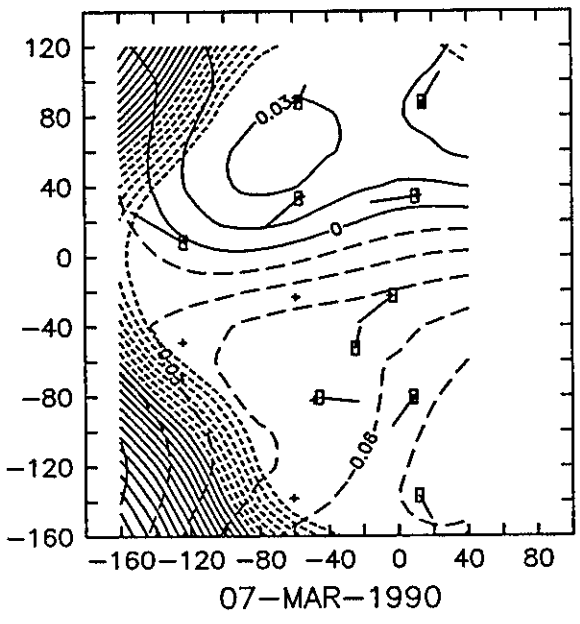
120
80
40
0
−40
−80
−120
−160
−160 −120 −80 −40 0 40 80
0.03
0
0.03
0.06
07−MAR−1990

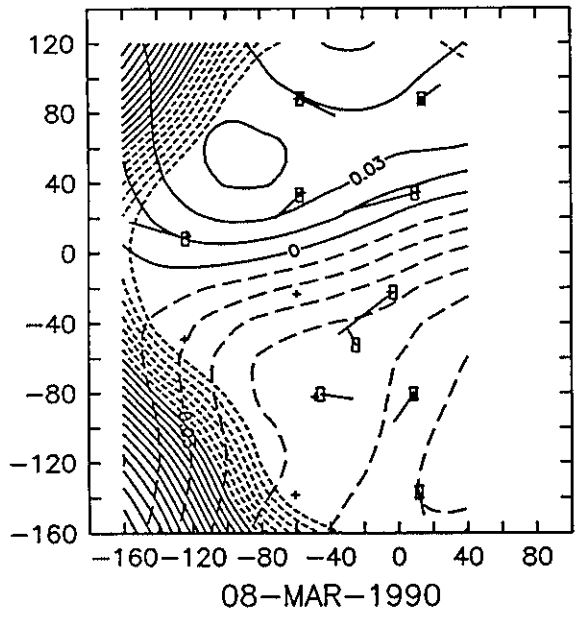
120
80
40
0
−40
−80
−120
−160
−160 −120 −80 −40 0 40 80
0.03
0
0.03
08−MAR−1990

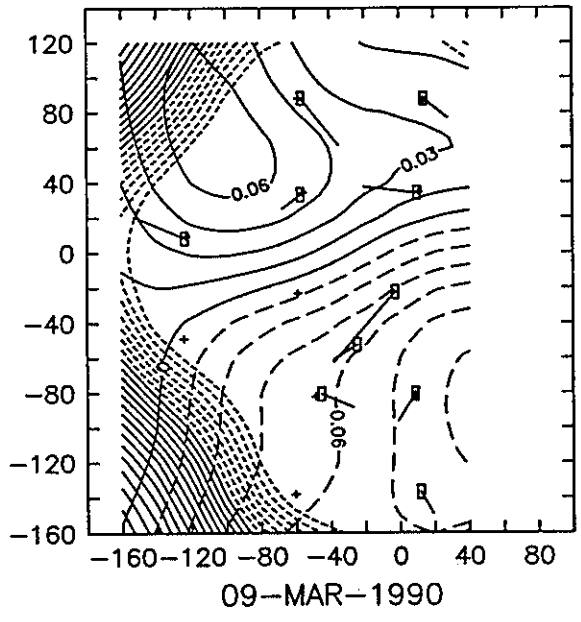
120
80
40
0
−40
−80
−120
−160
−160 −120 −80 −40 0 40 80
0.06
0.03
0.06
09−MAR−1990

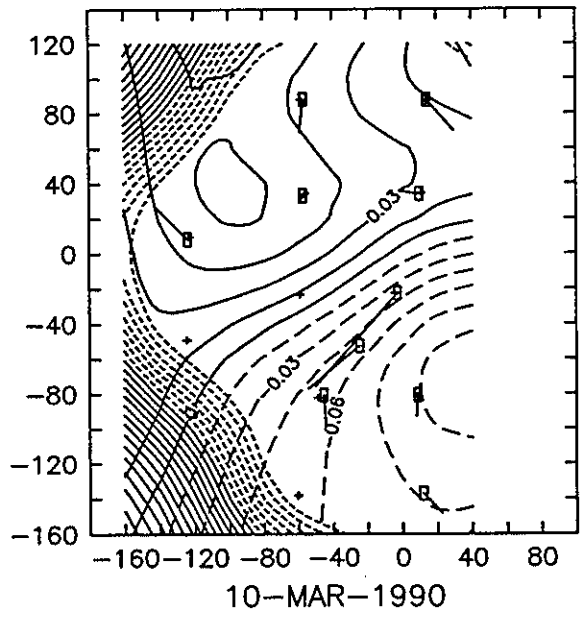
120
80
40
0
−40
−80
−120
−160
−160 −120 −80 −40 0 40 80
0.03
0.03
0.06
10−MAR−1990

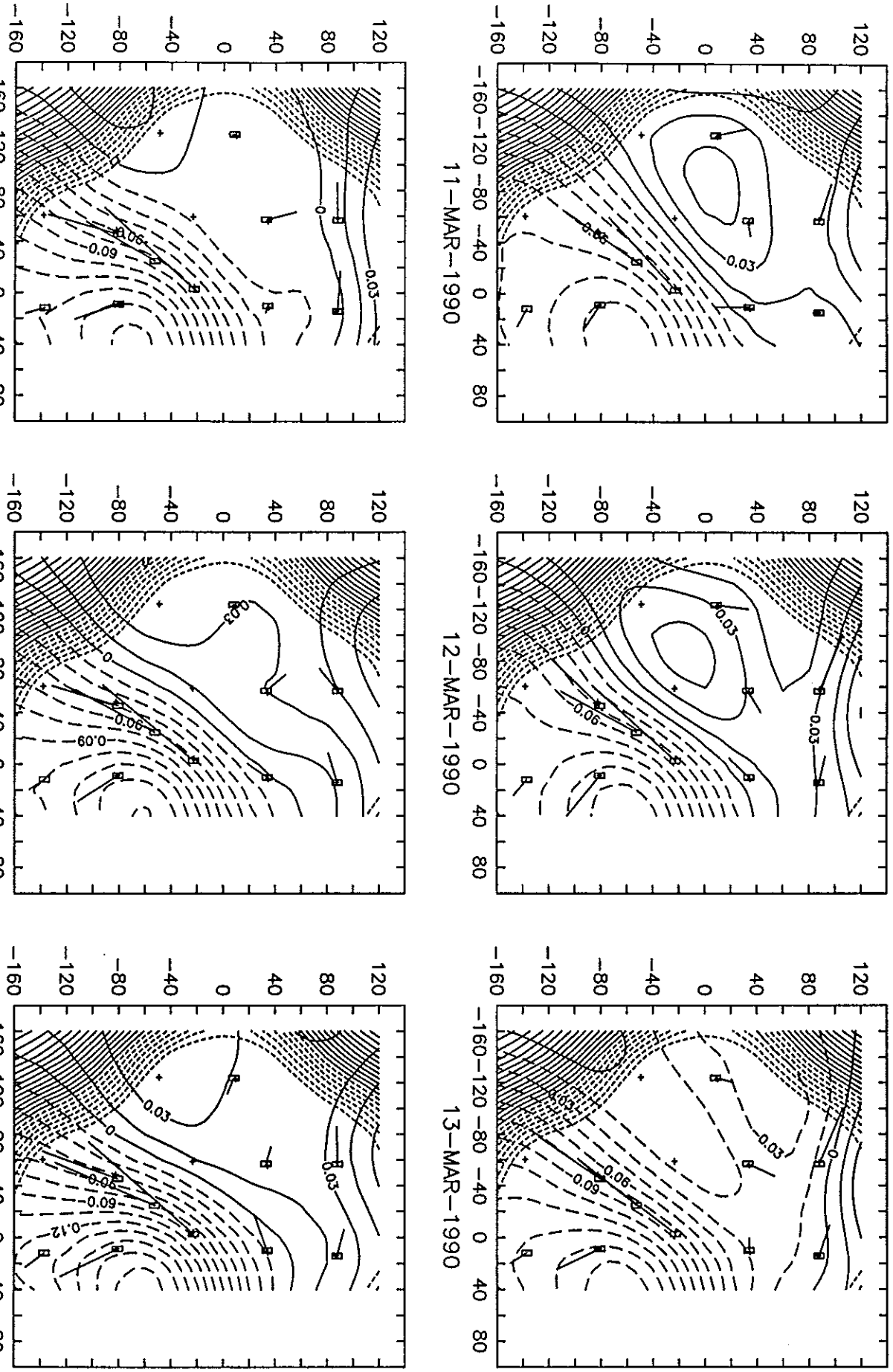
11-MAR-1990
12-MAR-1990
13-MAR-1990
14-MAR-1990
15-MAR-1990
16-MAR-1990

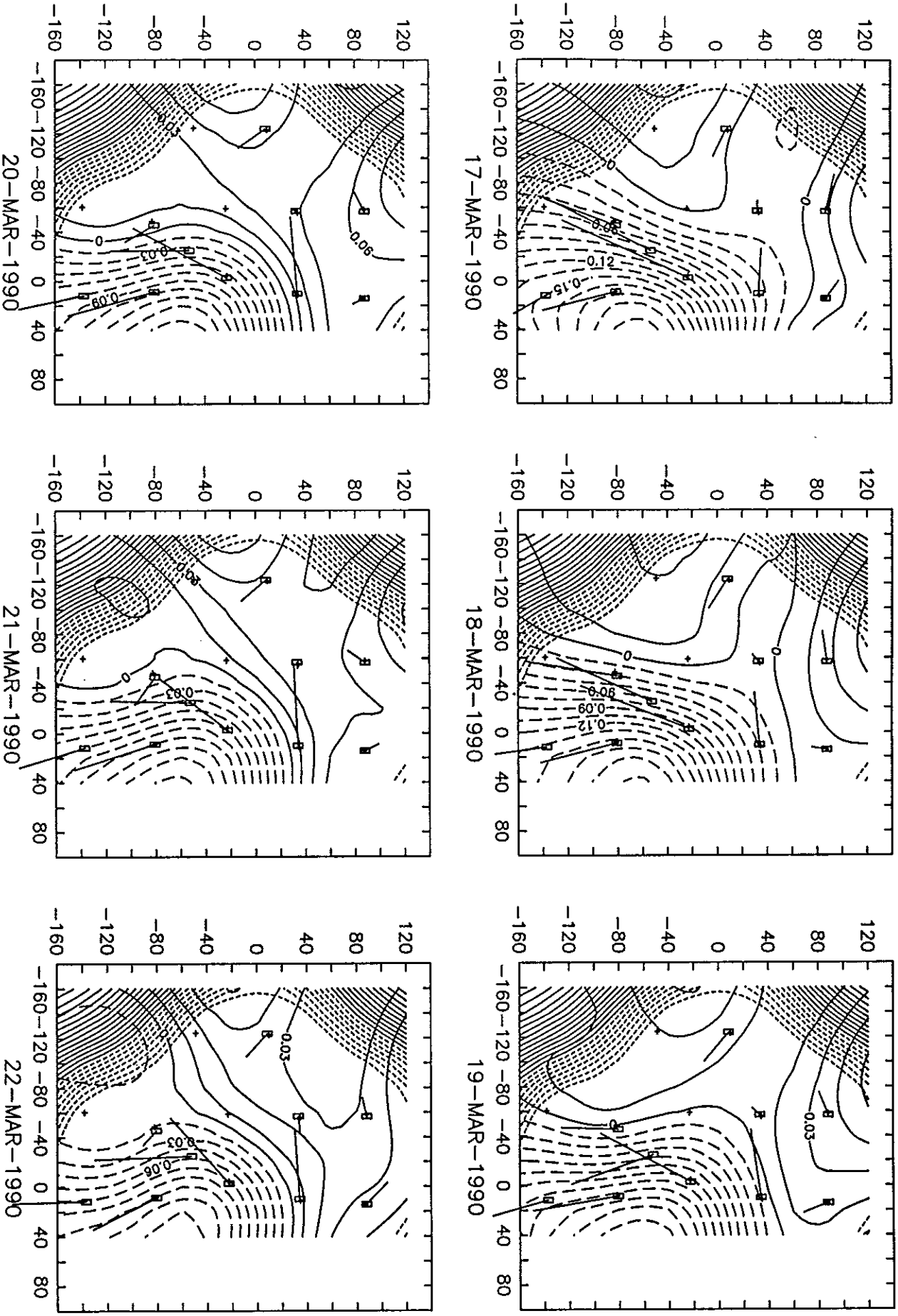
17-MAR-1990
18-MAR-1990
19-MAR-1990
20-MAR-1990
21-MAR-1990
22-MAR-1990

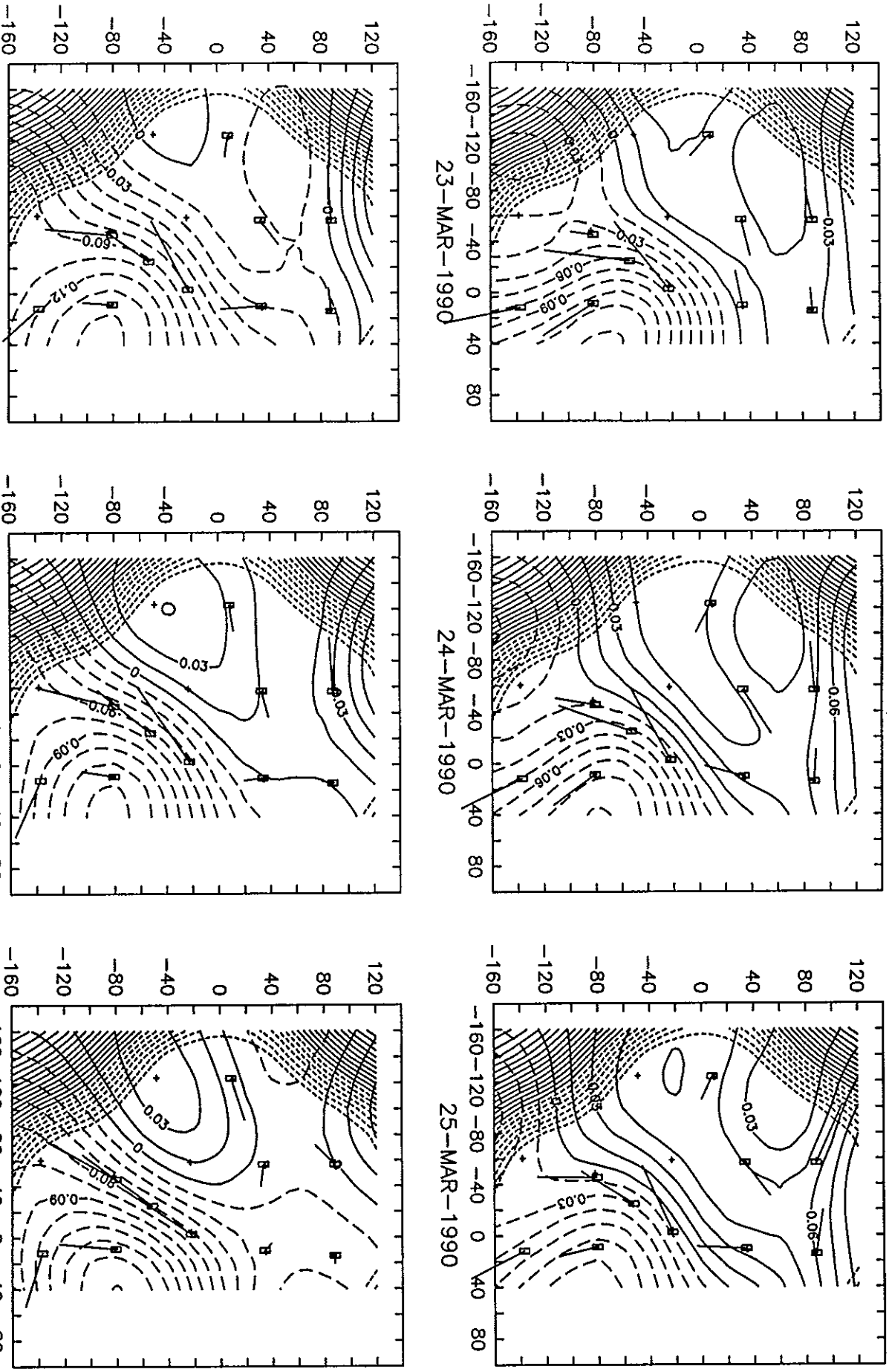
23-MAR-1990
24-MAR-1990
25-MAR-1990
26-MAR-1990
27-MAR-1990
28-MAR-1990

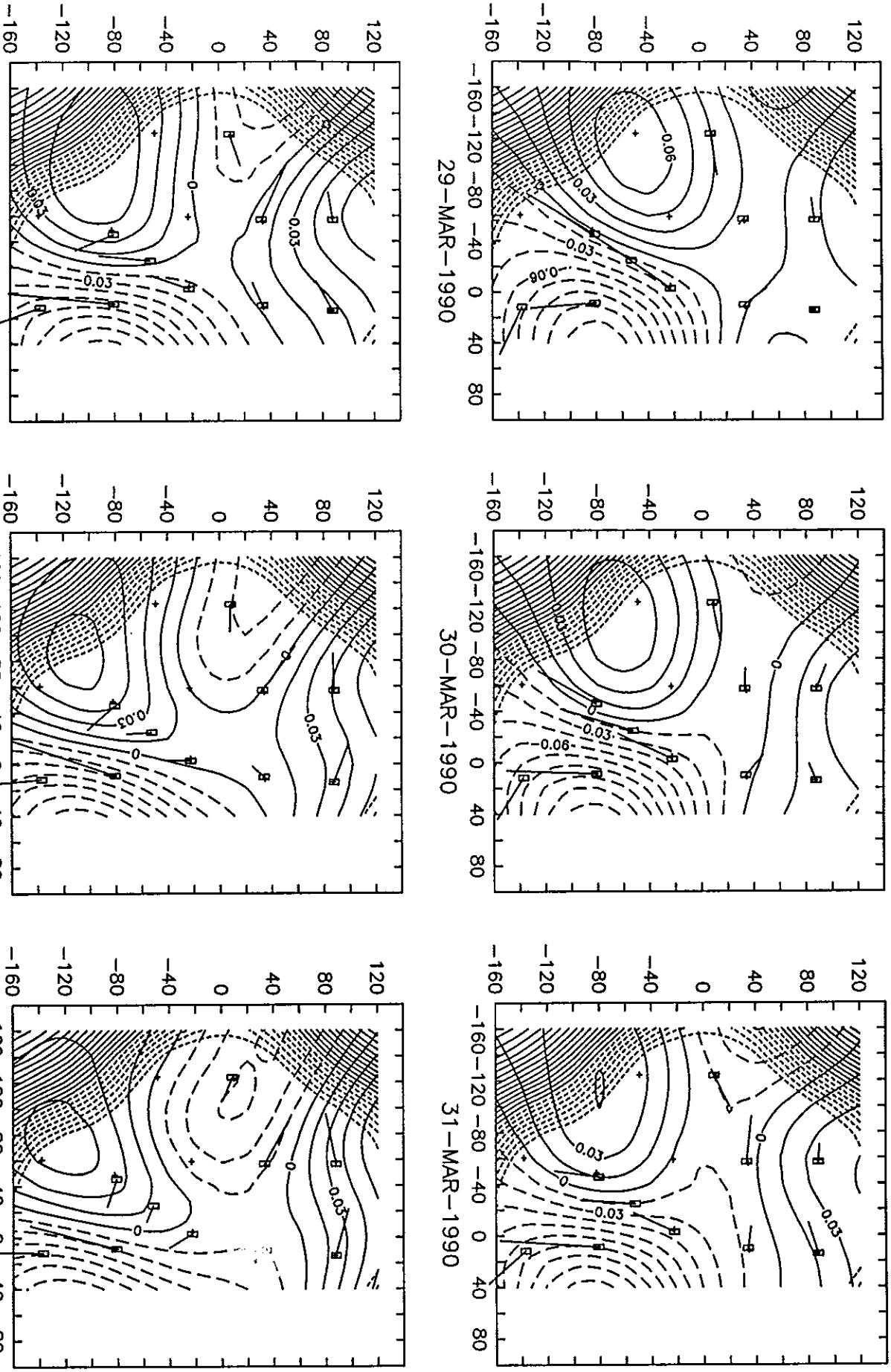
29-MAR-1990
30-MAR-1990
31-MAR-1990
01-APR-1990
02-APR-1990
03-APR-1990

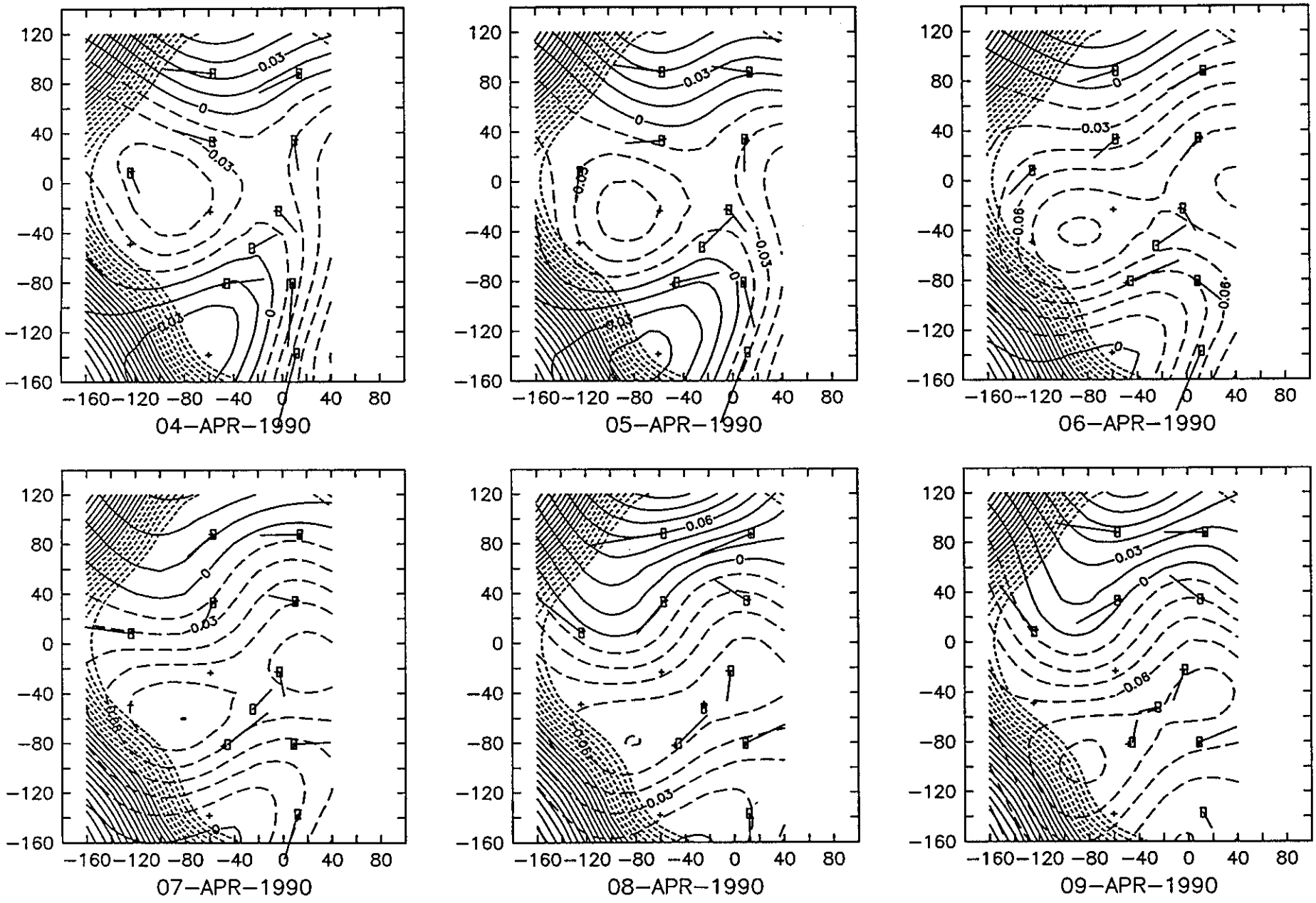
120
80
40
0
−40
−80
−120
−160
−160 −120 −80 −40 0 40 80
0.03
0
−0.03
04−APR−1990
05−APR−1990
0.06
−0.06
06−APR−1990
07−APR−1990
08−APR−1990
09−APR−1990

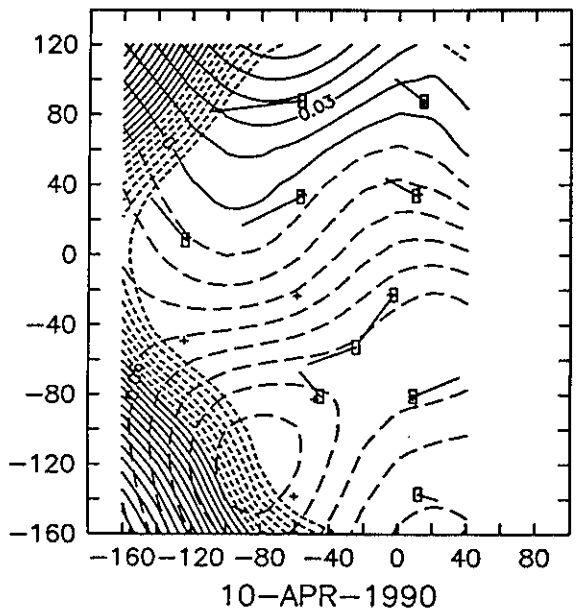
120
80
40
0
−40
−80
−120
−160
−160 −120 −80 −40 0 40 80
0.03
10−APR−1990

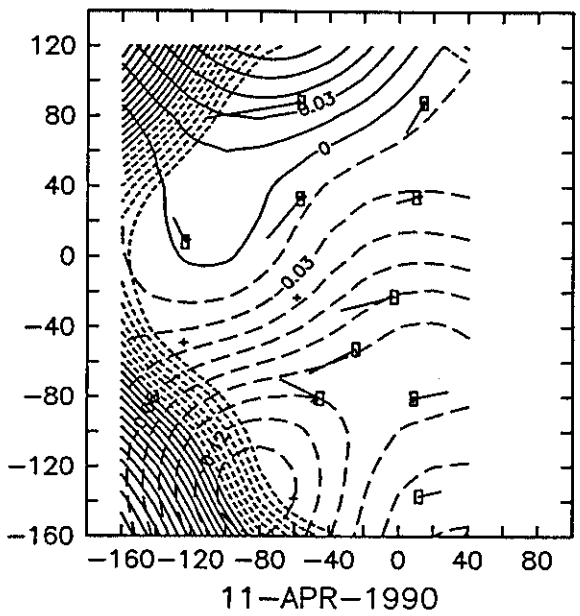
120
80
40
0
−40
−80
−120
−160
−160 −120 −80 −40 0 40 80
0.03
0
11−APR−1990

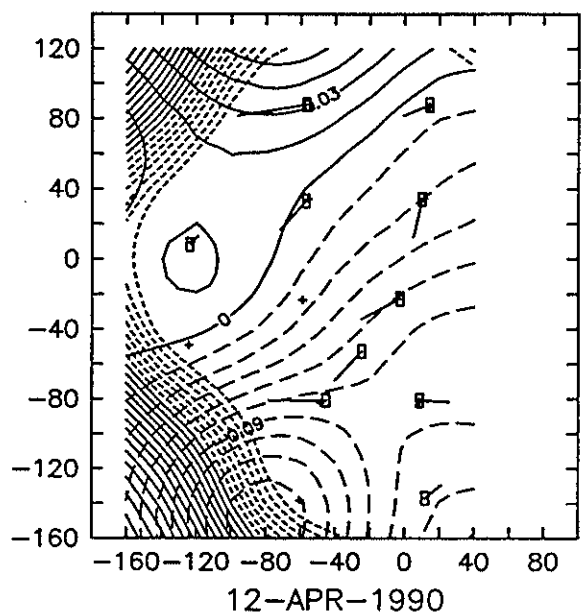
120
80
40
0
−40
−80
−120
−160
−160 −120 −80 −40 0 40 80
0.03
0
12−APR−1990

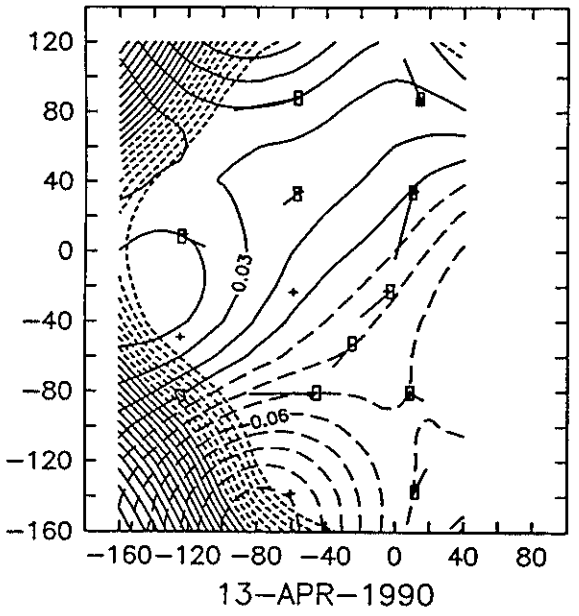
120
80
40
0
−40
−80
−120
−160
−160 −120 −80 −40 0 40 80
0.03
0.06
13−APR−1990

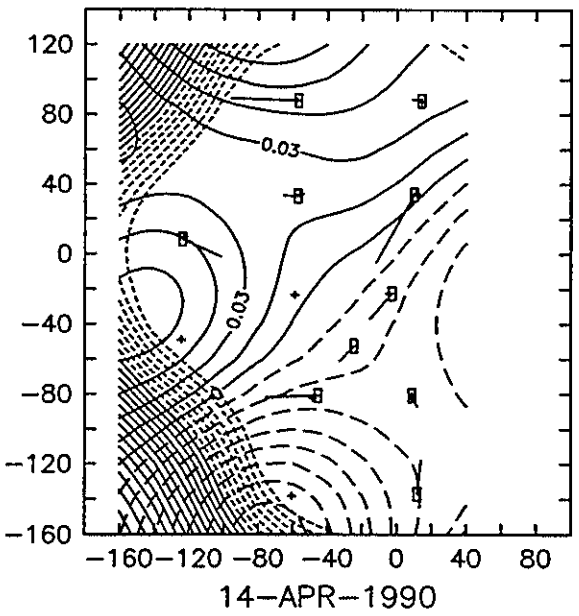
120
80
40
0
−40
−80
−120
−160
−160 −120 −80 −40 0 40 80
0.03
14−APR−1990

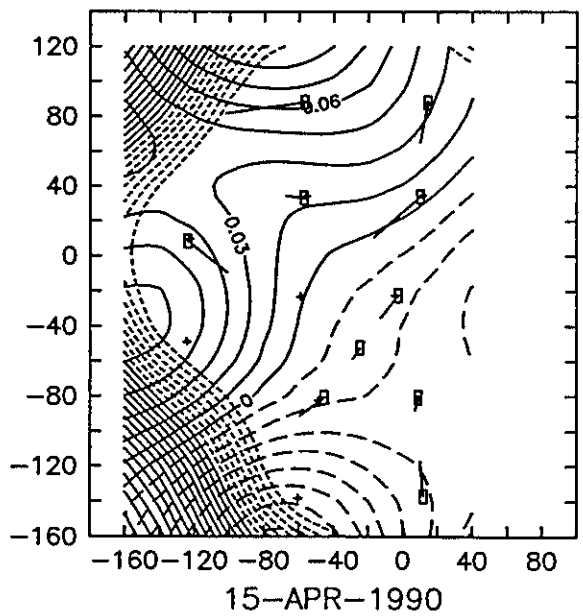
120
80
40
0
−40
−80
−120
−160
−160 −120 −80 −40 0 40 80
0.06
0.03
15−APR−1990

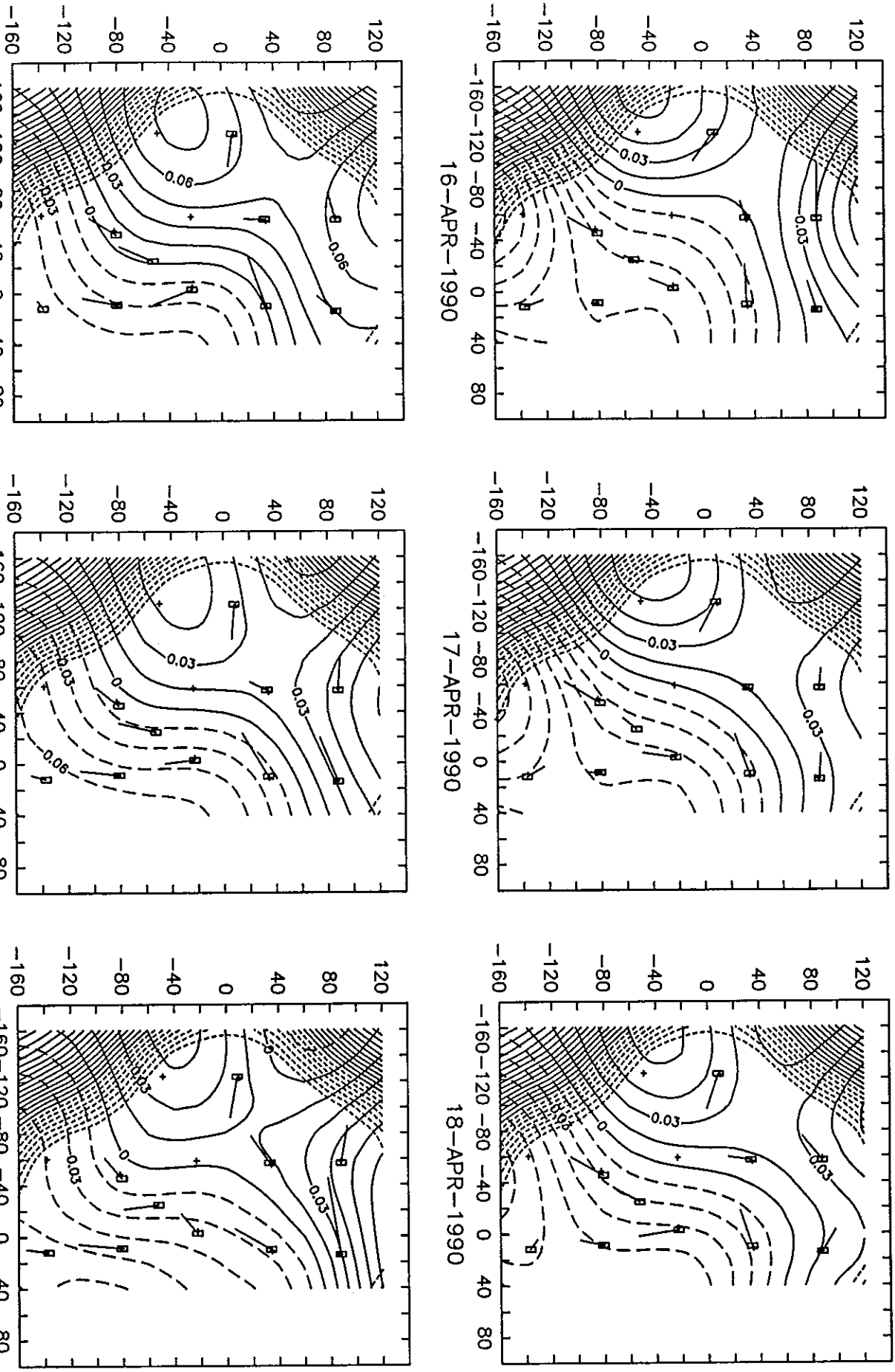
16-APR-1990
17-APR-1990
18-APR-1990
19-APR-1990
20-APR-1990
21-APR-1990
0.03
0
0.06

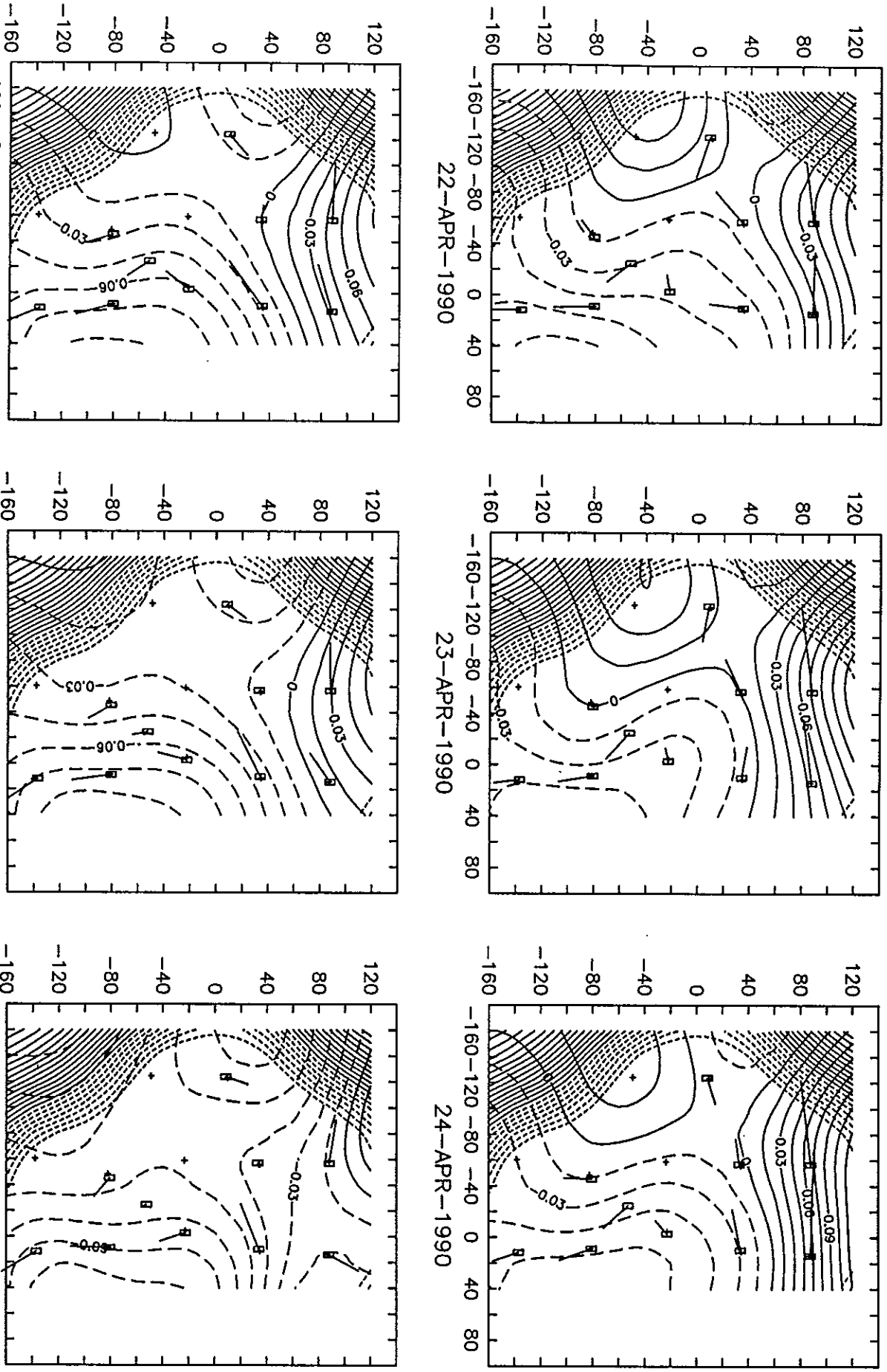
22-APR-1990
23-APR-1990
24-APR-1990
25-APR-1990
26-APR-1990
27-APR-1990

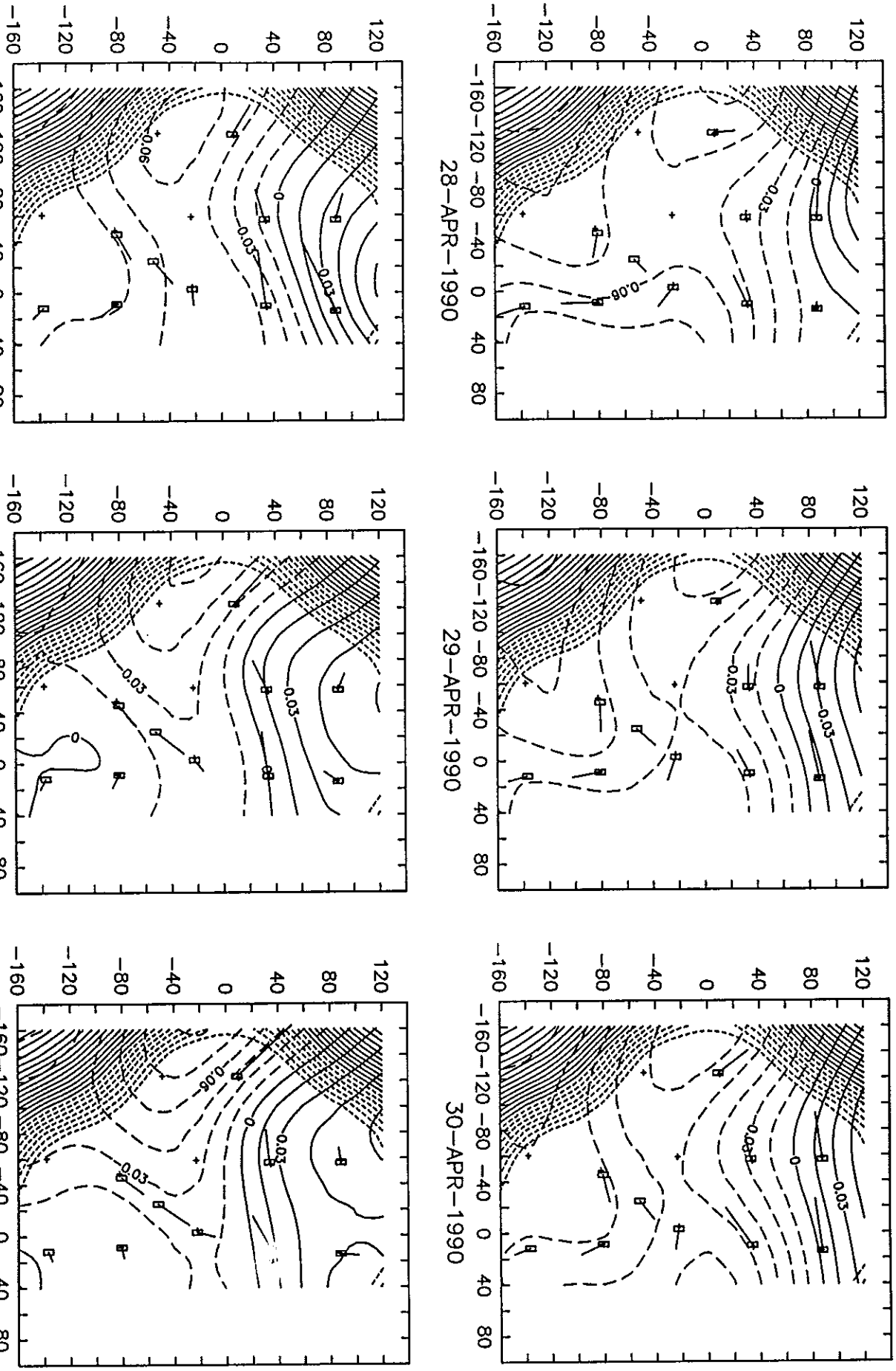
28-APR-1990
29-APR-1990
30-APR-1990
01-MAY-1990
02-MAY-1990
03-MAY-1990

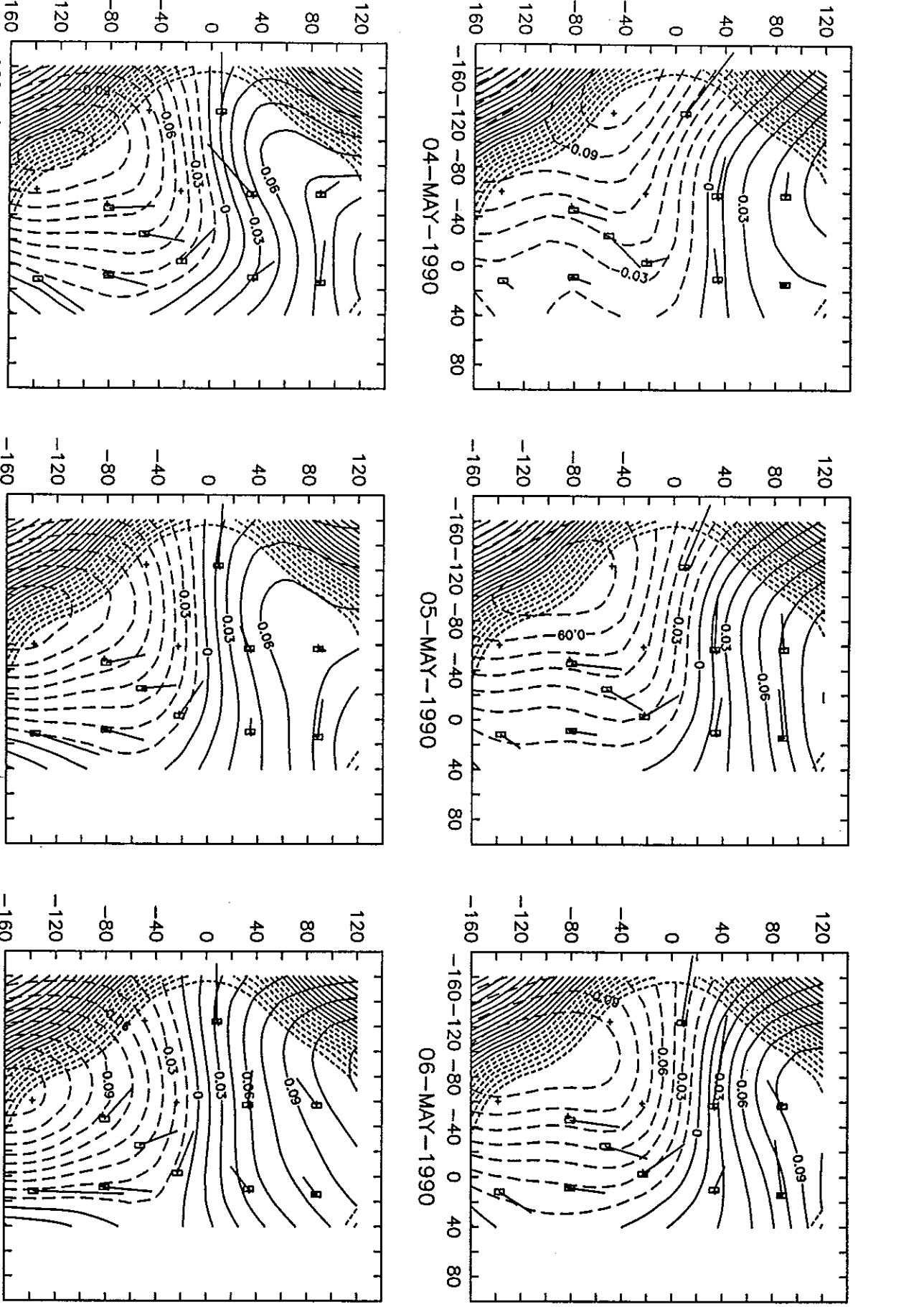
04-MAY-1990
05-MAY-1990
06-MAY-1990
07-MAY-1990
08-MAY-1990
09-MAY-1990

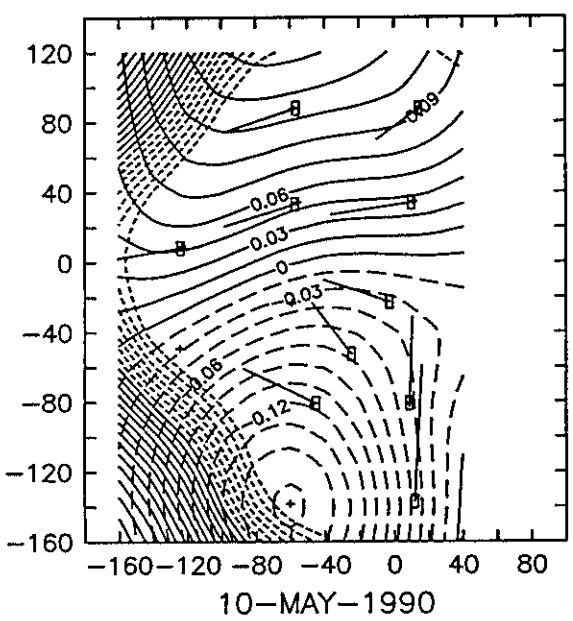
120
80
40
0
−40
−80
−120
−160
−160 −120 −80 −40 0 40 80
0.09
0.06
0.03
0
−0.03
−0.06
−0.12
10−MAY−1990

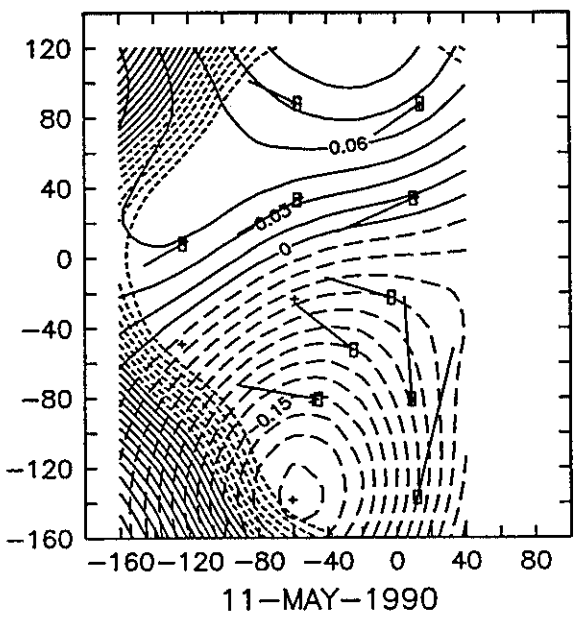
120
80
40
0
−40
−80
−120
−160
−160 −120 −80 −40 0 40 80
0.06
0.03
0
−0.03
−0.15
11−MAY−1990

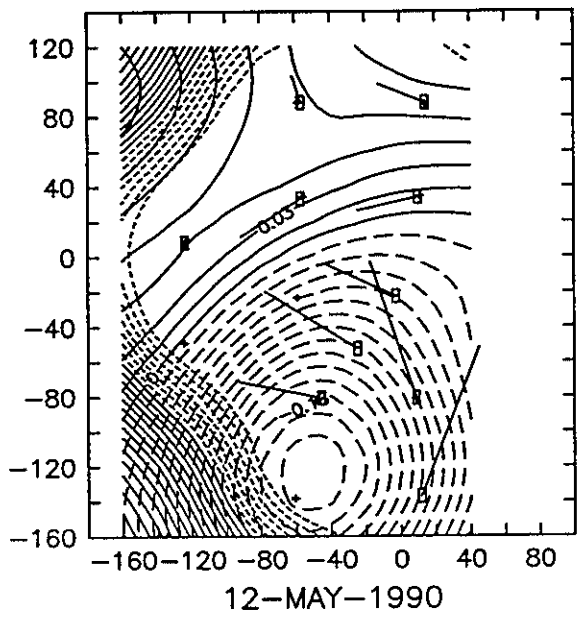
120
80
40
0
−40
−80
−120
−160
−160 −120 −80 −40 0 40 80
0.03
0
12−MAY−1990

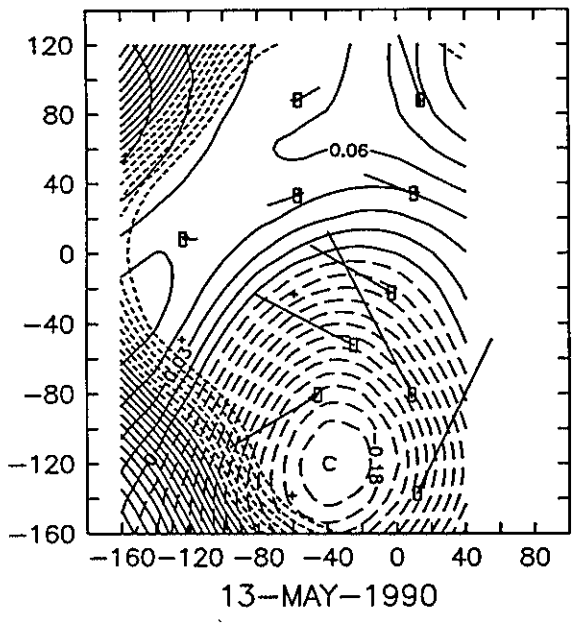
120
80
40
0
−40
−80
−120
−160
−160 −120 −80 −40 0 40 80
0.06
−0.03
−0.18
C
13−MAY−1990

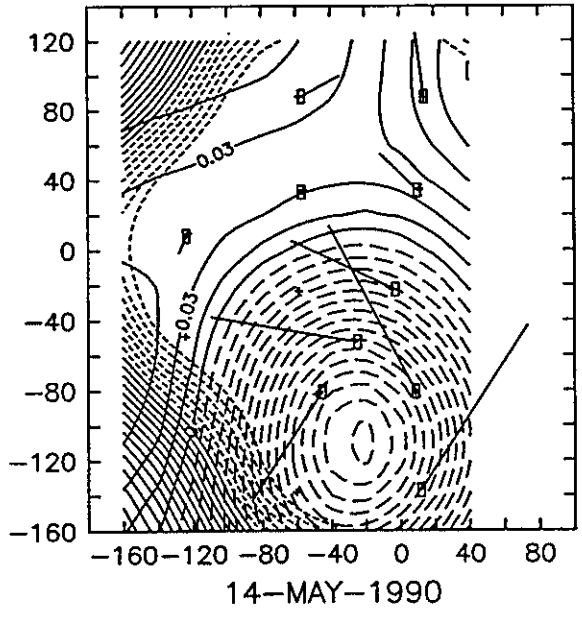
120
80
40
0
−40
−80
−120
−160
−160 −120 −80 −40 0 40 80
0.03
−0.03
14−MAY−1990

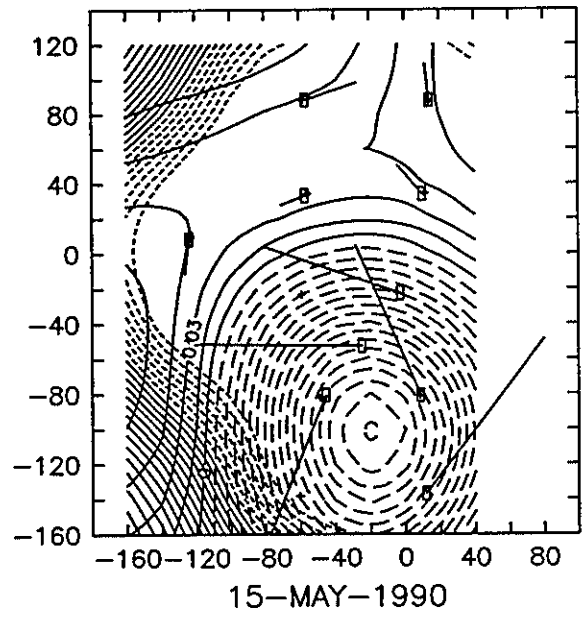
120
80
40
0
−40
−80
−120
−160
−160 −120 −80 −40 0 40 80
−0.03
C
15−MAY−1990

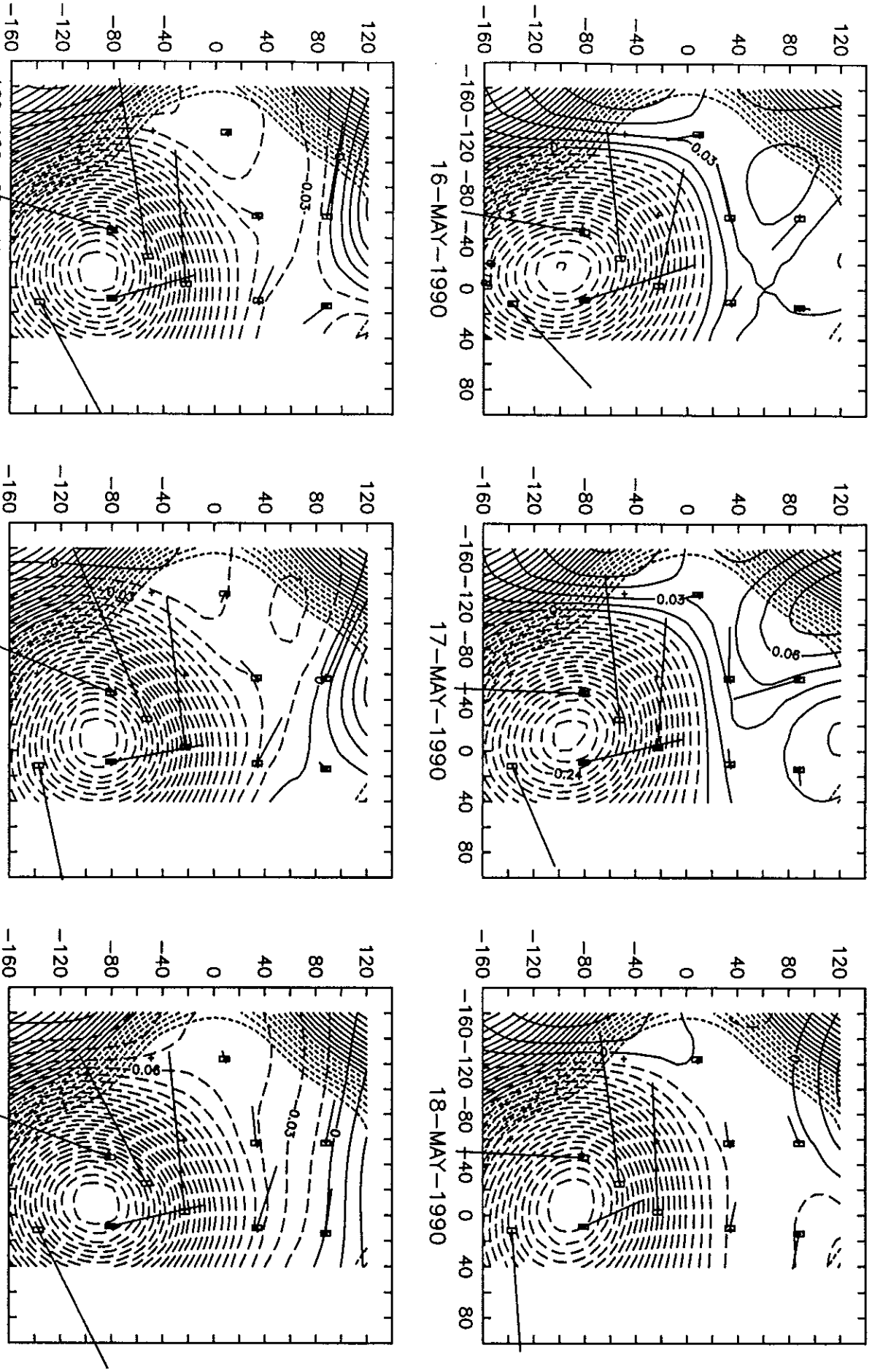
16-MAY-1990
17-MAY-1990
18-MAY-1990
19-MAY-1990
20-MAY-1990
21-MAY-1990

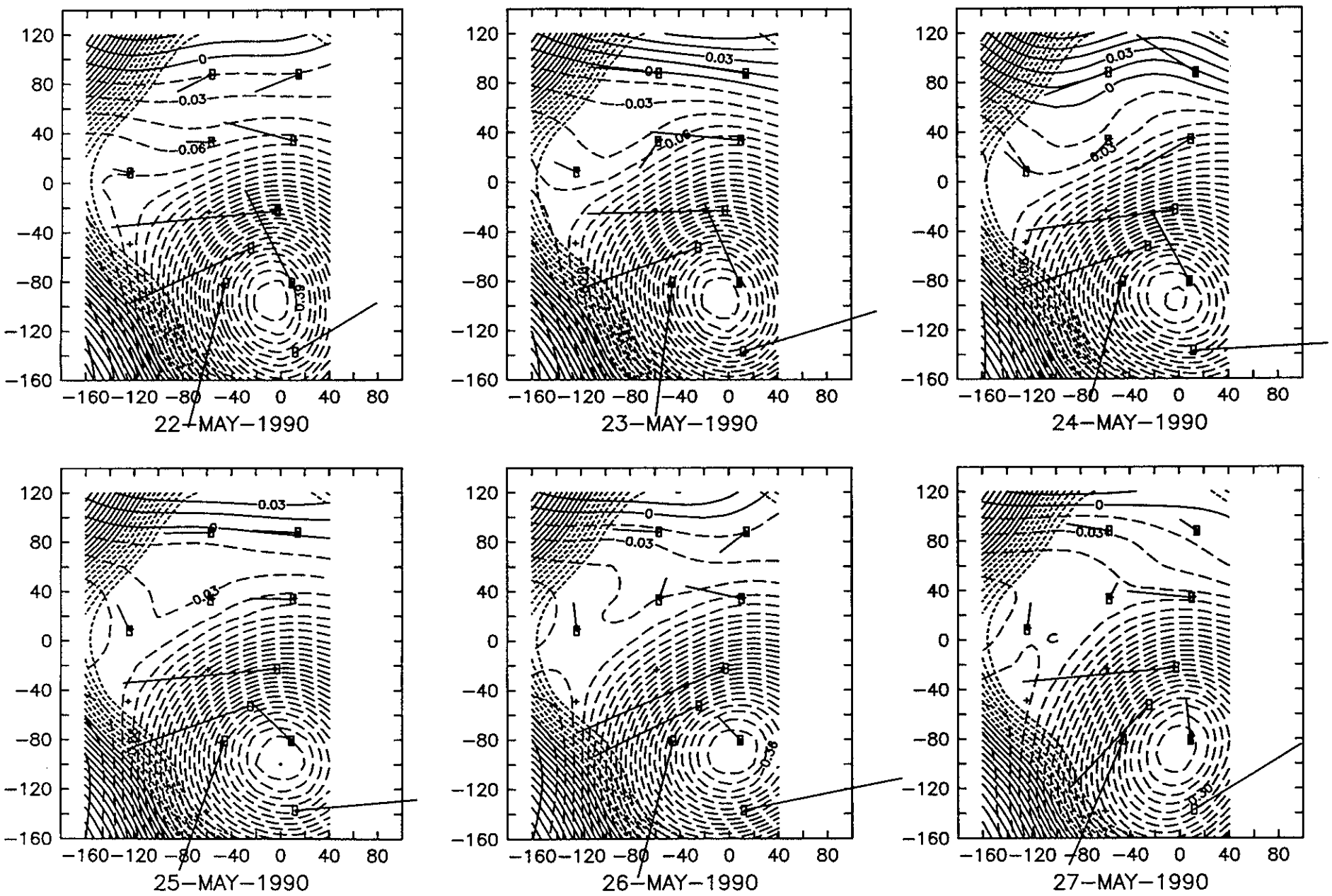
22–MAY–1990
23–MAY–1990
24–MAY–1990
25–MAY–1990
26–MAY–1990
27–MAY–1990
120
80
40
0
−40
−80
−120
−160
−160 −120 −80 −40 0 40 80
0
0.03
0.06
0.09

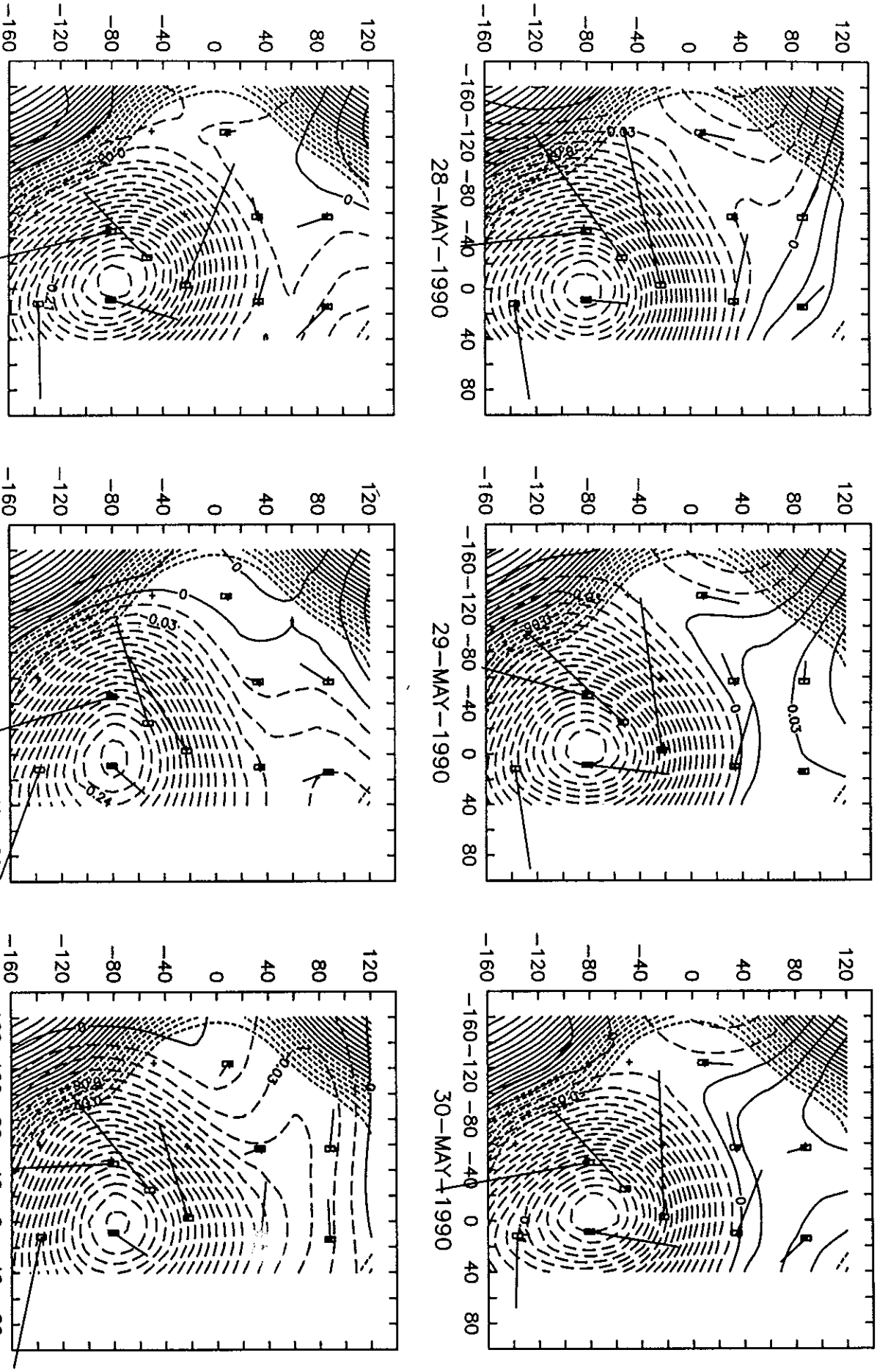
28-MAY-1990
29-MAY-1990
30-MAY-1990
31-MAY-1990
01-JUN-1990
02-JUN-1990

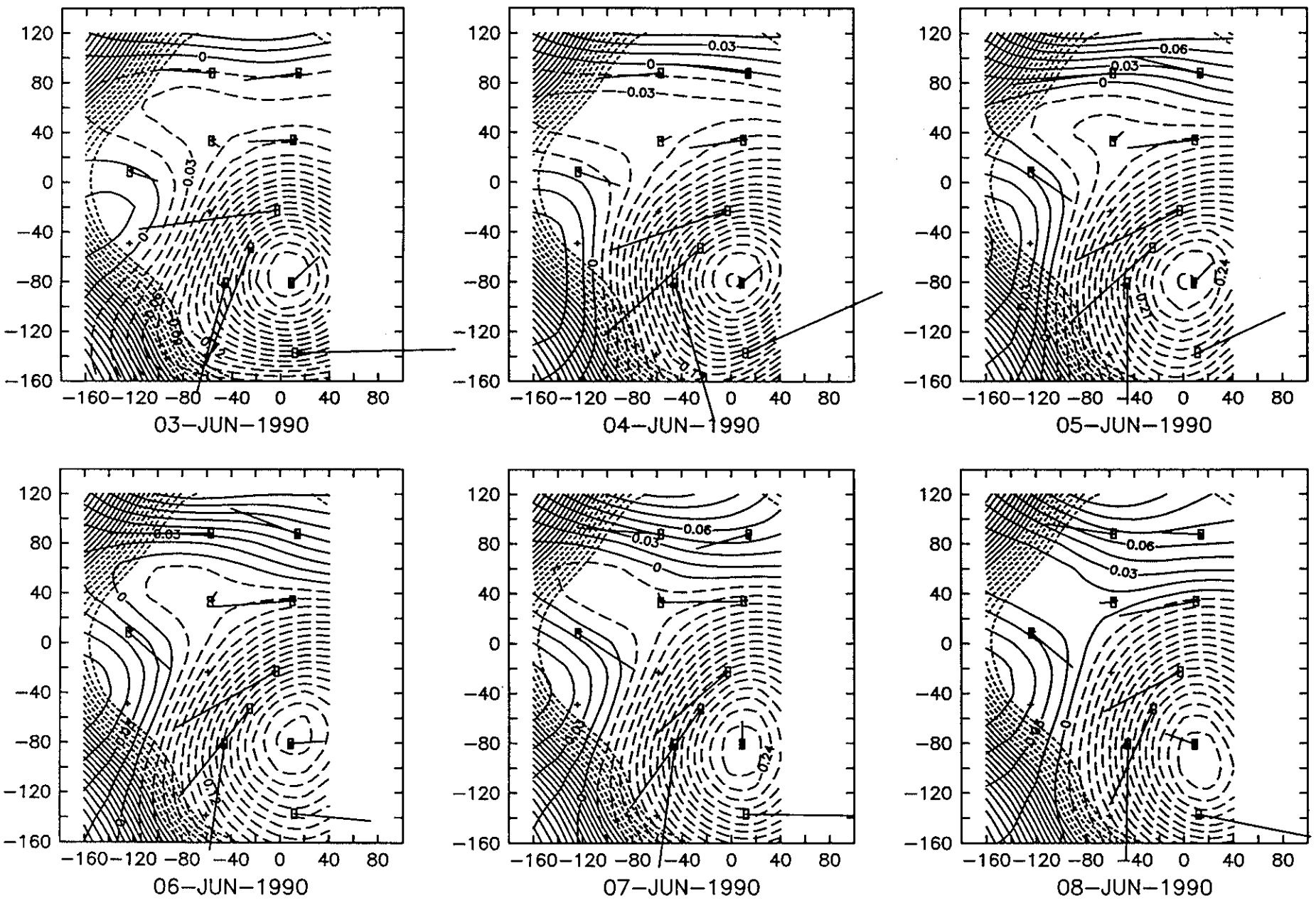
03–JUN–1990
04–JUN–1990
05–JUN–1990
06–JUN–1990
07–JUN–1990
08–JUN–1990

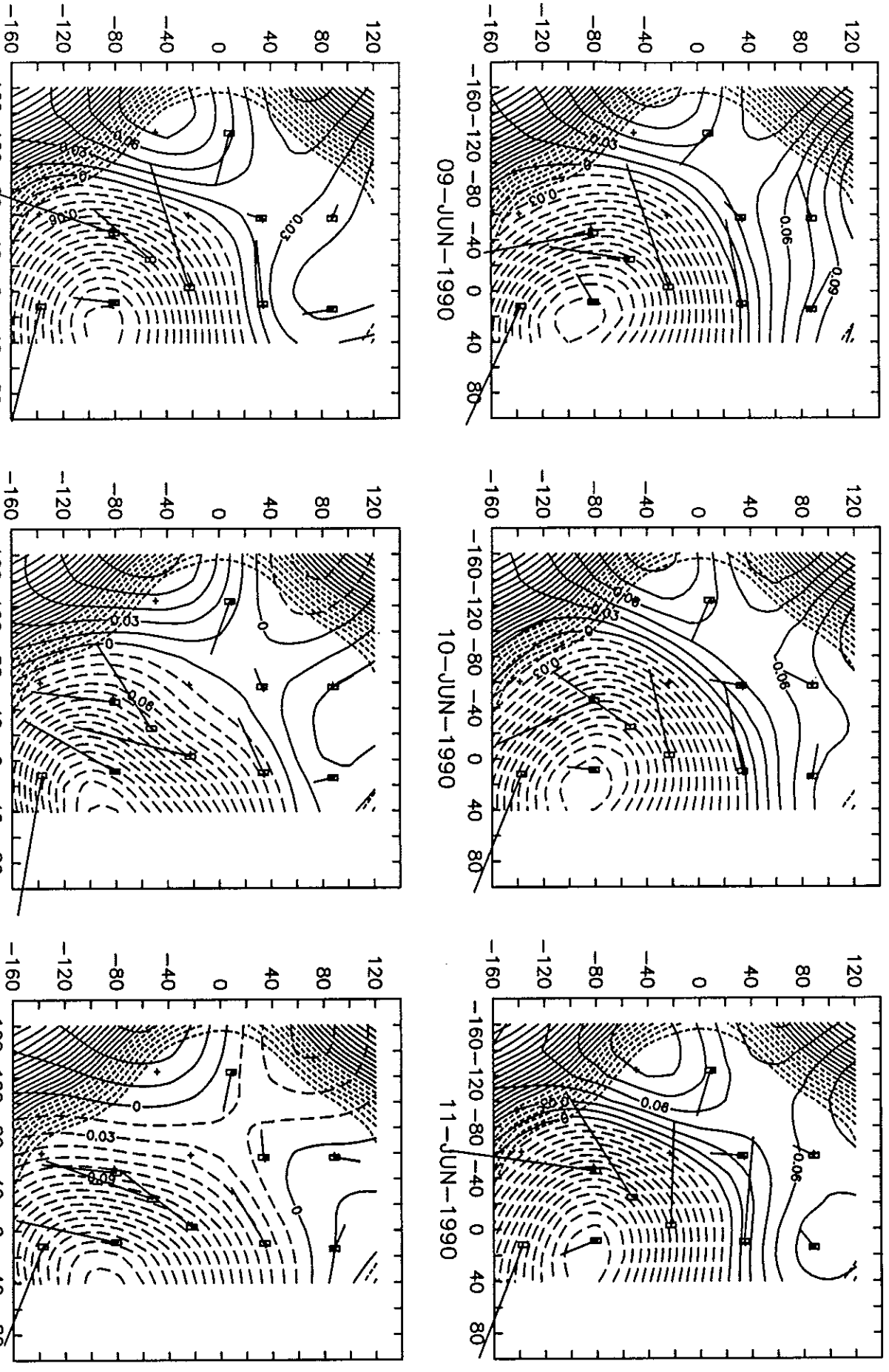
09-JUN-1990
10-JUN-1990
11-JUN-1990
12-JUN-1990
13-JUN-1990
14-JUN-1990

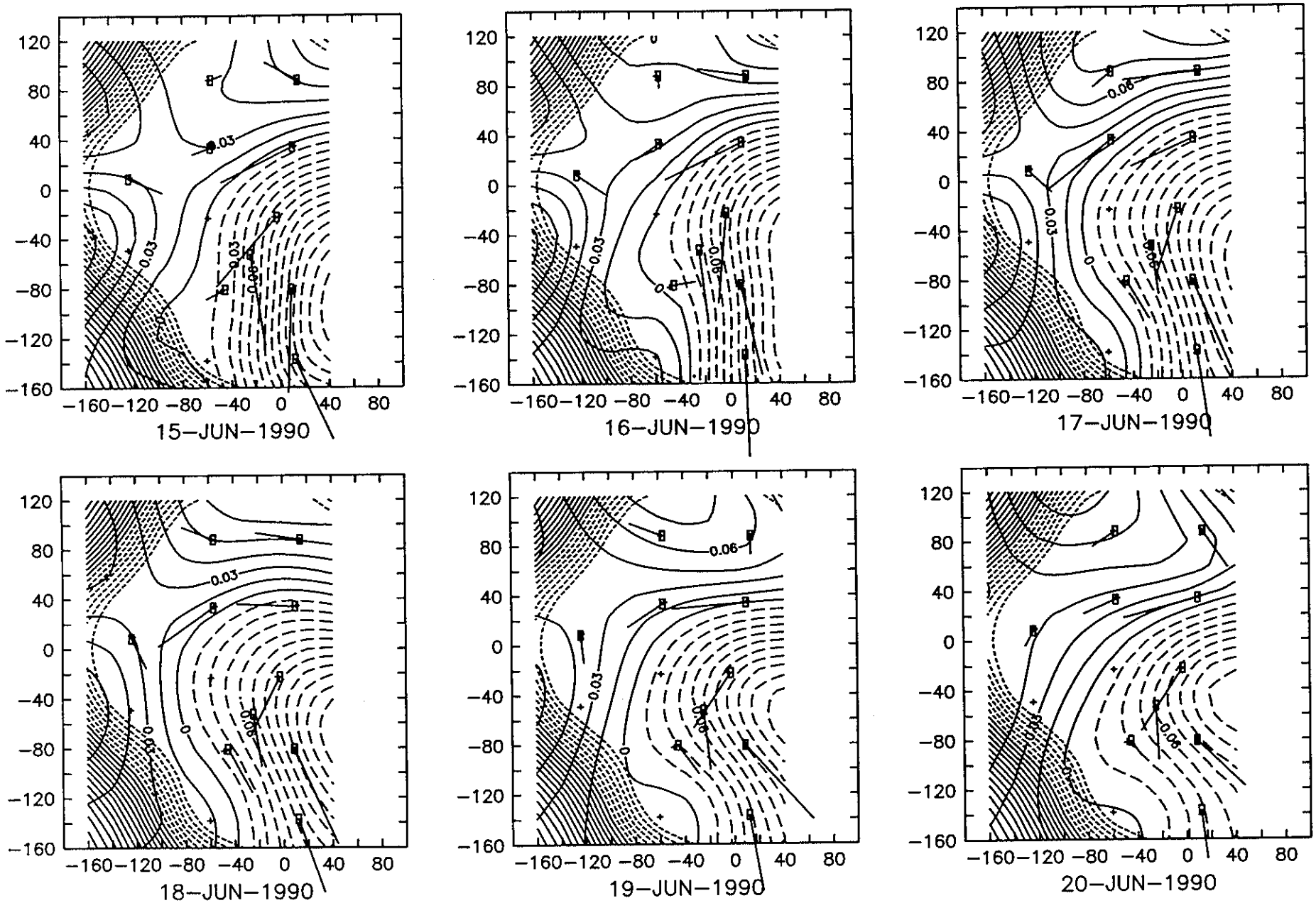
15–JUN–1990
16–JUN–1990
17–JUN–1990
18–JUN–1990
19–JUN–1990
20–JUN–1990

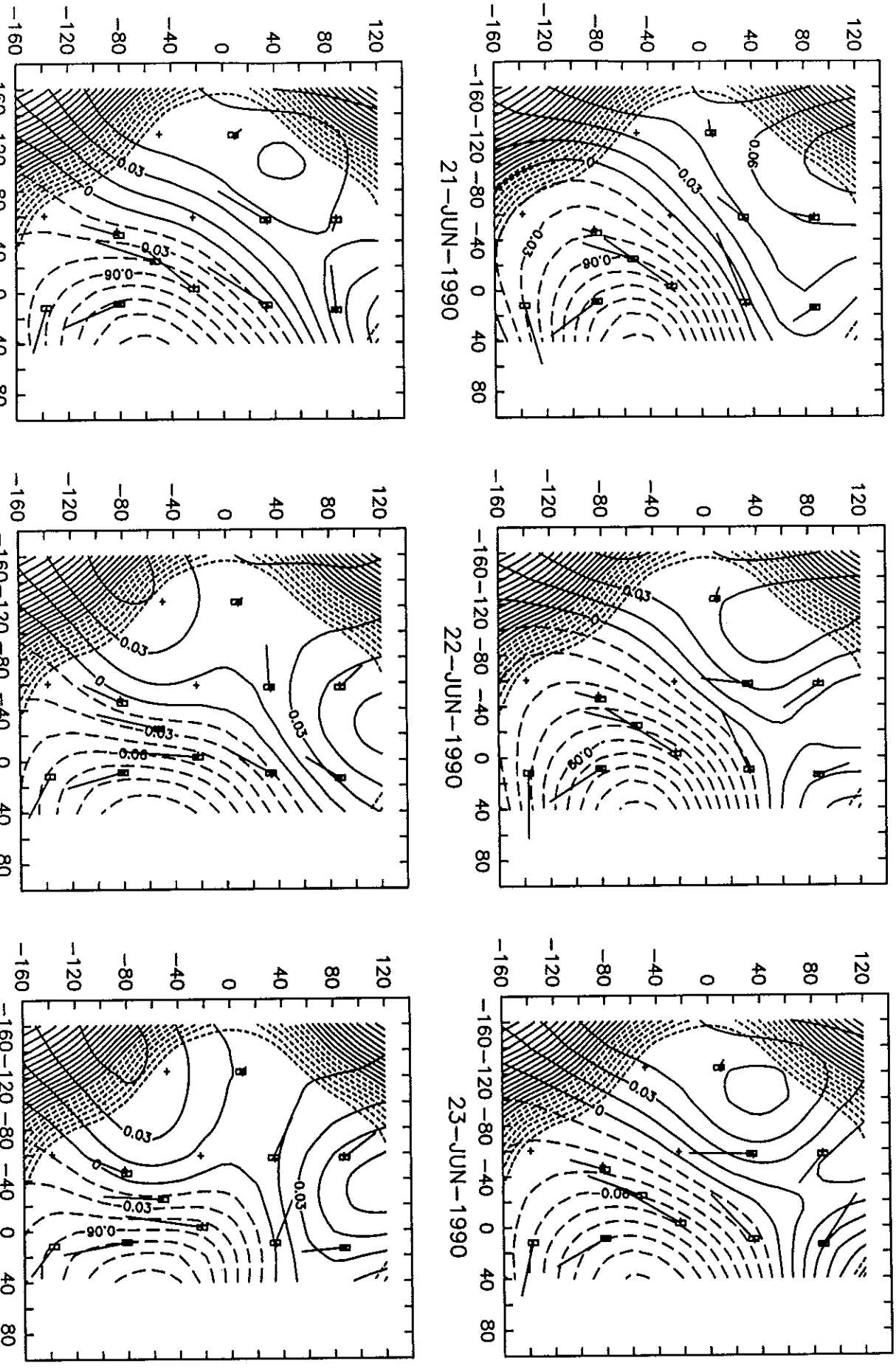
21-JUN-1990
22-JUN-1990
23-JUN-1990
24-JUN-1990
25-JUN-1990
26-JUN-1990

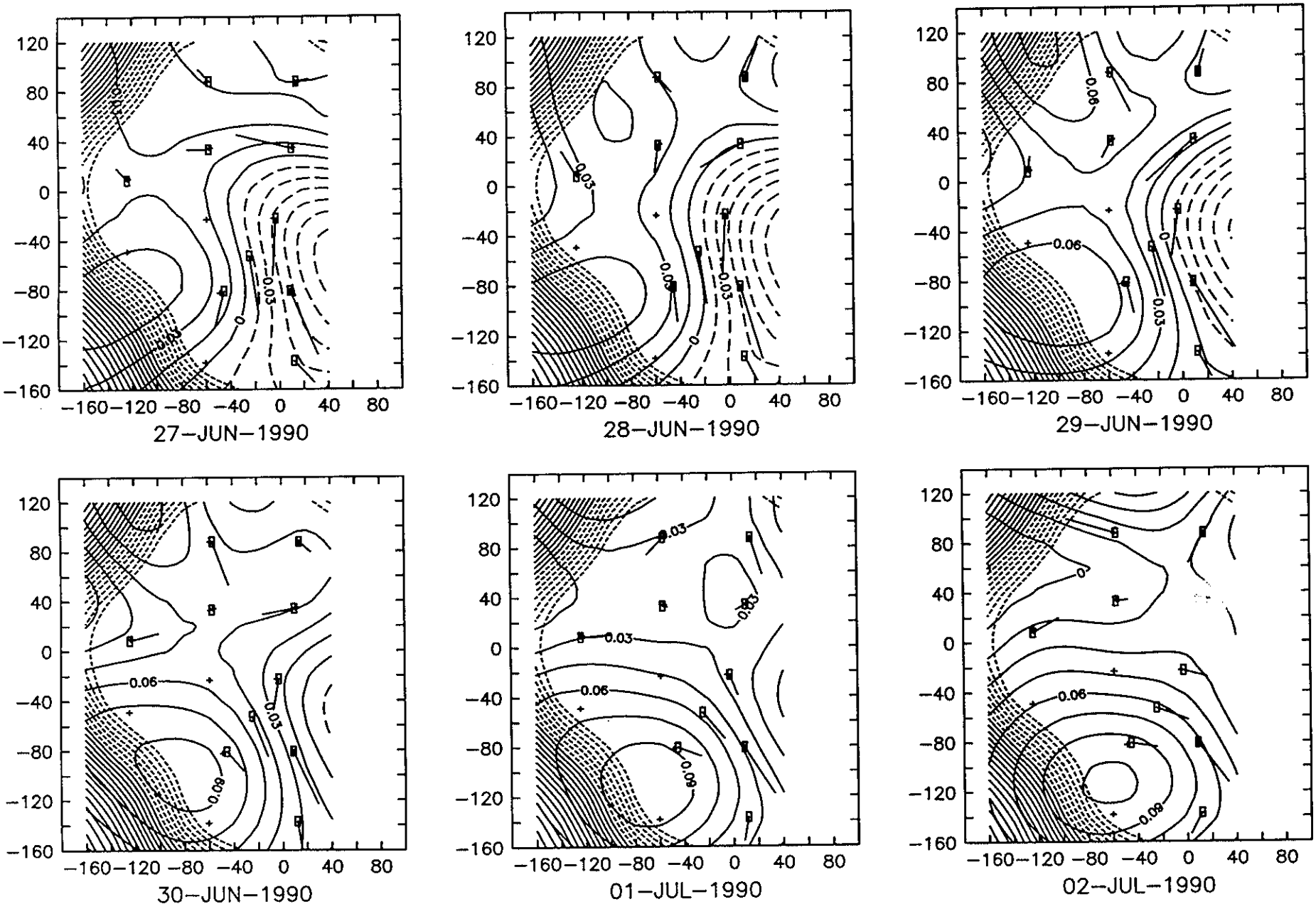
120
80
40
0
−40
−80
−120
−160
−160 −120 −80 −40 0 40 80
27−JUN−1990
28−JUN−1990
29−JUN−1990
30−JUN−1990
01−JUL−1990
02−JUL−1990
0.06
0.03
0
0.09

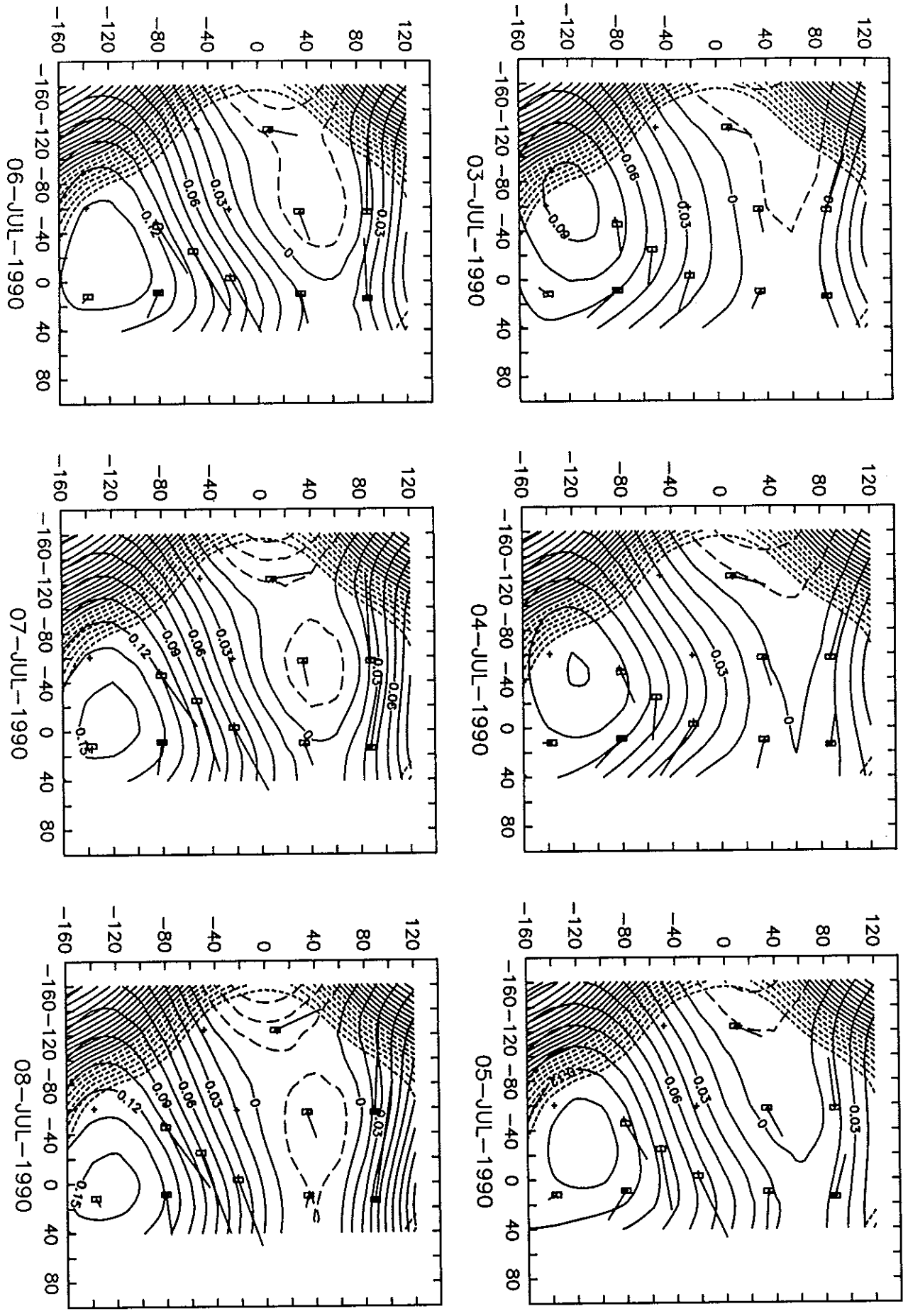
03-JUL-1990
04-JUL-1990
05-JUL-1990
06-JUL-1990
07-JUL-1990
08-JUL-1990

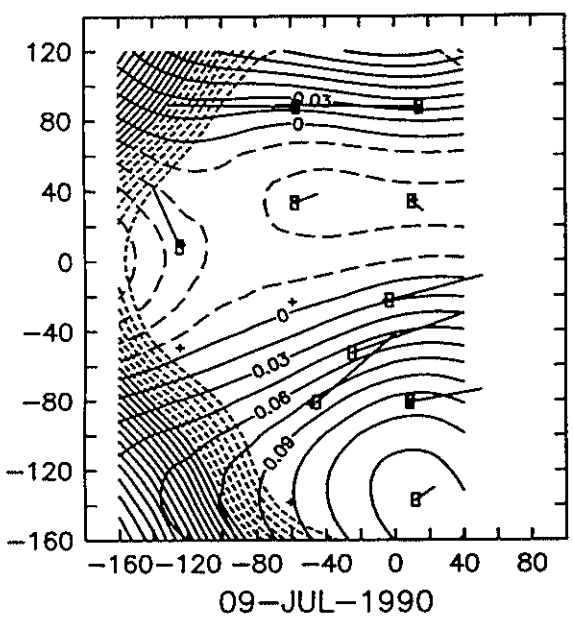
120
80
40
0
−40
−80
−120
−160
−160 −120 −80 −40 0 40 80
0.03
0
0.03
0.06
0.09
09−JUL−1990

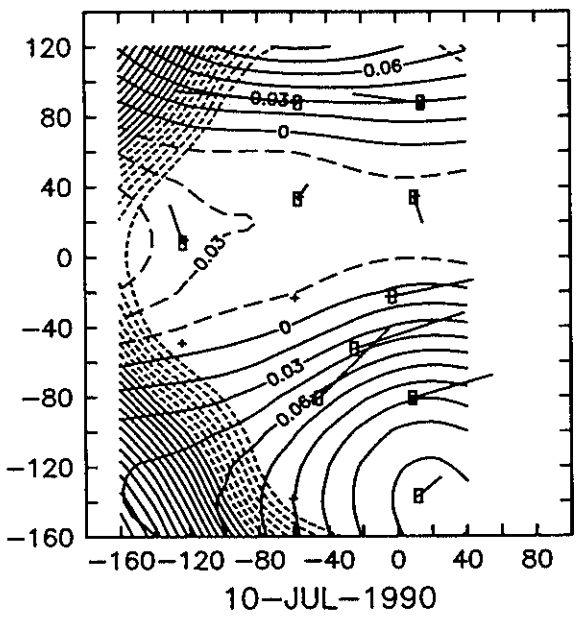
120
80
40
0
−40
−80
−120
−160
−160 −120 −80 −40 0 40 80
0.06
0.03
0
0.03
0
0.03
0.06
10−JUL−1990

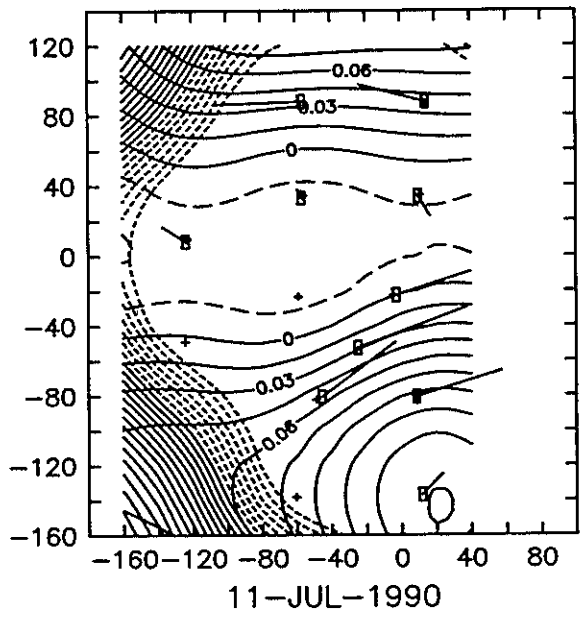
120
80
40
0
−40
−80
−120
−160
−160 −120 −80 −40 0 40 80
0.06
0.03
0
0
0.03
0.06
11−JUL−1990

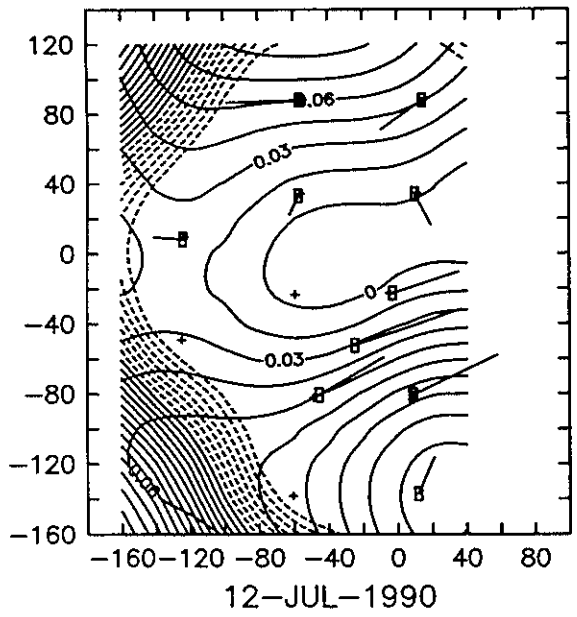
120
80
40
0
−40
−80
−120
−160
−160 −120 −80 −40 0 40 80
0.06
0.03
0
0.03
12−JUL−1990

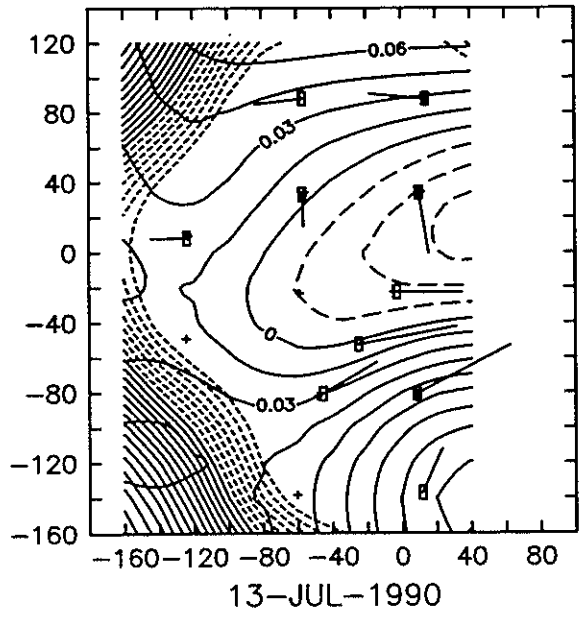
120
80
40
0
−40
−80
−120
−160
−160 −120 −80 −40 0 40 80
0.06
0.03
0
0.03
13−JUL−1990

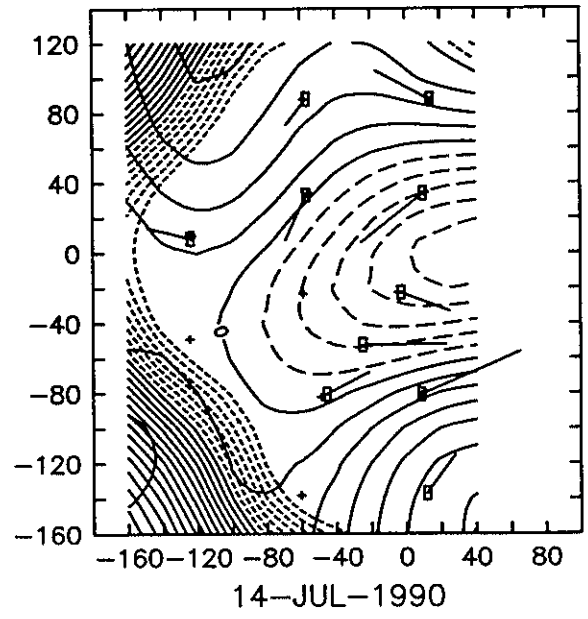
120
80
40
0
−40
−80
−120
−160
−160 −120 −80 −40 0 40 80
0
14−JUL−1990

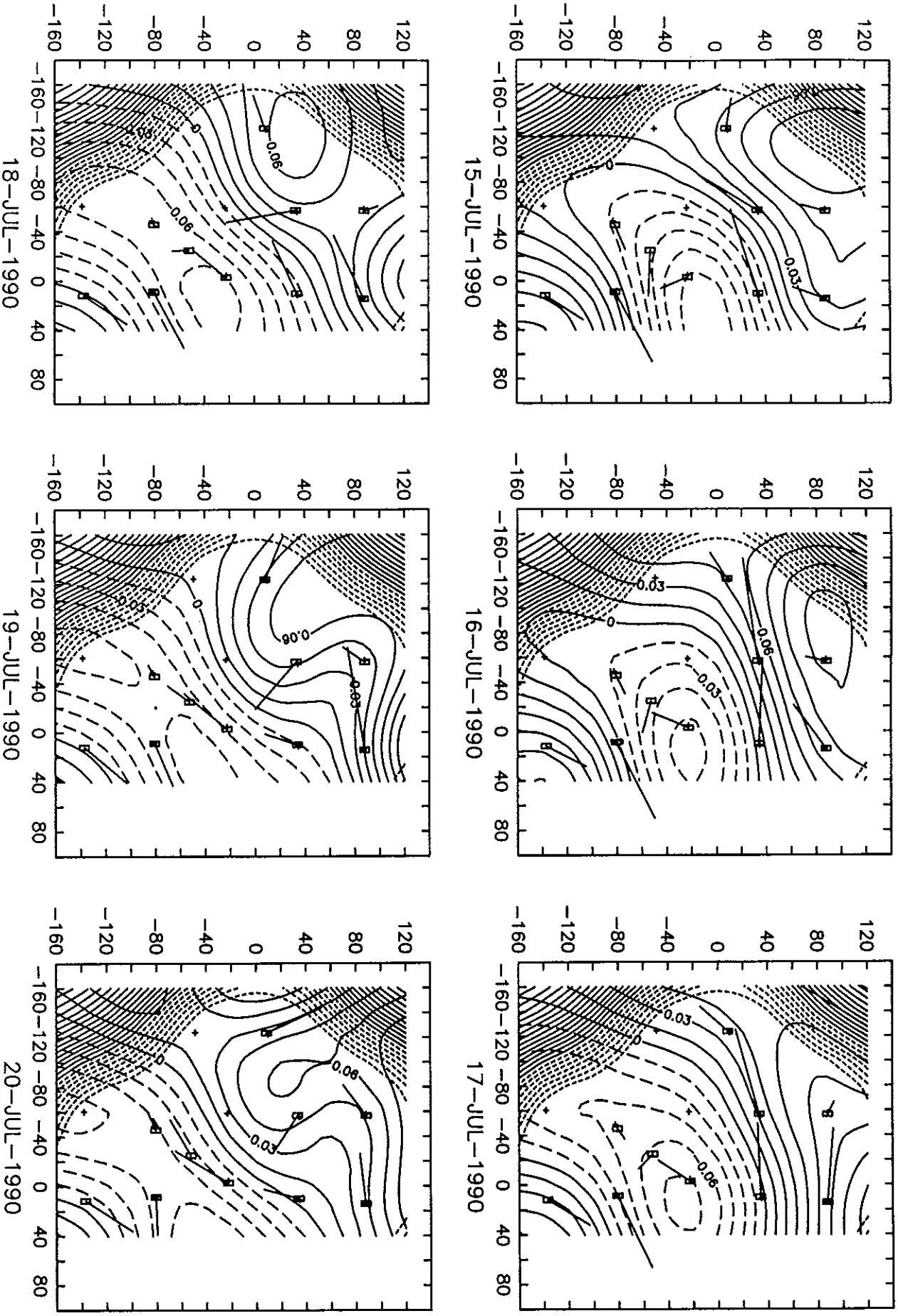
15-JUL-1990
16-JUL-1990
17-JUL-1990
18-JUL-1990
19-JUL-1990
20-JUL-1990

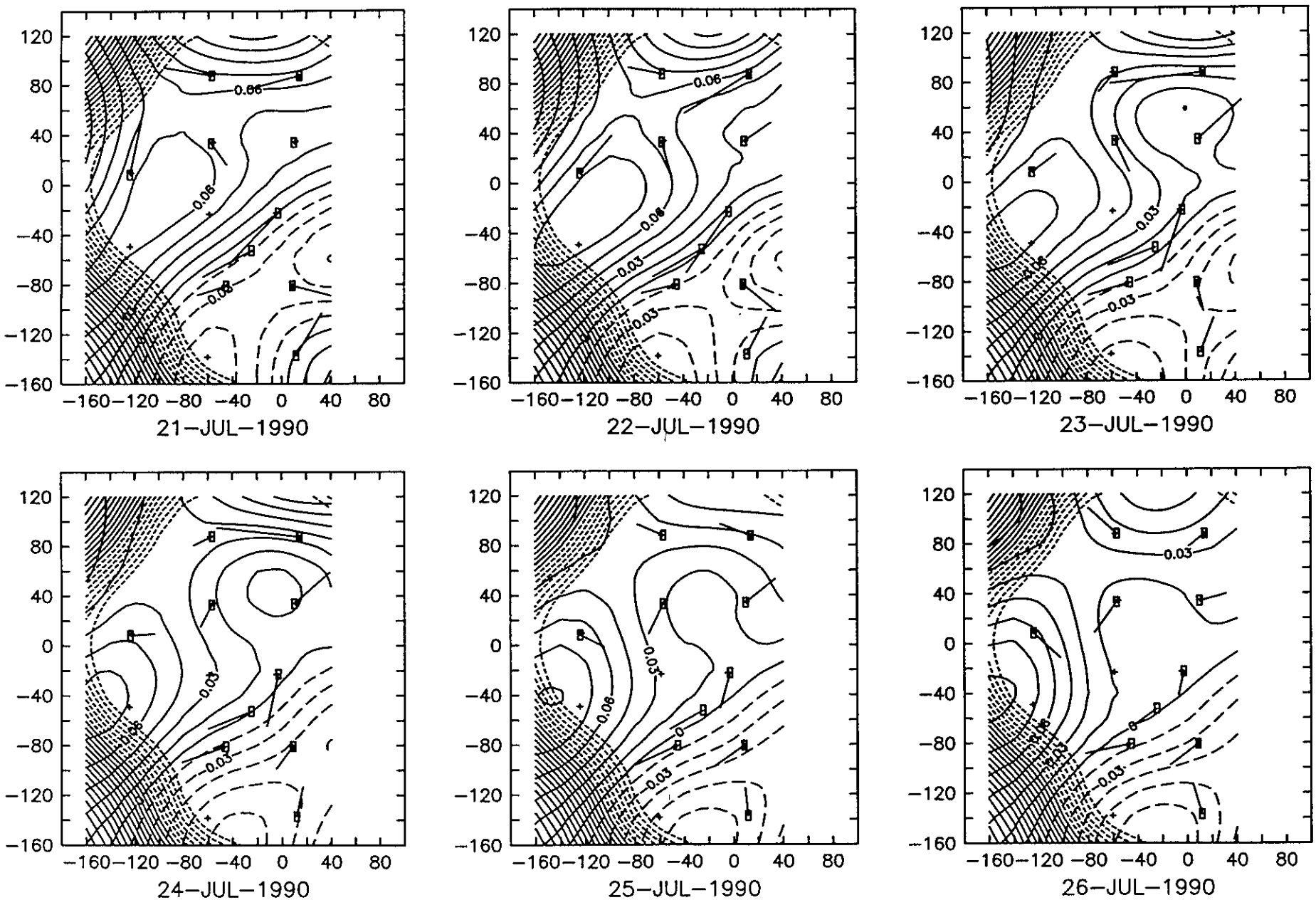
120
80
40
0
−40
−80
−120
−160
−160 −120 −80 −40 0 40 80
0.06
0.03
21−JUL−1990
22−JUL−1990
23−JUL−1990
24−JUL−1990
25−JUL−1990
26−JUL−1990

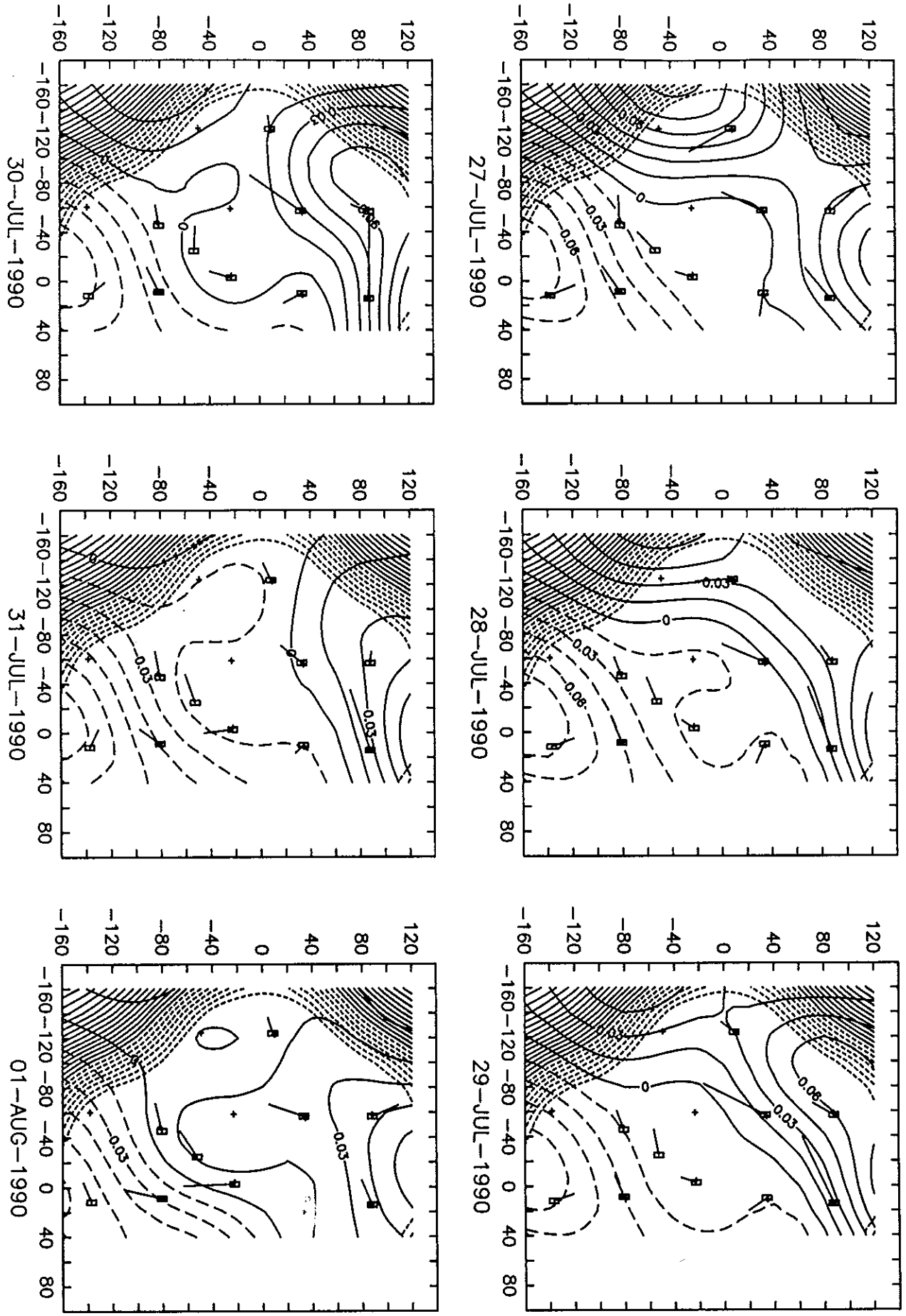
27-JUL-1990
28-JUL-1990
29-JUL-1990
30-JUL-1990
31-JUL-1990
01-AUG-1990

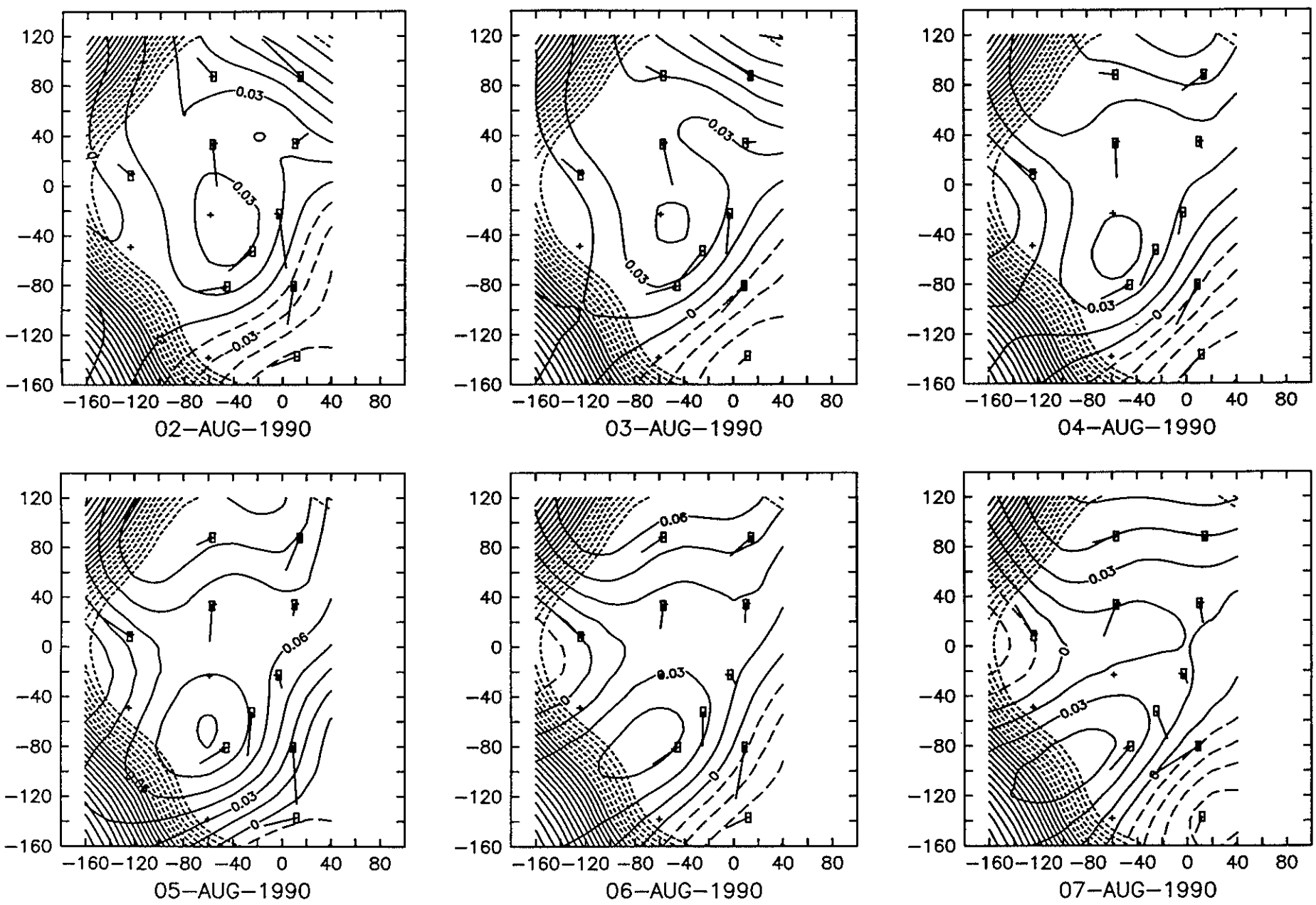
120
80
40
0
−40
−80
−120
−160
−160 −120 −80 −40 0 40 80
0.03
0
02−AUG−1990
03−AUG−1990
04−AUG−1990
0.06
05−AUG−1990
06−AUG−1990
07−AUG−1990

References

[1] Francis P. Bretherton, Russ E. Davis, and C. B. Fandry. A technique for objective analysis and design of oceanographic experiments applied to MODE-73. *Deep-Sea Research*, 23:559–582, 1976.

[2] Erik Fields and D. Randolph Watts. The SYNOP Experiment: Inverted echo sounder data report for May 1988 to August 1989. Technical Report 90–2, University of Rhode Island, Graduate School of Oceanography, 1990.

[3] Erik Fields and D. Randolph Watts. The SYNOP Experiment: Inverted echo sounder data report for June 1989 to September 1990. Technical Report 91–2, University of Rhode Island, Graduate School of Oceanography, 1991.

[4] C. Gilman and P. Cornillon. Gulf stream position time series. *J. Geophys. Res.* (Submitted).

[5] A. Papoulis. *Probability, Random Variables and Stochastic Processes.* McGraw-Hill book Company, 2nd edition, 1984.

[6] Robert S. Pickart, Xiaoshu Qian, and D. Randolph Watts. The SYNOP Inlet Experiment: Bottom current meter data report for October 1987 to August 1990 mooring period. Technical Report 91–1, University of Rhode Island, Graduate School of Oceanography, 1991.

[7] Xiaoshu Qian, Karen L. Tracey, Erik Fields, and D. Randolph Watts. The SYNOP Experiment: Inverted echo sounder data report for October 1987 to May 1988. Technical Report 90–3, University of Rhode Island, Graduate School of Oceanography, 1990.

[8] Karen L. Tracey and D. Randolph Watts. The SYNOP Experiment: Thermocline depth maps for the Central Array, October 1987 to August 1990. Technical Report 91–5, University of Rhode Island, Graduate School of Oceanography, 1991.

[9] Karen L. Tracey and D. Randolph Watts. The SYNOP Experiment: Thermocline depth maps for the Inlet Array, October 1987 to August 1990. Technical Report 91–6, University of Rhode Island, Graduate School of Oceanography, 1991.

Acknowledgements

The SYNOP Experiment was supported by the Office of Naval Research under contract number N00014-90-J-1568 and the National Science Foundation under grant number OCE87-17144. We thank Nelson Hogg for providing two MATLAB programs for objective analysis that facilitated our coding process.

Appendices

A OA Program List

A.1 '1 to 1' OA program

```
function [pi,ei]=oa11(xi,yi,xm,ym,pm,Vn,CLENGTH)
%function [pi,ei]=oa11(xi,yi,xm,ym,pm,Vn,CLENGTH)
% scalar objective analysis
% pi     : interpolated values with columns being the time and
%          rows being the interpolation points (NI by NT);
% ei     : estimated error in percentage of signal variance (NI by 1);
% xi, yi: x-y coordinates of interpolation points (NI by 1);
% xm, ym: x-y coordinates of measurement sites (NM by 1);
% pm     : array of measured values with columns being the time
%          and rows being the measurement sites (NM by NT);
% Vn     : noise variance in percentage of signal variance (scalar or 1 by NM);
% CLENGTH: correlation length (scalar);
% units: xi,yi,xm,ym and CLENGTH should have the same units;
%        input pm and output pi should have the same units.
%

NM = length(xm);                          %number of measurement sites.
NI = length(xi);                          %number of interpolation points.

% construct correlation matrices
r = sqrt( ( xm*ones(1,NM) - ones(NM,1)*xm' ).^2 +...
          ( ym*ones(1,NM) - ones(NM,1)*ym' ).^2 );
A = CFUNpp(r,CLENGTH);                    % pick correlation function here.
                                          % CFUNpp(r,L) = exp(-(r/L).^2);
A(1:NM+1:NM^2)=A(1:NM+1:NM^2).*(1 + Vn); % taking care of measurement errors.

r = sqrt( ( xi*ones(1,NM) - ones(NI,1)*xm' ).^2 +...
          ( yi*ones(1,NM) - ones(NI,1)*ym' ).^2 );
C = CFUNpp(r,CLENGTH);                   % pick correlation function here.

% mapping
pi = C*(A\pm);
ei = 1 - diag((C/A)*C')/CFUNpp(0,CLENGTH); % pick correlation function here.
```

A.2 '2 to 1' OA program

```
function [pi,ei]=oa21(xi,yi,xm,ym,um,vm,Vn,CLENGTH)
%function [pi,ei]=oa21(xi,yi,xm,ym,um,vm,Vn,CLENGTH)
% "2 to 1" objective analysis
% pi    : interpolated values with columns being the time and
%         rows being the interpolation points (NI by NT);
% ei    : estimated error in percentage of signal variance (NI by 1);
% xi, yi: x-y coordinates of interpolation points (NI by 1);
% xm, ym: x-y coordinates of measurement sites (NM by 1);
% um, vm: array of measured values with columns being the time
%         and rows being the measurement sites (NM by NT);
% Vn    : noise variance in percentage of signal variance (scalar or 1 by 2*NM);
% CLENGTH: correlation length (scalar);
% units: xi,yi,xm,ym and CLENGTH should have the same units;
%        units of inputs um,vm and output pi should have CONSISTENT units
%        with each other and with correlation functions CFUN??.
NM = length(xm);                    %number of current moorings.
NI = length(xi);                    %number of interpolation points.

% construct correlation matrices
dx = - xm*ones(1,NM) + ones(NM,1)*xm';     %dx(r,c)=xm_c - xm_r;
dy = - ym*ones(1,NM) + ones(NM,1)*ym';
Auu = CFUNuu(dx,dy,CLENGTH);        %pick correlation fun here.
Avv = CFUNvv(dx,dy,CLENGTH);        %pick correlation fun here.
Auv = CFUNuv(dx,dy,CLENGTH);        %pick correlation fun here.
A=[Auu, Auv; Auv', Avv];
L = 2*NM;
A(1:L+1:L^2) = A(1:L+1:L^2) .* (1 + Vn);    %take care of measurement errors.

dx = - xi*ones(1,NM) + ones(NI,1)*xm';      %dx(r,c)=xm_c - xi_r
dy = - yi*ones(1,NM) + ones(NI,1)*ym';
Cpu = CFUNpu(dx,dy,CLENGTH);        %pick correlation fun here.
Cpv = CFUNpv(dx,dy,CLENGTH);        %pick correlation fun here.
C=[Cpu, Cpv];

% mapping
pi = C*(A\[um;vm]);
ei = 1 - diag((C/A)*C')/CFUNpp(0,CLENGTH);   %pick correlation fun here.
```

A.3 '2 to 2' OA program

```
function [ui,vi,eu,ev]=oa22(xi,yi,xm,ym,um,vm,Vn,CLENGTH)
%function [ui,vi,eu,ev]=oa22(xi,yi,xm,ym,um,vm,Vn,CLENGTH)
% "2 to 2" objective analysis
% ui,vi : interpolated values with columns being the time and
%         rows being the interpolation points (NI by NT);
% eu,ev : estimated error in percentage of signal variance (NI by 1);
% xi, yi: x-y coordinates of interpolation points (NI by 1);
% xm, ym: x-y coordinates of measurement sites (NM by 1);
% um, vm: array of measured values with columns being the time
%         and rows being the measurement sites (NM by NT);
% Vn    : noise variance in percentage of signal variance (scalar or 1 by 2*NM);
% CLENGTH: correlation length (scalar);
% units: xi,yi,xm,ym and CLENGTH should have the same units;
%        units of inputs um,vm and output ui,vi should have CONSISTENT units
%        with each other and with correlation functions CFUN??.
NM = length(xm);                    %number of current moorings.
NI = length(xi);                    %number of interpolation points.

% construct correlation matrices
dx = - xm*ones(1,NM) + ones(NM,1)*xm'; % dx(r,c) = xm_c - xm_r
dy = - ym*ones(1,NM) + ones(NM,1)*ym';
Auu = CFUNuu(dx,dy,CLENGTH);        %pick correlation fun here.
Avv = CFUNvv(dx,dy,CLENGTH);        %pick correlation fun here.
Auv = CFUNuv(dx,dy,CLENGTH);        %pick correlation fun here.
A=[Auu, Auv; Auv', Avv];
L = 2*NM;
A(1:L+1:L^2) = A(1:L+1:L^2) .* (1 + Vn);    %take care of measurement errors.

dx = - xi*ones(1,NM) + ones(NI,1)*xm';      %dx(r,c)=xm_c - xi_r
dy = - yi*ones(1,NM) + ones(NI,1)*ym';
Cuu = CFUNuu(dx,dy,CLENGTH);        %pick correlation fun here.
Cuv = CFUNuv(dx,dy,CLENGTH);        %pick correlation fun here.
Cvu = CFUNvu(dx,dy,CLENGTH);        %pick correlation fun here.
Cvv = CFUNvv(dx,dy,CLENGTH);        %pick correlation fun here.
Cu=[Cuu, Cuv];
Cv=[Cvu, Cvv];

% mapping
ui = Cu*(A\[um;vm]);
vi = Cv*(A\[um;vm]);
eu = 1 - diag((Cu/A)*Cu')/CFUNuu(0,0,CLENGTH);   %pick correlation fun here.
ev = 1 - diag((Cv/A)*Cv')/CFUNvv(0,0,CLENGTH);   %pick correlation fun here.
```

A.4 '3 to 1' OA program

```
function [pi,ei]=oa31(xi,yi,xp,yp,p,xv,yv,u,v,Vn,CLENGTH)
%function [pi,ei]=oa31(xi,yi,xp,yp,p,xv,yv,u,v,Vn,CLENGTH)
% "3 to 1" objective analysis
% pi    : interpolated values with columns being the time and
%         rows being the interpolation points (NI by NT);
% ei    : estimated error in percentage of signal variance (NI by 1);
% xi, yi: x-y coordinates of interpolation points (NI by 1);
% xp, yp: x-y coordinates of pressure measurement sites (NP by 1);
% p     : measured pressures with columns being the time
%         and rows being the measurement sites (NP by NT);
% xv, yv: x-y coordinates of current measurement sites (NV by 1);
% u, v  : measured currents with columns being the time
%         and rows being the measurement sites (NV by NT);
% Vn    : noise variance in percentage of signal variance
%         (scalar or 1 by NP+2*NV);
% CLENGTH: correlation length (scalar);
% units: xi,yi,xp,yp,xv,yv and CLENGTH should have the same units;
%        units of inputs p,u,v and output pi should be CONSISTENT
%        with each other and with the correlation functions CFUN??.

NP = length(xp);        %number of pressure gauges.
NV = length(xv);        %number of current moorings.
NI = length(xi);        %number of interpolation points.

% construct correlation matrices
Rpp = sqrt( ( xp*ones(1,NP) - ones(NP,1)*xp' ).^2 +...
            ( yp*ones(1,NP) - ones(NP,1)*yp' ).^2 );
dxpv = - xp*ones(1,NV) + ones(NP,1)*xv'; % dxpv(r,c) = xv_c - xp_r
dypv = - yp*ones(1,NV) + ones(NP,1)*yv';
dxvv = - xv*ones(1,NV) + ones(NV,1)*xv';
dyvv = - yv*ones(1,NV) + ones(NV,1)*yv';
App = CFUNpp(Rpp,CLENGTH);              % pick correlation fun here.
Apu = CFUNpu(dxpv,dypv,CLENGTH);        % pick correlation fun here.
Apv = CFUNpv(dxpv,dypv,CLENGTH);        % pick correlation fun here.
Auu = CFUNuu(dxvv,dyvv,CLENGTH);        % pick correlation fun here.
Avv = CFUNvv(dxvv,dyvv,CLENGTH);        % pick correlation fun here.
Auv = CFUNuv(dxvv,dyvv,CLENGTH);        % pick correlation fun here.
A=[ App, Apu, Apv;...
    Apu',Auu, Auv;...
    Apv',Auv',Avv];
L = NP+2*NV;
A(1:L+1:L^2) = A(1:L+1:L^2).*(1 + Vn);  %taking care of measurement errors.
```

```
Rip = sqrt( ( xi*ones(1,NP) - ones(NI,1)*xp' ).^2 +...
            ( yi*ones(1,NP) - ones(NI,1)*yp' ).^2 );
dxiv = - xi*ones(1,NV) + ones(NI,1)*xv';      %dx(r,c)=xv_c - xi_r
dyiv = - yi*ones(1,NV) + ones(NI,1)*yv';
Cpp = CFUNpp(Rip,CLENGTH);            % pick correlation fun here.
Cpu = CFUNpu(dxiv,dyiv,CLENGTH);        % pick correlation fun here.
Cpv = CFUNpv(dxiv,dyiv,CLENGTH);        % pick correlation fun here.
C=[Cpp, Cpu, Cpv];

% mapping
pi = C*(A\[p;u;v]);
ei = 1 - diag((C/A)*C')/CFUNpp(0,CLENGTH);   %pick correlation fun here.
```

A.5 '3 to 2' OA program

```
function [ui,vi,eu,ev]=oa32(xi,yi,xp,yp,p,xv,yv,u,v,Vn,CLENGTH)
% [ui,vi,eu,ev]=oa32(xi,yi,xp,yp,p,xv,yv,u,v,Vn,CLENGTH)
% "3 to 2" objective analysis
% ui,vi : interpolated values with columns being the time and
%         rows being the interpolation points (NI by NT);
% eu,ev : estimated error in percentage of signal variance (NI by 1);
% xi, yi: x-y coordinates of interpolation points (NI by 1);
% xp, yp: x-y coordinates of pressure measurement sites (NP by 1);
% p     : measured pressures with columns being the time
%         and rows being the measurement sites (NP by NT);
% xv, yv: x-y coordinates of current measurement sites (NV by 1);
% u, v  : measured currents with columns being the time
%         and rows being the measurement sites (NV by NT);
% Vn    : noise variance in percentage of signal variance
%         (scalar or 1 by NP+2*NV);
% CLENGTH: correlation length (scalar);
% units: xi,yi,xp,yp,xv,yv and CLENGTH should have the same units;
%        units of inputs p,u,v and output ui,vi should be CONSISTENT
%        with each other and with the correlation functions CFUN??.

NP = length(xp);        %number of pressure gauges.
NV = length(xv);        %number of current moorings.
NI = length(xi);        %number of interpolation points.

% construct correlation matrices
Rpp = sqrt( ( xp*ones(1,NP) - ones(NP,1)*xp' ).^2 +...
          ( yp*ones(1,NP) - ones(NP,1)*yp' ).^2 );
dxpv = - xp*ones(1,NV) + ones(NP,1)*xv'; % dxpv(r,c) = xv_c - xp_r
dypv = - yp*ones(1,NV) + ones(NP,1)*yv';
dxvv = - xv*ones(1,NV) + ones(NV,1)*xv';
dyvv = - yv*ones(1,NV) + ones(NV,1)*yv';
App = CFUNpp(Rpp,CLENGTH);              % pick correlation fun here.
Apu = CFUNpu(dxpv,dypv,CLENGTH);        % pick correlation fun here.
Apv = CFUNpv(dxpv,dypv,CLENGTH);        % pick correlation fun here.
Auu = CFUNuu(dxvv,dyvv,CLENGTH);        % pick correlation fun here.
Avv = CFUNvv(dxvv,dyvv,CLENGTH);        % pick correlation fun here.
Auv = CFUNuv(dxvv,dyvv,CLENGTH);        % pick correlation fun here.
A=[ App, Apu, Apv;...
    Apu',Auu, Auv;...
    Apv',Auv',Avv];
L = NP+2*NV;
A(1:L+1:L^2) = A(1:L+1:L^2).*(1 + Vn);  %taking care of measurement errors.
```

```
dxip = - xi*ones(1,NP) + ones(NI,1)*xp';      %dx(r,c)=xp_c - xi_r
dyip = - yi*ones(1,NP) + ones(NI,1)*yp';
dxiv = - xi*ones(1,NV) + ones(NI,1)*xv';      %dx(r,c)=xv_c - xi_r
dyiv = - yi*ones(1,NV) + ones(NI,1)*yv';
Cup = CFUNup(dxip,dyip,CLENGTH);        % pick correlation fun here.
Cuu = CFUNuu(dxiv,dyiv,CLENGTH);        % pick correlation fun here.
Cuv = CFUNuv(dxiv,dyiv,CLENGTH);        % pick correlation fun here.
Cvp = CFUNvp(dxip,dyip,CLENGTH);        % pick correlation fun here.
Cvu = CFUNvu(dxiv,dyiv,CLENGTH);        % pick correlation fun here.
Cvv = CFUNvv(dxiv,dyiv,CLENGTH);        % pick correlation fun here.
Cu=[Cup, Cuu, Cuv];
Cv=[Cvp, Cvu, Cvv];

% mapping
ui = Cu*(A\[p;u;v]);
vi = Cv*(A\[p;u;v]);
eu = 1 - diag((Cu/A)*Cu')/CFUNuu(0,CLENGTH);   %pick correlation fun here.
ev = 1 - diag((Cv/A)*Cv')/CFUNvv(0,CLENGTH);   %pick correlation fun here.
```

A.6 Cross-correlation Functions

```
===> function y = CFUNpp(x,L)
     y = exp(-(x/L).^2);

===> function Cpu = CFUNpu(dx,dy,CLENGTH)
     lambda = 1/CLENGTH^2;
     r = sqrt( dx.^2 + dy.^2 );
     Cpu = dy .* (2*lambda * CFUNpp(r,CLENGTH));

===> function Cpv = CFUNpv(dx,dy,CLENGTH)
     lambda = 1/CLENGTH^2;
     r = sqrt( dx.^2 + dy.^2 );
     Cpv = - dx .* (2*lambda * CFUNpp(r,CLENGTH));

===> function Cup = CFUNup(dx,dy,CLENGTH)
     Cup = -CFUNpu(dx,dy,CLENGTH);

===> function Cuu = CFUNuu(dx,dy,CLENGTH)
     lambda = 1/CLENGTH^2;
     r = sqrt( dx.^2 + dy.^2 );
     Cuu = (1 - 2*lambda*dy.^2) .* (2*lambda * CFUNpp(r,CLENGTH));

===> function Cuv = CFUNuv(dx,dy,CLENGTH)
     lambda = 1/CLENGTH^2;
     r = sqrt( dx.^2 + dy.^2 );
     Cuv = 2*lambda*dx .* dy .* (2*lambda * CFUNpp(r,CLENGTH));

===> function Cvp = CFUNvp(dx,dy,CLENGTH)
     Cvp = -CFUNpv(dx,dy,CLENGTH);

===> function Cvu = CFUNvu(dx,dy,CLENGTH)
     Cvu = CFUNuv(dx,dy,CLENGTH);

===> function Cvv = CFUNvv(dx,dy,CLENGTH)
     lambda = 1/CLENGTH^2;
     r = sqrt( dx.^2 + dy.^2 );
     Cvv = (1 - 2*lambda*dx.^2) .* (2*lambda * CFUNpp(r,CLENGTH));
```

B Deriving cross-correlation functions

The relations in Table 4 and 5 are derived in this appendix. First recall the definitions of γ, α_x and α_y:

$$\gamma = \sqrt{(x_1 - x_2)^2 + (y_1 - y_2)^2}; \quad x_2 - x_1 = \gamma \cos\alpha_x, \quad y_2 - y_1 = \gamma \cos\alpha_y.$$

From these definitions follow these identities:

$$\frac{\partial\gamma}{\partial x_1} = -\cos\alpha_x; \quad \frac{\partial\gamma}{\partial x_2} = \cos\alpha_x; \quad \frac{\partial\gamma}{\partial y_1} = -\cos\alpha_y; \quad \frac{\partial\gamma}{\partial y_2} = \cos\alpha_y;$$

and

$$\frac{\partial\cos\alpha_y}{\partial y_1} = -\frac{1}{\gamma}\left(1 - \cos^2\alpha_y\right); \quad \frac{\partial\cos\alpha_y}{\partial x_1} = \frac{\partial\cos\alpha_x}{\partial y_1} = \frac{1}{\gamma}\cos\alpha_x\cos\alpha_y; \quad \frac{\partial\cos\alpha_x}{\partial x_1} = -\frac{1}{\gamma}\left(1 - \cos^2\alpha_x\right).$$

By these identities and Equation (32), $F_{\psi u}$ and $F_{\psi v}$ can be derived:

$$F_{\psi u} = E\{\psi(x_1,y_1)u(x_2,y_2)\} = -E\{\psi(x_1,y_1)\frac{\partial\psi(x_2,y_2)}{\partial y_2}\} = -\frac{\partial F(\gamma)}{\partial y_2} = -\frac{\partial\gamma}{\partial y_2}\frac{dF}{d\gamma} = -\cos\alpha_y\frac{dF}{d\gamma};$$

$$F_{\psi v} = E\{\psi(x_1,y_1)v(x_2,y_2)\} = E\{\psi(x_1,y_1)\frac{\partial\psi(x_2,y_2)}{\partial x_2}\} = \frac{\partial F(\gamma)}{\partial x_2} = \frac{\partial\gamma}{\partial x_2}\frac{dF}{d\gamma} = \cos\alpha_x\frac{dF}{d\gamma}.$$

Similarly, we have

$$F_{u\psi} = \cos\alpha_y\frac{dF}{d\gamma} \quad \textit{and} \quad F_{v\psi} = -\cos\alpha_x\frac{dF}{d\gamma}.$$

The remaining four relations in Table 4 follow from the above two equations and the identities before:

$$\begin{aligned} F_{uu} &= E\{u(x_1,y_1)u(x_2,y_2)\} = -E\{\frac{\partial\psi(x_1,y_1)}{\partial y_1}u(x_2,y_2)\} = -\frac{\partial F_{\psi u}}{\partial y_1} \\ &= \frac{\partial\cos\alpha_y\frac{dF}{d\gamma}}{\partial y_1} = -\cos^2\alpha_y\frac{d^2F}{d\gamma^2} - (1-\cos^2\alpha_y)\frac{1}{\gamma}\frac{dF}{d\gamma}; \end{aligned}$$

$$\begin{aligned} F_{uv} &= E\{u(x_1,y_1)v(x_2,y_2)\} = -E\{\frac{\partial\psi(x_1,y_1)}{\partial y_1}v(x_2,y_2)\} = -\frac{\partial F_{\psi v}}{\partial y_1} \\ &= -\frac{\partial\cos\alpha_x\frac{dF}{d\gamma}}{\partial y_1} = \cos\alpha_x\cos\alpha_y\left(\frac{d^2F}{d\gamma^2} - \frac{1}{\gamma}\frac{dF}{d\gamma}\right) = F_{vu} \end{aligned}$$

and

$$\begin{aligned} F_{vv} &= E\{v(x_1,y_1)v(x_2,y_2)\} = E\{\frac{\partial\psi(x_1,y_1)}{\partial x_1}v(x_2,y_2)\} = \frac{\partial F_{\psi v}}{\partial x_1} \\ &= \frac{\partial\cos\alpha_x\frac{dF}{d\gamma}}{\partial x_1} = -\cos^2\alpha_x\frac{d^2F}{d\gamma^2} - (1-\cos^2\alpha_x)\frac{1}{\gamma}\frac{dF}{d\gamma}. \end{aligned}$$

The results in Table 5 are obtained by substituting $F(\gamma)$ in Table 4 by a Gaussian function:

$$F(\gamma) = V_\psi \exp(-\lambda\gamma^2).$$

Thus we have

$$F'(\gamma) = -2\lambda\gamma F, \qquad F''(\gamma) = -(1 - 2\lambda\gamma^2) \cdot 2\lambda F$$

and then

$$F_{\psi u} = \gamma \cos\alpha_y \cdot 2\lambda F(\gamma) = -F_{u\psi}, \qquad F_{\psi v} = -\gamma \cos\alpha_x \cdot 2\lambda F(\gamma) = -F_{v\psi};$$

$$F_{uu} = [\cos^2\alpha_y(1 - 2\lambda\gamma^2) + \sin^2\alpha_y] \cdot 2\lambda F = (1 - 2\lambda\gamma^2\cos^2\alpha_y) \cdot 2\lambda F(\gamma);$$

$$F_{uv} = \cos\alpha_x \cos\alpha_y \left[-(1 - 2\lambda\gamma^2) + 1\right] \cdot 2\lambda F = 2\lambda\gamma^2 \cos\alpha_x \cos\alpha_y \cdot 2\lambda F(\gamma) = F_{vu};$$

$$F_{vv} = [\cos^2\alpha_x(1 - 2\lambda\gamma^2) + \sin^2\alpha_x] \cdot 2\lambda F = (1 - 2\lambda\gamma^2\cos^2\alpha_x) \cdot 2\lambda F(\gamma).$$

C Time series plots

Two sets of time series plots are collected in this appendix. The first set plots (Figure 9) the pressure time series which are interpolated to the PIES sites from the final pressure maps (dashed lines) and the absolute pressure on the PIES sites determined in section 3.3.2 (solid lines). The second set (Figures 10 and 11) displays the time series of geostrophic current on current meter sites derived from the pressure maps (dashed lines) and the current measurements on the corresponding sites (solid lines).

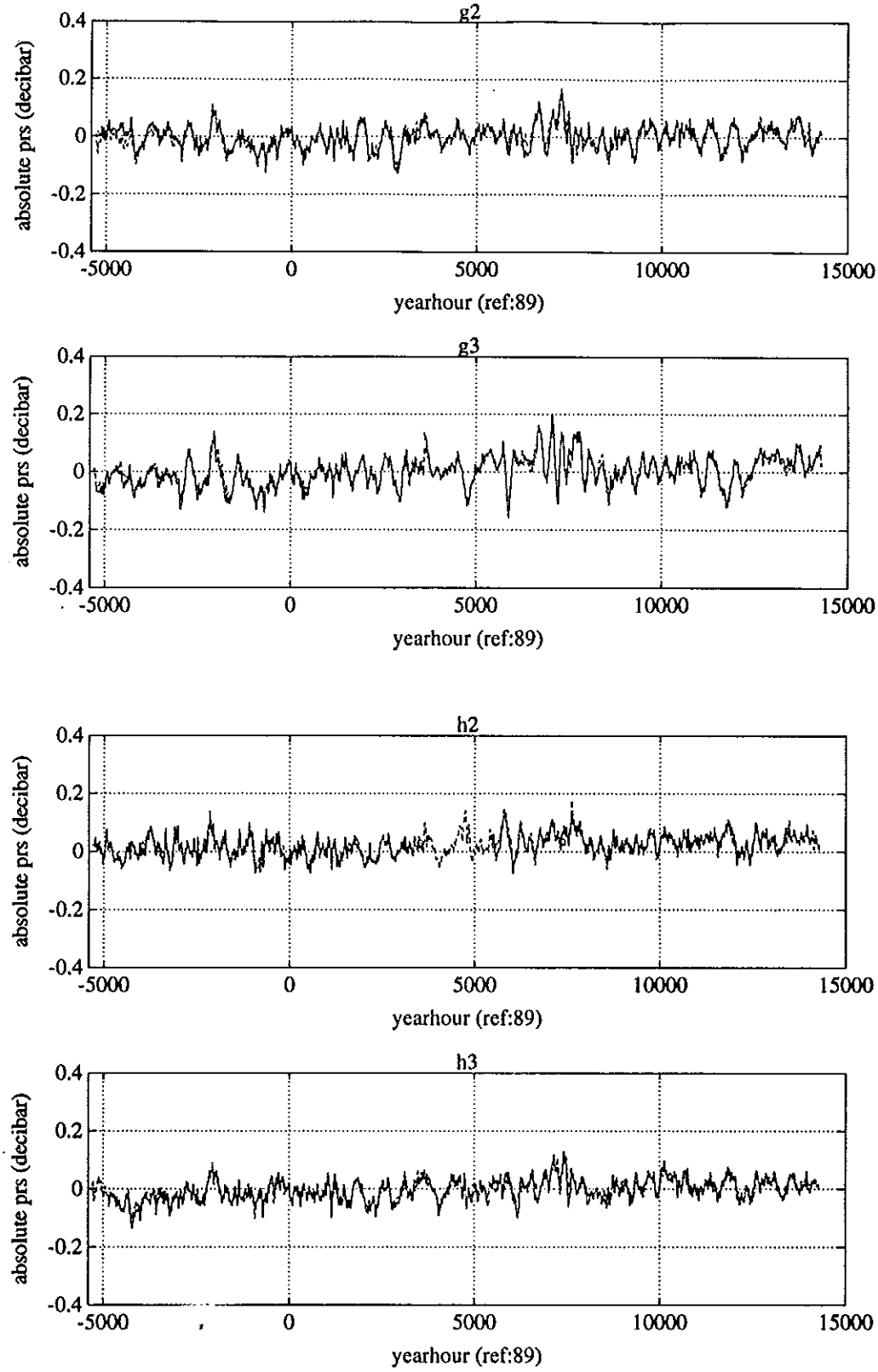

Figure 9: Measured pressure (solid) with mapped pressure (dashed)

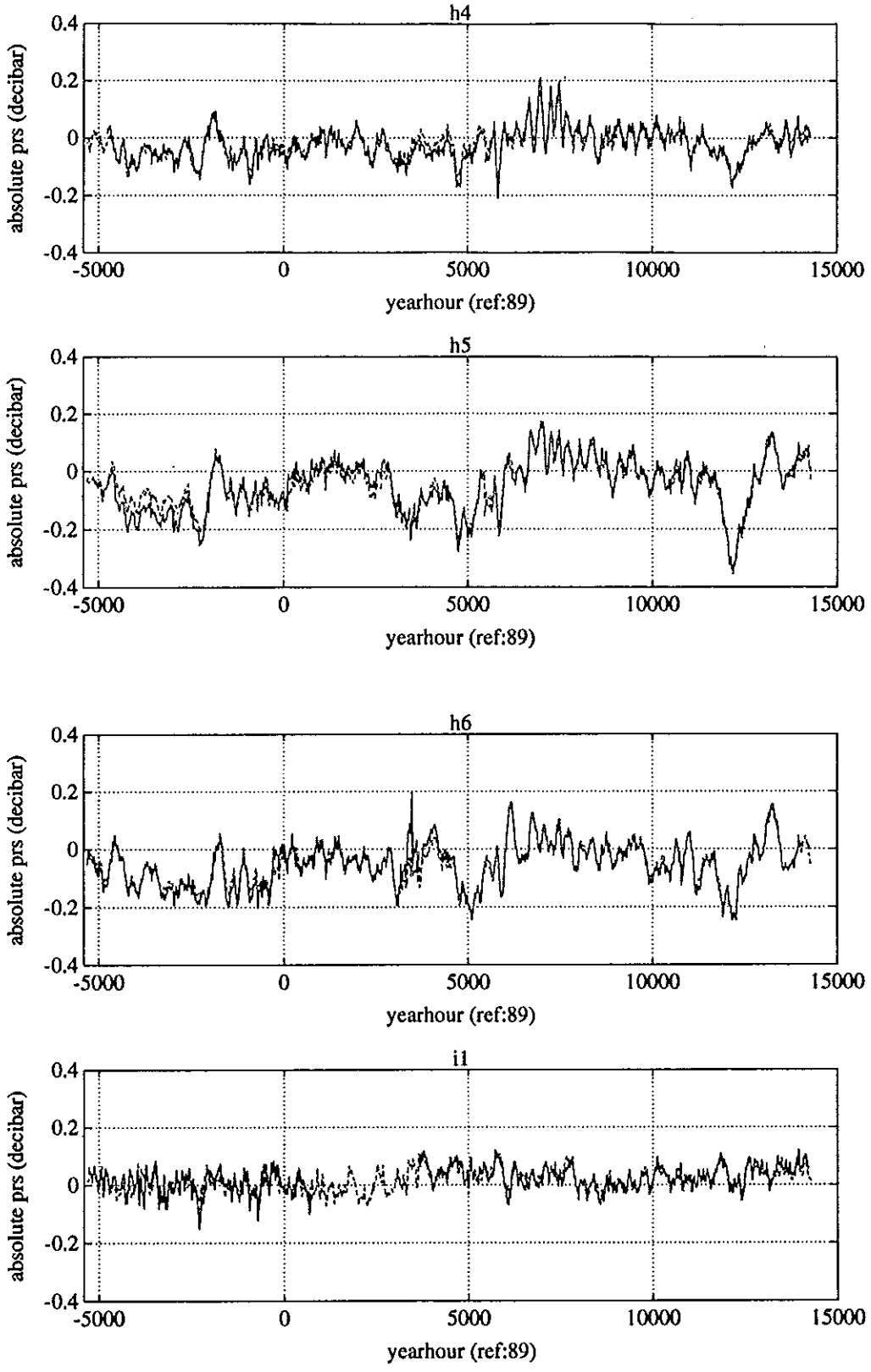

Figure 9: (*Continued*)

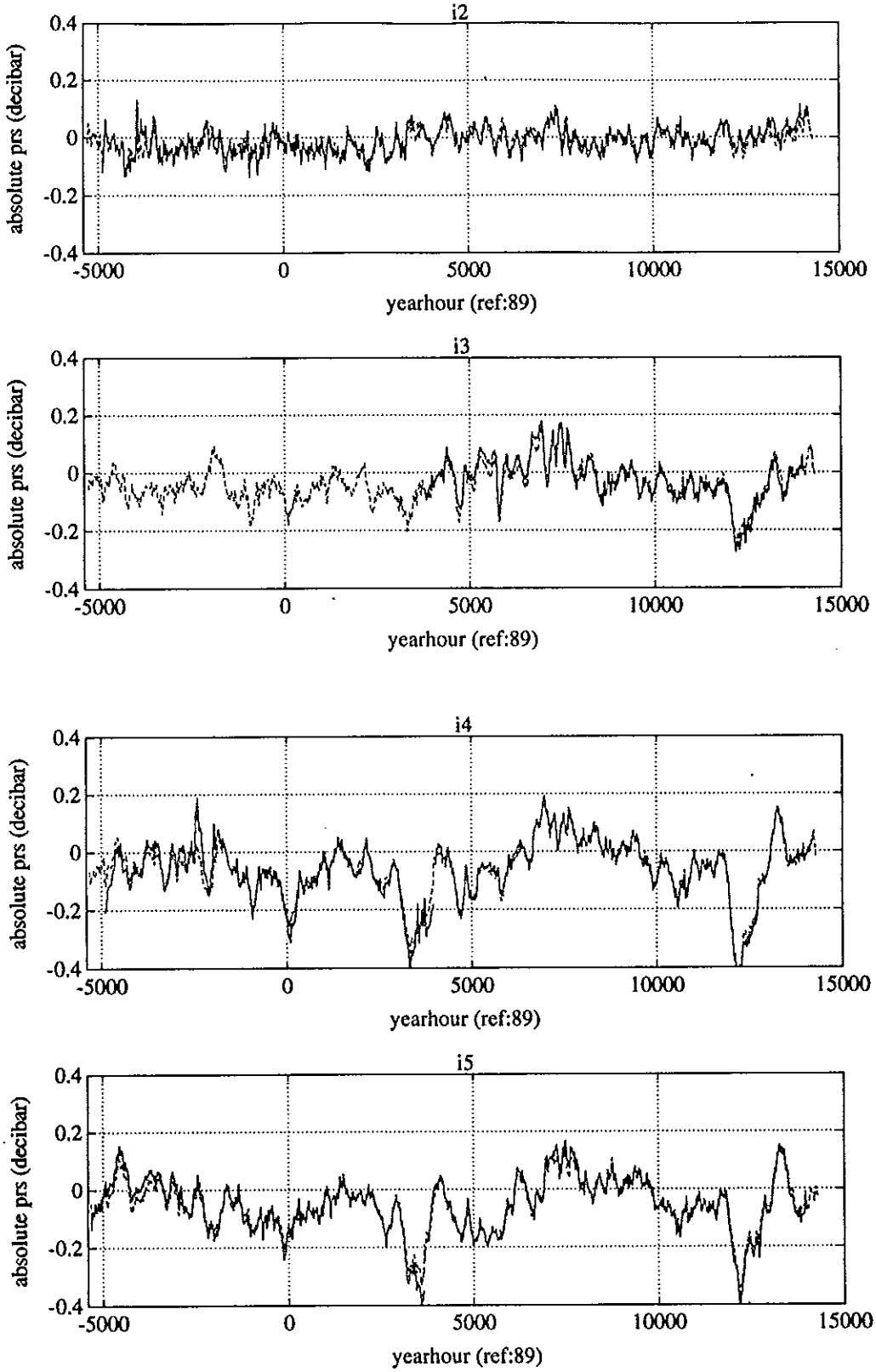

Figure 9: (*Continued*)

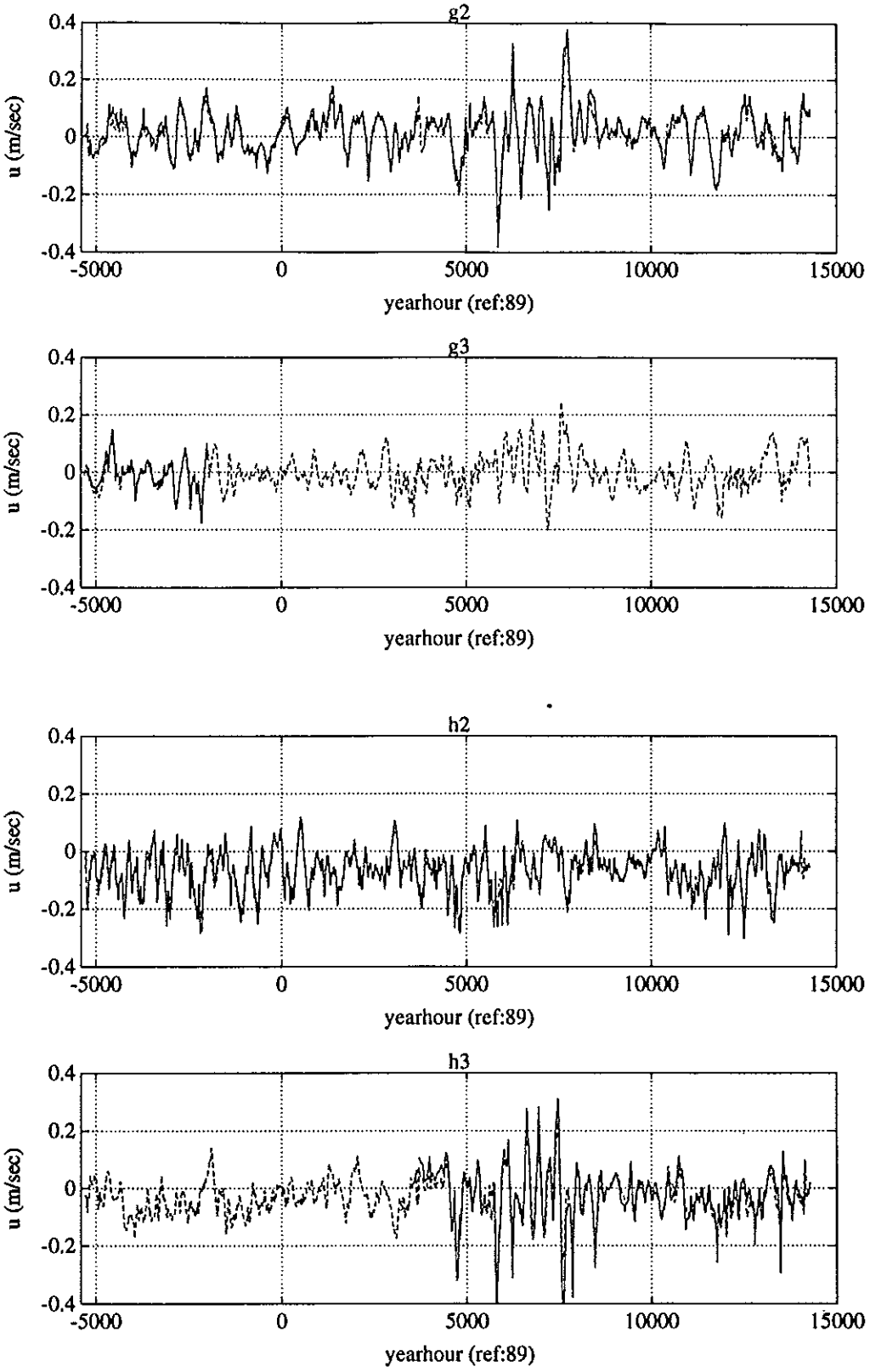

Figure 10: Measured (solid) and mapped currents (dashed) (u component)

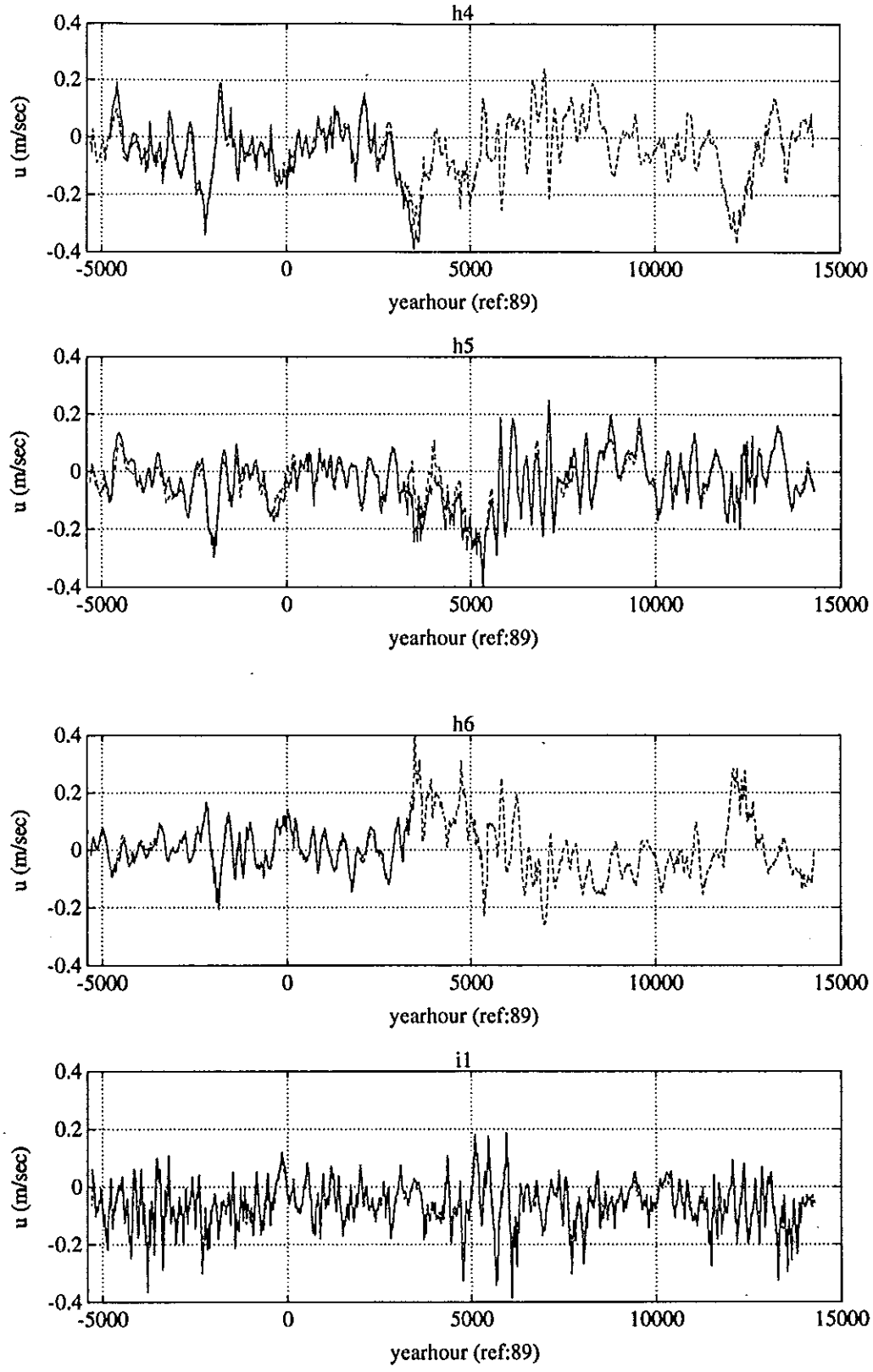

Figure 10: (*Continued*)

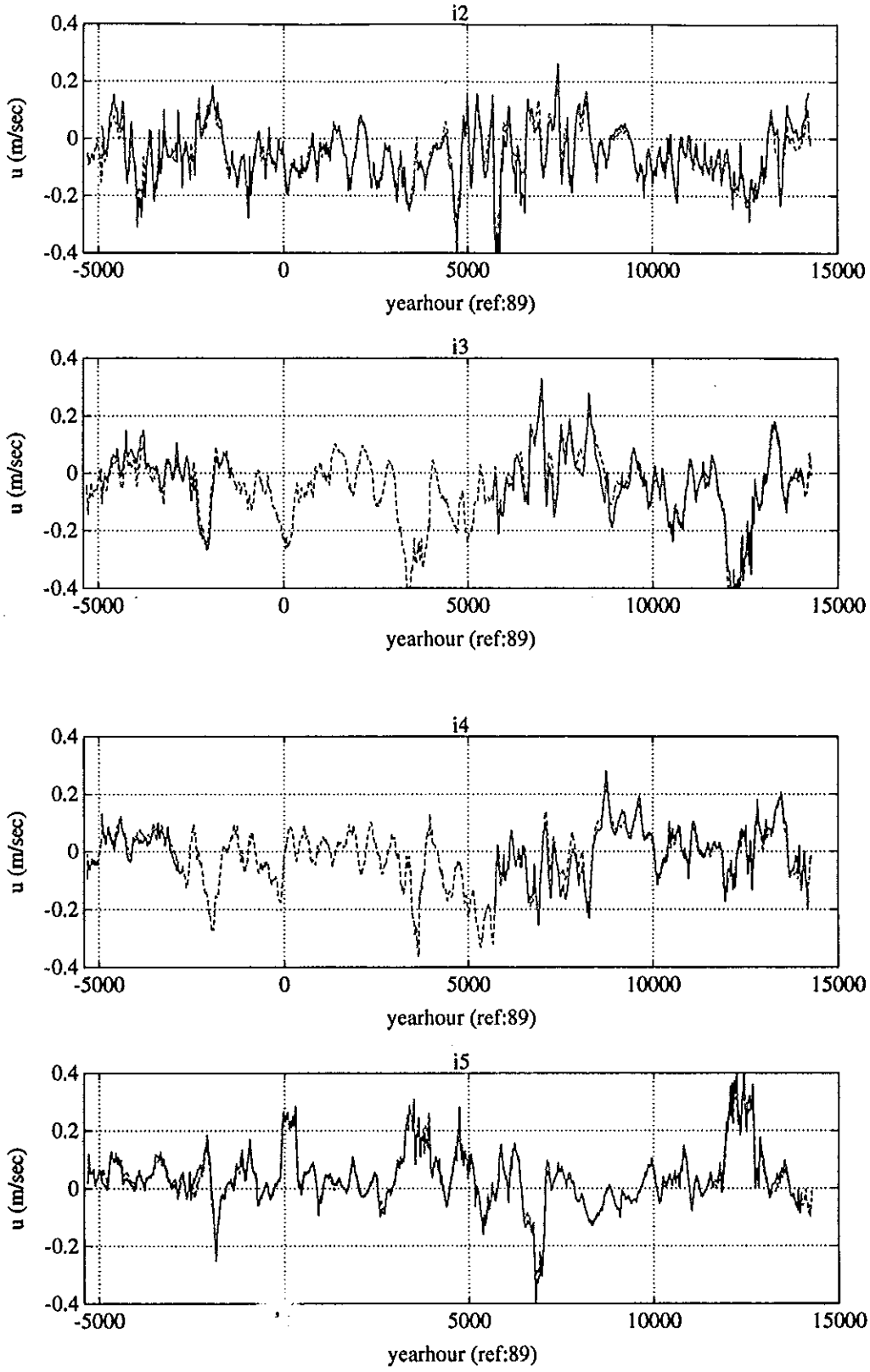

Figure 10: (*Continued*)

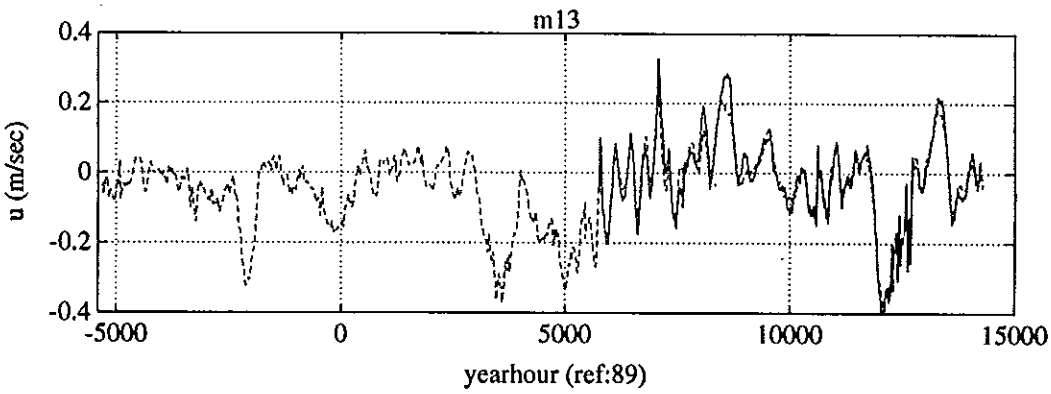

Figure 10: (*Continued*)

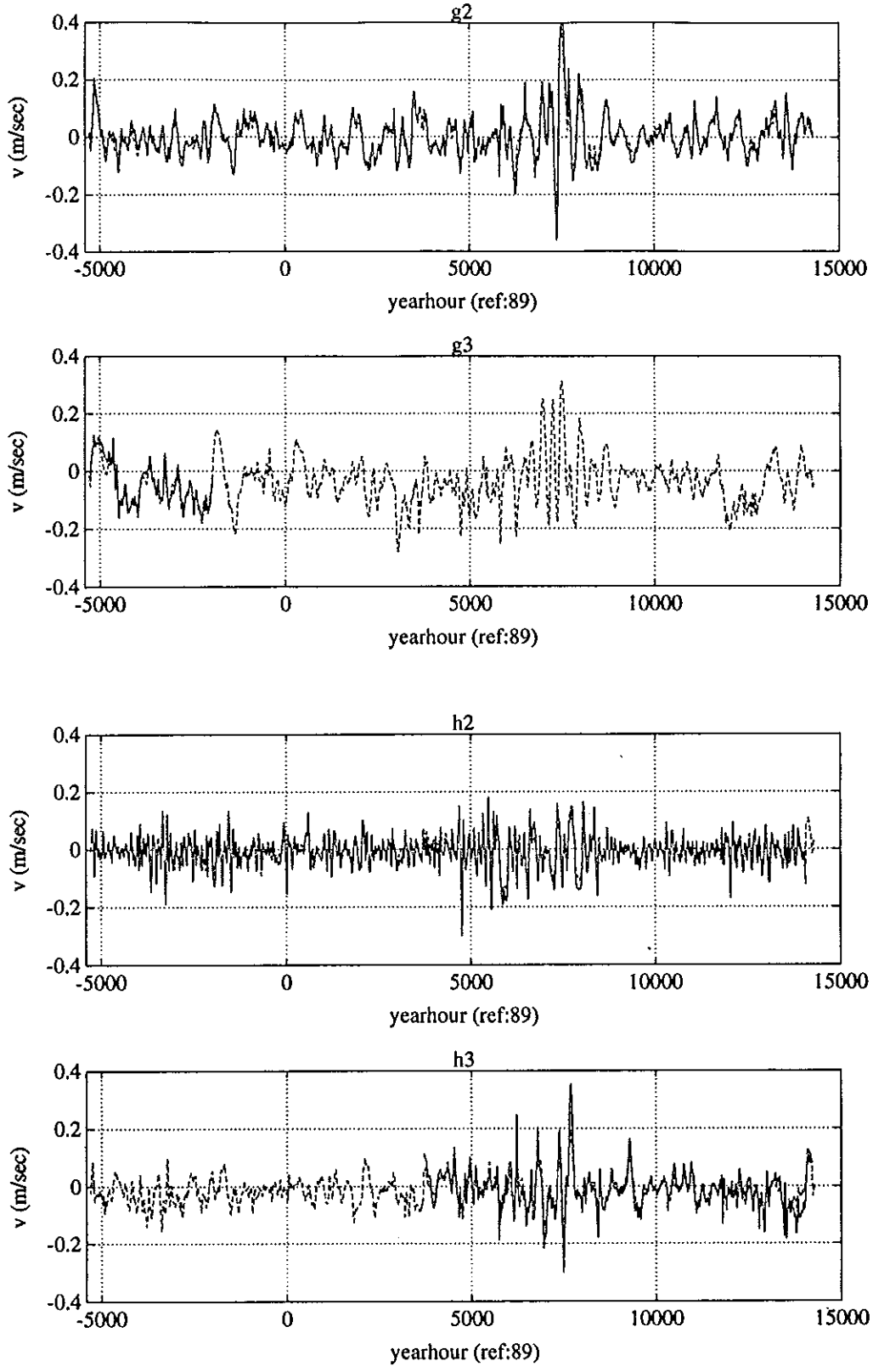

Figure 11: Measured (solid) and mapped currents (dashed) (v component)

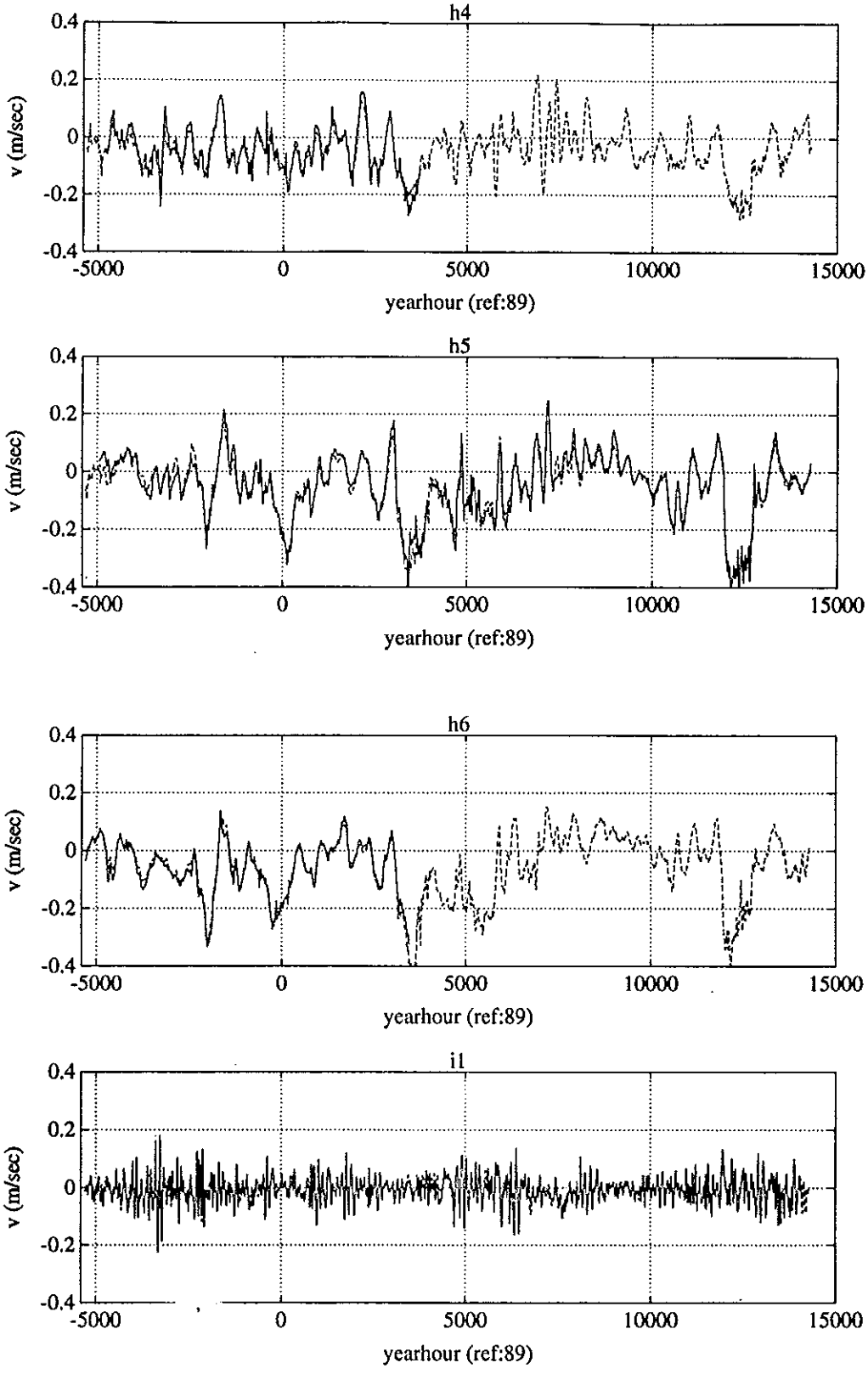

Figure 11: (*Continued*)

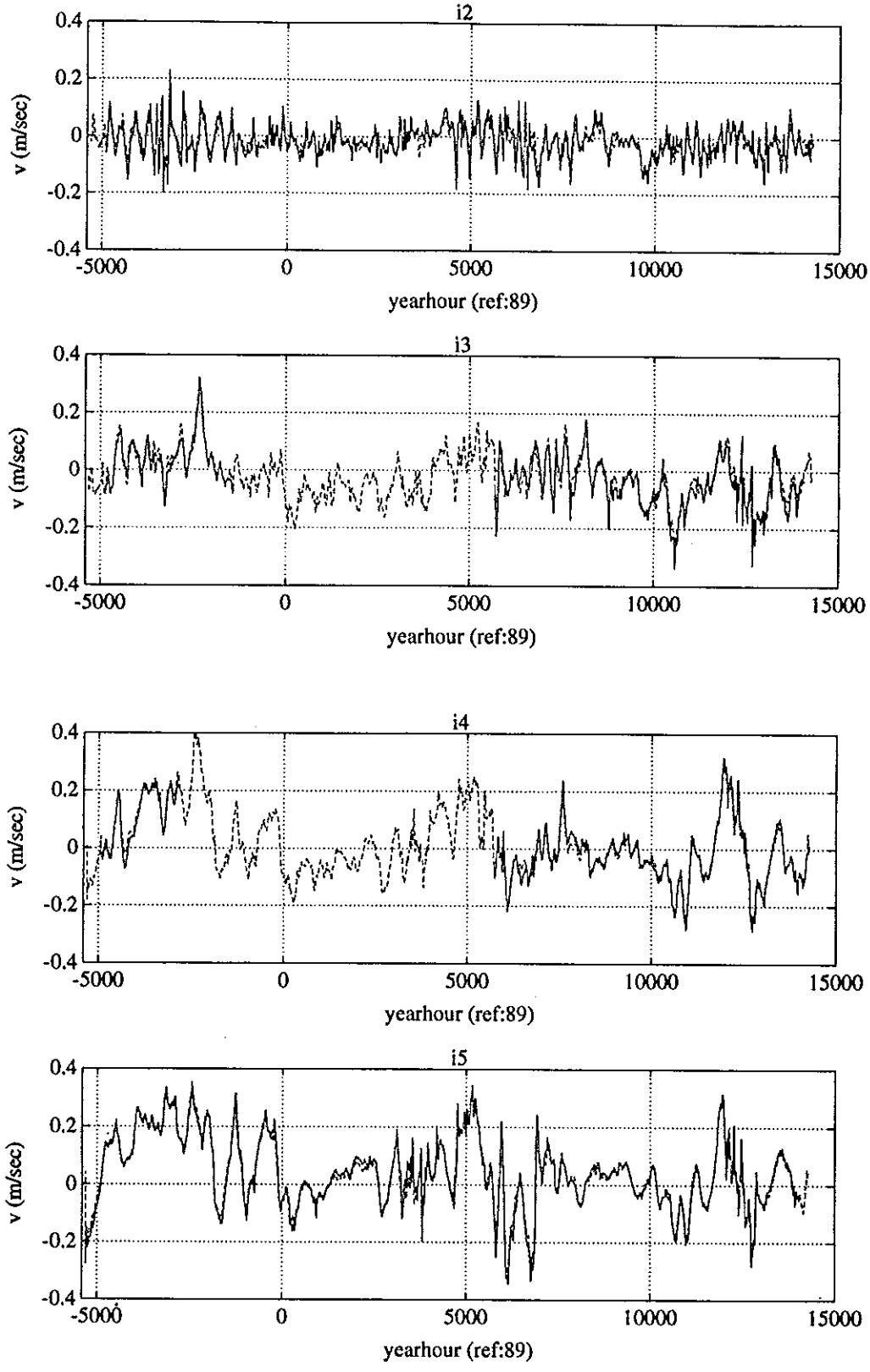

Figure 11: (*Continued*)

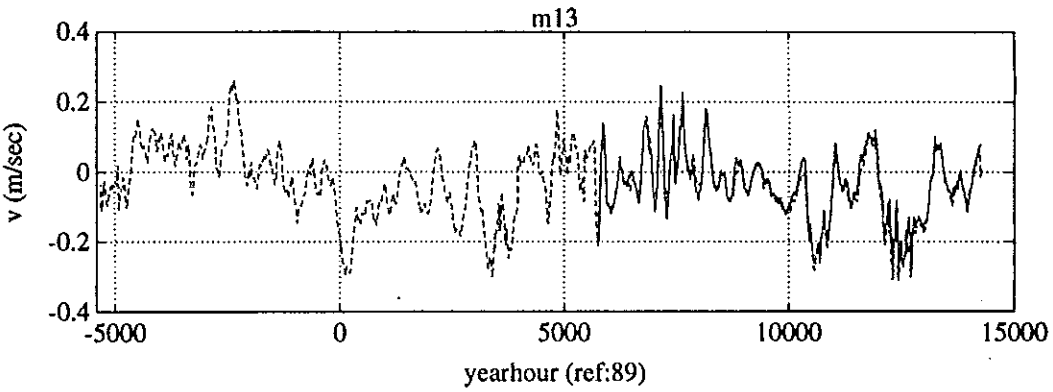

Figure 11: (*Continued*)

SECURITY CLASSIFICATION OF THIS PAGE

REPORT DOCUMENTATION PAGE

1a. REPORT SECURITY CLASSIFICATION Unclassified	1b. RESTRICTIVE MARKINGS
2a. SECURITY CLASSIFICATION AUTHORITY	3. DISTRIBUTION/AVAILABILITY OF REPORT Distribution for Public release; Distribution is unlimited.
2b. DECLASSIFICATION/DOWNGRADING SCHEDULE	
4. PERFORMING ORGANIZATION REPORT NUMBER(S) University of Rhode Island Graduate School of Oceanography GSO Technical Report 91-6	5. MONITORING ORGANIZATION REPORT NUMBER(S)
6a. NAME OF PERFORMING ORGANIZATION Univ. of Rhode Island Grad. School of Oceanography 6b. OFFICE SYMBOL (If applicable) 1122 PO	7a. NAME OF MONITORING ORGANIZATION
6c. ADDRESS (City, State, and ZIP Code) South Ferry Road Narragansett, RI 02882	7b. ADDRESS (City, State, and ZIP Code)
8a. NAME OF FUNDING/SPONSORING ORGANIZATION Office of Naval Research National Science Foundation 8b. OFFICE SYMBOL (If applicable)	9. PROCUREMENT INSTRUMENT IDENTIFICATION NUMBER
8c. ADDRESS (City, State, and ZIP Code) 800 N. Quincy St., Arlington, VA 22217 1800 G. St., N.W., Washington, DC 20550	10. SOURCE OF FUNDING NUMBERS PROGRAM ELEMENT NO. / PROJECT NO. / TASK NO. / WORK UNIT ACCESSION NO.

11. TITLE (Include Security Classification)
THE SYNOP EXPERIMENT: Bottom Pressure Maps for the Central Array
May 1988 to August 1990

12. PERSONAL AUTHOR(S)
Xiaoshu Qian and D. Randolph Watts

13a. TYPE OF REPORT	13b. TIME COVERED	14. DATE OF REPORT (Year, Month, Day)	15. PAGE COUNT
Technical	FROM 5/88 TO 8/90	July 1992	194

16. SUPPLEMENTARY NOTATION

17. COSATI CODES			18. SUBJECT TERMS (Continue on reverse if necessary and identify by block number)
FIELD	GROUP	SUB-GROUP	Gulf Stream, SYNOP, Ocean Bottom Pressure, Currents, Pressure Maps

19. ABSTRACT (Continue on reverse if necessary and identify by block number)

This report documents our procedures and the accuracy of objective maps of bottom pressure in the Synop Central Array region between June 1988 and August 1990. The pressure maps are made by using multivariate objective analysis procedures to combine data from bottom pressure measurements by Inverted Echo Sounders (PIES) and bottom current meter measurements in the Central Array between June 1988 and August 1990.

A key new feature is that all daily maps can be adjusted to a fixed reference level by combining measurements of bottom pressure and near-bottom currents, (P_b, u,v). While objective stream functions mapped from (u,v) alone are spatially consistent, the reference levels vary temporally from map to map. On the other hand, each bottom pressure record P_b has a temporally consistent reference but the reference can vary from site to site. The combination allows us to adjust all to a common, consistent reference level in multivariate objective maps.

The pressure maps and error maps are displayed daily for 26 months with overlaid measured current vectors. Mapping procedures are documented along with error analyses and comparisons

20. DISTRIBUTION/AVAILABILITY OF ABSTRACT ☒ UNCLASSIFIED/UNLIMITED ☐ SAME AS RPT. ☐ DTIC USERS	21. ABSTRACT SECURITY CLASSIFICATION
22a. NAME OF RESPONSIBLE INDIVIDUAL	22b. TELEPHONE (Include Area Code) / 22c. OFFICE SYMBOL

DD FORM 1473, 84 MAR 83 APR edition may be used until exhausted. All other editions are obsolete.

SECURITY CLASSIFICATION OF THIS PAGE

19. ABSTRACT

with measured fields. The results produce bottom pressure and current fields with typical error of only 2 mbar and 2 cm/sec, compared to typical signal standard deviation of 6 mbar and 9 cm/s.

The report is one of a series of data reports that document aspects of our participation in the SYNoptic Ocean Prediction (SYNOP) experiment.